ANALYSIS AND DESIGN OF RELIABLE AND SECURE CHAOTIC COMMUNICATION SYSTEMS FOR OPTICAL AND WIRELESS LINKS

THESIS

Submitted in partial fulfillment of the requirements for the degree of

DOCTOR OF PHILOSOPHY

By

LWAA FAISAL ABDULAMEER

Reg. No.: 100787EC10F02

DEPARTMENT OF

ELECTRONICS AND COMMUNICATION ENGINEERING

NATIONAL INSTITUTE OF TECHNOLOGY

KARNATAKA SURATHKAL, MANGALORE- 575 025

AUGUST, 2014

DECLARATION

I hereby declare that the Research Thesis entitled **Analysis and Design of Reliable and Secure Chaotic Communication Systems for Optical and Wireless Links** which is being submitted to the **National Institute of Technology Karnataka**, **Surathkal** in partial fulfillment of the requirements for the award of the Degree of **Doctor of Philosophy in Electronics and Communication Engineering** is a bonafide report of the research work carried out by me. The material contained in this Research Thesis has not been submitted to any University or Institution for the award of any degree.

LWAA FAISAL ABDULAMEER

EC10F02,

Department of **Electronics and Communication Engineering**

Place: NITK- Surathkal

Date:

CERTIFICATE

This is to certify that the Research Thesis entitled "**Analysis and Design of Reliable and Secure Chaotic Communication Systems for Optical and Wireless Links"** submitted by **LWAA FAISAL ABDULAMEER (Register Number: EC10F02)** as the record of the research work carried out by him, is accepted as the Research Thesis submission in partial fulfillment of the requirements for the award of degree of Doctor of Philosophy.

Dr. U. Sripati

Research Guide

(Name and Signature with Date and Seal)

Dr. Muralidhar Kulkarni

Research Guide

(Name and Signature with Date and Seal)

Dr. M. S. Bhat

Chairman, DRPC

Dedicated To My Mother, My Father, My Wife,

And

My Kids

Acknowledgements

This thesis is the end of my journey in obtaining my Ph.D. This thesis has been kept on track and been seen through to completion with the support and encouragement of numerous people including my well wishers, my friends, colleagues and various institutions. At the end of my thesis I would like to thank all those people who made this thesis possible and an unforgettable experience for me. At the end of my thesis, it is a pleasant task to express my thanks to all those who contributed in many ways to the success of this study and made it an unforgettable experience for me.

Foremost, I would like to express my sincere gratitude to my advisors ***Professor U. Sripati*** and ***Professor Muralidhar Kulkarni*** for the continuous support of my Ph.D study and research, for their patience, motivation, enthusiasm, and immense knowledge. Their guidance helped me in all the time of research and writing of this thesis. I could not have imagined having a better advisors and mentors for my Ph.D study. I hope that one day I would become as good advisors to my students as ***Professor U. Sripati and Professor Muralidhar Kulkarni*** have been to me.

I thank my RPAC members, Dr. Ashwini Chaturvedi and Dr. M. N. Satyanarayan for their helpful suggestions and comments during my progress report presentations.

Deep respect to **I**ndian **C**ouncil **C**ultural **R**elations **(ICCR)** – India for give me Ph.D fellowship throw indo-Iraq exchange relations program.

I would also like to acknowledge Ministry of Higher Education and Scientific Research, **University of Baghdad**, ALKHWARIZMI College of Engineering and **Iraqi Cultural Office** in Iraqi Embassy-New Delhi for all fiancées supporting during for allowing me to study

Special thanks to my friend Mr. Jokhakar Jignesh D. for his help and support. I and Mr. Jignesh worked together on several different phases of project, and without his efforts my job would have undoubtedly been more difficult. I greatly benefited from his keen scientific insight, his knack for solving seemingly intractable practical difficulties, and his ability to put complex ideas into simple terms.

I cannot imagine my current position without the love and support from my family. I thank my parents, for striving hard to provide a good education for me and my siblings. I always fall short of words and felt impossible to describe their support in words. If I have to mention one thing about them, among many, then I would proudly mention that my parents are very simple and they taught me how to lead a simple life. I would simply say, “Mama, Baba you are great!”.

Most importantly, none of this would have been possible without the love and patience of my wife (Samraa Mohammed), my Daughter (Sura Lwaa) and my son (Ahmed Lwaa). My family, to whom this dissertation is dedicated to, has been a constant source of love, concern, support and strength all these years. I would like to express my heart-felt gratitude to my family.Thanks to my dear brother Ameer Faisal for bringing my family to India while I was busy in my course work and also he helped me during all these years.

My sincere thanks to all research scholars of the Department of Electronics and Communication Engineering, NITK, Surathkal, without them this research pursuit would not have been possible.

I am also grateful to all staff at the Department of Electronics and Communication Engineering, NITK for their various forms of support during my research work.

Also I would like to thank all staff of Al-Khwarizmi Engineering College for their support.

Many friends have helped me through these difficult years. Their support and care helped me overcome setbacks and stay focused on my study. I greatly value their friendship. I am also grateful to the Indian people in Mangalore that helped me adjust to a new country. Special thanks to my best friend Muhannad Waleed who supported me during my time here.

LWAA FAISAL ABDULAMEER

ABSTRACT

There has been growing interest in the use of chaotic techniques for enabling secure communication in recent years. A number of researchers have focused their energies to develop communication strategies based on the discipline of chaotic mechanics. This need has been motivated by the emergence of a number of wireless services which require the channel to provide very low Bit-Error-Rate (BER), high bandwidth efficiency along with information security. Simultaneous provision of these three conflicting requirements is difficult to achieve with conventional communication strategies. This has motivated researchers in the Communication Engineering community to explore new domains in their search for efficient and secure communication techniques.

This work reported in this thesis has aimed at the study, design and validation (via analysis and simulation) of techniques derived from chaotic mechanics to enhance security and BER performance at physical layer for wireless communication. Both RF and Optical Wireless system domains have been included in our study. Conventional techniques aiming to provide security enhancement at the physical layer have employed spreading sequences. The use of these techniques requires bandwidth expansion, and the amount of security is limited. Further, the security provided by these techniques comes with a penalty in BER performance and bandwidth efficiency. As a consequence of rapidly increasing demand for wireless services and limited licensed bandwidth, there is a strong need for bandwidth efficient secure systems. In our work, we have designed and verified (by analysis and simulation) chaos-based systems with enhanced BER performance and bandwidth efficiency similar to that offered by conventional PN sequence based systems. We have also proposed techniques that are applicable to the emerging domain of Free Space Optical (FSO) communication because this technology has the potential of providing fiber like unlicensed bandwidth for high speed short distance communication links.

We have started the discussion with a study of the issues involved in synchronization between master and slave chaotic systems. We have suggested the use of Low Density

Parity Check (LDPC) error correcting code in the system to reinforce the ability of the system resist noise and facilitate the synchronization between master and slave systems in presence of AWGN. In addition, it is shown that synchronization can be achieved even when the spreading factor is decreased to low values ($\beta = 4$).

We have proposed a dual chaotic encryption algorithm to solve the dynamical degradation problem. An important feature in the analysis of the dynamical systems is system stability, which can be determined using the Lyapunov Exponent (LE). We have computed the LE for the single and dual chaotic maps. We have also investigated the BER for different types of dual and single chaotic maps by employing Chaos Shift Keying (CSK) modulation scheme with Multiple-Input-Multiple-Output (MIMO) communication system under AWGN channel. Simulation results indicate that the single tent map gives acceptable security and superior BER performance as compared to dual tent map which gives the superior security but with relatively lesser BER performance.

Although the chaotic sequences are more secure as compared to PN sequences, they are inferior in terms of bandwidth efficiency and BER performance. In order to overcome this limitation, we have proposed the use of a chaotic modulation schemes in MIMO channels. The BER performance of coherent and non-coherent chaotic modulation schemes combined with 2×1 and 2×2 Alamouti schemes over AWGN channel and Rayleigh fading channel have been evaluated and compared.

Continuing further in our efforts to propose superior communication strategies, we have proposed a concatenated scheme involving the combination of LDPC and MIMO schemes based on chaotic technique. The security and BER performance of this Chaotic-LDPC scheme with two transmit antennas and two receive antennas under various channel models has been evaluated. We have discussed the theory and carried out detailed analysis pertaining to encoding/decoding of chaotic modulation schemes, the use of suitable LDPC codes and MIMO schemes for providing secure and reliable communication over the AWGN channel, the Rayleigh fading channel and the Gamma-Gamma fading channel.

To improve security and reliability with enhanced throughput, we have proposed a Quadrature Chaos Shift Keying (QCSK) modulation scheme with high rate STBC. The bandwidth efficiency of chaos based communication schemes is inferior to that of the traditional communication schemes. To address this problem, we have designed a rate-$\frac{5}{4}$ and rate-$\frac{6}{4}$ full diversity orthogonal STBC for QCSK and 2 transmit antennas and 2 receive antennas. Simulation results indicate that these high rate codes achieve better throughputs in the high SNR region. It is seen that a rate-$\frac{5}{4}$ code achieves a 25% improvement in information rate and -$\frac{6}{4}$ code achieves a 50% improvement in information rate increase compared to the traditional Alamouti scheme for Differential Chaos Shift Keying (DCSK).

To evaluate the performance of these techniques in multi-user environment, we have analyzed and evaluated the anti-jamming performance of CSK in a MIMO channel. The BER performance analysis for three common types of jamming, namely single-tone jamming, pulsed sinusoidal jamming and multi-tone jamming under different levels of noise power over AWGN channel has been derived and evaluated. We have also discussed the design and evaluated the performance of a communication system that combines a MIMO scheme with a chaotic sequence based Direct Sequence Code Division Multiple Access (DS-CDMA) scheme.

In the last part of our work, we have considered the application of the chaotic techniques in the Free-Space Optical (FSO) communication system. The design analysis, simulation and BER performance evaluation of different optical chaotic modulation schemes with MIMO-FSO communication system are presented. Simulations were carried out using available simulators from Rsoft, OPTSIM version 5.2.

The main aim of this work is to assess the feasibility of employing Space-Time Coded chaotic communications over MIMO communication channels (both RF and Optical). Our analyses and simulations show that it is feasible to develop reliable and secure communication systems based on chaotic modulation schemes combined with MIMO

and channel codes. These systems can provide the benefits of information integrity, security and enhanced throughput. It is hoped that the use of tools from chaotic mechanics will enable communication engineers to devise strategies that will allow wide dissemination of wireless services to all of humankind.

Key Words: Chaotic Technique, Wireless Communications, MIMO, LDPC, FSO

Table of Contents

List of Figures

List of Tables

List of Abbreviations

APD	Avalanche Photo Diode
AWGN	Additive White Gaussian Noise
E_b/N_0	Bit Energy to Noise Ratio
BER	Bit Error Rate
BP	Belief Propagation
BPSK	Binary Phase Shift Keying
C	Chaotic
CSK	Chaos Shift Keying
CDSK	Correlation Delay Shift Keying
CDMA	Code Division Multiple Access
CSS	Chaotic Spreading Sequence
CPF	Chebyshev Polynomial Function
CAT	Chaotic Analog Turbo
CG	Coding Gain
CPM	Chaotic Parameter Modulation
DES	Data Encryption Standard
DCSK	Differential Chaos Shift Keying
DS	Direct Sequence
DD	Direct Detection
EOM	Electro-Optical Modulation
FSO	Free Space Optics
FM-DCSK	Frequency Modulation- Differential Chaos Shift Keying
FM-QCSK	Frequency Modulation-Quadrature Chaos Shift Keying
GA	Gaussian Approximation
HRSTBC	High Rate Space Time Block Code
IM	Intensity Modulation
LE	Lyapunov Exponent

LDPC	Low Density Parity Check
LPI	Low Probability of Interception
LLR	Log Likelihood Ratio
LED	Light Emitted Diode
MIMO	Multiple Input Multiple Output
ML	Maximum Likelihood
MMSE	Minimum Mean Square Error
MPPC	Maximum Pic of Periodic Correlation
MPAC	Maximum Pic of Aperiodic Correlation
OPTSIM	Optical Simulator
PN	Pseudo Noise
pdf	Probability Density Function
PLM	Piecewise Linear Map
PMRP	Peak-to-Minimum Power Ratio
QCSK	Quadrature Chaos Shift Keying
QAM	Quadrature Amplitude Modulation
QDCSK	Quadrature Differential Chaos Shift Keying
QOSTBC	Quasi-Orthogonal Space Time Block Code
STBC	Space Time Bloch Code
SNR	Signal-to-Noise Ratio
SS	Spread Spectrum
UWB	Ultra Wideband
WPAN	Wireless Personal Area Network
WLAN	Wireless Local Area Network
ZF	Zero Forcing

List of Notations

β	Spreading Factor
x_n, y_n	Current symbol of the chaotic sequence
n	Number of iteration of chaotic map
x_{n+1}, y_{n+1}	Next symbol of the chaotic sequence
x_0	Initial value of chaotic sequence
e_n	Current error system
e_{n+1}	Next error system
e_0	Initial value of error
u_n	Nonlinear control factor
S_n	Inputted digital code
B	Control factor matrix
p	Control parameter of tent map
X_n	Transmitted signal
X_r	Received Signal
H	Parity check matrix
c	Codeword
N	Codeword length
K	Message length
v_i	Variable nodes
c_i	Check nodes
G	Generator matrix
T_s	Symbol duration
T_c	Chip duration
f	Chaotic map
μ	Control factor of logistic map
δ_0	The change in initial value
λ	Lyapunov exponent
D_{si}	Decision variable
E_b	Bit energy

α	Channel coefficient
W_l	Noise after dispreading and integration
γ_b	Chi-Square distribution
h_{ij}	Channel gain
H	Channel matrix
$erfc$	Complementary error function
I_k	$k \times k$ identity matrix
R	Code rate
$Œ_1$	Energy of transmitted codeword
$Œ_2$	Energy of data
$Œ$	Difference energy
ϰ	Power scaling factor
φ	Optimum rotation angle
P_x	power of chaotic signal
$c_y(t)$	Hilbert transform of chaotic signal
F	Normalized jamming frequency
P_{jam}	Jamming power
P_s	Signal power
ρ	Duty factor
M	Level of digital modulation
N_j	Number of jamming frequency
N_f	Number of frequency in the total bandwidth
θ	Initial phase angle of jamming signal
ζ	Responsively
h_P	Planck's constant $6.6 \times 10^{-34}\,\frac{m^2 Kg}{s}$
η	Quantum efficiency
e	Electron charge $1.6 \times 10^{-19}\,C$
$Q_i(n)$	LFSR sequence
E_i	Data information

CHAPTER 1

INTRODUCTION

1.1 Introduction to Chaotic Techniques

The study and understanding of chaotic phenomenon in nature gained popularity in the minds of the general populace with the publication of "Chaos: Making A New Science", by James Gleick in 1987. Since then, the study of chaotic dynamics has found its way into many fields. Chaotic sequences are very difficult to predict and identify due to the nonperiodic nature and instability of the chaotic sequences [Anjam R. and Maaruf A., 2008].

One very important application has been in the fields of information security and secure communication. This is because systems providing information security and secure communication require features such as the characteristics of internal randomness and sensitive dependence on initial conditions both of which are readily provided by chaotic systems. Chaotic circuits and their applications for secure communications have received a great deal of attention since Pecora and Carroll [1990] proposed a method to synchronize two identical chaotic systems [Jing P, Yanbin Z., Lei N. and Qun D. 2012,].

Generally speaking, the complex dynamics of the process of a chaotic system has following characteristics:

(1) Small change in initial conditions can produce highly dissimilar output sequences. (Highly sensitive dependence on initial conditions).
(2) The largest Lyapunov Exponent is greater than zero;
(3) Chaotic attractor in the phase space is bounded on the whole, but it has a high degree of instability of orbits in the attractors [Wang Y, Wang J and Si F, 2013].

Figure 1.1 illustrates the trace of two chaotic sequences based on an identical chaotic map with a slightly difference in their initial conditions. In this plot, x_n represents the current symbols of the chaotic sequence [Wai T, Francis L and Chi T, 2007]. Note that the blue line represents of one chaotic sequence while the red line represents the trace of the other sequence. Although the difference in initial conditions is very small, it is observed that the two chaotic signals separate rapidly from each other after a short time period. Therefore, by using initial values separated by small amounts, it is possible to produce a large number of chaotic signals.

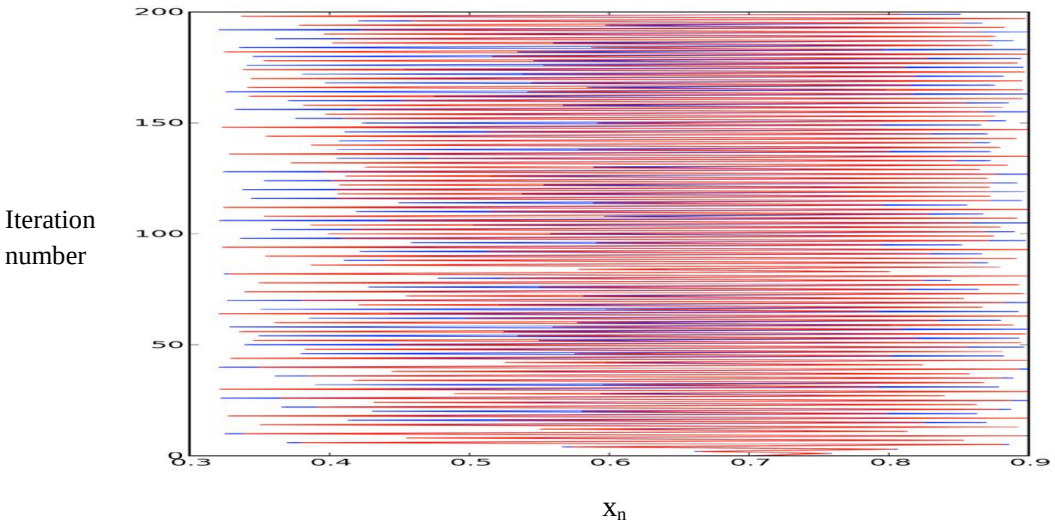

Figure 1.1 Waveforms of two chaotic signals

It is well known that as compared to wired links, wireless links are more prone to hazards like eavesdropping, hacking and external monitoring by unknown entities.

The aim of this thesis is to propose solutions to the problems of enhancing the reliability and security of wireless RF and Optical communication links by employing techniques from Chaos dynamics.

In conventional links, security can be achieved on network layer by implementing various security algorithms such as Data Encryption Standard (DES), triple DES, various key generation and exchange algorithms, etc [Ranjan B. and Amitabha B.,1996]. An alternative method to achieve security is by using orthogonal sequence

for data scrambling on physical layer. Some of the well known sequences that have been employed include Pseudo Noise (PN), Gold and Walsh sequences. The drawback of using these sequences is that they are periodic in nature (however, they can be designed to have very large periods) and can be predicted by observing a long sequence of scrambled data. The use of chaotic sequences has been proposed to overcome this drawback [Stavroulakis P., 2006].

The use of chaotic sequences has the disadvantage that though they are more secure as compared to PN sequences, they are inferior in terms of bandwidth efficiency and (Bit Error Rate) BER performance [Lawrence L, Jia L and Lev T, 2006].

In the light of these facts, the objective of our research work has been to develop various schemes to enhance reliability and security of RF and Optical wireless links by a combination of Chaotic Modulation combined with Space Time Block Codes (STBC) and various channel codes.

Free Space Optical (FSO) communication systems are affected by this trend. Thus, it is necessary to design a technique that can maintain the security of information against unauthorized eavesdroppers as well as protecting information against channel induced perturbations and errors in both Radio Frequency and Optical Wireless communication systems.

Optical Wireless systems have attracted the interest of the academic and Communication Engineering community with inherent advantages such as high bandwidth, low electromagnetic interference, high data rate and ease of deployment. Thus, there is an urgent need to develop techniques well suited to the Optical Wireless Channel in addition to techniques that are designed for conventional RF/ microwave based wireless systems which can secure information against eavesdroppers and channel induced distortion.

In [2006], it was demonstrated by Zhi et.al that a correctly designed wireless communication method which employs chaotic sequences for providing security can

be regarded as being secure. Distinctive features of chaotic signals that make their deployment in wireless systems attractive are robustness against channel induced impairments in multipath environments and resistance to jamming. Chaotic signals are nonperiodic, broadband, and difficult to predict and reconstruct. These are properties which match with requirements for signals used to secure data in wireless communication systems.

1.2 Chaotic Communication Systems; A review

The simple block diagram of chaotic communication system is shown in Figure 1.2. The chaotic modulation technique employed at the transmitter side and synchronization at the receiver side provide good security.

In conventional communication systems, data are transmitted from one point to another by convert a bit sequences to symbols, and convert symbols to sample functions. In a traditional communication system the sample functions passed through the channel are weighted sums of sinusoids waveform; in chaotic communication systems the sample functions which are generated from chaotic attractors are segments of chaotic waveforms. This chaotic sample function for a given symbol is non-periodic and different from one symbol interval to another which represents the principle difference between the chaotic carrier and traditional periodic carrier.

When a sinusoidal carrier is used, the transmitted power is concentrated in narrow band, that way resulting in high power spectral density causing very high attenuation over narrow frequency bands especially in a multipath propagation. In addition, because of high transmitted power spectral density, the probability of interception in narrow band communications is high and cause high levels of interference with other users.

These difficulties can be overcome by using spread spectrum communications, which uses pseudorandom spreading sequences. The drawbacks of these sequences are: it is not possible to achieve synchronization under poor propagation conditions. In

addition, these the pseudorandom sequences required additional circuitry in spreading and dispreading processing.

The difficulties summarized above can be overcome by using chaotic signals which characterized by a wideband signals that can be generated using very simple circuitry. [Geza K., Michael K. and Leon C., 1997, Geza K., Michael K. and Leon C., 1998].

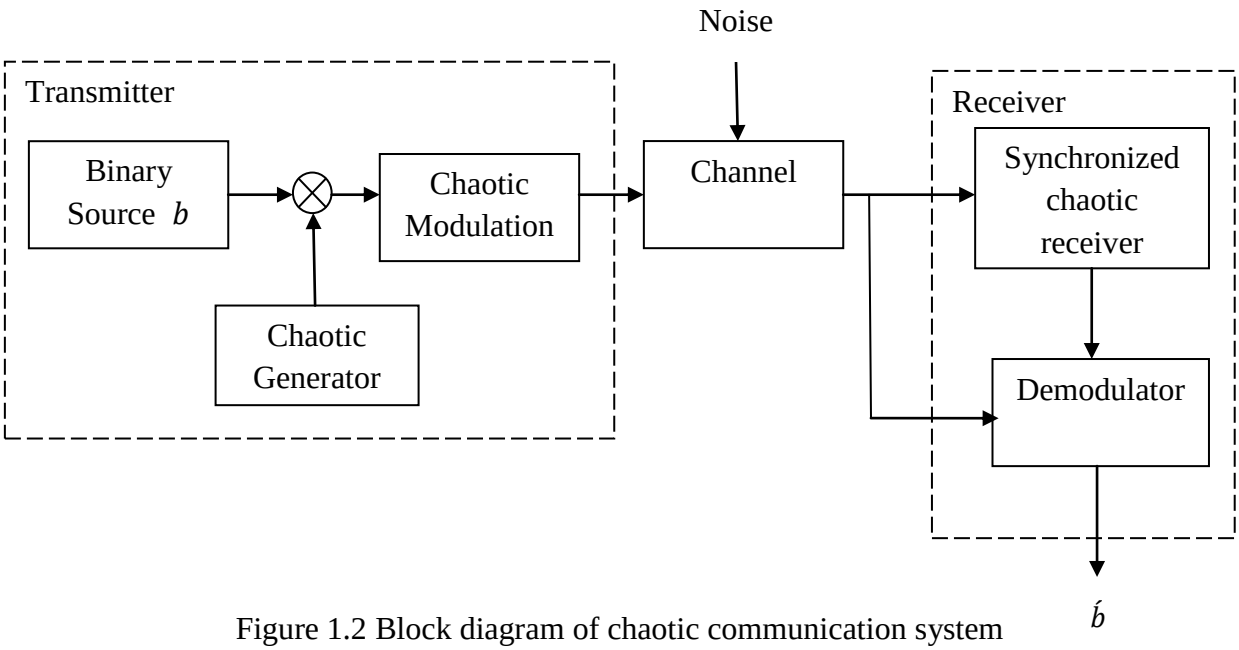

Figure 1.2 Block diagram of chaotic communication system

The interest of the Communication Engineering community to this field dates back to the work of Pecora and Carroll [Pecora M. and Carroll L., 1990] who investigated the linking of two chaotic systems with common signals. It has been shown that when the sign of Lyapunov exponents for the subsystems are all negative, the system will synchronize. It has been found that the synchronization appears to be structurally stable.

These ideas have been applied to several well-known systems (e.g. Lorenz and Rossler) as well as to the construction of physical set of chaotic synchronization circuits. In [1993], Frey D. proposed a method to use chaotic signals in the digital domain for secure communications. The method used a nonlinear digital filter with finite precision (8 bits) in conjunction with inverse filter to implement an encoder and

decoder respectively. Jaijin L. and Douglas W. [1995] investigated a secure communication scheme using chaotic system. This system employed a noise reduction method which reduces the dynamical error. It was further realized that this system did not require synchronization of the receiver to the transmitter and was robust against channel induced noise.

In the year [2000], Jianmeng Z. and Shuqing W. Presented a method to use chaotic signals in the digital domain for secure communications. This method uses a well-trained multilayer neural network to generate the chaotic sequence whose randomness properties are excellent. It was demonstrated that this method has good immunity to interference and can be implemented easily. Thus they concluded that a chaotic secure communication system based on neural network can be designed to be robust with respect to information security considerations.

In [2002], Zhong presented a new technique to transmit and receive an information-bearing signal by employing chaotic systems. In contrast to existing systems characterized by the use of one transmission line, a two channel transmission method was proposed. It was demonstrated that this technique had the advantage of faster synchronization and higher security. In [2004], Guopeng T. et al has been proposed a secure communication system based on symbolic dynamics. The masked message sequence was tracked with a symbolic sequence generated by another tent map. It was concluded that this algorithm had many desired properties such as high speed, ease simple implementation and high security. In [2005], Safwan and Chadi proposed a secure spread spectrum communication system, using chaotic spreading sequences and also developed a digital chaotic codec. Zhi D. et al in [2006] presented a secure communication method based on chaotic synchronization. This scheme has the characteristics of simple design, fast synchronization speed and high security.

Hang K. and The L. [2009] proposed a scheme that improved the security and accuracy of transmitted information that proposed a new wireless communication structure based on three coupled chaotic systems. The performance of this scheme including the calculation of BER as a function of SNR in the AWGN channel has

been verified. Li. F. and Gang Z., [2010] investigated a chaotic secure communication scheme based on Logistic map. The synchronization method was based on nonlinear control by Logistic map. It has been found that with this method, the system synchronization can always be achieved with just a single iteration.

Stamatios V. [2010] studied the security vulnerabilities of FSO links by using chaos (logistic map). In [2012], Chi C. and Chao C. developed a robust synchronization scheme for two different chaotic systems exposed to bounded noise. It was shown that decryption attempts using a slightly incorrect key failed and recovery of the original message was not possible.

In addition to using chaos sequences to enhance information security, many researchers have attempted to design digital communication systems similar to phase modulation schemes (PSK) by employing the idea of chaotic modulation. In [1996], Ling C. and Sun S. proposed coherent demodulation of Chaos Shift Keying (CSK) using Lorenz-based chaotic circuits. They have proposed a simple solution to the synchronization problem and the allowable bit rate has been assessed.

In [1996], Liu J. et al presented a chaotic secure communication via CSK modulation using a receiver with feedback control. The transmitter and receiver have been built with Chua's circuits. Henry L. and Jennifer L. [1997] proposed chaotic modulation for Spread Spectrum (SS) and Code Division Multiple Access (CDMA) communication. The demodulation of this communication scheme has been built using an adaptive filter. It has been found that an adaptive filter can reduce the effect of channel noise. Geza K. et al [1998] combined the Differential Chaos Shift Keying (DCSK) technique with frequency modulation (FM) in order to improve the BER performance of DCSK and keep the bit energy constant.
In [2001], Chris W. addressed the issues of communicating over radio channel with continuous time chaotic signal with synchronized and non-synchronized methods. He proposed models for radio channels (which included modeling of multipath and Doppler effects).

In [2001] Liu J. et al studied chaotic optical-communication systems using semiconductor lasers. The dynamics, synchronization, message encoding and decoding have been modeled and studied numerically and experimentally for two systems based on optical injection and delayed optoelectronic feedback of semiconductor lasers in an autonomous nonlinear system with three dynamic variables. In [2002], Zakria N. et al presented a new approach for the design of DS-CDMA signal by performing modulation using CSK. The chaotic generator was based on Lorenz system which was modified in order to control the amplitude and frequency of the chaotic signal as well as provide synchronization between the receiver and transmitter. The results have indicated that the receiver can recover the transmitted information without any degradation and with high security. In [2002], Wang J. and Xu Z. proposed a new version of DCSK which can double the data rate without an increase in complexity of the chaotic communication system. In [2004], Ji Y. discussed the effect of the chaotic map employed in CSK communication systems. He has deduced the conditions to be satisfied for an optimal map. In addition, he has also presented simulation results using the optimal map and has compared these with those obtained by the use of commonly used chaotic maps. The design of both coherent and non-coherent CSK systems, with spreading factor of two, has been presented. In [2005], Yuu S. and Zahir H. investigated an approach in CSK for secure communication systems. Two different chaotic maps namely logistic map and modified logistic map for chaos shift keying modulation scheme has been proposed in this study. Additional control parameters have been provided to increase the randomness of chaotic behavior. In [2006] Guangyi W. et al investigated the BER performance analysis of chaos shift keying modulation scheme in noisy multiuser environment. The Logistic map was used to provide the discrete chaos generator. The BER in terms of signal-to-noise ratio has been derived. In [2007], Kaddoum G.et al studied the coherent reception of DS-CDMA by using chaotic sequences in the place of conventional PN spreading code. A Piecewise Linear Map (PLM) has been used as Chaotic Spreading Sequence (CSS). An analytical expression of the bit error rate in the single user case was presented. In [2008], Zhibo Z. et al employed an exact method to analyze the BER performance of DCSK communication system over fading channels. The exact BER performance of DCSK in Nakagami-m, Rayleigh and

Rician fading channels was studied. Gaussian Approximation (GA) method has been compared with the exact method. Jiamin P. and He Z. in [2009] investigated an enhanced chaos shift keying which they named as FM-QACSK. They concluded that this scheme improves the speed of chaos shift keying and its noise performance is better than other chaotic communication systems, such as DCSK and QDCSK. In the same year, Songsheng Z. et al [2009] presented the design of a QDCSK communication system. The scheme is developed from M-ary phase shift keying and Quadrature Chaos Shift Keying (QCSK). This scheme combines the advantages of and characteristics of chaotic communication systems with higher efficiency of bandwidth usage and transmitting speed. In [2010], Chunyan H. and Fenguan M. used a simple and effective approach for analyzing the multiuser performance of coherent CSK system in the presence of noise. They have provided a quantitative description of the performance of multi-user chaos based communications in the presence of noise. Using Logistic map as the chaotic signal generator and assuming ideal synchronization at receiver, the BER of CSK has been derived in term of noise intensity. Long M., Chen Y. and Peng F., [2012] improved the BER of CSK for an AWGN by applying trimming operation to the Chebyshev polynomial function of order 2 and the piecewise linear map to make the input source possess a distribution which is more Gaussian. Numerical results show that the proposed method can achieve performance gains of up to 3.5 dB in signal-to-noise ratio over the conventional method without trimming.

Yuu L. et al [2005] showed that the use of CSK with a transmit diversity technique such as beamforming and space-time coding can provide a secure communication link with improvement in the system performance. Zheng G. et al [2008] investigated the problem of secure communication based on Multiple Input Multiple Output (MIMO) chaotic systems. The proposed scheme also has been improved into an amplitude independent one. Huanfei M. and Haibin K. [2009] investigated the feasibility of using chaotic communications in MIMO channel. DCSK modulation has been chosen as a bench mark and Alamouti space-time code scheme has been used for the 2 transmit and 2 receiver antennas wireless system. Based on the evaluation of system performance, improvements have been also discussed. Jose L. and Sebastien R.

[2010] presented a technique that provides spatial diversity for a CSK transceiver. It has been found that the MIMO systems greatly improve the BER performance of a chaotic communications over the Rayleigh channel. Shilian W. and Xiaodong W. [2010] investigated M-DCSK in MIMO wireless multipath fading channels. Two transceiver systems which require no channel state information either at transmitter or at receiver have been proposed. The first system employs a distinct chaotic signal at each transmit antenna and the second scheme employs a single chaotic spreading sequence and make use of adaptive transmit and receive beamforming. It has been concluded that the both schemes can effectively exploit the spatial diversity of the underlying MIMO system and that the adaptive beamforming scheme significantly outperforms the ominidirectional transmission. Eiji O. in [2011] presented a chaos MIMO transmission scheme to achieve secure on physical layer, low-error rate, and low complexity transmission. The joint MIMO detection and chaos decoding have been done by Maximum Likelihood Decoding (MLD) at the receiver. The Bernoulli shift map has been used to generate the chaotic sequence. Kaddoum G. et al [2011] investigated the performance of CSK in MIMO communications systems using second-order Chebyshev Polynomial Function (CPF) as a chaotic generator. An Alamouti space-time code scheme has been combined with CSK system for two transmit - two receive antennas. Kaddoum G. et al [2011] analyzed the performance of DCSK communications in MIMO system. The Alamouti space-time code for 2 transmitter and 2 receiver antennas has been used to improve the performance of such system. A new approach for computing the BER performance has been provided and the analytical BER expression has been derived. Pingping C., Lin and W. Francis L., [2013] have been proposed an analog STBC-DCSK scheme. The proposed scheme can suppress the inter-transmit-antenna interference in order to recover the transmitted information and to achieve the full diversity. Yi F., Jing X. and Guanrong C., [2013] have been proposed a multi-access MIMO relay DCSK cooperative diversity system. It has been show that the proposed system stands out as a good candidate or alternative for energy-constrained wireless communications based on chaotic modulation, especially for low-low-power and low-cost WPANs.

Zakira et. al [2002] have presented a new approach for the design of DS-CDMA signal by performing modulation using CSK. In this study, the chaotic generator was based on Lorenz system which was modified in order to control the amplitude and frequency of the chaotic signal as well as provide synchronization between the receiver and transmitter. The results have indicated that with this scheme, the receiver is able to recover fully the transmitted information without any degradation and with high security. Soobul et. al [2002] have investigated a chaotic code and its performance compared with conventional PN sequences in an AWGN and Rayleigh fading channel. Kaddoum et. al [2007] have studied the coherent reception of DS-CDMA in SISO system by using chaotic sequences in the place of conventional PN spreading code. A Piecewise Linear Map (PLM) has been used as chaotic Spreading Sequence (CSS). An analytical expression of the bit error rate in the single user case has been presented. Cherni et. al [2011] have highlighted the role of the spread spectrum sequence on the performance of the CDMA MIMO system. They considered a family of sequences generated by nonlinear system selected according to criteria Maximum `Pic' of Periodic Correlation (MPPC) and Maximum `Pic' of Aperiodic Correlation (MPAC) correlation. They showed that the use of these sequences improves the performance of conventional receiver.

Martin H. and Thomas S. [2002] analyzed the potential of chaos in digital communication using the AWGN channel model. An example using the Bernoulli shift map has been presented to illustrate the fact that the use of chaotic piecewise linear maps has no systematic negative effect for digital communication applications.

In [2003], Thomas and Martin examined the use of chaotic system based on the iteration of 1-D and 2-D piecewise linear chaotic maps in a coded modulation scheme.

The transmitted information was imposed on the chaotic system by a small perturbation control method. Lin W. and Guanrong C. in [2004] enhanced the performance of FM-DCSK using LDPC codes. Through system design and simulation it has been shown that the enhanced system is superior to that without LDPC codes by

at least 8 dB over AWGN channel. Moreover, it has been concluded that the longer the frame, the greater its coding gain.

Kai X. et al. [2009] proposed a novel construction of analog codes based on nonlinear chaotic dynamical systems in general and the tent map in particular. The proposed construction exploits useful ideas of interleaving and parallel concatenation from classical coding theory to protect symbolic coding and subsequently chaotic state. The resultant new codes have been labeled as Chaotic Analog Turbo (CAT) codes. Kwok W. et al [2010] studied a simultaneous arithmetic coding and encryption scheme in which the chaotic map model for arithmetic coding has been determined by a secret key and keeps changing. The compressed sequence has been masked by a pseudorandom key stream generated by another chaotic map. This two-level protection enhances its security level, which results in high key and plaintext sensitivity.

Sushanta D. [2006] et al. have proposed a scheme employing two transmit antennas by enlarging the set of signals used in Alamouti code by applying constellation power scaling and constellation of rotation. This scheme has the advantage that a low-complexity ML decoding algorithm can be used for decoding. Duy N. et al. [2008] constructed a rate 6/4 full-diversity STBC for QPSK and 2 transmit antennas by applying constellation scaling and rotation to the set of quaternions used in Alamouti code. Also a rate-9/8 full diversity QOSTBC for 4 transmit antennas has been given.

Mihir M. et al. in [2011] considered space–time block coding, for communication over Rayleigh fading channels using multiple transmit antennas.

Shilian W., Jiang Z. and Jie Z., [2012] have been proposed non-coherent chaotic communication system with Low Probability of Intercept (LPI) based on OFDM. It has been shown that the proposed scheme outperforms DCSK under AWGN with high bandwidth efficiency.

1.3 Organization of the Thesis

This research work presented in this thesis has been organized as follows. In Chapter 2 of the thesis we have discussed the technique used to maintain synchronization between the transmitter and receiver and the performance enhancement resulting from the use of Low Density Parity Check (LDPC) channel codes. In addition, this chapter of the thesis discusses the security enhancement obtained by the use of dual maps, their Lyapunov exponent and the corresponding BER performances implementing 2×2 Alamouti schemes.

In chapter 3 we have shown that various chaotic modulation schemes like CSK, DCSK and CDSK enhance security but suffer from BER degradation. To counteract this problem we propose the use of MIMO techniques of various orders. In particular, we have considered the use of Alamouti 2×1 and 2×2 schemes. Further, a comparison is made between various chaotic modulation schemes implementing various Alamouti techniques in term of BER under Rayleigh fading channel and AWGN.

Detection schemes can be categorized into coherent and non-coherent types. In coherent detection, (employed in CSK systems), the receiver has to reproduce the same chaotic carrier which has been used to carry the information through the process known as chaos synchronization. This can be difficult to achieve in practice. In non-coherent systems, however, the chaotic carrier does not need to be generated at the receiver. Usually, non-coherent (DCSK and Correlation Delay Shift Keying (CDSK)) detection makes use of some distinguishable properties of the transmitted signals, which can be some inherent deterministic properties, or fabricated by a suitable bit arrangement, or some statistical properties [Francis L., Chi T., Ming Y. and Sau H., 2004]. So, non-coherent communication schemes, which do not require the reproduction of the chaotic signals at the receiving end, are more feasible in practice [Wai T, Francis L., and Chi T., 2006].

In this chapter, we have compared the performance of coherent and non-coherent Chaotic communication systems over AWGN and Rayleigh fading channels.

In Chapter 4 of the thesis, we have taken into consideration the use of regular and irregular LDPC codes for enhancing information integrity in Chaos modulated communication systems. We have compared the performance of chaotic systems implementing regular and irregular LDPC codes, 2×2 MIMO techniques in terms of BER performance.

In chapter 5 of the thesis, we discuss the drawbacks of low bandwidth efficiency in chaotic systems and suggest solutions for this problem. We conclude that the use of QCSK modulation technique and higher rate STBC schemes can increase the effective throughput. Unlike DCSK which divides symbol period into two parts for one data bit (symbol), QCSK divides the symbol period into four parts for two bit data without increasing in spreading factor (β). The thesis proposes the use of high rate STBC like rate-$\frac{5}{4}$ and rate-$\frac{6}{4}$ to further increase the effective throughput.

A wireless communication system is always prone to jamming signals hampering the expected performance of the system. So, in chapter 6 of the thesis, we have studied the performance of CSK schemes under the influence of a strong jamming signal along with AWGN noise. We have considered three different types of jamming in our study, that is, sinusoidal jamming, pulse sinusoidal jamming and multi-tone jamming. The BER performance of CSK-MIMO (2×1 and 2×2 Alamouti schemes) system is analyzed in the presence of jamming signals and the robustness of the system against jamming has been quantified.

In CDMA applications, PN sequences have been conventionally used for spreading scrambling and authentication. In Chapter 7 of the thesis, we propose the use of chaotic sequences instead of PN sequences and illustrate the BER performance of the systems under Rayleigh fading and Gamma-Gamma fading channel conditions.

The BER performance enhancement by using Alamouti MIMO techniques (2×1 and 2×2) is discussed and comparison between various chaotic maps is made. In addition, we have also considered the effect of reduction of spreading factor to $\beta = 10$ from $\beta = 64$ for conventional CDMA systems. The effect of the number of users in a cell on the BER performance is discussed for both CSK-CDMA-SISO and CSK-CDMA-MIMO systems.

In Chapter 8, we have proposed the use of chaotic techniques to enhance the security of FSO systems. The BER degradation due to the use of chaotic techniques is resolved by using optical MIMO schemes. This arrangement has the advantage of minimizing BER degradation while maintaining information security.

We conclude the thesis in Chapter 9 by summarizing the obtained results, and giving directions for further research work in this area.

CHAPTER 2

CHAOTIC SECURE COMMUNICATION SYSTEMS BASED ON CHAOTIC MAPS

2.1 Introduction

The majority of efficient communication systems are coherent systems. Such systems require synchronization between the clock signals (equivalently oscillators) at the transmitter and receiver. This is especially true of digital communication systems, spread spectrum systems and systems designed to protect the integrity or security of information during its passage over the channel. The requirement that the generating chaotic signal and the local version generated at the receiver be perfectly synchronized is an essential requirement for chaotic communication systems as well.
In this chapter, we shall discuss the design of a scheme for synchronizing the chaotic generators at the transmitter and receiver and then discuss the design of secure communication systems based on chaotic maps. In the first part of this chapter, we have discussed the master-slave concept of chaotic system synchronization. A method of designing and deriving nonlinear control factor for the synchronization of the chaotic map master-slave system has been presented. The general approach to master-slave chaotic map synchronization is demonstrated on the one dimensional chaotic tent map. Jovic and Unsworth [2010] have demonstrated that synchronization can be achieved and maintained in a chaotic system employing spreading factor $\beta = 400$ in the absence of noise. In this thesis, we have demonstrated the synchronization of noiseless system with spreading factor $\beta = 250$. While this constitutes an improvement on the earlier system, it is found that it cannot achieve synchronization in the presence of noise. In addition, synchronization has been achieved with a relatively high value of spreading factor. Since the principle source of error in a digital communication system is the channel, quantifying the performance of a chaotic modulation technique by assuming an ideal channel will not be accurate. A realistic

channel model must at least include Additive White Gaussian Noise (AWGN). Chaotic synchronization is greatly limited by its sensitivity to noise.

Even small amounts of noise added to the synchronizing signal can degrade synchronization quality and it might not be possible to reconstruct the original chaotic signal at the receiver. To overcome these difficulties, we have suggested the use of LDPC error correcting code in the system to reinforce the ability of the system resist noise and thus facilitate the synchronization between master and slave systems in presence of AWGN. In addition, it is shown that this scheme allows synchronization can be achieved even when the spreading factor is decreased to low values ($\beta = 4$). Low values of β are helpful in the maintenance of chaotic properties. Large value of spreading factor leads to loss of chaotic signal properties such as non-periodicity [Kaddoum G., Mai V. and Francois G., 2011]. In the second part of this chapter, we have discussed the design and performance of dual chaotic system encryption algorithm which is a stream cipher algorithm employing two chaotic maps with different system parameters and different initial conditions. This gives additional flexibility to the designer to create more complex chaotic signals which can resist strong eavesdropper attacks. While single chaotic systems are simple to generate, they are realized with limited precision and this can lead to dynamical degradation of the original system [Yi C, Li Z. and Yifang W., 2010]. To solve the dynamical degradation problem, we have introduced a new kind of dual chaotic encryption algorithm. In the analysis of the dynamical system an important feature is the system stability, which can be determined using the Lyapunov Exponent (LE). In this chapter, we have performed numerical computation of the LE for the single and dual chaotic maps.

Contributions of the thesis in Chapter 2:

- Demonstrate that coherent chaotic communications systems can be practically designed and deployed by devising techniques to achieve synchronization between transmitter and receiver.

- Evaluate the security of single and dual chaotic maps and compute their Lyapunov Exponent (LE).

2.2 Communication System Employing Chaotic Map with LDPC Codes and Master-Slave Synchronization

It is well known that keeping information secure via wireless access is difficult, for while the wireless information is being broadcast, any person equipped with a suitable receiver can intercept information from wireless transmission in the local area. Further, it is hard to discover such interceptions. So security of wireless transmission is very important. Chaotic systems are characterized by sensitive dependence on initial conditions. It is seen that the trace of a chaotic system appears to be completely random, making the chaotic signals appear to be unpredictable. This creates a strong ability of intercepting avoidance and capture for a longer period time. So, it is said that the wireless communication method based on chaotic system is a secure communication scheme [Zhi D., Bing W. and Peng L, 2006]. Since the synchronization in the scheme proposed by Jovic and Umsowrth [2010] cannot be maintained when the spreading factor is less than 400 (large values of spreading factor are detrimental to preservation of chaotic signal properties), one of the problems addressed in this thesis is to device schemes which can achieve and maintain synchronization with a reduced value of spreading factor. This necessitates the use of a suitable channel code. We have used LDPC codes in this thesis. The various issues pertaining to the design of robust chaotic communication systems in the presence of AWGN are discussed and addressed in the remaining part of this chapter.

2.2.1 Synchronization of Chaotic Map

In this section a theorem for the design of nonlinear controllers [Jovic B., 2011] for the chaotic map master –slave system is presented.

Theorem:

Let, e_n, and e_{n+1}, (where $e_n = y_n - x_n$) represent the system errors associated with current and next state A_n and U_n respectively.

Suppose:

$$e_{n+1} = A_n e_n + U_n e_n, \forall n \geq 0, |eig(A_n + U_n)| = |eig(B)| < 1. \quad (2.1)$$

Then: $\|e_n\| \to 0$, as $n \to \infty$, $\forall e_0 \in R^n$.

Notation: $|\ \ |$ denotes the magnitude of the Eigen values of matrix while brackets $\|\ \ \|$ denote the Euclidean norm.

This theorem states that the equilibrium 0, of the error system e_{n+1}, is globally asymptotically stable if and only if all eigenvalues of $B = A_n + U_n$ have magnitude less than one. A special case of interest is stated below.

Special case: If the matrix B is a function of n, then the condition that $\|B_{n+1} - B_n\|$ remains bounded must also be satisfied.

Proof of special case:

Since

$$e_{n+1} = B_n e_n \quad (2.2)$$

Then $e_{n+2} = B_{n+1} e_{n+1} \to e_{n+2} = B_{n+1} B_n e_n \to e_{n+i} = B_{n+i} B_{n+(i-1)} \dots B_n e_n, \forall i > 1$

To ensure that the system represented by equation (2.1) remains bounded it must be ensured that all the matrix components of $B_{n+i} B_{n+(i-1)} \dots B_n e_n$ remain bounded, that is, the condition that $\|B_{n+1} - B_n\|$ remains bounded, must be satisfied.

2.2.2 System Structure

In this section, we have discussed the design procedure of the synchronizing nonlinear control factor for master-slave synchronization of the chaotic tent map. Tent map has been chosen because of the simplicity in terms of generating chaotic sequences. The mapping has a constant coefficient p, referred to as the peak value.

This is the point at which the dependent variable reaches its maximum output value.

The dynamics of the tent map is defined by,

$$x_{n+1} = \begin{cases} \frac{x_n}{p}, & x_n < p \\ \frac{1-x_n}{1-p}, & x_n \geq p \end{cases} \quad (2.3)$$

In equation (2.3), x_n and x_{n+1} represent the current and next symbols of the chaotic sequence respectively and p represents the control parameter of the chaotic tent map [Mozsary A., Azzinari L., Krol K. and Porra V., 2001].

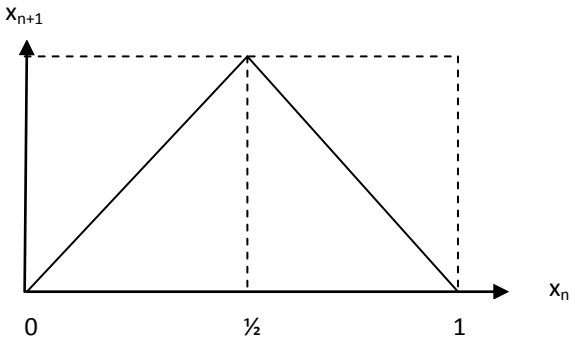

Figure 2.1 The dynamic (input-output) relationship of the tent map

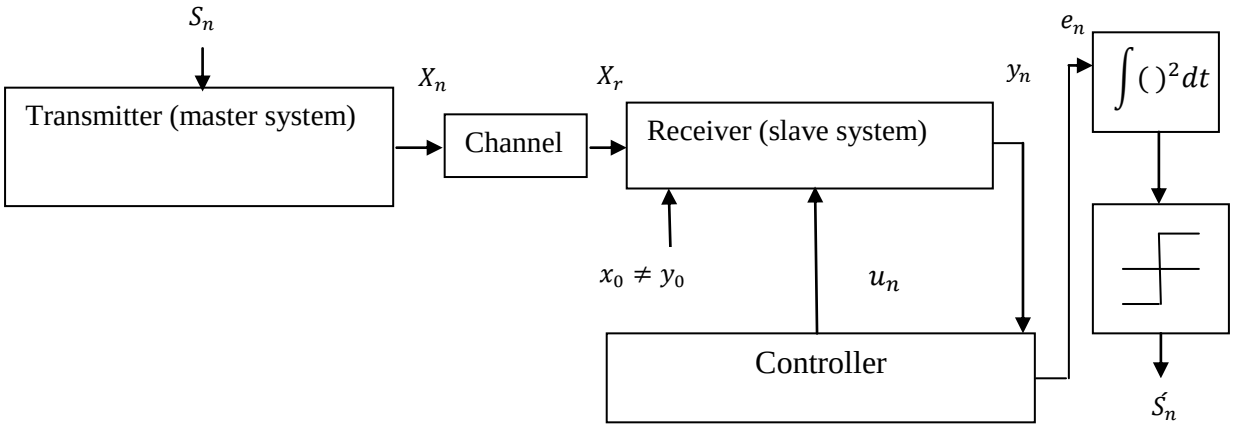

Figure 2.2 Chaotic map communication system based on parameter modulation concept (first proposed by Jovic [2010]).

Where in Figure 2.2, u_n is the nonlinear control factor.

At the transmitter

$$x_{n+1} = \begin{cases} \frac{x_n}{p+0.1S_n}, & x_n < p \\ \frac{1-x_n}{1-(p+0.1S_n)}, & x_n \geq p \end{cases} \quad (2.4)$$

where S_n is input digital symbol (code) which can take on two values 0 and 1.

At the receiver,

$$y_{n+1} = \begin{cases} \frac{y_n}{p} + u_n & y_n < p \\ \frac{1-y_n}{1-p} + u_n, & y_n \geq p \end{cases} \quad (2.5)$$

y_n and x_n can be synchronized by nonlinear control factor.

The error between y_n and x_n is

$$e_n = y_n - x_n \quad (2.6)$$

Design of nonlinear control factor u_n for the chaotic tent map

For $y_n, x_n < p$, assuming $S_n = 0$,

$e_{n+1} = \frac{y_n}{p} - \frac{x_n}{p} + u_n = \frac{y_n - x_n}{p} + u_n = \frac{e_n}{p} + u_n$

e_{n+1} denotes the error between the chaotic sequence at the transmitter and chaotic sequence generated at the receiver. This error is due to the loss of synchronization between receiver and the transmitter. u_n is the control factor which we add to achieve synchronization or force synchronization. In order to achieve synchronization, e_{n+1} should be zero.

$e_{n+1} = A_n e_n + U_n e_n$ ([From equation (2.3)])

then

$e_{n+1} = \frac{e_n}{p} + U_n e_n$

$A_n = \frac{1}{p},\ u_n = U_n e_n$

and

$B = A_n + U_n$

Then

$B = \frac{1}{p} + U_n$

$U_n = B - \frac{1}{p}, \qquad -1 < B < 1$

Then

$U_n = -\frac{1}{p}$

$u_n = U_n e_n$

$$u_n = \frac{-e_n}{p} \tag{2.7}$$

For $y_n, x_n > p$,

$e_{n+1} = \frac{1-y_n}{1-p} - \frac{1-x_n}{1-p} + u_n = \frac{x_n - y_n}{p} + u_n = \frac{-e_n}{1-p} + u_n$

But

$e_{n+1} = A_n e_n + U_n e_n$

$A_n = \frac{-1}{1-p},\ u_n = U_n e_n$

$B = A_n + U_n$

$U_n = B - (\frac{-1}{1-p}),$ $\quad -1 < B < 1$

$U_n = \frac{1}{1-p}$

$$u_n = \frac{e_n}{1-p} \tag{2.8}$$

$S_n = 0$ represents bit 0

$S_n = 1$ represents bit 1

So synchronization at the receiver can be achieved when 0 is transmitted, while a-synchronization occurs when transmitting signal is 1.

A series often bits that are transmitted are shown in Figure 2.3. The corresponding transmitted sequence X_n is shown in Figure 2.4. Figure 2.5 shows the corresponding squared synchronization error e_n^2 under noiseless conditions. The received bits are detected by squaring and integrating the error e_n. The output of the integrator is then compared to the predetermined threshold and the decision is made whether a bit 0 or bit 1 was sent. Figure 2.6 shows the detected signal which is matched to S_n.

In Figure 2.2, a spreading factor $\beta = 250$ has been used to represent one bit. Note that the spreading factor is the number of chips associated with each bit interval. This value of spreading factor is very high.

The use of high values of spreading factor β results in the sequence losing some characteristics of chaotic behavior. So we have suggested a new secure communication scheme based on synchronization of chaotic tent map master-slave system corrupted by AWGN with spreading factor ($\beta = 4$) which employs a LDPC error correcting code.

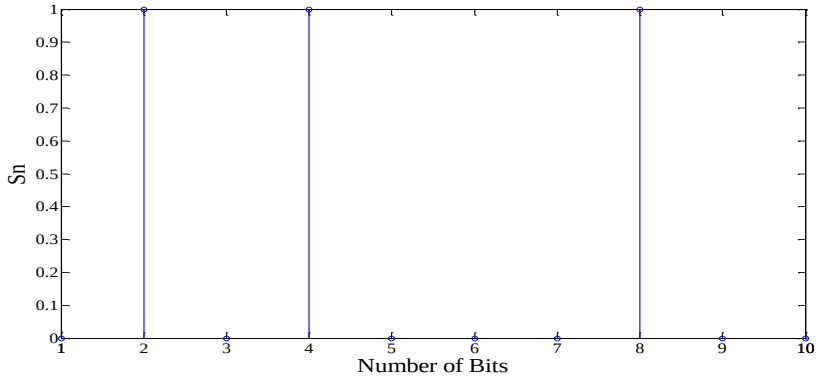

Figure 2.3 The input signal

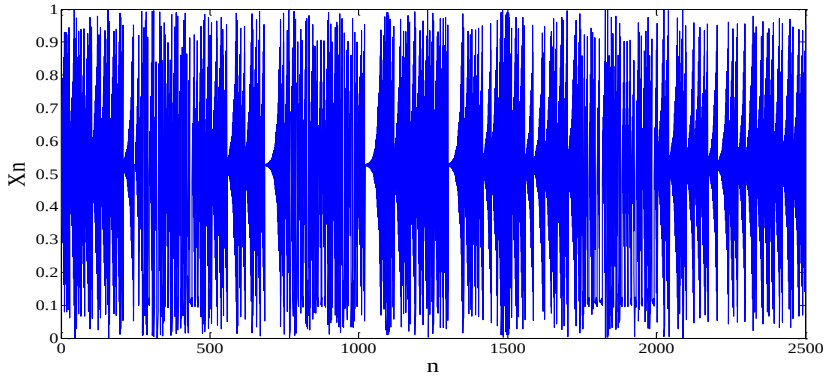

.Figure 2.4 The transmitted signal X_n

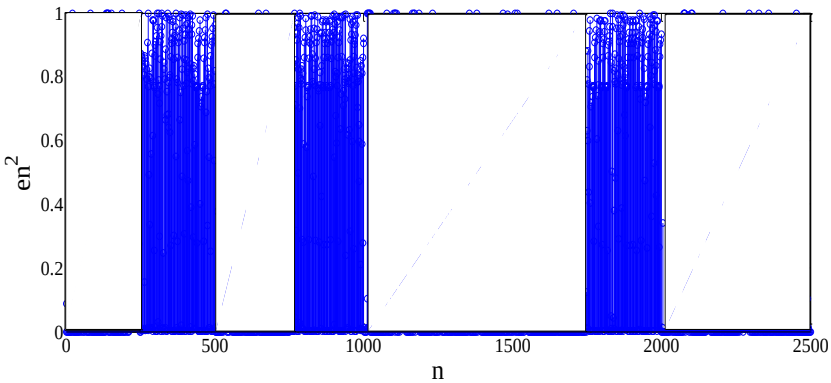

Figure 2.5 Squared synchronized error e_n^2

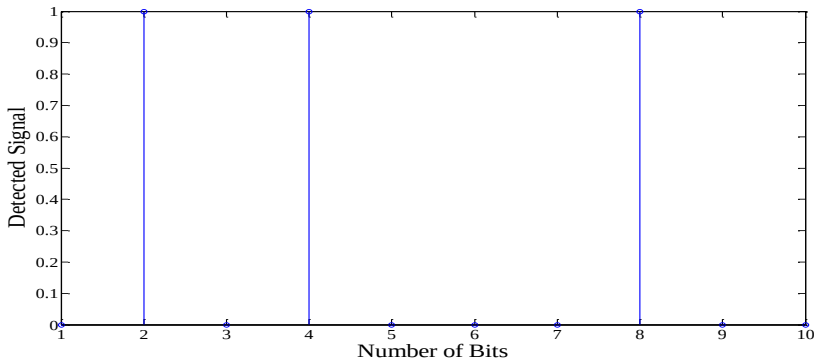

Figure 2.6 The detected signal

2.2.3 Representation of LDPC Codes

The simplest LDPC code is a binary linear block code that can be denoted as (N, w_c, w_r) where N is the code length, w_c is the column weight (i.e., the number of nonzero elements in a column of the parity-check matrix), and w_r is the row weight (i.e., the number of nonzero elements in a row of the parity check matrix). For regular LDPC codes, w_c and w_r remain invariant for all columns and rows, while for irregular ones, w_c and $w_r$may vary for different columns and rows. All LDPC codes, must satisfy

$$\mathbf{H}.\underline{c} = 0 \tag{2.9}$$

where $\underline{c}$ is a codeword and **H** is a sparse (i.e., most elements are zero elements) parity-check matrix. It is the sparseness of **H** that guarantees the low computing complexity. Suppose there are K source bits in each N-bit codeword. Then **H** is a matrix with $(N - K)$ rows, each denoting one check, and N columns, each denoting one bit. Each bit in **H** participates in $w_c$checks while each check involves $w_r$bits [Zongjie T Shiyong Z., 2007].

Tanner graphs, which are essentially bipartite graphs, can be used to represent LDPC Codes. The nodes in a Tanner graph fall into two categories: variable nodes, each representing one column of the parity-check matrix, and check nodes, each representing one row of the parity-check matrix. If each N-bit codeword contains K

source bits, as is the case for the simplest LDPC code mentioned earlier, there will be N variable nodes and $(N-K)$ check nodes in the Tanner graph. An edge will be present between variable node *j* and check node *i* if the corresponding element in the parity-check matrix **H,** $\mathbf{h_{ij}}$, is nonzero. It is apparent that there is at most one edge between a variable node and a check node. When the edge does exist, the variable node and the check node are adjacent to each other. A typical Tanner graph is illustrated in Figure 2.7. In the decoding procedures, belief (i.e. message) is propagated along edges between variable nodes and check nodes.

MacKay, et al. [1999] discovered that cycles, especially short ones, tended to degrade decoding performance of LDPC codes. Therefore, it is of pivotal importance that short cycles be avoided in the construction of LDPC codes.

The decoding of LDPC codes is usually performed using iterative decoding. Optimum performance is achieved by the use of sum-product algorithm (or Belief Propagation (BP) algorithm) with soft-decision decoding. The process of decoding works as follows:

- Initialization: Set the maximum number of iterations, and initialize log-likelihood ratios (LLR's) sent from the check node to variable node and the LLR sent from the variable node to check node respectively based on modulation technique in use and probabilistic characteristics of noise on the channel.
- Calculating iterative the message from bit to check which is the sum of the sum-product algorithm
- Calculating iteratively the message from check to bit which is product of sum-product algorithm.
- Calculating the posterior probability of bits;
- Making a decision (estimate of the transmitted bit) [Sae C., Daived G., Thomas R. and Rudiger U, 2001, Zongjie T, Shiyong Z., 2007].

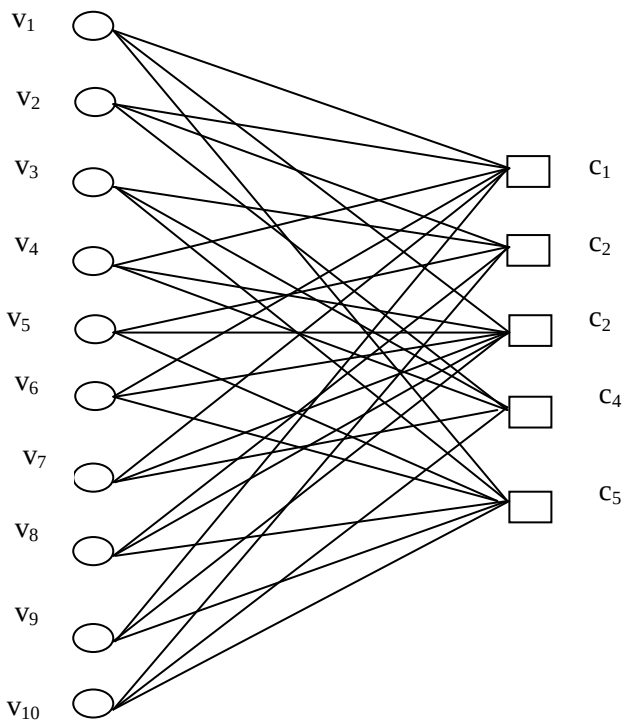

Figure 2.7 A typical Tanner Graph

2.2.4 Communication System Based on Synchronization of Chaotic-LDPC Master-Slave under AWGN

The system proposed by us is illustrated in Figure 2.8.

Figure 2.9 shows the chaotic sequences at the transmitter and receiver. It can be observed that even with $\beta = 4$, the two signal plots closely overlap each other and synchronization can be achieved. We found that whenever the synchronization is lost, the proposed synchronization technique regains the synchronization within a time period of 2 chip samples ($2T_c$). Thus, in this technique, synchronization can be achieved and maintained with a very small spreading factor ($\beta = 4$) as compared to the work described in [Jovic B. and Unsowrth C. P., 2010] which employs a spreading factor of $\beta = 400$. Hence the proposed technique has lesser complexity in chaotic modulation block which partially compensates for increase in complexity due to the addition of block comprising of LDPC encoder/ decoder.

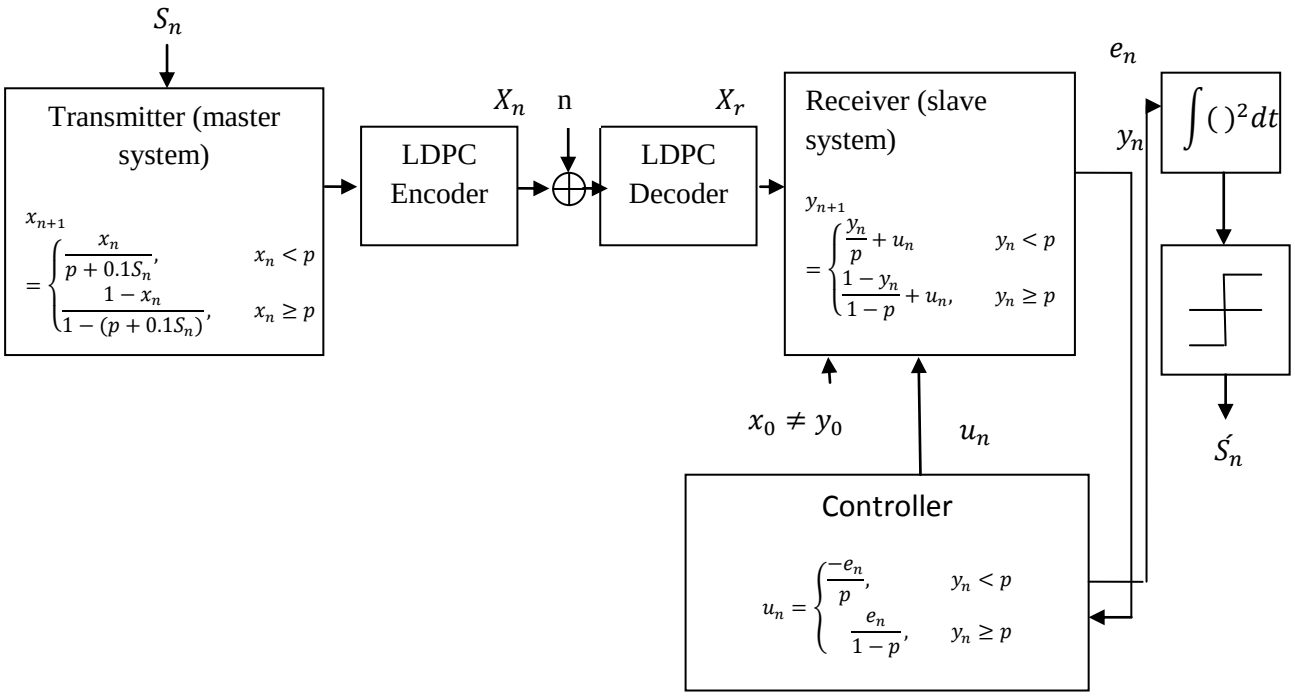

Figure 2.8 Chaotic tent map communication system based on parameter modulation concept and LDPC under AWGN

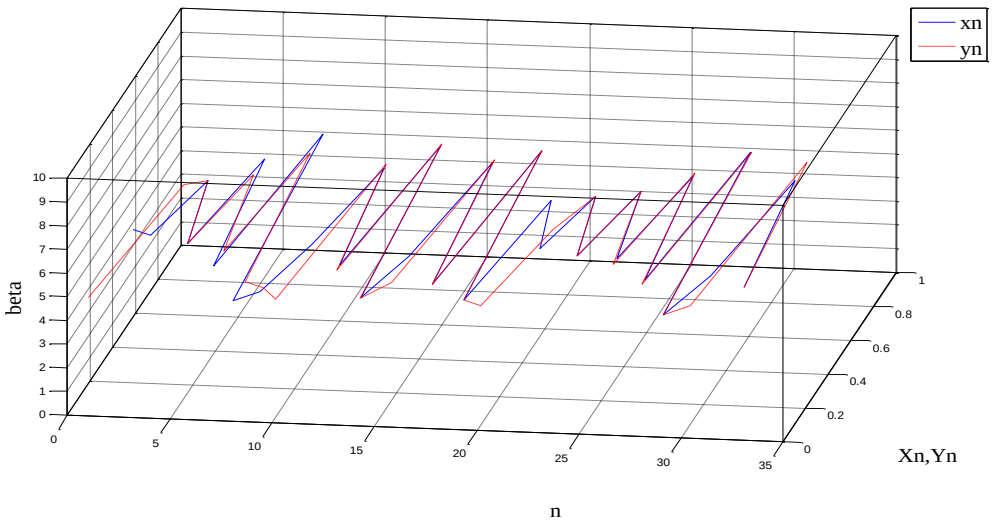

Figure 2.9 Synchronization between sequences at transmitter and receiver for $\beta = 4$

The LDPC code is characterized by w_r =6 and w_c =3. We set the block length to $N = 10000$ for LDPC codes and the code rate $\frac{K}{N} = 0.5$).

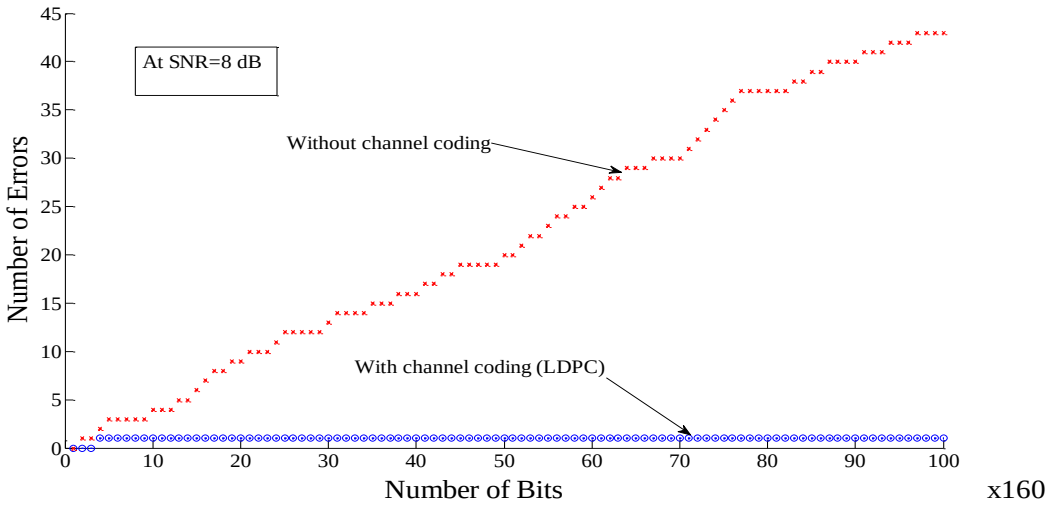

Figure 2.10 Illustration of the number average number of errors for the chaotic-SISO system under AWGN

In reported literature [Jovic B. and Unsowrth C. P., 2011], it has been shown that when 50000 data samples are sent at SNR of 8dB, the system employing chaotic Single-Input-Single-Output (SISO) technique gives 43 errors (on an average).

After implementation of LDPC channel coding, the number of errors for same data size at identical SNR value (8dB) reduces to 1 error (on an average) as shown in Figure2.10. This illustrates the fact that the use of LDPC codes can drastically improve information integrity at the receiver.

This has motivated us to study the performance of communication system comprising of chaotic modulation, LDPC coding followed by Alamouti STBC on various RF and Optical wireless channels. These topics will be discussed in chapter four.

2.3 On the security of chaotic maps based on Dual chaotic System with Lyapunov Exponent (LE)

A chaotic signal is defined as being deterministic, aperiodic and presenting sensitivity to initial conditions. The last property means that, if the generator system is initialized

with a slightly different initial condition, the obtained signal diverges very quickly from the original one **[**Daniela K. and Marcio E., 2007**]**.

A chaotic signal possesses good randomness properties, especially after being processed in some certain ways. Chaotic system can be used to generate high security key stream for data encryption algorithm. However, a single chaotic system is vulnerable to be attacked by chaotic reconstruction because of it has less control parameters and is simple in term of generation. High-dimensional chaotic system have more complex form and more parameters for adjustment [Kathleen A., Tim S. and James Y,1996, Jiu F and Chi T, 2008]. However, the corresponding complexity load is heavy**.** The dual chaos system represent a balance those two factors [Yi C, Li Z. and Yifang W, 2010]. We have proposed a dual-chaos system that consists of two one dimensional logistic maps and two one dimensional tent maps.

In order to characterize a chaotic attractor, determination of a quantitative measure of the degree of sensitivity on the initial conditions is of great importance.
The Lyapunov Exponent (LE) describes the (average) growth of small perturbations in different directions of the state space on a logarithmic scale. When at least one LE is positive, the attractor under investigation possesses the property of sensitive dependence on initial conditions and may thus be characterized as possessing chaotic properties.

When the equations of motion of the dynamical system are known the computation of LEs is straightforward task [Parlitz U., 1993**]**. In this chapter of the thesis, we have derived the LEs for dual logistic chaotic maps and dual tent chaotic map.

2.3.1 Dynamics of Chaotic Maps:

2.3.1.1 Dynamics of Tent Map:

Let us consider the tent map f: [0,1] given by equation (2.3)
It is noninvertible transformation of the unit interval onto itself. It depends on the parameter `p' which satisfies, $0 < p < 1$. .

A typical trajectory $x(k)$ of the dynamical system is obtained by iterating this map, i.e.,

$$x(k) = f^n[x(0)] = f(\{\dots f[x(0)] \dots\}) \quad n=0,1,2,\dots\dots \tag{2.10}$$

2.3.1.2 Dynamics of Logistic Map

Logistic map is a typical nonlinear chaotic equation. The model of logistic map is illustrated in equation (2.11) [Abir A., Safwan. A, Wang Q. Calin V. and Bassem. B., 2008]

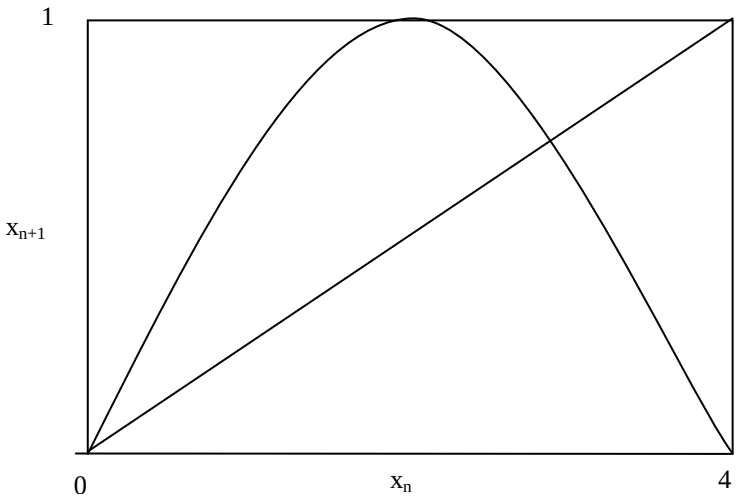

Figure 2.11 The dynamic (input-output) relationship of the logistic map $[0 \leq \mu \leq 4]$

$$x_{n+1} = \mu x_n(1 - x_n), \qquad \mu \in [0,4], x_n \in (0,1) \tag{2.11}$$

When the value of parameter μ is determined, an arbitrary initial value $x_0 \in (0,1)$ can generate a fixed sequence $\{x_1, x_2, \dots x_n\}$. For different values of parameter μ, logistic sequence will present different characteristics.

2.3.2 Dual Chaotic System Design

Most of single chaotic systems are vulnerable to be attacked by chaotic reconstruction because they have lesser number of control parameters. High-dimensional chaotic

system has more complex form and more parameters for precise control**.** However, these systems present heavy computational load. Dual chaos system present balance between these two factors. We have designed and characterized dual-chaos systems comprising of two one dimensional logistic maps and two one dimensional tent maps.

2.3.2.1 Dual Logistic Map

The chaotic map is represented here by LOG1 and LOG2 where

LOG1: $x_{n+1} = \mu x_n(1 - x_n), \qquad \mu \in [3.57,4], x_n \in (0,1)$ (2.12)

LOG2: $y_{n+1} = \eta y_n(1 - y_n), \qquad \eta \in [3.57,4], y_n \in (0,1)$ (2.13)

where μ and η are control parameters. In this dual-chaos system, x_{n+1} is the output of chaotic system LOG1, y_{n+1} is the output of chaotic system LOG2 with $y_0 = x_{n+1}$.

So, chaotic sequence $\{y_n\}$ is the final output of this two dual-chaos system. It is produced by composing (placing in cascade) chaotic system LOG1 and chaotic system LOG2 [Yi C, Li Z. and Y. Ifang W, 2010].

2.3.2.2 Dual Tent Map

The equation of TENT1 and TENT2 are shown in equations (2.14) and (2.15)

TENT1: $x_{n+1} = \begin{cases} \frac{x_n}{p} & , \ 0 \le x_n < p \\ \frac{1-x_n}{1-p} & , \ p \le x_n < 1 \end{cases}$ (2.14)

TENT2: $y_{n+1} = \begin{cases} \frac{y_n}{b} & , \ 0 \le y_n < b \\ \frac{1-y_n}{1-b} & , \ b \le y_n < 1 \end{cases}$ (2.15)

where p and b are control parameters, x_0 and y_0 represent the initial values respectively in the equations (2.14) and (2.15). In this dual-chaos system, x_{n+1} is the output of chaotic system TENT1, y_{n+1} is the output of chaotic system TENT2 with $y_0 = x_{n+1}$. So, chaotic sequence $\{y_n\}$ is the final output of this dual-tent map arrangement. It is produced by composing chaotic system TENT1 and chaotic system TENT2 in cascade.

This technique makes chaotic behavior more complex. It also results in the output chaotic sequence having better randomness properties.

2.3.3 Lyapunov Exponent

Let us define $|\delta_n| = f^n(x_0 + \delta_0) - f^n(x_0)$, where n is the number of iterations of the chaotic map, x_0 the initial condition and δ_0 an arbitrary small number. In the limit when $\delta_0 \to 0$, an accurate and computationally useful formula for evaluating the LE can be obtained as, [Ibarra E., Vazquez R., Cruz M. and Del-RioJ., 2008]

$$\lambda = \frac{1}{n} ln \left|\frac{\delta_n}{\delta_0}\right| = \frac{1}{n} ln \left|(f^n)'(x_0)\right| \tag{2.16}$$

The term within the algorithm can be expanded, so that the LE can be approximated by the following expression,

$$\lambda = \frac{1}{n} \sum_{i=0}^{n-1} ln \left|f'(x_i)\right| \tag{2.17}$$

Evaluating this equation in the limit as $n \to \infty$, then the LE for the orbit that begin in x_0 is

$$\lambda = \lim_{n\to\infty} \{\frac{1}{n} \sum_{i=0}^{n-1} ln \left|f'(x_i)\right|\} \tag{2.18}$$

Note that λ depends on x_0. It has been shown that for cycle to be stable, λ should be negative. On the contrary, for chaotic attractors λ is positive [Ljupco K., Janusz S., Jose A. and Igor T., 2006, Ibarra E., Vazquez R., Cruz M. and Del-RioJ., 2008].

2.3.3.1 LE of Single Logistic MAP

From equation (2.11) and equation (2.18)

$$\lambda = \lim_{n\to\infty}\{\frac{1}{n}\sum_{i=0}^{n-1}\ln(\mu) - \ln(2\mu x_i)\} \tag{2.19}$$

2.3.3.2 LE of Single Tent MAP [Martin H and Yuri M, 1997]

From equation (2.3) and equation (2.18)

$$\lambda = \int_0^p ln\left|\frac{1}{p}\right| dx + \int_a^1 \left|\frac{1}{1-p}\right| dx \tag{2.20}$$

2.3.2.3 LE of Dual Logistic Map

The LEs of a trajectory x_n obtained by iteration of the map $f:\mathbb{R}^n \to \mathbb{R}^n$ are defined to be eigenvalues of the matrix

$$\lambda = \lim_{n\to\infty}\frac{1}{2n}\ln[D_n^T D_n] \tag{2-21}$$

whenever, D_n is well-defined and the limit exists. Here D_n^T denotes the transpose of D [Martin H and Yuri M, 1997]. From equation (2.18) and equation (2.19) we derived the LE of dual logistic map as follows

Let, $x_{n+1} = \mu x_n(1-x_n)$, $x_{n+1}^{'} = \mu - 2\mu x_n$
For Dual logistic map,

$$\lambda = \lim_{n\to\infty}\frac{1}{2n}\sum_{i=1}^{n-1}\ln\{[\mu - 2\mu x_n]^T[\mu - 2\mu x_n] - \delta_0\} = \lim_{n\to\infty}\frac{1}{2n}\sum_{i=1}^{n-1}\ln\{\mu(1-2x_n)]^T[\mu(1-2x_n)] - \delta_0\} \tag{2.22}$$

where δ_0 is the change in initial value.

2.3.2.4 LE of Dual Tent Map

From equation (2.18) and equation (2.20) we can derive the LE of dual tent map as follows. The dynamic equation of chaotic tent map is as described in equation (2.14)
The LE for dual chaotic tent map is given as follows:

$$\lambda = \lim_{n\to\infty} \frac{1}{2n}\left\{\left[\int_0^p ln\left|\frac{1}{p}\right| dx + \int_p^1 \left|\frac{1}{1-p}\right| dx\right]^T \left[\int_0^p ln\left|\frac{1}{p}\right| dx + \int_p^1 \left|\frac{1}{1-p}\right| dx\right] - \delta_0\right\} \quad (2.23)$$

2.3.4 Simulation Results

In Figure 2.12 a) we have sketched the behavior of a single logistic map showing chaotic behavior beyond control parameter value $\mu = 3.57$. This map is most chaotic (secure) at control parameter value $\mu = 3.8$, where the value of LE is 0.5.

In Figure 2.13 a) we observe that single tent map is chaotic within the range (0,1) of control parameter p. It is most secure for control parameter values above 0.5 where the value of LE is 0.85.

The sketch of dual logistic map is shown in Figure 2.14 a). It is seen that it exhibits chaotic behavior for values of control parameter μ greater than 1.25 and less than 4. The maximum security is achieved at $\mu = 4$ where the value of LE is 0.81.

In Figure 2.15 a) a sketch of the dual tent map is presented. It is evident that this map exhibits chaotic behavior for the range of values (0,1) of control parameter p. It most secure at $p = 0.5$ and the maximum value of LE at $p = 0.5$ is 1.2.

Another important property of chaotic sequences is exhibited by Figure 2.12 b). In this plot the difference between the values of chaotic sequences with a difference in initial values equal to 10^{-16} for the Logistic map has been plotted. We see that in the beginning (small values of iteration numbers), the difference between two pseudo-random sequence is very small. In Figure 2.13 b), the difference between the values of

chaotic sequences with a difference in initial values equal to 10^{-16} for the tent map has been plotted. Again, we observe that for small values of iteration numbers, the difference between the two pseudo-random sequence s is very small. However, with the increase of the iteration number above 20, the difference gradually increases. For the dual logistic map sketched in Figure 2.14 b), this separation in the values of increases when the iteration number exceeds 40.

In dual tent map (Figure 2.15 b)) we can see the difference between two pseudo-random sequences takes on large values for small iteration numbers. Thus the system is very sensitive to initial conditions. We conclude that the dual tent map shows superior sensitivity to initial conditions than other maps considered here. Further, the single tent map gives better sensitivity than dual single and logistic maps.

The values of LE for different chaotic maps are summarized in the following table.

values of LE are specified in Table 2.1

Chaotic map	LE
Single logistic map	0.5
Single tent map	0.85
Dual logistic map	0.81
Dual tent map	1.2

Table 2.1

From the values presented in the Table 2.1, we infer that dual tent map is most secure whereas single logistic map is least secure.

The correlation characteristics of chaotic sequence are also regarded as indicators of cryptography security. These characteristics are divided into two categories, auto-correlation and cross-correlation.

Let x_n and y_n be two sequences of length L. The autocorrelation function and the crosscorrelation function are defined as in equation (2.24) and equation (2.25) [Yi C, Li Z. and Yifang W, 2010].

$$R_x(j) = \frac{1}{L}\sum_{i=1}^{L} x_i x_{i+j} \tag{2.24}$$

$$R_{xy}(j) = \frac{1}{L}\sum_{i=1}^{L} x_i y_{i+j} \tag{2.25}$$

where L is the length of sequence and j is the distance between two elements in chaotic sequence. Figure 2.16 shows a sketch of the autocorrelation function for the dual tent map. It can be observed that the autocorrelation is maximum at zero time shifts (δ – like). Figure 2.17 shows the plot of cross correlation plots of single and dual tent map. It is seen that the cross-correlation function is nearer to zero value (maximum value 0.0085) for the single tent map as compared to dual tent map (maximum value 0.028). Hence two consecutive sequences of single tent map exhibit greater degree of orthogonality than dual tent map shown in Figure 2.17

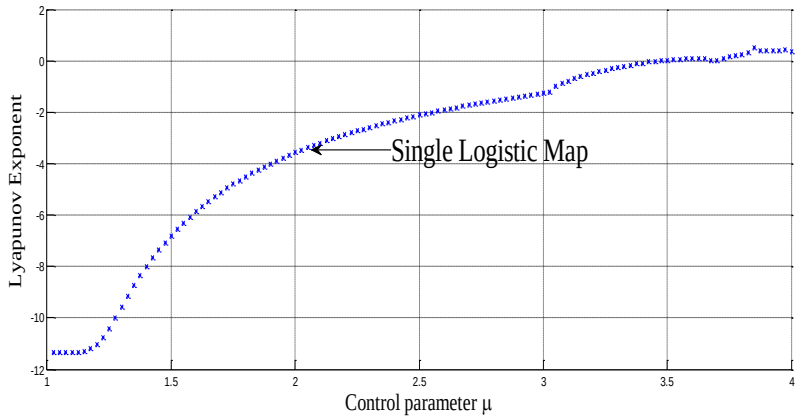

(a)

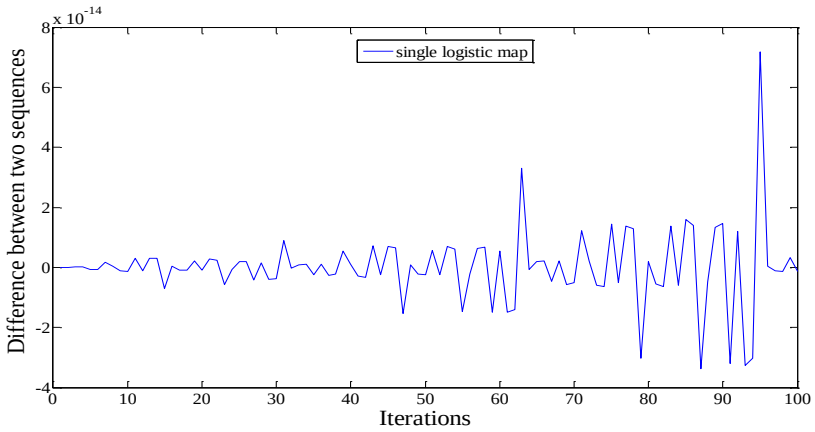

(b)

Figure 2.12 a) Plot of LE b) The difference between two chaotic sequences with different x_0 in single logistic map

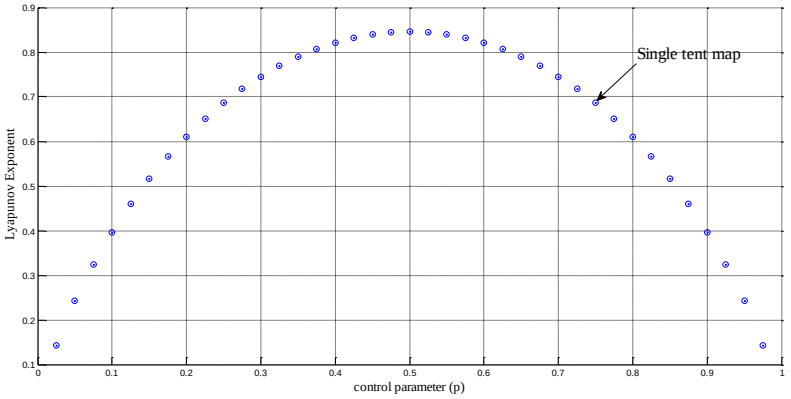

(a)

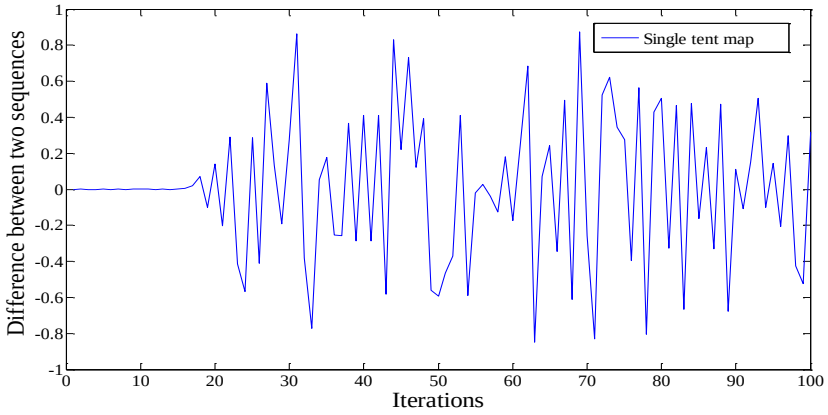

(b)

Figure 2.13 a) Plot of LE

b) The difference between two chaotic sequences with different x_0 in single tent map

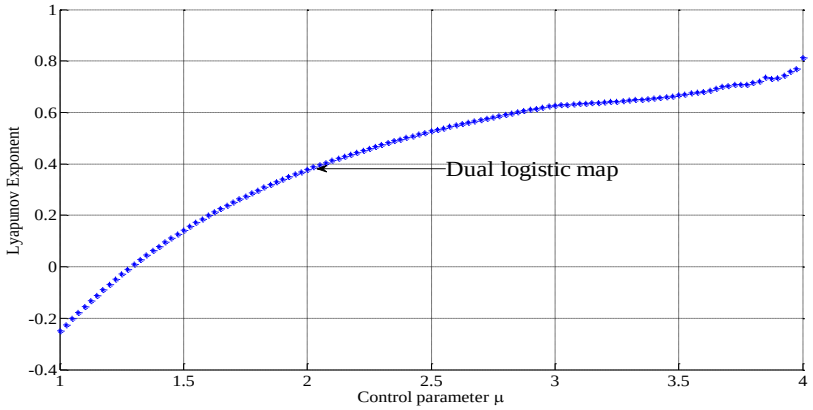

(a)

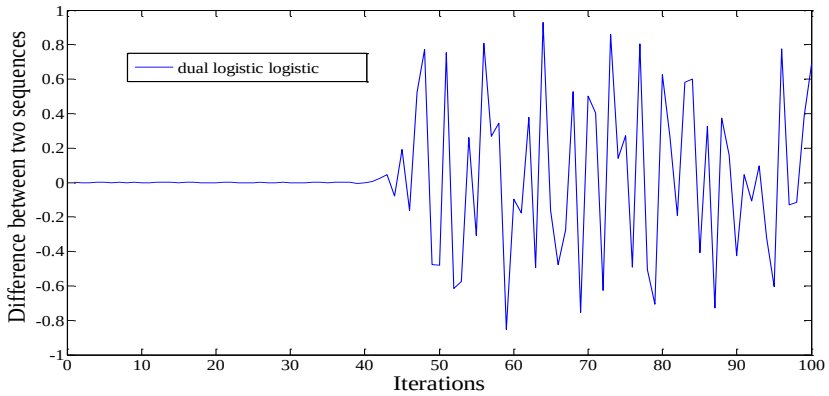

(b)

Figure 2.14 a) Plot of LE b) The difference between two chaotic sequences with different x_0 in dual logistic map

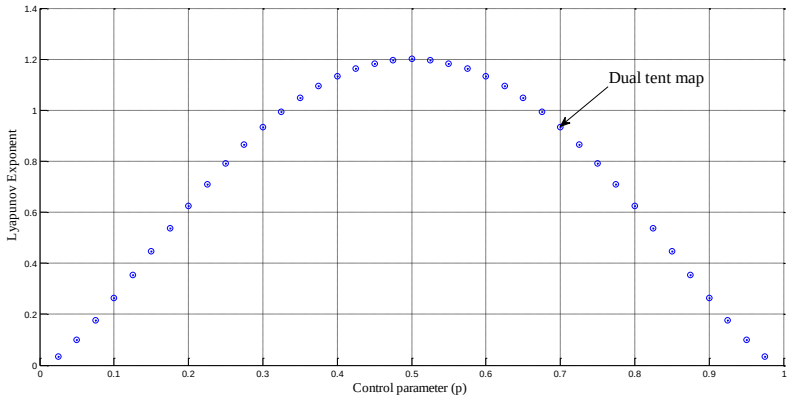

(a)

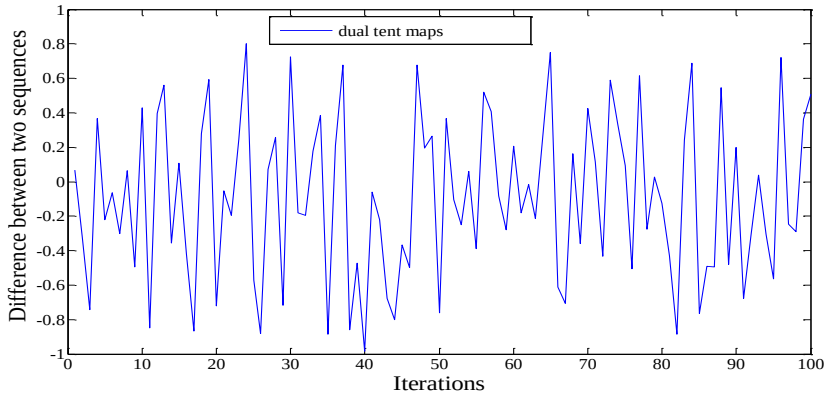

(b)

Figure 2.15 a) Plot of LE b) The difference between two chaotic sequences with different x_0 in dual tent map

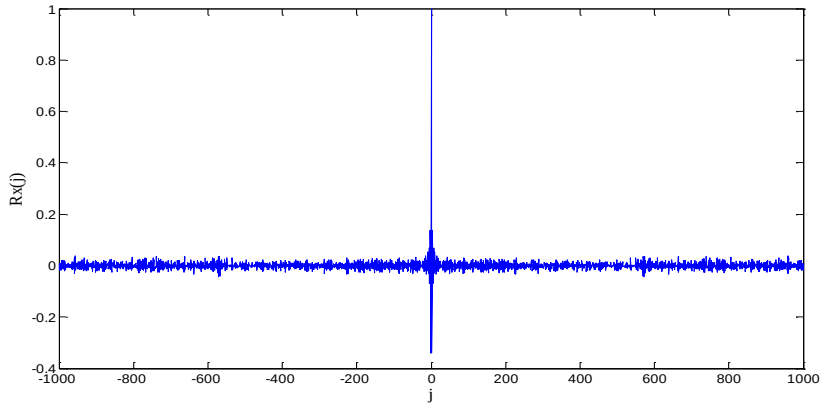

Figure 2.16 Plot of auto-correlation of dual tent

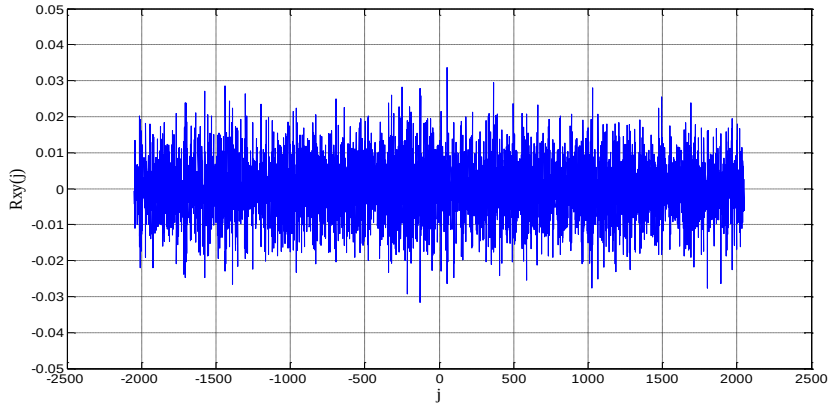

(a)

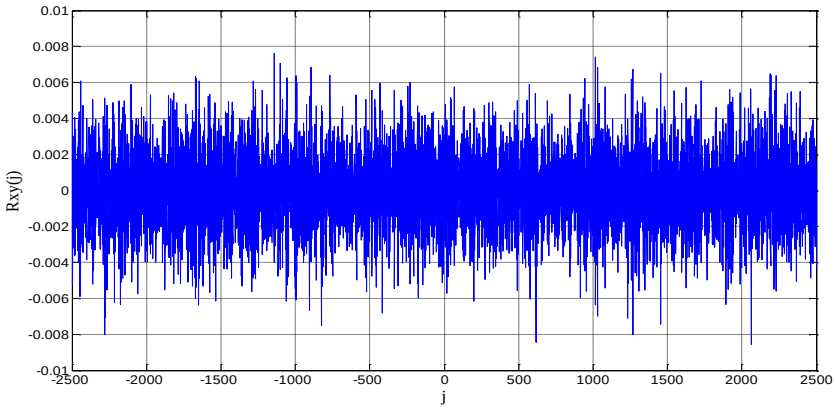

(b)

Figure 2.17 cross-correlation of tent map depicted in a) Plot of dual tent map b) Plot of single tent map

2.4 **Conclusions**

A method of synchronizing chaotic maps and its implementation within a chaotic communication system has been proposed and evaluated in this chapter. The general approach to master-slave chaotic map synchronization has been presented on the one-dimensional chaotic tent map without noise and with AWGN. The control factor of chaotic tent map has been designed in such away to reduce the error of the system.

The use of channel code has enabled reduction of the spreading factor from 400 in [Jovic B. and Unsowrth C. P., 2010] to 4 in our enhanced system. This means that the properties of chaotic signals have been maintained. Reduction in spreading factor (β) helps in reducing the complexity of the system. At the same time, the required energy per symbol reduces with reduction in β. The proposed technique thus helps in reduction in complexity and energy per symbol without compromising in security due to non-periodic behavior of chaotic sequences.

The data encryption algorithm based on dual chaotic system has excellent security when compared with the work of [Marco S., 1996] [average value of LE is 0.6] who worked with chaotic continuous systems such as Lorenz system and [Parlitz U.,1993] [average value of LE is 0.24] who computed the value of LE for the Chua's circuit. In addition, we have also described a system of dual chaotic maps by combining two chaotic maps with different initial conditions to generate more complex chaotic sequences. The values of LE for the dual maps and the values taken by them as a function of iteration number have been computed. These results will be invoked in later chapters to design Chaos sequence based communication systems that can mitigate the effects of channel induced error as well as present resistance to eavesdroppers trying to gather privileged information being communicated over wireless channels.

In chapter three we will discuss the feasibility of using different chaotic modulation schemes such as CSK, DCSK and CDSK in a MIMO channel. A comparison will be made between various chaotic modulation schemes implementing various Alamouti techniques in term of BER under AWGN and Rayleigh fading channel.

CHAPTER 3

BER PERFORMANCE ENHANCEMENT BASED ON CHAOTIC-MIMO COMMUNICATION SYSTEM

3.1 Introduction

Transfer of information by wireless means has become ubiquitous with the development and widespread deployment of personal communication devices that support voice as well as data communication. However, these modes of communication have their own challenges which have to be overcome. One major challenge has been that has attracted the attention of researchers is the design of techniques that can protect sensitive information against being accessed by unauthorized eavesdroppers during its transmission. This is because with suitable receivers, any person with requisite equipment can intercept information from wireless transmission in the local area. In addition, it is difficult to discover such interceptions. Techniques derived from the study of chaos have presented researchers with new tools for ensuring information security during transmission and storage. It has been demonstrated that even one dimensional discrete chaotic system is able to provide a high level of security [Hong Z., Xie T. and Jun Y., 1997]. Chaotic signals can be used in secure communications due to their wideband property and sensitive dependence on initial conditions. The use of Chaotic Shift Keying (CSK) provides strong resistance against interception and capture over long intervals of time. Hence, researchers have concluded that wireless communication methods based on chaotic modulation schemes can be designed to provide robust and secure communications [Liu J., Cai. T., Xiao J., Zhang Y. and Wu Y, 1996, Zhi D., Bing W. and Peng L, 2006]. Various methods for chaos-based secure transmission of private information signals have been proposed by several authors [Jaejin L., Chungyong L. and Williams D.,1995], [Zhinggou L., Kun L., Changyun W. and Yeng S, 2003], [Guoping T., Xiaofeng L, Di X. and Chuandong l.., 2004] and [Yuu S. and Zahir H., 2005]. In addition, the problem of synchronization of chaotic systems and their

potential application in securing communication has received a lot of attention in the past decade [Pecora M. and Carroll L., 1990]. Kaddoum et.al [2009] have studied the performance of coherent CSK communication systems under the assumption that perfect synchronization between transmitter and receiver has been achieved

It is well known that detection schemes can be categorized into coherent and non-coherent types. In coherent detection, such as in CSK systems, the receiver has to reproduce the same chaotic carrier which has been used to carry the information, through the process known as chaos synchronization which is difficult to achieve in practice over channels which are time varying and perturbed by noise. In non-coherent systems, however, the chaotic carrier does not need to be generated at the receiver. Thus non-coherent schemes are attractive from implementation point of view. One important non coherent scheme that has attracted the attention of the research community is Differential Chaos Shift Keying (DCSK) which has been studied by a number of researchers. A DCSK system represents a robust non-coherent scheme. These schemes do not require exact knowledge of the chaotic signal used to modulate the data at the transmitter end for demodulation purposes. Further, Ma H. and Kan H. [2009] have claimed that DSCK system is one of the most promising chaos-based communications schemes for a feasible implementation and that these schemes are very robust against channel imperfections. The relaxation of the chaos synchronization requirement ensures that non-coherent systems represent very practical forms of chaos based communication [Lau F., Tse M C. and Hau S., 2004]. Because of sensitivity on initial conditions, the task of reliably synchronizing the chaotic signals on the transmitter and receiver sides of a communication channel is a challenging task. Therefore, non-coherent chaos communication systems which do not need chaos synchronization have attracted the attention of the researchers developing efficient and practical secure communication systems. DCSK is a typical non-coherent chaos-based communication scheme, almost insensitive to channel distortion, with reasonably good immunity to noise [Ben M., Akachouri A. and Samet M., 2006]. The Correlation Delay Shift Keying (CDSK) scheme is one of the non-coherent detection schemes, which is similar to the DCSK scheme in that a reference chaotic signal is embedded in the transmitted signal. Unlike in DCSK, however, the

reference signal and the information bearing signal are now added together with a certain time delay in CDSK. As a consequence, the transmitted signal sample includes the reference signal and the information bearing signal. Both the signals are added together with a certain time delay in CDSK [Wai T, Francis L., and Chi T., 2006]. Moreover, by eliminating the switch required to perform the switching DCSK system, CDSK allows a certain operation of transmitter. In this scheme, the transmitted signal is more homogenous and less prone to interception. However, because the sum of two chaotic signals is sent, more uncertainty (interference) is produced when the received signal correlates with its delayed version at the receiving side. Therefore, the performance of CDSK is inferior to that of DCSK when employed over real world channels perturbed by noise. In these schemes, a chaos generator is used to generate CSK, DCSK and CDSK sequences, where different sequences can be generated using the same generator but with different initial conditions. In this thesis, we have investigated the performance of the CSK-MIMO, DCSK-MIMO and CDSK-MIMO scheme over wireless channels.

The channel perturbations are modeled using the Rayleigh distribution. This is because Rayleigh fading channel is widely accepted as a realistic channel model for understanding the behavior of wireless links. We have tried to propose and study the performance of secure communication links with an optimum BER performance which are required to protect information integrity against channel induced impairments and criminal activity directed at wireless communication systems [Lau Y., Lin K. and Zahir H., 2005]. In wireless communications the presence of reflecting objects and scatterers in the medium can disturb the propagation of signal energy, leading to multiple versions of the transmitted signal arriving at the receiver with different amplitudes, phases and time delays. The multipath waves combine at the receiver, causing the received signal to vary greatly in amplitude and phase. Multipath fading limits the performance in wireless applications. In the presence of multiple users accessing a common communication channel in a multipath environment multipath effects are compounded by interference.

The simultaneous presence of these two signal degrading phenomenon can cause the signal at the receiver to distort and fade significantly, leading to higher BER. The BER performance of the chaos based communication system for the Single Input Single Output (SISO) channels has been studied by several researchers [Kaddoum G., Mai V. and Gagnon F., 2011].

It is now well established that exploitation of channel diversity via the use of MIMO techniques by utilizing multiple antennas is an optimum method to combat fading in wireless communications [Huanfei M. and Haibin. K. 2009]. Motivated by these considerations, we have investigated the feasibility of employing chaotic techniques to enhance information security in MIMO channels by implementing space-time coding schemes combined with CSK, DCSK and CDSK modulation schemes. Further, Space Time Block Codes (STBCs) have attached much attention in radio wireless communications because they provide both space and time diversity by coding over multiple antennas and several time slots. A very simple and effective STBC was introduced by Alamouti [Siavash M. Alamouti 1998, Hiroshi Y. and Tomoaki O., 2003]. In practice, non-coherent (DCSK and CDSK) detection make use of some distinguishable property of the transmitted signal, which can be some inherent deterministic property, a feature fabricated by a suitable bit arrangement, or some statistical property [Francis L., Chi T., Ming Y. and Sau H, 2004]. Non-coherent communication schemes, which do not require the reproduction of the chaotic signals at the receiving end, are more feasible in practice [Wai T, Francis L., and Chi T., 2006]. This is primarily because a major drawback of coherent chaos-based communication systems such as the CSK is that they require synchronization between the chaotic carrier signals between the transmitter and receiver [Kaddoum G., Francois G., Pascal C and Daniel R, 2010]. With coherent receiver, the chaotic signal used as a spreading sequence to spread the data information signal, must be exactly reproduced at the receiver to de-spread the received information bearing signal. After de-spreading a correlator and a threshold detector are used in order to reconstruct the signal. On the other hand, with DCSK, chaotic synchronization is not required on the receiver side. However, as has been shown by Kaddoum et.al [2011], DCSK system is less secure, and does not perform as well as the coherent chaos-based communication systems. The DCSK technique offers one significant advantage over CSK. The noise

performance of a DCSK communication system in measured in terms of BER versus E_b/N_0 outperforms the performance of a standard non-coherent CSK system. For sufficiently large bit duration, the noise performance of DCSK is comparable to that of a conventional sinusoid based modulation scheme. Also, because synchronization is not required, a DCSK receive can be implemented using very simple circuitry.

A DCSK is not as sensitive to channel distortion as coherent methods since both the reference and the information bearing signal pass through the same channel [Jiu F. and Chi Tse, 2008]. Because of the non periodic nature of chaotic signals, the transmitted bit energy after passing through the chaotic modulator varies from one bit to another. However, most researchers have computed the BER performance by considering the bit energy as constant. This approximation, which is widely known as Gaussian Assumption (GA), suffers from a low precision when the spreading factor is low. Another approach integrates the BER expression for a given chaotic map over all possible spreading sequences associated with a given spreading factor. This latter method when compared with the BER computation under the Gaussian Assumption, gives more accurate results, but suffers from high computation complexity. Another accurate computation is the exact BER performance for coherent and non coherent chaos based communication systems.

The idea of this approach is to first compute the PDF of the bit energy, and then use the computed PDF to compute the BER expression [Tam W., Lau F., Tse C. and Lawrance A., 2004]. We have employed this last method in our study.

Contributions of the thesis in Chapter 3:

- Investigate the feasibility of, and advantages derived by employing chaotic communications in Multiple Input Multiple Output (MIMO) channels and quantify their performance.
- Evaluate the BER performance of different chaotic modulation schemes (coherent CSK and noncoherent DCSK and CDSK) with different chaotic maps under AWGN and Rayleigh fading channels.

3.2 Chaotic Generators

The most commonly used PN sequence is the m-sequence which is generated by linear feedback shift register. The number of distinct m-sequences that can be generated with a given shift register is limited. By using code clock extraction techniques, an interceptor can wipe out the spreading sequences and extract the un-spread modulated user information. In this context, chaotic sequences, which have superior data masking characteristics compared with m-sequences, can be used to improve the covertness of the communication. Noise-like chaotic sequences can be used to effectively conceal the information bearing signals. Several chaotic maps, such as Tent map, Logistic map, Chebyshev map and Bernoulli map have been used to generate chaotic sequences [Jin Y., Hanyu L., Yu Y. and Neil V., 1999]. In the following section, a brief description of various chaotic maps used to generate random sequences is presented.

3.2.1 Tent Map

A piece-wise one dimensional representation of the tent map is presented in Figure 2.1.
Associated with the map is a constant coefficient 'p' referred to as the peak value.

This is the point at which the map reaches its maximum output value. In the example shown in Figure 2.1, x_{n+1} takes on maximum value at $x_n = p = 0.5$. Above and below this value x_{n+1}decreases linearly to reach to zero at $x_n = 0$ and $x_n = 1$. The dynamic (input-output) relationship of the tent map is specified by equation (2.3) which is reproduced here for reference [Dornbusch A. and Gyvez J., 1999].

$$x_{n+1} = \begin{cases} \dfrac{x_n}{p}, & x_n < p \\ \dfrac{1 - x_n}{1 - p}, & x_n \geq p \end{cases}$$

3.2.2 Logistic Map

The iterated input-output relationship of the logistic map is given by equation (2.11) which is reproduced here for reference [Abir A, Safwan A.., Wang Q., Calin V. and Bassem B., 2008].

$$x_{n+1} = \mu x_n(1 - x_n), \qquad \mu \in [0,4], x_n \in (0,1)$$

3.2.3 Chebyshev Map

The 2nd order Chebyshev polynomial function has been chosen in this thesis for generation of chaotic sequences. It is described in equation (3.1). The dynamic input-output relationship is sketched in Figure 3.1[Shilian W. and Xiaodong W., 2010].

$$x_{n+1} = 1 - 2x_n^2 \tag{3.1}$$

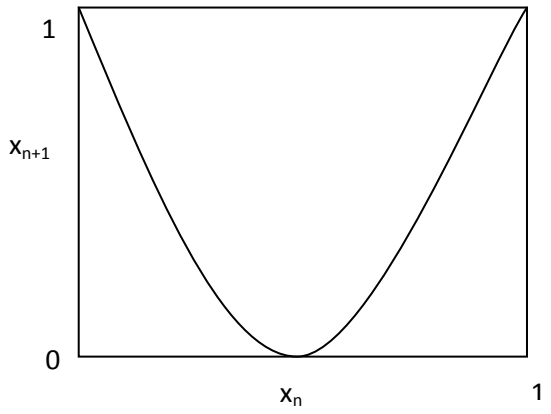

Figure 3.1 The dynamic (input-output) relationship of the Chebyshev map

3.2.4 Bernoulli Map

The iterated input-output relationship of the Bernoulli map is given by equation (3.2) and is sketched in Figure3.2 [Mozsary A., Azzinari K. and Porra V., 2001].

$$x_{n+1} = 2x_n \tag{3.2}$$

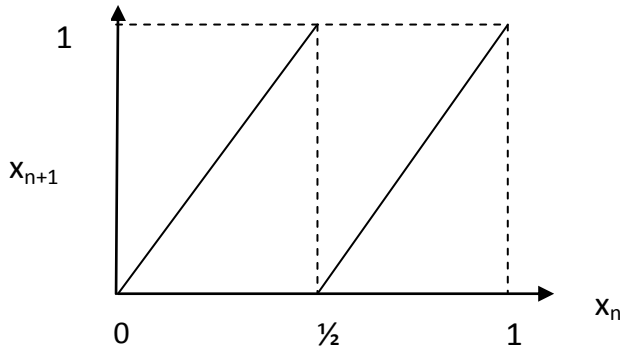

Figure 3.2 The dynamic (input-output) relationship of the Bernoulli map

In equations (2.3), (2.11), (3.1) and (3.2), x_n and x_{n+1} represent the current and next symbols of the chaotic sequence respectively.

3.3 CSK-MIMO Communication System

This section examines the feasibility of using chaotic communications over MIMO channels. While the use of chaotic maps can enhance security, it is seen that the overall BER performance gets degraded when compared to conventional communication schemes. In order to overcome this limitation, we have proposed the use of a combination of chaotic modulation and Alamouti Space Time Block Code.

The performance of CSK with 2×1 and 2×2 Alamouti schemes for different chaotic maps over wireless channels has been studied. It has been shown that the use of these schemes can provide security enhancement without the penalty of degradation of BER performance.

In CSK communication system the signal x(t) is first generated by one of the chaotic maps defined in section (3.2). If a "$+1$" is to be transmitted, the chaotic signal is sent. If "-1" is to be transmitted, an inverted copy of the chaotic signal is conveyed. Hence the transmitted signal $s(t)$ can be expressed as,

$$s(t) = \begin{cases} x(t), & when\ symbol\ "+1"s\ transmitted \\ -x(t), & when\ symbol\ "-1"s\ transmitted \end{cases} \quad (3.3)$$

Consider the data information symbols ($s_l = \pm 1$) with period T_s.

A chaotic sample (or chip) is generated at every time interval equal to $T_c (x_k = x(kT_C))$. The transmitted signal at the output of the transmitter is:

$$u(t) = \sum_{l=0}^{\infty} \sum_{k=0}^{\beta-1} s_l x_{l\beta+k} \quad (3.4)$$

where the spreading factor β is equal to the number of chaotic samples in symbol duration T_s, ($\beta = \frac{T_s}{T_c}$). The received signal is modeled as,

$$r(t) = hu(t) + n(t) \quad (3.5)$$

where, h is the channel coefficient and $n(t)$ represents a sample function of the AWGN process. In order to demodulate the transmitted bits, the received signal is first despread by employing the locally generated chaotic sequence.

The resulting symbols are then integrated over symbol duration T_s. Finally, the transmitted bits are estimated by computing the sign of the decision variable at the output of correlator,

$$Ds_l = sign\ (s_l T_c \sum_{k=0}^{\beta-1} (x_{l\beta+k})^2 + w_l) = sign(s_l E_b^{(l)} + w_l) \quad (3.6)$$

Where $sign(.)$ is the sign operator, $E_b^{(l)}$ is the bit energy of the lth bit and w_l is the noise after despreading and integration.

3.3.1 The Channel

In every communication channel noise is always present. Furthermore, other disturbances which cause the transmitted signal to change, such as fading, may also be present. In most cases, AWGN is used to evaluate the performance of a communication system over a noisy channel. This is an idealized form of noise where the term additive refers to the fact that noise is added directly onto the transmitted signal. The term white, denotes the fact that this type of noise is of theoretically infinite bandwidth, with power spectral density of:

$$S_W(f) = \frac{N_0}{2} \tag{3.7}$$

Rayleigh Fading Channel [Zhibo. Z., Jinxiang W and Yizheng Y. 2010].

Fading is a phenomenon in wireless transmission whereby a signal has traveled along many paths from the transmitter to the receiver.

The different components combine constructively or destructively at the receiver. As a result the net signal received varies in amplitude and phase over time in an unpredictable manner.

Let H be a Rayleigh distributed random variable with parameters α and σ^2. The pdf is specified as,

$$f_\alpha(h) = \frac{\alpha}{2\sigma^2} e^{\frac{-\alpha^2}{2\sigma^2}}, \quad \alpha > 0 \tag{3.8}$$

In this case, $\gamma_b = \alpha^2 E_b/N_0$ is Chi-square distribution and has the form

$$f_{Rayleigh}(\gamma_b) = \frac{1}{\grave{\gamma_b}} e^{-\frac{\gamma_b}{\grave{\gamma_b}}}, \ \gamma_b \geq 0 \tag{3.9}$$

3.3.2 CSK-2×1 Alamouti Scheme

The block diagram of CSK-2×1 communication system is shown in Figure 3.3

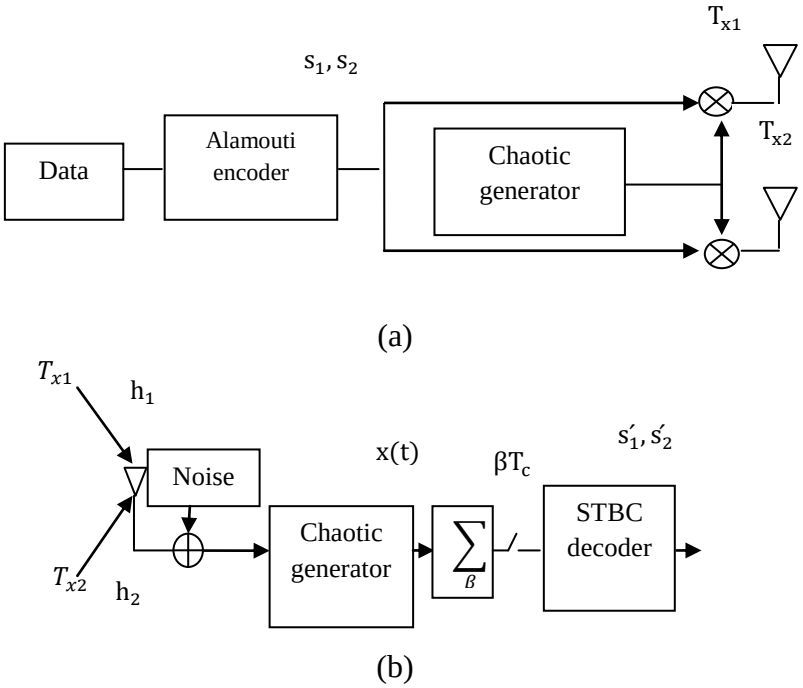

Figure 3.3 CSK-MIMO communication system a) Transmitter with two antennas, b) Receiver with one antenna.

The Alamouti matrix for symbols s_1 and s_2 is

$$S = \begin{bmatrix} s_1 & -s_2^* \\ s_2 & s_1^* \end{bmatrix} \tag{3.10}$$

The transmitted symbols over two time slots from two antennas is specified in Table 3.1

Time	$s_1(t)$from T_{x1}	$s_2(t)$from T_{x2}
$[0, \beta T_c]$	$s_1 x_k$	$s_2 x_k$
$[\beta T_c, 2\beta T_c]$	$-s_2^* x_{k+\beta}$	$s_1^* x_{k+\beta}$

Table 3.1

The received signal (base band) of the 2×1 Alamouti is specified in Table (3.2)

Time	Received signal
$[0, \beta T_c]$	$h_1 s_1 x_k + h_2 s_2 x_k + n_k^1$
$[\beta T_c, 2\beta T_c]$	$-h_1 s_2^* x_{k+\beta} + h_2 s_1^* x_{k+\beta} + n_k^2$

Table 3.2

The extracted decision variables are specified in Table 3.3.

Time	The equivalent baseband model of the received symbol
$[0, \beta T_c]$	$Y_1 = E_b(h_1 s_1 + h_2 s_2) + N_1$
$[\beta T_c, 2\beta T_c]$	$Y_2 = E_b(-h_1 s_2^* + h_2 s_1^*) + N_2$

Table 3.3

The energy of a given bit l is $E_b^{(l)} = \sum_{k=1}^{\beta} x_k^{(l)2}$. N_1 and N_2 represent noise components while $h_1$and h_2 specify the channel gains.

The channel model can be written as

$$Y = E_b HS + N \tag{3.11}$$

The transmitted bits are estimated by multiplying the signal Y by the conjugate transpose of the channel matrix H:

$$\begin{pmatrix} D_{s1} \\ D_{s2} \end{pmatrix} = H^* Y \tag{3.12}$$

Kaddoum et.al [2011] has provided a proof of this equation.

The estimated bits are computed from the sign of the decision variables,

$$\acute{s}_1 = sign\ D_{s1}; \quad \acute{s}_2 = sign\ D_{s2} \tag{3.13}$$

3.3.3 CSK-2 × 2 Alamouti Scheme

The transmitter of 2 × 2Alamouti Scheme is identical to the 2× 1 Alamouti scheme and is specified in Figure 3.3, the receiver is shown in Figure 3.4.

The Alamouti matrix for symbols s_1 and s_2 is as specified in equation (3.10).

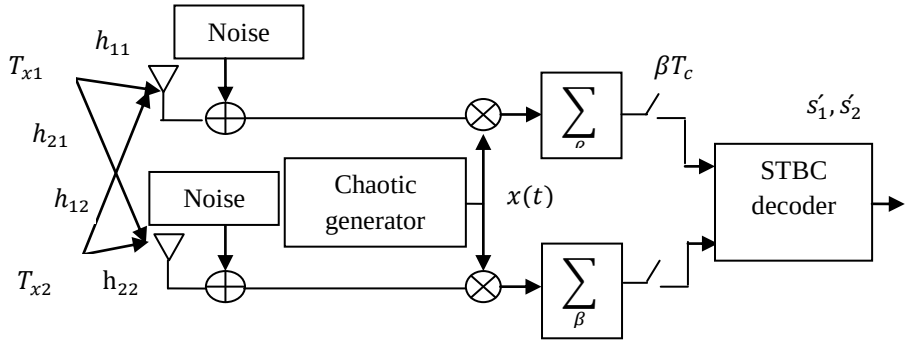

Figure 3.4 CSK-MIMO communication system with two receive antennas

The design of the transmitted signal of 2 × 2Alamouti is specified in Table (3.1).

The received signal on R_{x1} is specified in Table 3.4

Time	Received signal on R_{x1}
$[0, \beta T_c]$	$h_{11}s_1x_k + h_{21}s_2x_k + n_k^1$
$[\beta T_c, 2\beta T_c]$	$-h_{11}s_2^*x_{k+\beta} + h_{21}s_1^*x_{k+\beta} + n_k^2$

Table 3.4

The received signal on R_{x2} is specified in Table 3.5

Time	Received signal on R_{x2}
$[0, \beta T_c]$	$h_{12}s_1x_k + h_{22}s_2x_k + n_k^1$
$[\beta T_c, 2\beta T_c]$	$-h_{12}s_2^*x_{k+\beta} + h_{22}s_1^*x_{k+\beta} + n_k^2$

Table 3.5

The decision variables extracted from the symbols received from the first receive antenna are given by,

Time	The equivalent baseband model of the received symbol on the first antenna R_{x1}
$[0, \beta T_c]$	$Y_{11} = E_b(h_{11}s_1 + h_{21}s_2) + N_{11}$
$[\beta T_c, 2\beta T_c]$	$Y_{21} = E_b(-h_{11}s_2^* + h_{21}s_1^*) + N_{21}$

Table 3.6

$N_{11} = \sum_{K=1}^{\beta} n_k^1 x_k$ and $N_{21} = \sum_{K=1}^{\beta} n_k^2 x_{k+\beta}$ represent noise components.

The decision variables extracted from the symbols received from the second receive antenna are given by,

Time	The equivalent baseband model of the received symbol on the second antenna R_{x2}
$[0, \beta T_c]$	$Y_{12} = E_b(h_{12}s_1 + h_{22}s_2) + N_{12}$
$[\beta T_c, 2\beta T_c]$	$Y_{22} = E_b(-h_{12}s_2^* + h_{22}s_1^*) + N_{22}$

Table 3.7

$N_{12} = N_{11}$ and $N_{22} = N_{21}$ represent noise components and h_{11}, h_{21}, h_{12} and h_{22} are the channel gains. The channel model, estimation and computation of the transmitted bits is similar to 2×2 Alamouti scheme using equations (3.11), (3.12) and (3.13) respectively.

3.3.3 Performance Analysis of CSK-MIMO Communication System

The main objective of this chapter is to study the performance of the CSK-MIMO system under channels perturbed by AWGN and fading channels modeled using Rayleigh pdf. The channel gains for both 2×2 Alamouti and 2×1 Alamouti are constant under the AWGN assumption. The overall BER expression of the CSK-MIMO system for 2×1 Alamouti and 2×2 Alamouti are given in (3.14) and (3.15) respectively [Tam W., Lau F., Tse C. and Lawrance A, 2004].

$$P_e\left(E_b^{(l)}\right) = \frac{1}{2} erfc\left(\sqrt{\frac{(h_1^2+h_2^2)E_b^{(l)}}{N_0}}\right)$$

Now,

$E_{xi}[Q\{E(x)/\sqrt{Var(x)}\}]$ where $Q(x) = \int_x^{+\infty} \frac{1}{\sqrt{2\pi}} \exp(-u^2/2)$

$$BER = \sum_{n=1}^{2} h_n^2 \sum\nolimits_{l=0}^{\beta-1} E_{xi} \left(\sum_{i=0}^{\beta-1} \frac{x_i^2}{N_0}\right)^2 = \sum\nolimits_{l=0}^{\beta-1} E_{xi} \left(\sum_{i=0}^{\beta-1} \frac{x_i^2}{N_0}\right)^{\frac{1}{2}} (h_1^2 + h_2^2) E_b^{(l)}$$

$\sum_{i=0}^{\beta-1} x_i^2 = E_b^{(l)}$ is the chaotic symbol energy, and $E_{xi} = \int_0^{\infty} p\left(E_b^{(l)}\right) dE_b^{(l)}$,

Then

$$BER = \int_0^{\infty} \frac{1}{2} erfc\left(\sqrt{\frac{(h_1^2+h_2^2)E_b^{(l)}}{N_0}}\right) p\left(E_b^{(l)}\right) dE_b^{(l)} \qquad (3.14)$$

For 2×2 Alamouti, the BER expression is given by

$$P_e\left(E_b^{(l)}\right) = \frac{1}{2} erfc\left(\sqrt{\frac{(h_{11}^2 + h_{12}^2 + h_{21}^2 + h_{22}^2)E_b^{(l)}}{N_0}}\right)$$

$$BER = \int_0^{\infty} \frac{1}{2} erfc\left(\sqrt{\frac{(h_{11}^2+h_{12}^2+h_{21}^2+h_{22}^2)E_b^{(l)}}{N_0}}\right) p\left(E_b^{(l)}\right) dE_b^{(l)} \qquad (3.15)$$

In these expressions, $p\left(E_b^{(l)}\right)$ is the probability density function of the energy $E_b^{(l)}$. The BER expression is the result of the integral given in equations (3.14) and (3.15).

To compute the integral in (3.14) and (3.15), we must first have the bit energy distribution. Since the pdf seems to be intractable, the only way to evaluate the BER is to compute the histogram of the bit energy followed by a numerical integration.

Figure 3.5 shows the histogram of the bit energy, for spreading factor β=4 and 50000 samples obtained by simulation.

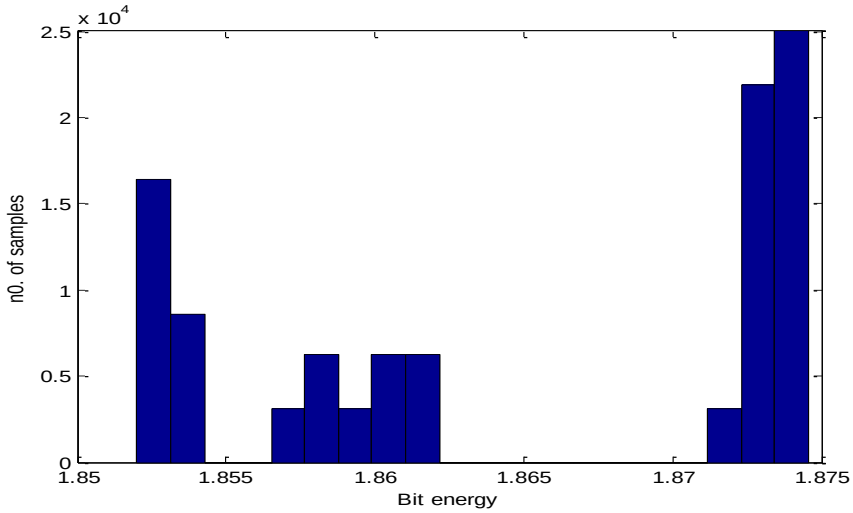

Figure 3.5 Histogram of the bit energy for a CSK-MIMO communication system

After numerical integration the BER expression for 2×1 Alamouti is given by,

$$BER = \sum_{l=1}^{m} \frac{1}{2} erfc\left(\sqrt{\frac{(h_1^2+h_2^2)E_b^{(l)}}{N_0}}\right) p\left(E_b^{(l)}\right) \tag{3.16}$$

For 2× 2 Alamouti, the corresponding BER is given by,

$$BER = \sum_{l=1}^{m} \frac{1}{2} erfc\left(\sqrt{\frac{(h_{11}^2+h_{12}^2+h_{21}^2+h_{22}^2)E_b^{(l)}}{N_0}}\right) p(E_b^{(l)}) \tag{3.17}$$

In these equations, m represents the number of histogram classes and $p\left(E_b^{(l)}\right)$is the probability of having the energy in interval centered on $E_b^{(l)}$.

3.3.4 Simulation Results and Discussions

In this section, we have compared the performance of various chaotic maps (assuming CSK modulation) under AWGN and Rayleigh fading conditions for a spreading factor (β=4), with Single Input-Single Output (SISO) and MIMO (Alamouti) communication schemes. Our aim is to identify the scheme that provides the best BER performance with acceptable security. From Figure 3.6 we observe that 2×2 single tent map gives the best BER performance with a given level of security when compared to all other chaotic maps. We also observed that 2×2 dual tent gives 1.5 dB gain as compared to 2×2 single logistic map. Finally, the 2×2 single tent map exhibits 3 dB gain when compared 2×2 single tent map with 2×2 dual logistic map under AWGN channel.

In Figure 3.7 we have compared the performance of different chaotic maps under AWGN for the spreading factor (β=4) and $T_c = 1$. Our simulations indicate that the BER performance of tent map is superior to the performance offered by other chaotic maps. Hence, the design of a combined system offering security as well as superior BER over AWGN channels can be achieved by a CSK scheme which uses tent map combined with Alamouti scheme. Our simulation results indicate that the use of 2×2 Alamouti scheme can provide a gain of approximately 6 dB at a BER of 10^{-5} as compared to SISO systems when both schemes employ chaotic modulation techniques. A careful inspection of Figure 3.7 reveals that the performance of 2×2Alamouti scheme without chaos and the performance of CSK modulated 2×2Alamouti scheme are nearly identical. This implies that the BER degradation seen with the use of chaotic schemes has been successfully overcome by the 2×2Alamouti STBC. Thus this system offers security as well as good BER performance. It is observed that the black graph represent BER curve for simulated CSK-tent map which is a large extent align with the green curve represented theoretical BER computed in equation (3.17).

In Figure 3.8 we have compared the performance of different chaotic maps under Rayleigh fading channel (spreading factor (β=4)). We observed that there is gain of 3 dB as compared to SISO communication system.

The BER performance of 2×1Alamouti schemes combined with CSK for different chaotic maps under AWGN have been computed and plotted in Figure 3.9.

It is observed in Figure 3.10 that under Rayleigh fading conditions, tent map gives superior BER performance as compared to other maps. Further, it can be observed that the 2×1 Alamouti scheme combined with CSK gives approximately 2 dB improvement (at a BER of 10^{-4}) when compared to SISO scheme employing CSK. Also a careful inspection of Figure 3.10 reveals that the performance of 2×1 Alamouti scheme without chaotic modulation and the performance of CSK modulated 2×1 Alamouti scheme are nearly identical (A difference of 0.75 dB at a BER of 10^{-5} is observed).

It is clear that the use of antenna diversity combined with a suitable channel code (Alamouti scheme) reduces the degradation seen when CSK techniques are used over fading channels. Such combined MIMO-CSK schemes can be judiciously employed on channels where high levels of data integrity and security are simultaneously required. This improvement is realized with only a marginal increase in computational complexity at the transmitter and receiver.

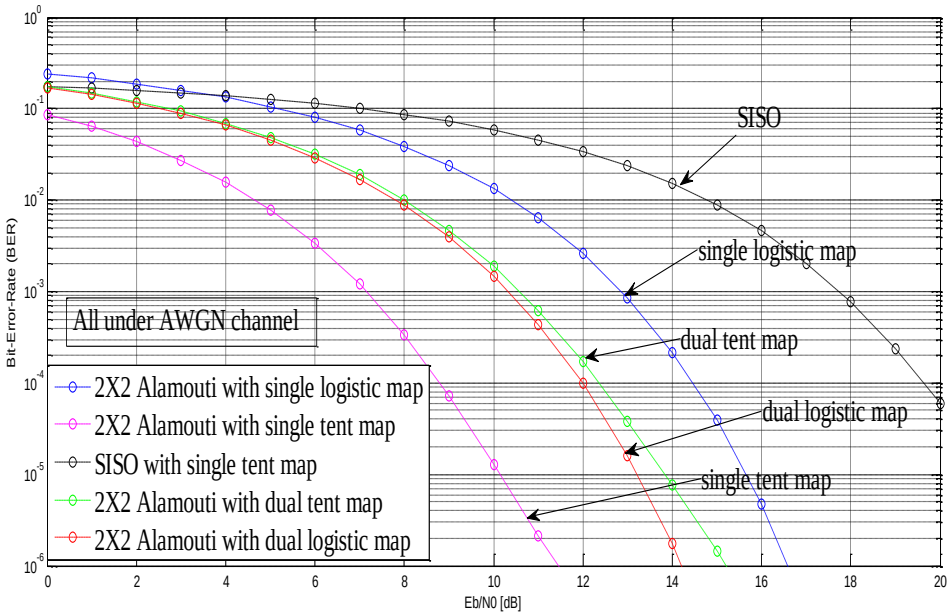

Figure 3.6 BER performances for different chaotic maps using 2 × 2 Alamouti and SISO communication systems under AWGN channel assumption

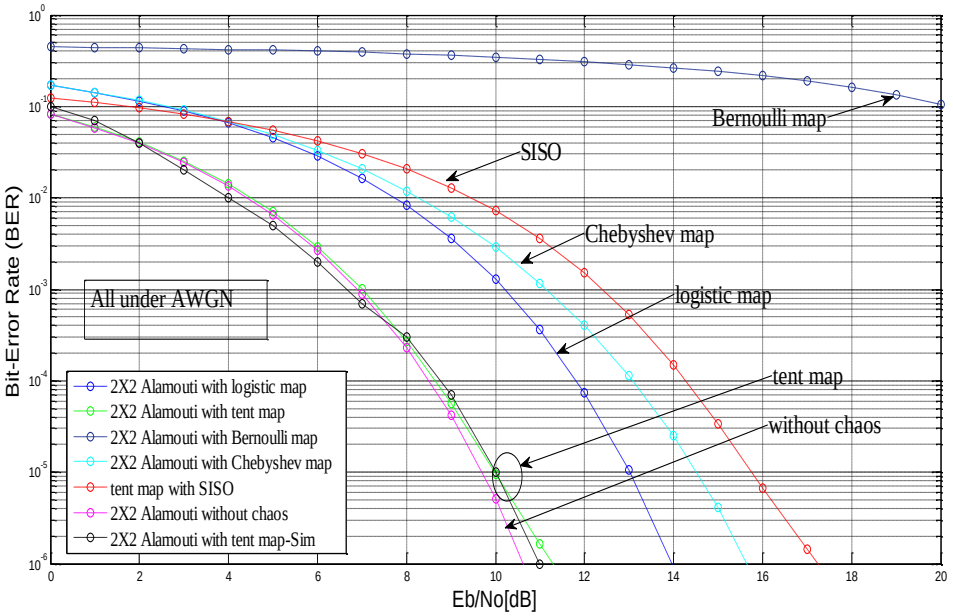

Figure 3.7 BER of 2 × 2 Alamouti for various types of chaotic maps under AWGN

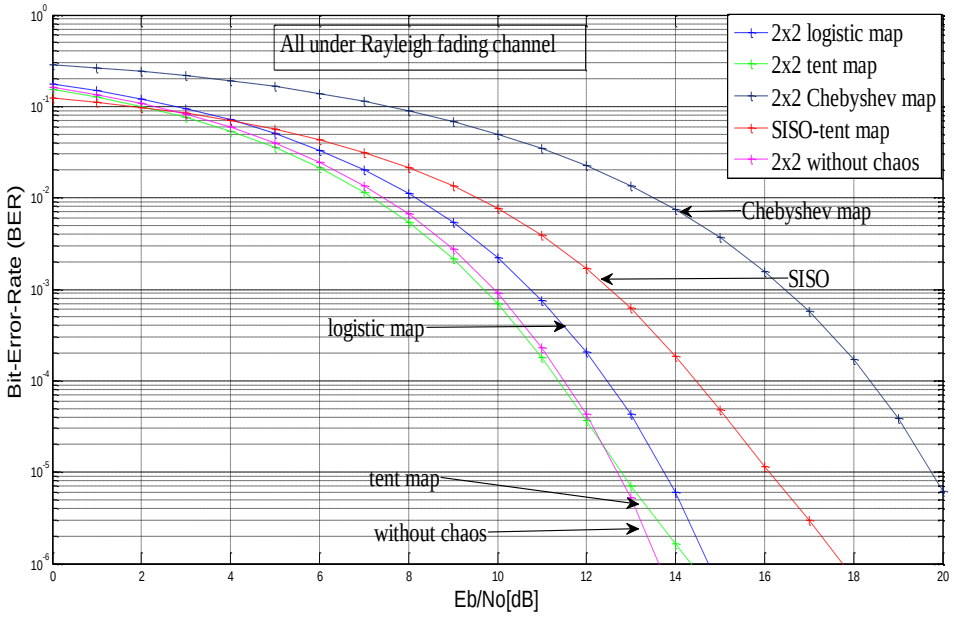

Figure 3.8 BER of 2 × 2 Alamouti for various types of chaotic maps under Rayleigh fading channel

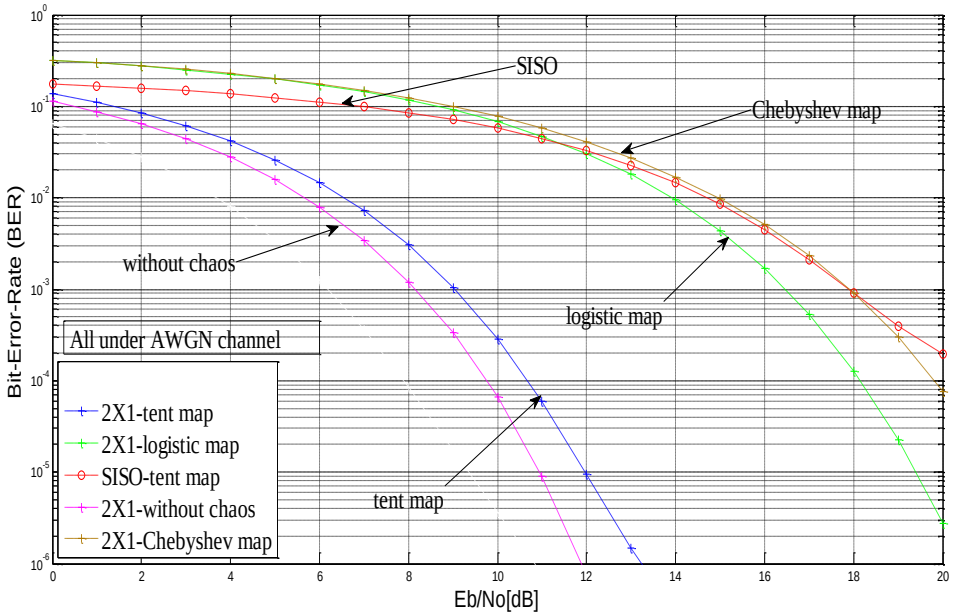

Figure 3.9 BER of 2 × 1 Alamouti for various types of chaotic maps under AWGN channel

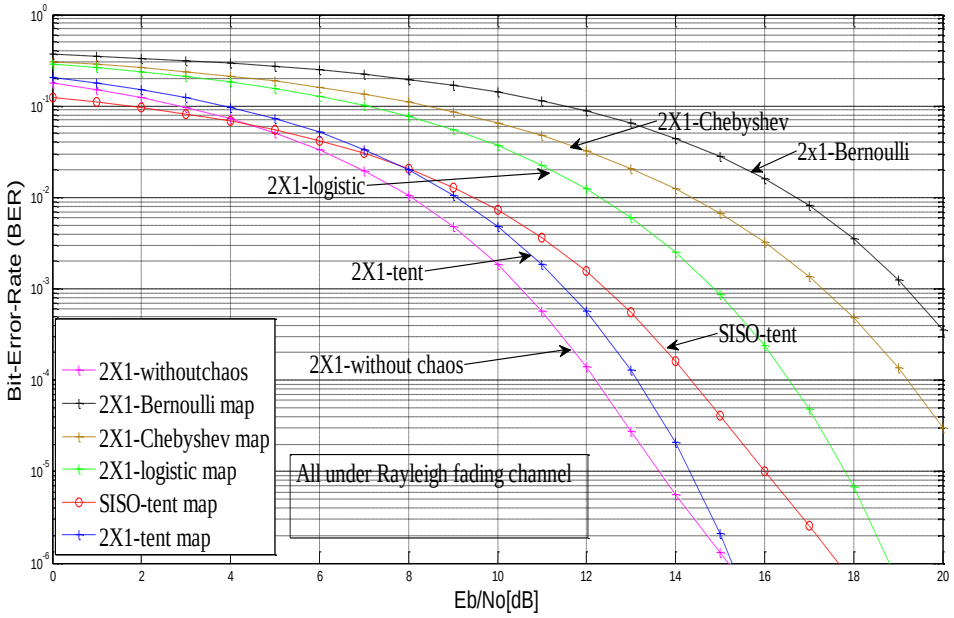

Figure 3.10 BER of 2 × 1 Alamouti for various types of chaotic maps under Rayleigh fading channel

3.4 DCSK-MIMO Communication System

3.4.1 Differential Chaos Shift Keying (DCSK)

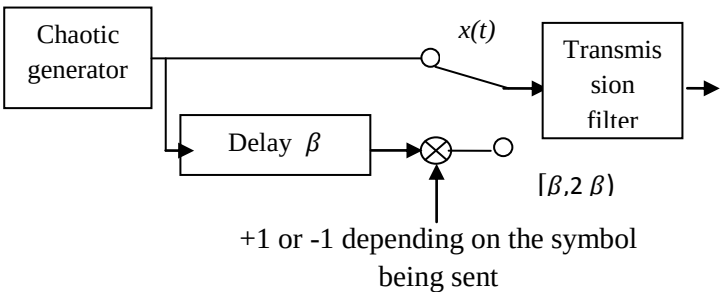

Figure 3.11 DCSK modulator

Figure 3.11 shows the block diagram of a DCSK modulation scheme in which every transmitted symbol is represented by two consecutive segments of chaotic signals. The first one serves as the reference signal whereas the second one carries the information bearing symbol. If a "+1" is to be transmitted, the data-bearing signal will be identical to the reference signal, and if a "-1" is to be transmitted, an inverted

version of the reference signal will be used as the data-bearing signal. [Stavroulakis P., 2006]. Let 2β be the spreading factor, defined as the number of chaotic samples sent for each bit, where β is an integer. During the lth bit duration, the output of the transmitter e_x is

$$e_x = \begin{cases} x_k & for\ 1 < k \leq \beta \\ s_l x_{k-\beta} & for\ \beta < k \leq 2\beta \end{cases} \tag{3.18}$$

Where x_k is the chaotic sequence used as reference and $x_{k-\beta}$ is the delayed version of the reference sequence. At the receiver, the correlation of the reference signal and the data bearing signal is achieved. This can be accomplished by correlating the incoming signal with half symbol-delayed version of itself as shown in Figure 3.12.

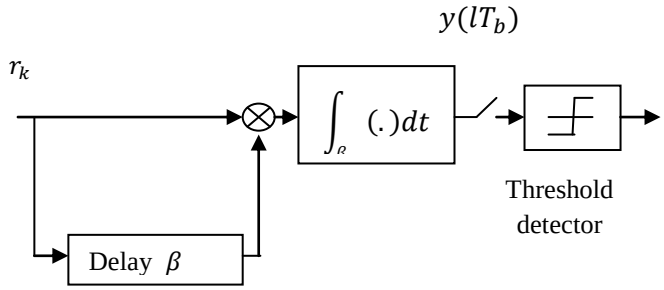

Figure 3.12 DCSK demodulator

3.4.2 DCSK-2×2 Alamouti Scheme

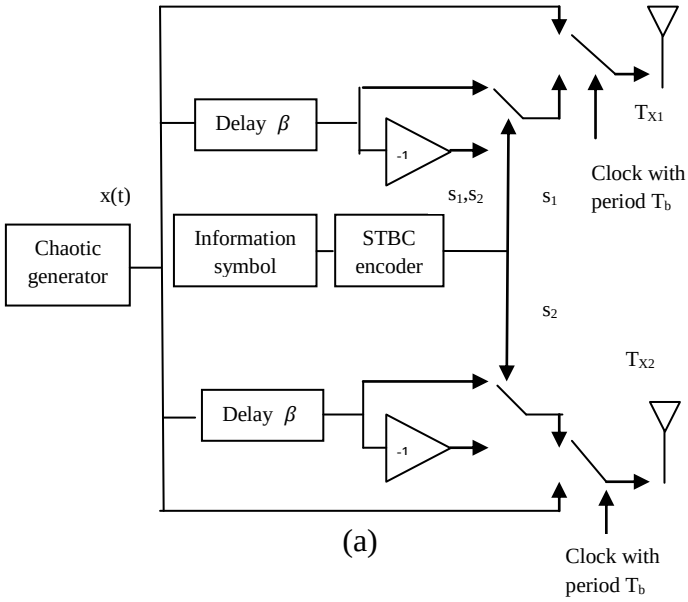

(a)

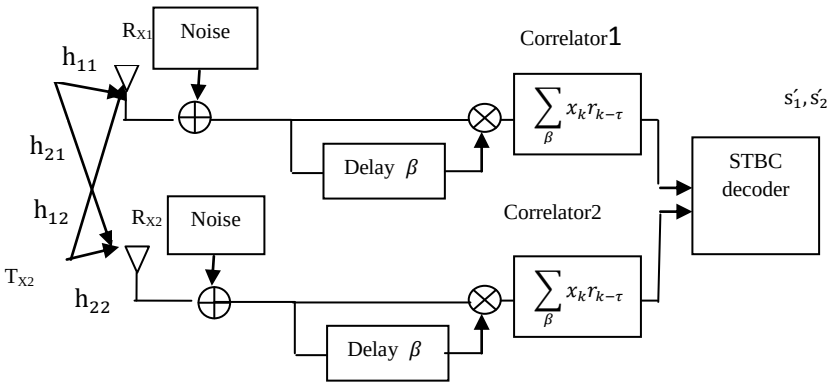

(b)

Figure 3.13 DCSK-MIMO a) Transmitter with two antennas, b) Receiver with two antennas [Huanfei M. and Haibin K., 2009]

In Figure 3.13, we consider an Alamouti scheme with two transmitter antennas and two receiver antenna. The Alamouti matrix for symbol s_1 and s_2 is as in equation (3.10). This matrix form leads to the design of the block diagram for the DCSK with the STBC coder, which is illustrated in Figure 3.13a.

On the receiver side, in addition to fading, the distorted and noisy signal is received as shown in Figure 3.13b. The correlator is used to estimate the symbols by correlating the two chips and then decoded by STBC decoder.

Equations below show the structure of the transmitted signal in time $2T_b = 4\beta T_c$, where the time symbol $T_b = 2\beta T_c$, and T_c is the time chip.

The design of the transmitted signal for time $[0, \beta T_c]$ from T_{x1} and T_{x2} is x_k.

The design of the transmitted signal for time $[\beta T_c, 2\beta T_c]$ from T_{x1} and T_{x2} is

$$U_{[\beta T_c, 2\beta T_c]}(t) = s_1 x_{k-\beta} + s_2 x_{k-\beta} \tag{3.19}$$

The design of the transmitted signal for time $[2\beta T_c, 3\beta T_c]$ from T_{x1} and T_{x2} is $x_{k-2\beta}$

The design of the transmitted signal for time $[3\beta T_c, 4\beta T_c]$ from T_{x1} and T_{x2} is

$$U_{[3\beta T_c, 4\beta T_c]}(t) = -s_2^* x_{k-3\beta} + s_1^* x_{k-3\beta} \tag{3.20}$$

The communication channels is received on the first antenna R_{x1} , where h_{11}, h_{21}, h_{12} and h_{22} are the channel gain as shown in Figure 3.13b, the received signal is first correlated to delayed replica of the received signal, and then decoded by STBC decoder. We consider the time chip T_c=1.

The received signal on R_{x1} for time $[0, \beta T_c]$

$$r_{11}(t) = h_{11}x_k + h_{21}x_k + n_{k,1} \tag{3.21}$$

The received signal on R_{x1} for time $[\beta T_c, 2\beta T_c]$

$$r_{21}(t) = h_{11}s_1x_{k-\beta} + h_{21}s_2x_{k-\beta} + \mathrm{n_{k,1}} \tag{3.22}$$

The received signal on R_{x1} for time $[2\beta T_c, 3\beta T_c]$

$$r_{31}(t) = h_{11}x_{k-2\beta} + h_{21}x_{k-2\beta} + \mathrm{n_{k,2}} \tag{3.23}$$

The received signal on R_{x1} for time $[3\beta T_c, 4\beta T_c]$

$$r_{41}(t) = -h_{11}s_2^*x_{k-3\beta} + h_{21}s_1^*x_{k-3\beta} + \mathrm{n_{k,2}} \tag{3.24}$$

The received signal on R_{x2} for time $[0, \beta T_c]$

$$r_{12}(t) = h_{12}x_k + h_{22}x_k + n_{k,1} \tag{3.25}$$

The received signal on R_{x2} for time $[\beta T_c, 2\beta T_c]$

$$r_{22}(t) = h_{12}s_1x_{k-\beta} + h_{22}s_2x_{k-\beta} + \mathrm{n_{k,1}} \tag{3.26}$$

The received signal on R_{x2} for time $[2\beta T_c, 3\beta T_c]$

$$r_{32}(t) = h_{12}x_{k-2\beta} + h_{22}x_{k-2\beta} + \mathrm{n_{k,2}} \tag{3.27}$$

The received signal on R_{x2} for time $[3\beta T_c, 4\beta T_c]$

$$r_{42}(t) = -h_{12}s_2^* x_{k-3\beta} + h_{22}s_1^* x_{k-3\beta} + \mathrm{n_{k,2}} \tag{3.28}$$

The energy of a given bit l is $E_b^{(l)} = \sum_{k=1}^{\beta} x_k^{(l)2}$.

After correlation $(r_k, r_{k-\beta})$, the output of correlator 1 y_{11} in Figure 3.13, after time block $[0,2\beta T_c]$ is

$$y_{11} = \sum_{k=1}^{\beta}\left[h_{11}s_1x_k^{(l)} + h_{21}s_2x_k^{(l)} + n_{k+\beta}\right]\left[h_{11}x_k^{(l)} + h_{21}x_k^{(l)} + n_k\right]$$

$$= \sum_{k=1}^{\beta}\left(h_{11}^2 s_1 x_k^{(l)2} + h_{11}h_{21}s_1x_k^{(l)2} + h_{11}s_1x_k^{(l)}n_k\right) +$$

$$\sum_{k=1}^{\beta}(h_{21}h_{11}s_2x_k^{(l)2} + h_{21}^2 s_2 x_k^{(l)2} + h_{21}s_2x_k^{(l)}n_k)$$

$$+ \sum_{k=1}^{\beta}(h_{11}x_k^{(l)}n_{k+\beta} + h_{21}x_k^{(l)}n_{k+\beta} + n_k n_{k+\beta})$$

The equivalent baseband model on $[0,2\beta]$ of the received symbol on the first antenna is

$$y_{11} = E_b^{(l)}(h_{11}^2 s_1 + h_{21}^2 s_2) + \left(h_{11}h_{21}(s_1 + s_2)\right)\sum_{k=1}^{\beta} x_k^{(l)2} + (h_{11}s_1$$

$$+ h_{21}s_2)\sum_{k=1}^{\beta} x_k^{(l)}n_k + (h_{11} + h_{21})\sum_{k=1}^{\beta} x_k^{(l)}n_{k+\beta} + \sum_{k=1}^{\beta} n_k n_{k+\beta}$$

The equivalent baseband model of the received symbol on the first antenna R_{x1} for time $[0,2\beta T_c]$

$$y_{11} = E_b^{(l)}(h_{11}^2 s_1 + h_{21}^2 s_2) + E_b^{(l)}(h_{11}h_{21}(s_1 + s_2)) + N_{11} \tag{3.29}$$

$$y_{11} = E_b^{(l)}(h_{11}^2 s_1 + h_{21}^2 s_2 + \mathrm{h_{11}h_{21}s_1} + \mathrm{h_{11}h_{21}s_2}) + \mathrm{N_{11}}$$
$$= E_b^{(l)}\big((h_{11}^2 + h_{11}h_{21})s_1 + (h_{21}^2 + h_{11}h_{21})s_2\big) + N_{11}$$

Let , $h_{11}^2 + \mathrm{h_{11}h_{21}} = H_{11}$ and $h_{21}^2 + \mathrm{h_{11}h_{21}} = H_{21}$

Then,

$$Y_{11} = E_b^{(l)}(H_{11}s_1 + H_{21}s_2) + N_{11} \tag{3.30}$$

Similarly,

The equivalent baseband model of the received symbol on the first antenna R_{x1} for time $[2\beta T_c, 4\beta T_c]$

$$Y_{21} = E_b^{(l)}(-H_{11}s_2^* + H_{21}s_1^*) + N_{21} \tag{3.31}$$

where N_{11} and N_{21} are zero mean Gaussian noise component, from above equations

$$(h_{11}s_1 + h_{21}s_2)\sum_{k=1}^{\beta} x_k^{(l)} n_k + (h_{11} + h_{21})\sum_{k=1}^{\beta} x_k^{(l)} n_{k+\beta} + \sum_{k=1}^{\beta} x_k^{(l)} n_{k+\beta} = N_{11} \tag{3.32}$$

and

$$(-h_{11}s_2^* + h_{21}s_1^*)\sum_{k=1}^{\beta} x_k^{(l)} n_k + (h_{11} + h_{21})\sum_{k=1}^{\beta} x_k^{(l)} n_{k+\beta} + \sum_{k=1}^{\beta} n_k n_{k+\beta} = N_{21} \tag{3.33}$$

The equivalent baseband model of the received symbol on the second antenna $\mathrm{R_{x2}}$ for time $[0,2\beta\mathrm{T_c}]$

$$Y_{12} = E_b^{(l)}(H_{12}s_1 + H_{22}s_2) + N_{12} \tag{3.34}$$

The equivalent baseband model of the received symbol on the second antenna $\mathrm{R_{x2}}$ for time $[2\beta\mathrm{T_c}, 4\beta\mathrm{T_c}]$

$$Y_{22} = E_b^{(l)}(-H_{12}s_2^* + H_{22}s_1^*) + N_{22} \tag{3.35}$$

Where $h_{12}^2 + \mathrm{h_{12}h_{22}} = H_{12}$, $h_{22}^2 + h_{12}h_{22} = H_{22}$ and $N_{12} = N_{11}$ and $N_{22} = N_{21}$.

The channel model, estimation and computation of the transmitted bits is similar to 2×2 Alamouti scheme using equations (3.11), (3.12) and (3.13) respectively.

3.4.3 DCSK-2×1 Alamouti Scheme

The Alamouti matrix for symbol s_1 and s_2 is as in equation (3.10).

The design of the transmitted signal of 2×1 Alamouti is as in Almouti 2×2 above.

The received signal for time $[0, \beta T_c]$

$$r_1(t) = h_1 x_k + h_2 x_k + n_{k,1} \tag{3.36}$$

The received signal for time $[\beta T_c, 2\beta T_c]$

$$r_2(t) = h_1 s_1 x_{k-\beta} + h_2 s_2 x_{k-\beta} + n_{k,1} \tag{3.37}$$

The received signal for time $[2\beta T_c, 3\beta T_c]$

$$r_3(t) = h_1 x_{k-2\beta} + h_2 x_{k-2\beta} + n_{k,2} \tag{3.38}$$

The received signal for time $[3\beta T_c, 4\beta T_c]$

$$r_4(t) = -h_1 s_2^* x_{k-3\beta} + h_2 s_1^* x_{k-3\beta} + n_{k,2} \tag{3.39}$$

The equivalent baseband model of the received symbol for time $[0,2\beta T_c]$

$$Y_1 = E_b^{(l)}(H_1 s_1 + H_2 s_2) + N_1 \tag{3.40}$$

The equivalent baseband model of the received symbol for time $[2\beta T_c, 4\beta T_c]$

$$Y_2 = E_b^{(l)}(-H_1 s_2^* + H_2 s_1^*) + N_2 \tag{3.41}$$

where $N_1$and N_2 represent noise components while $h_1$and h_2 represent the channel gains.

The channel model, estimation and computation of the transmitted bits is similar to 2×2 Alamouti scheme using equations (3.11), (3.12) and (3.13) respectively.

3.4.4 BER Performance Analysis

Considering the bit energy (or chaotic chips) as a deterministic variable, the decision variable at the output of the correlator is necessarily a random Gaussian variable. The overall error probability expression of the DCSK-MIMO system for 2×2 Alamouti and 2 × 1 Alamouti are given in (3.42) and (3.43) respectively.

$$P_e\left(E_b^{(l)}\right) = \frac{1}{2} erfc\left(\sqrt{\frac{2(H_{11}^2+H_{12}^2+H_{21}^2+H_{22}^2)E_b^{(l)}}{N_0}(3+\frac{\beta N_0}{4E_b^{(l)}})^{-1}}\right) \quad (3.42)$$

For 2×1 Alamouti, the error probability expression is given by

$$P_e\left(E_b^{(l)}\right) = \frac{1}{2} erfc\left(\sqrt{\frac{2(H_1^2+H_2^2)E_b^{(l)}}{N_0}(3+\frac{\beta N_0}{4E_b^{(l)}})^{-1}}\right) \quad (3.43)$$

$$BER = Q[E(x)/\sqrt{Var(x)}]$$

Where

$$Q(x) = \int_x^{+\infty} \frac{1}{\sqrt{2\pi}} \exp(-u^2/2)$$

$$BER = Q[E_{xi} \times 2(\sum_{n,p=1}^{2} H_{n,p}^2)^{\frac{1}{2}}(\sum_{i=0}^{\beta-1} \frac{x_i^{(l)2}}{N_0(\beta\sigma^2)})^{\frac{1}{2}}(3+\frac{\beta N_0}{4E_b^{(l)}})^{-1} \ ] = E_{xi} \times$$

$$(\sum_{i=0}^{\beta-1} \frac{x_i^{(l)2}}{N_0(\beta\sigma^2)})^{\frac{1}{2}} 2(H_{11}^2 + H_{12}^2 + H_{21}^2 + H_{22}^2)^{\frac{1}{2}}.(3+\frac{\beta N_0}{4E_b^{(l)}})^{-1}$$

$\sum_{i=0}^{\beta-1} x_i^{(l)2} = E_b^{(l)}$ is the chaotic symbol energy, and $(\sum_{i=0}^{\beta-1} \frac{E_{xi}}{(\beta\sigma_X^2)^{\frac{1}{2}}}) = \int_0^{\infty} p\left(E_b^{(l)}\right) dE_b^{(l)}$,

then

$$BER = \int_0^{\infty} \frac{1}{2} erfc\left(\sqrt{\frac{2(H_{11}^2+H_{12}^2+H_{21}^2+H_{22}^2)E_b^{(l)}}{N_0}(3+\frac{\beta N_0}{4E_b^{(l)}})^{-1}}\right) p\left(E_b^{(l)}\right) dE_b^{(l)} \quad (4.44)$$

and for 2×1 Alamouti-DCSK is

$$BER = Q[E_{xi} \times 2(\sum_{n=1}^{2} H_n^2)^{\frac{1}{2}}(\sum_{i=0}^{\beta-1} \frac{x_i^{(l)2}}{N_0(\beta\sigma^2)})^{\frac{1}{2}}(3 + \frac{\beta N_0}{4E_b^{(l)}})^{-1} \ ] =$$

$$E_{xi} \times (\sum_{i=0}^{\beta-1} \frac{x_i^{(l)2}}{N_0(\beta\sigma^2)})^{\frac{1}{2}} 2(H_1^2 + H_1^2)^{\frac{1}{2}}.(3 + \frac{\beta N_0}{4E_b^{(l)}})^{-1}$$

$\sum_{i=0}^{\beta-1} x_i^{(l)2} = E_b^{(l)}$ is the chaotic symbol energy, and $(\sum_{i=0}^{\beta-1} \frac{E_{xi}}{(\beta\sigma_X^2)^{\frac{1}{2}}}) = \int_0^{\infty} p\left(E_b^{(l)}\right) dE_b^{(l)}$,

then

$$BER = \int_0^{\infty} \frac{1}{2} erfc\left(\sqrt{\frac{2(H_1^2+H_2^2)E_b^{(l)}}{N_0}(3 + \frac{\beta N_0}{4E_b^{(l)}})^{-1}}\right) p\left(E_b^{(l)}\right) dE_b^{(l)} \qquad (3.45)$$

where $p\left(E_b^{(l)}\right)$ is the probability density function of the energy $E_b^{(l)}$. The BER expression is the result of the integral given in equations (3.44) and (3.45). We must first determine the bit energy distribution. Since the pdf seems to be intractable, the only way to evaluate the BER is to compute the histogram of the bit energy followed by a numerical integration. Figure 3.14 shows the histogram of the bit energy, for $\beta = 10$ and 50000 samples.

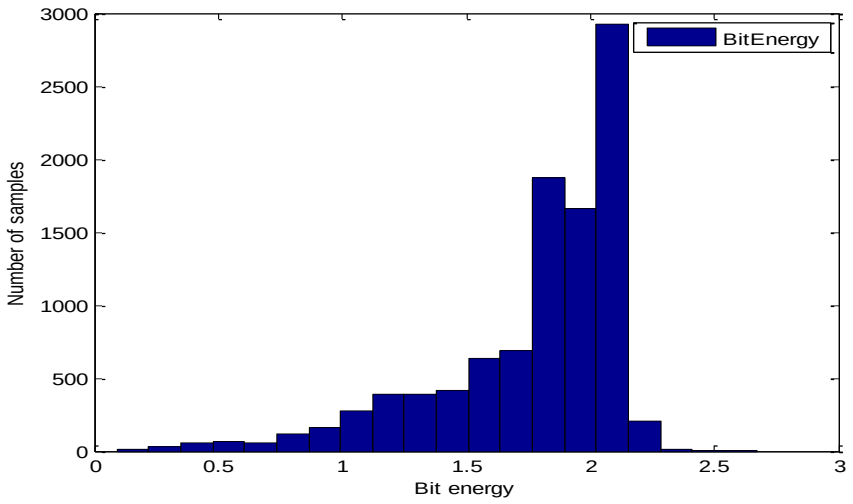

Figure 3.14 Histogram of the bit energy for a DCSK-MIMO communication system

After numerical integration the BER expression for 2×2 Alamouti is given by,

$$BER \approx \sum_{l=1}^{m} \frac{1}{2} erfc\left(\sqrt{\frac{2(H_{11}^2+H_{12}^2+H_{21}^2+H_{22}^2)E_b^{(l)}}{N_0}} \left(3+\frac{\beta N_0}{4E_b^{(l)}}\right)^{-1} \right) p\left(E_b^{(l)}\right) \quad (3.46)$$

For 2× 1 Alamouti, the corresponding BER is given by,

$$BER \approx \sum_{l=1}^{m} \frac{1}{2} erfc\left(\sqrt{\frac{2(H_1^2+H_2^2)E_b^{(l)}}{N_0}} \left(3+\frac{\beta N_0}{4E_b^{(l)}}\right)^{-1} \right) p\left(E_b^{(l)}\right) \quad (3.47)$$

Where m is the number of histogram classes and $p\left(E_b^{(l)}\right)$is the probability of having the energy.

3.4.5 Simulation Results and Discussion

In Figure 3.15 we have compared the performance of different chaotic maps under AWGN. The spreading factor (β=10) and $T_c = 1$. Our simulations indicate that the tent map gives best performance when compared to other chaotic maps. Hence, the use of tent map is preferred over other maps because it offers superior BER performance in addition to security. Additionally, our simulation results indicate that the use of 2×2 Alamouti scheme provides a gain of 2 dB as compared to SISO when both schemes employ chaotic techniques. In SISO systems using BPSK, chaotic techniques give a degradation of 5 dB in BER performance. This degradation is compensated by the use of MIMO systems.

From Figure 3.15 it can be seen that up to a BER of 10^{-5}, chaos systems maintain approximately the same BER performance as BPSK without using chaos. Additionally they provide security against eavesdroppers.

In Figure 3.15 the circle graph (black) represent BER curve for simulated DCSK-tent map which is overlapped with a maximum deviation of 0.5 dB by the blue curve represented theoretical BER computed in equation (3.46) with maximum deviation 0.5 dB.

It is observed in Figure 3.16 that under AWGN conditions, tent map gives the best BER performance as compared to other maps.

In Figure 3.17 it is observed that with the use of 2×2 and 2×1 Alamouti schemes under Rayleigh fading conditions, the performance of the 2×2 Alamouti scheme is superior by 2 dB when compared to 2×1 Alamouti scheme at 10^{-5} BER. In addition, under Rayleigh fading conditions, the performance degrades by only 1 dB for 2×2 and approximately 3 dB for 2×1 Alamouti scheme as compared to AWGN-SISO.

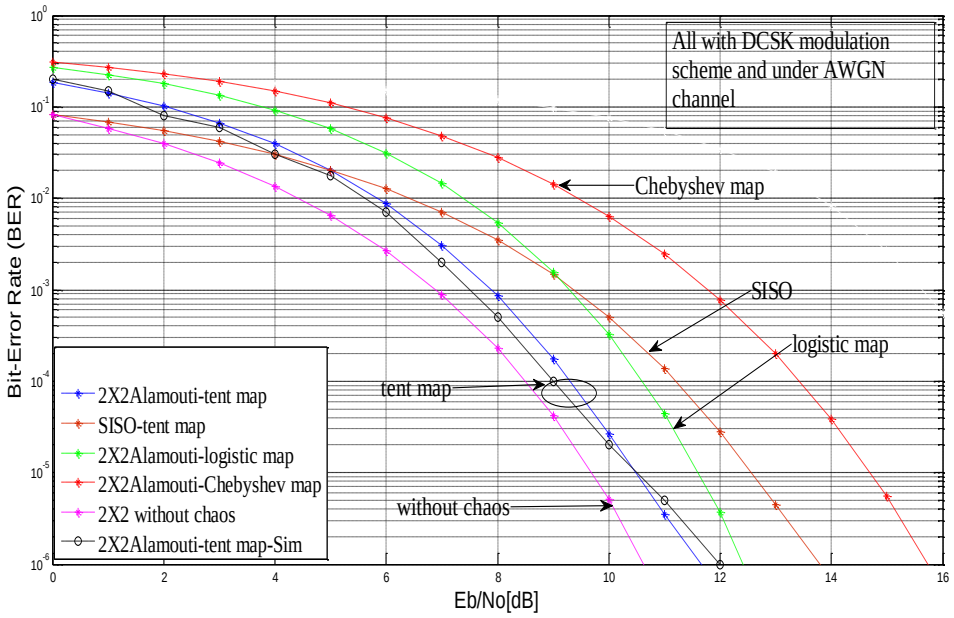

Figure 3.15 BER of 2×2 Alamouti and SISO for various types of chaotic maps

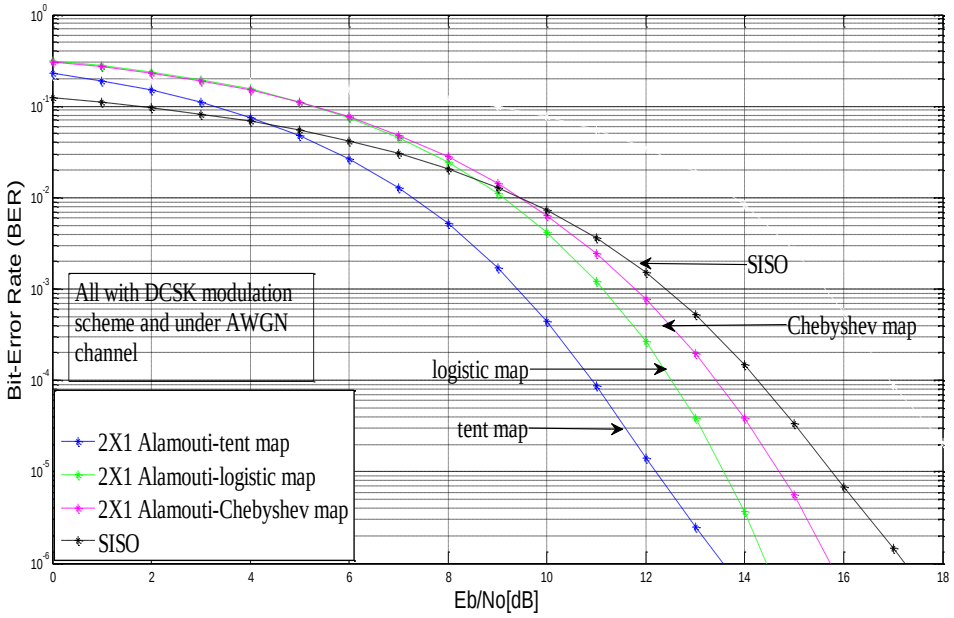

Figure 3.16 BER of 2×1 Alamouti and SISO for various types of chaotic maps

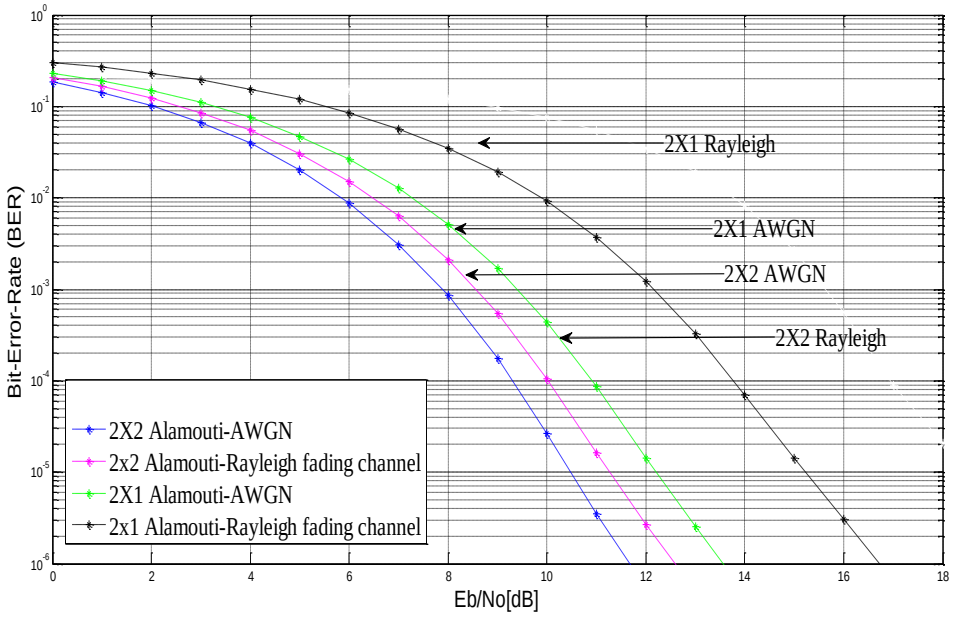

Figure 3.17 BER performances of AWGN and Rayleigh fading channel for 2×2 and 2×1 Alamouti schemes

3.5 CDSK-MIMO Modulation Scheme

In this section, we have analyzed the performance of CDSK-MIMO scheme. In the DCSK modulation scheme, the reference signal is transmitted separately from the information bearing signal. Consequently, half of the symbol duration is not used to carry information. CDSK has been proposed to transmit the information continuously and enhance the bandwidth efficiency and thus mitigate this disadvantage. [Zhibo. Z., Jinxiang W and Yizheng Y., 2010 , Stavroulakis P 2006]. The transmitted signal is the sum of the chaotic signal and a delayed version of the chaotic signal modulated by the transmitted symbol. Therefore, the transmitted signal contains both the reference signal and the information bearing signal. During the lth symbol period, the transmitted signal is given by

$$s(t) = \begin{cases} x_{k,} + x_{k-\beta}, & when\ symbol\ "+1"s\ transmitted \\ x_k - x_{k-\beta}, & when\ symbol\ "-1"s\ transmitted \end{cases} \tag{3.48}$$

Figure 3.18 shows the block diagram of a CDSK modulation scheme [Gokcen C. and Cabir V., 2010].

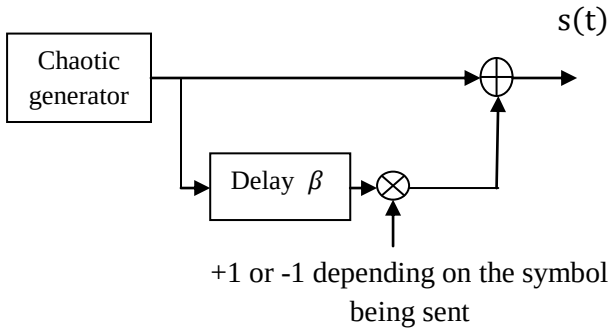

Figure 3.18 CDSK modulator

3.5.1 CDSK-2×1 Alamouti Scheme

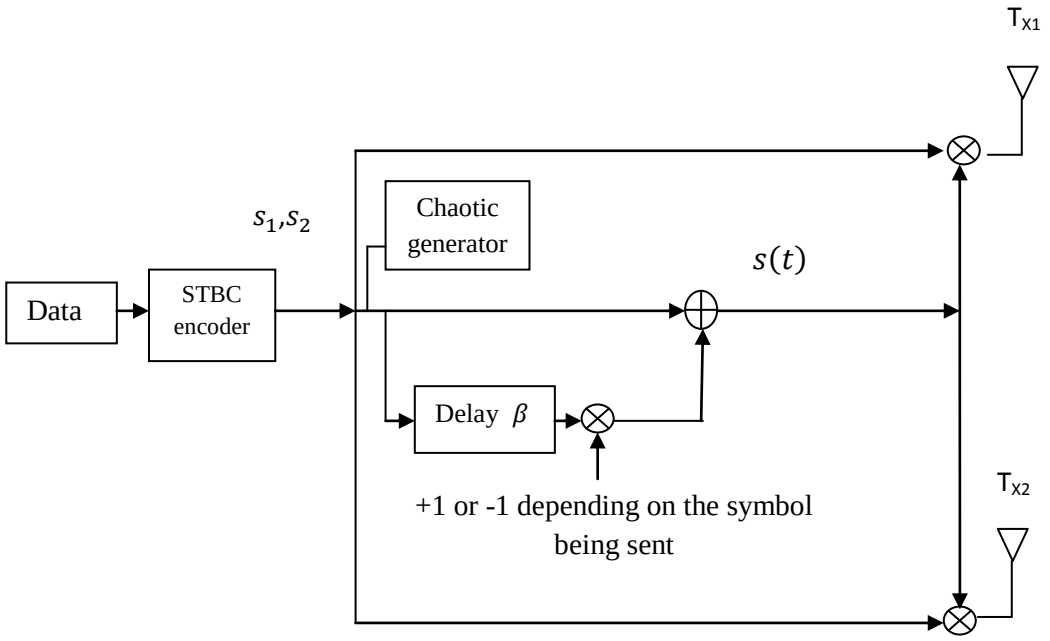

Figure 3.19 Proposed CDSK transmitter with two antennas

The Almouti matrix for symbols s_1 and s_2 is as in equation (3.10).

Figure 3.19 illustrates the transmitter side of the CDSK system with an STBC coder.

The two transmitted symbols s_1 and s_2 are spread by the chaotic sequences and then transmitted from transmitter antenna T_{x1} and transmitter antenna T_{x2}.

The design of transmitted signal of CDSK Alamouti scheme is specified in Table (3.8).

Time	$s_1(t)$from T_{x1}	$s_2(t)$from T_{x2}
$[0, \beta T_c]$	$s_1 x_k$	$s_2 x_k$
$[\beta T_c, 2\beta T_c]$	$-s_2^*(x_k + x_{k-\beta} b_l)$	$s_1^*(x_k + x_{k-\beta} b_l)$

Table 3.8

The CDSK receiver and the channel model, estimation and computation of the transmitted bits is similar to 2×2 Alamouti scheme for CDSK is same as DCSK receiver [Georges K., Francois G. and Mai V, 2011, Wai T, Francis L and Chi T, 2007, Mekhail S, Lev T. and Alexander V., 2000].

The CDSK receiver is same as the DCSK receiver. Therefore, the receiver can detect the information by multiplying the received signal and its delayed signal [Dornbusch A., 1999].

3.5.2 CDSK-2×2 Alamouti Scheme

The transmitter of CDSK-2×2 Alamouti Scheme is same as in Figure 3.20. The CDSK receiver and the channel model, estimation and computation of the transmitted bits is similar to 2×2 Alamouti scheme for CDSK is same as DCSK receiver [Mekhail S, Lev T. and Alexander V., 2000].

3.5.3 BER Performance Analysis of CDSK-MIMO

In CDSK, the output of correlator, r, in Figure 3.12.

$$y(lT_b) = \int_{(l-1)T_b}^{lT_b} r(t)r(t-\beta)dt = \int_{(l-1)T_b}^{lT_b} [x(t)+n(t)][x(t)-\beta)+n(t-\beta)dt =$$

$$\int_{(l-1)T_b}^{lT_b} x(t)x(t-\beta)dt + \int_{(l-1)T_b}^{lT_b} x(t)n(t-\beta)dt + \int_{(l-1)T_b}^{lT_b} n(t)x(t-$$

$$\beta)dt + \int_{(l-1)T_b}^{lT_b} n(t)n(t-\beta)dt =$$

$$(-1)^{m+1}\int_{(l-1)T_b}^{lT_b} x^2(t-\beta)dt + \int_{(l-1)T_b}^{lT_b} n(t)x(t-\beta)dt + (-1)^{m+1}\int_{(l-1)T_b}^{lT_b} x(t-\beta)n(t-\beta)dt + \int_{(l-1)T_b}^{lT_b} n(t)n(t-\beta)dt \quad (3.49)$$

For CDSK-MIMO

$$y(lT_b) = \int_{(l-1)T_b}^{(lT_b)} [h_{11}s_1x(t-\beta)\} + h_{21}s_2x(t-\beta) + n_1(t)].[h_{11}x(t-\beta)\} + h_{21}x(t-\beta) + n_1(t-\beta)]\,dt =$$
$$(h_{11}^2s_1 + h_{11}h_{21}s_2 + h_{11}h_{21}s_1 + h_{21}^2s_2)\int_{(l-1)T_b}^{lT_b} x^2(t-\beta)dt + (h_{11}s_1 + h_{21}s_2)\int_{(l-1)T_b}^{l(T_b)} x(t-\beta)n_1(t)dt + \int_{(l-1)T_b}^{lT_b} n_{1(t-\beta)}n_1(t)dt \quad (3.50)$$

The overall error probability expression of the CDSK-MIMO system for 2×2 Alamouti is given in (3.33).

$$P_e\left[E_b^{(l)}\right] = \frac{1}{2}erfc\left(\sqrt{\frac{(h_{11}^2+h_{12}^2+h_{21}^2+h_{22}^2)\mathrm{E_b^{(l)}}}{2N_0(1+\frac{E_b^{(l)}}{2\beta N_0}+\frac{\beta N_0}{4E_b^{(l)}})}}\right) \quad (3.33)$$

The overall BER expression of the 2×2 Alamouti -CDSK system is then given by:

$$BER = \int_0^\infty \frac{1}{2}erfc\left(\sqrt{\frac{(h_{11}^2+h_{12}^2+h_{21}^2+h_{22}^2)\mathrm{E_b^{(l)}}}{2N_0\left(1+\frac{E_b^{(l)}}{2\beta N_0}+\frac{\beta N_0}{4E_b^{(l)}}\right)}}\right)\mathrm{p}\left(\mathrm{E_b^{(l)}}\right)d\mathrm{E_b^{(l)}} \quad (3.51)$$

To compute the integral in equation (3.51), we must first have the bit energy distribution. Since the pdf seems to be intractable, the only way to evaluate the BER is to compute the histogram of the bit energy (Figure 3.13) followed by a numerical integration. After numerical integration the BER expression for 2×2 Alamouti is given by,

$$BER = \sum_{L=1}^{m} \frac{1}{2} erfc\left(\sqrt{\frac{(h_{11}^2+h_{12}^2+h_{21}^2+h_{22}^2)\mathrm{E}_\mathrm{b}^{(\mathrm{l})}}{2N_0\left(1+\frac{E_b^{(l)}}{2\beta N_0}+\frac{\beta N_0}{4E_b^{(l)}}\right)}} \right) \mathrm{p}\left(\mathrm{E}_\mathrm{b}^{(\mathrm{l})}\right) \quad (3.52)$$

3.6 Comparison between Different Chaotic Modulation Schemes

In this part of chapter three, we compare between digital modulations schemes with MIMO communication system for coherent and non-coherent chaos-based communications. The performance of coherent and non-coherent chaotic modulation schemes combined with MIMO communication system over AWGN channel and Rayleigh fading channel is evaluated and compared.

In case of SISO-AWGN channel as shown in Figure 3.20, the order of increasing BER performance can be observed as non-coherent CDSK, DCSK and coherent CSK with $\beta = 8$. Coherent CSK gives 3 dB gain in BER performance at 10^{-5} as compared to non-coherent DCSK. Similarly, non-coherent DCSK gives a gain of 1.5 dB at 10^{-5} BER as compared to non-coherent CDSK. But, when we consider a fading channel (in this case, SISO-Rayleigh fading channel), the order of increasing BER performance charges to CDSK, CSK and DCSK. In this case, non-coherent DCSK gives 2 dB gain as compared to coherent CSK at 10^{-4} BER. Similarly, coherent CSK gives 1dB gain as compared to non-coherent CDSK at BER of 10^{-4}. Thus these simulations seem to indicate that for wireless applications, non-coherent DCSK can be preferred over coherent CSK and non-coherent CDSK in term of BER performance but it is less secure. In case of AWGN channel implementing 2×2 Alamouti scheme, as shown in Figure 3.21, the order of increasing BER performance is CDSK, DCSK and CSK. Coherent CSK gives 2.5 dB gain as compared to non-coherent DCSK. Similarly, non-coherent DCSK gives 3 dB gain as compared to non-coherent CDSK.

As compared to CSK-SISO, implementing 2×2 Alamouti scheme gives 5 dB gain in BER performance under AWGN channel. In case of fading channel (Rayleigh), implementing 2×2 Alamouti scheme as shown in Figure 3.22, the increasing order of

BER performance comes out to be CDSK,CSK and DCSK. Non-coherent DCSK gives 2 dB gain as compared to coherent CSK.

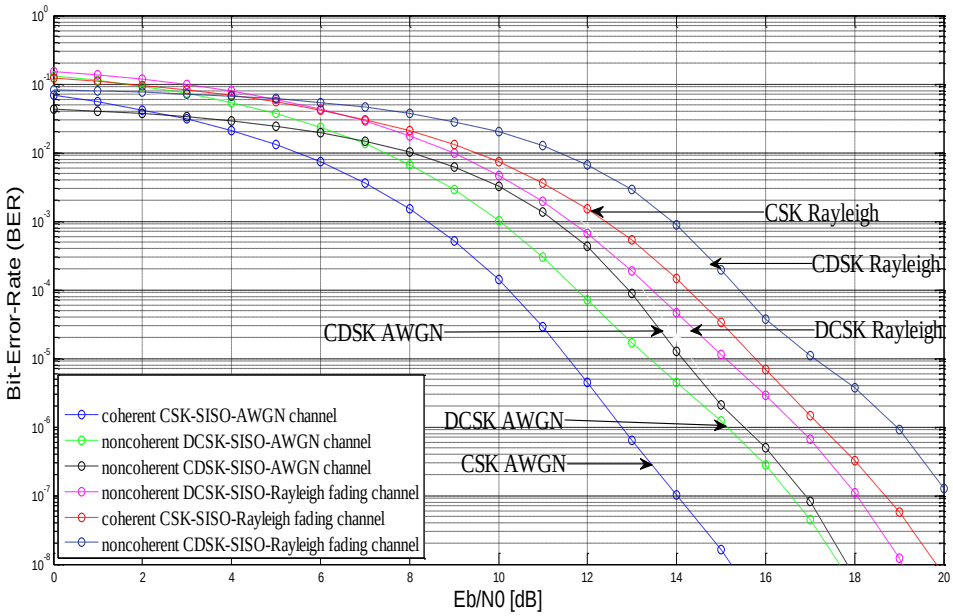

Figure 3.20 Coherent and non-coherent chaotic-SISO under AWGN and Rayleigh fading channels

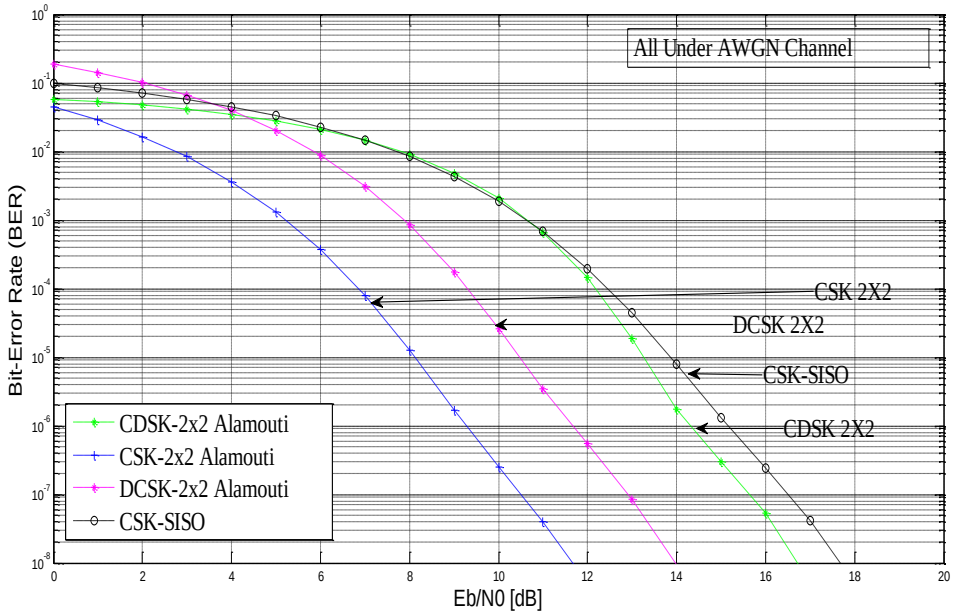

Figure 3.21 Coherent and non-coherent chaotic-2×2 under AWGN channel

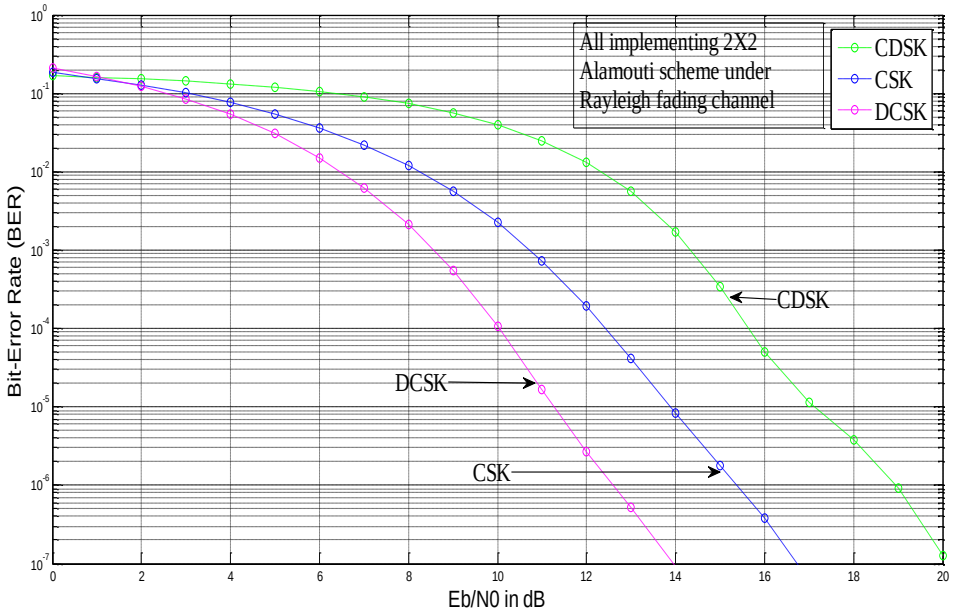

Figure 3.22 Coherent and non-coherent chaotic-2×2under Rayleigh fading channel

3.7 Conclusions

The BER performance of 2×2 Alamouti and 2×1 Alamouti schemes combined with CSK and DCSK for different chaotic maps under AWGN and Rayleigh fading channel conditions have been computed and plotted. These schemes can provide additional benefit of improved data security along with superior BER performance. In addition, the BER performance of 2×2 Alamouti and 2×1 Alamouti schemes combined with DCSK for different chaotic maps under different fading channel conditions have been computed and plotted.

It can be concluded from these results that implementing 2×2 Alamouti scheme with DCSK modulation technique yields better BER performance. Hence, it is the superior option for wireless applications under poor channel conditions.

We have compared our work implementing tent map with papers implementing Chebyshev and logistic chaotic maps [Wai T, Francis L., and Chi T., 2006, Chen Y, Shi Y and Li H., 2009]. For a SISO-DCSK technique under AWGN channel,

implementing chaotic tent map gives 4 dB gain as compared to Chebyshev map and 1.5 dB as compared to logistic map in BER performance for BER of 10^{-4} for β=8. For a SISO-DCSK technique under Rayleigh fading channel, implementing chaotic tent map gives 3 dB gain as compared to logistic in BER performance for BER of 10^{-2}. For a SISO-CDSK technique under AWGN channel, implementing chaotic tent map gives 3 dB gain as compared to Chebyshev chaotic map [Wai T, Francis L., and Chi T, 2006].

The Chaotic modulation schemes are combined with MIMO technique to increase the BER performance under AWGN and Rayleigh fading channel.

Low spreading factor (β) helps in reducing the complexity of the system and for a high β, the energy tends to be constant and the chaotic properties such as non-periodicity will be lost. At the same time, the required energy per symbol reduces with reduction in β. The proposed technique thus helps in reduction in complexity and energy per symbol without compromising in security due to non-periodic behavior of chaotic sequences.

BER performance for different chaotic modulation schemes is computed using exact approach based on the probability density function of the bit energy of the chaotic sequences.

To further improve BER performance and reduce the degradation of the signal caused by multi-path fading, we propose in chapter four to use LDPC channel codes in MIMO channels.

CHAPTER 4

BER PERFORMANCE ANALYSIS OF CHAOTIC-LDPC CODED STBC SYSTEM

4.1 Introduction

The problem of ensuring information security as it is transacted over a physical channel is a very challenging problem which has attracted the attention of a number of researchers from the Communication Engineering and Computer Science community.

An eavesdropper equipped with a suitable receiver can intercept information from a wireless channel and in addition, such interceptions can go largely unnoticed. In this context, communication systems based on chaotic modulation possess certain attractive properties. Chaotic systems possess sensitive dependence on initial conditions. Further, with suitable design, it can be ensured that two chaotic systems even though starting with the same initial condition trace independent paths. This makes the trajectory of chaotic signals highly unpredictable to a potential eavesdropper and hence provides a strong foundation for interception avoidance and signal capture for long periods of time. Hence, researchers have concluded that wireless communication schemes employing chaotic modulation can be designed to be secure [Zhi D., Bing W. and Peng L, 2006]. MIMO schemes have attracted the interest of the academia and industry because they have the potential to offer a many fold increase in capacity of wireless channels when compared to conventional SISO systems.

The performance of these systems can be further improved by the use of a suitably designed Space Time Block Code (STBC) or a Space Time Trellis Code (STTC). A STBC for two transmit antennas was proposed by Alamouti [Siavash A., 1998]. Many other STBC and STTC schemes have been proposed by different researchers [Vahid T. Hamid J. and Robert C., 1999, Akinori O. and Tomoaki O., 2004].

Although the technology of multiple antennas can improve the channel capacity, the use of multiple input and multiple output antennas will also bring issues of higher computation complexity associated with signal detection and reconstruction at the receiving end of system. The main detection algorithms used in decoding of MIMO systems are Zero Forcing (ZF), Minimum Mean Square Error (MMSE) and Maximum Likelihood (ML). Amongst the algorithms specified, the ML algorithm has the best detection performance. However, this approach also has the highest computation complexity.

We have employed the simple and effective Alamouti scheme as the STBC employed along with multiple antenna transmission and reception in our study. The main advantage of this arrangement is that it improves signal quality at the receiver by simple processing across two antennas on the transmitter side. This is achieved without any feedback from the receiver to the transmitter. The additional computational complexity incurred is small.

The use of chaotic modulation can improve information security but usually compromises the BER performance [Lawrence L, Jia L and Lev T., 2006, Shilian W. and Xiaodong W., 2010].

Most communication systems operate with certain BER specifications that are specified by the user. In this chapter, we have attempted to design and evaluate suitable combinations of chaotic modulation and channel coding schemes which can provide information security along with protection against errors caused by channel impairments and noise.

The field of channel coding has been revolutionized by the discovery and deployment Low Density Parity Check Codes (LDPC) which can achieve error rate performance close to the Shannon limit [Gallager, R.G , 1962, Mackay, D.J.C. 1999, Akinori O. and Tomoaki O, 2004].

LDPC codes are a sub-class of linear block error correction codes, defined by sparse parity-check matrices using bipartite graphs [Wang L. and Li W., 2007]. Many researchers have proposed combinations of LDPC codes and MIMO systems (termed as LDPC-MIMO) which can provide excellent levels of protection against errors induced by channel induced impairments and noise.

An important issue in LDPC-MIMO systems is the decoding of the LDPC coded bit stream received over multiple antennas. A LDPC decoder should operate on soft outputs produced by the MIMO detector for the best performance [Nuwan B., Pradeepa Y., Telex N. and Attahiru A., 2009].

LDPC codes can be decoded by using a probability propagation algorithm known as the sum-product or Belief Propagation (BP) algorithm. [Wang L. and Li W., 2007].

Contributions of the thesis in Chapter 4:

- Evaluate the security and BER performance of synchronized Low-Density-Parity-Check (LDPC)-MIMO system based on chaotic technique for wireless communication systems.

4.2 Design and Mathematical Model of Chaotic-LDPC-MIMO System

4.2.1 System Structure

The block diagram (both transmitter and receiver) of the Chaotic-LDPC-MIMO communication system proposed in this thesis is shown in Figure 4.1

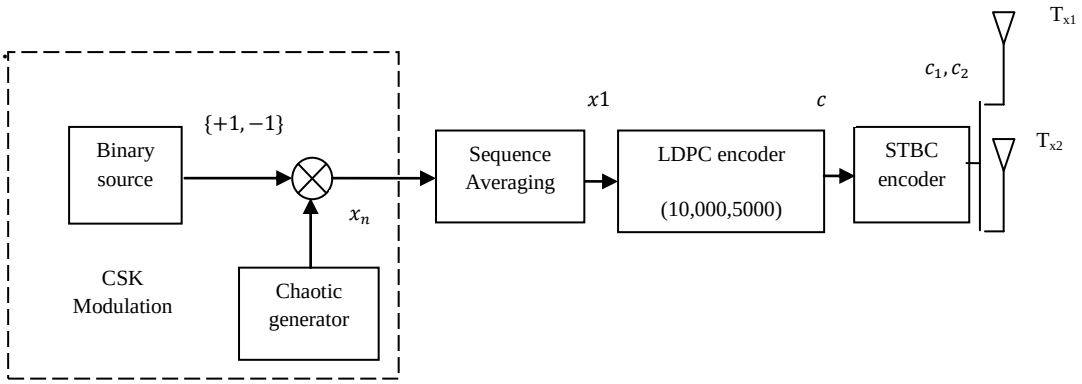

(a)

.

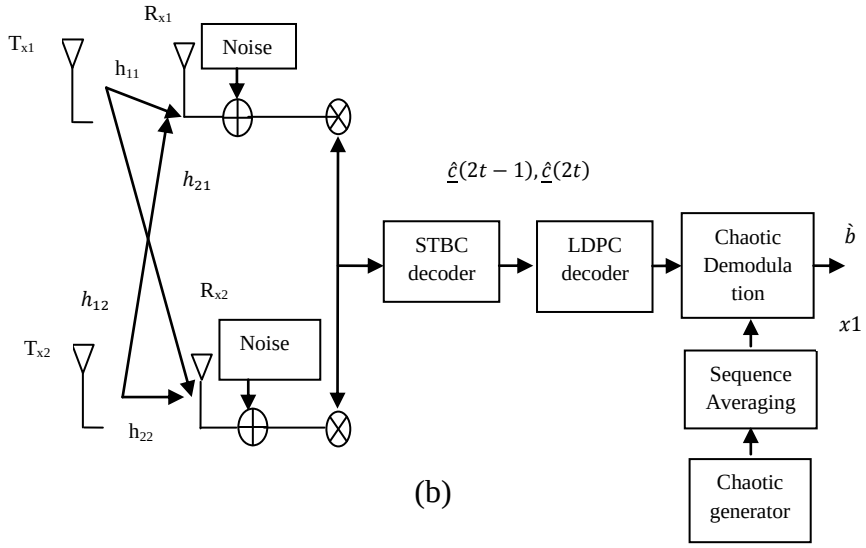

Figure 4.1 Proposed C-LDPC-MIMO system structure a) Transmitter, b) Receiver

4.2.2 Mathematical Model

The data information symbols ($B = \mp 1$) with period T_s are spread by a chaotic sequence x_k. A new chaotic sample (or chip) is generated at every time interval equal to T_c.

The real valued chaotic sequence generated by the chaotic tent map in equation (2.3) is converted into a binary valued sequence (to facilitate LDPC encoding) by the following process described in equation (4.1).

$$x1_{ik} = \begin{cases} 1, & x_{ik} < mean\ of\ x \\ 0, & x_{ik} \geq mean\ of\ x \end{cases} \tag{4.1}$$

In this equation, symbol x_{ik} represents real valued chaotic symbol and $x1_{ik}$ is the corresponding binary symbol. This processing is done by the sequence averaging block in Figure 4.1. The spread data sequence can be written as

$$U_{ik} = \sum_{i=1}^{B} \sum_{k=1}^{\beta} b_i x1_{ik} \tag{4.2}$$

The LDPC code is characterized by a generator matrix $G_{K\times N}$ (where the vector $\underline{x}$ has $K = B \times \beta$ elements), and the parity-check matrix $H_{(N-K)\times N}$. (the subscripts denote the size of the matrices). The code word is specified by,

$$c_{1\times N} = U_{1\times K}.\, G_{K\times N} \tag{4.3}$$

The generator matrix G is expressed in a systematic form,

$$G = [I_K \ : \ P_{K\times N}] \tag{4.4}$$

The MIMO scheme used in our discussion is the Alamouti design specified by,

$$c = \begin{pmatrix} c_1 & -c_2^* \\ c_2 & c_1^* \end{pmatrix} \tag{4.5}$$

where the rows of matrix represents time coordinate, the column of matrix represents space coordinate, and * represents complex transposition.
The data transmitted from transmitter 1 over time t can be given as

$$T_{x1}(t) = \begin{cases} \underline{c}(2t-1), & t = 2T_c - 1 \\ -\underline{c^*}(2t), & t = 2T_c \end{cases} \tag{4.6}$$

and the data transmitted from transmitter 2 is

$$T_{x2}(t) = \begin{cases} \underline{c}(2t-1), & t = 2T_c \\ \underline{c^*}(2t), & t = 2T_c - 1 \end{cases} \tag{4.7}$$

The receiver structure is shown in Fig. 4.1b. It consists of an Alamouti decoder followed by blocks performing LDPC decoding and chaotic demodulation. As illustrated in the Figure 4.1, the signals received by Rx-ant1 over two time slots are

$$r_0 = h_{11}c_1 + h_{21}c_2 + n_0 \tag{4.8}$$

$$r_1 = -h_{11}c_2^* + h_{21}c_1^* + n_1 \tag{4.9}$$

Similarly, the signals received by Rx-ant2 over two time slots are

$$r_2 = h_{12}c_1 + h_{22}c_2 + n_2 \tag{4.10}$$

$$r_3 = -h_{12}c_2^* + h_{22}c_1^* + n_3 \tag{4.11}$$

where n_0, n_1, n_2 and n_3 are the Gaussian noise components with zero mean and variance σ^2 over four MIMO channels.

The received signals on the both receivers are used to estimate the transmitted codeword.

$$\underline{\tilde{c}}(2t-1) = h_{11}^* r_0 + h_{21} r_1^* + h_{12}^* r_2 + h_{22} r_3^* = (|h_{11}^2| + |h_{21}^2| + |h_{12}^2| + |h_{22}^2|)c_1 + (h_{11}^* n_0 + h_{21} n_1^* + h_{12}^* n_2 + h_{22} n_3^*)$$
$$= (|h_{11}^2| + |h_{21}^2| + |h_{12}^2| + |h_{22}^2|)c_1 + w_0 \tag{4.12}$$

$$\underline{\tilde{c}}(2t) = h_{21}^* r_0 - h_{11} r_1^* + h_{22}^* r_2 - h_{12} r_3^* = h_{21}^*(h_{11}c_1 + h_{21}c_2 + n_0) - h_{11}(-h_{11}^* c_2 + h_{21}^* c_1 + n_1^*) + h_{22}^*(h_{21}c_1 + h_{22}c_2 + n_2) - h_{12}(h_{12}^* c_2 + h_{22}^* c_1 + n_3^*)$$
$$= (|h_{11}^2| + |h_{21}^2| + |h_{12}^2| + |h_{22}^2|)c_2 + (h_{21}^* n_0 - h_{11} n_1^* + h_{22}^* n_2 - h_{12} n_3^*)$$
$$= (|h_{11}^2| + |h_{21}^2| + |h_{12}^2| + |h_{22}^2|)c_2 + w_1 \tag{4.13}$$

Considering ML detection, the estimates of the transmitted symbols are given by,

$$\underline{\hat{c}}(2t-1) = arg \min_{c(2t-1)\in\{0,1\}} \left\| \underline{\tilde{c}}(2t-1) - (|h_{11}^2| + |h_{21}^2| + |h_{12}^2| + |h_{22}^2|)c_1 \right\|^2 \tag{4.14}$$

$$\underline{\hat{c}}(2t) = arg \min_{c(2t)\in\{0,1\}} \left\| \underline{\tilde{c}}(2t) - (|h_{11}^2| + |h_{21}^2| + |h_{12}^2| + |h_{22}^2|)c_2 \right\|^2 \tag{4.15}$$

4.2.3 LDPC Decoding

Let the sequence at the output of the Alamouti decoder (input of the LDPC encoder be specified as $r = (r_1, r_{2,\ldots} r_N)$. This is a binary valued sequence which is then given as an input to the LDPC decoder. The decoder decodes the received words and attempts to correct the errors introduced in the channel. We have used the message Sum-Product algorithm to decode the LDPC code. An estimate of the transmitted information vector (as existing at the sequence average block in the transmitter) is provided to the chaotic demodulator block.

4.2.4 Decoding of Chaotic Sequences

The output of the LDPC decoder is a binary valued sequence and contains the estimate of the sequence that was originally presented to the input of the LDPC encoder. At the final stage, we decode the chaotic sequence to get the original data.

This requires the generation of a chaotic sequence at the receiver which is exactly identical to that used at the transmitter end. The master-slave synchronizing arrangement discussed in chapter 2 is used to generate the local chaotic sequence matched to the sequence generated in the transmitter.

The LDPC decoded data is given as x_i where $1 \leq i \leq K$. x_i is correlated with the locally generated chaotic sequence as follows:

$$\underline{D_i} = \sum_{i=1}^{K} \underline{x_i}.\underline{x1_i} \tag{4.16}$$

Thus, it becomes mandatory to select the length of chaotic sequence (generated at the receiver) equal to K. Hence, it follows that

$$K = \beta.B \tag{4.17}$$

The output of the chaotic demodulator represents the information sequence as retrieved at the receiver.

4.3 Fading Channel Models

In addition to Rayleigh fading channel (section 3.3.1), Gamma-Gamma fading channel are widely used in wireless optical communication channels.

Gamma-Gamma Fading Channel [Peng L., Xueying W., Wakamori K., Pham T., Alam M. and Matsumoto M., 2011, Ehsan. B., Robert S. and Ranjan. M.,2008]

The atmospheric turbulence causes irradiance fluctuation known as scintillation, is mainly caused by temperature variations in the atmosphere. Different models have been proposed to describe the atmosphere turbulence by varying degrees of strength. For a wide range of turbulence conditions (weak to strong) the fading gain I_{mn} in FSO systems can be modelled by a Gamma-Gamma distribution.

$$f_I(I_{mn}) = \frac{2(\alpha\beta_c)^{\frac{\alpha+\beta_c}{2}}}{\Gamma(\alpha)\Gamma(\beta_c)} I^{\frac{\alpha+\beta_c}{2}-1} K_{\alpha-\beta_c}(2\sqrt{\alpha\beta_c I_{mn}}) \tag{4.18}$$

where parameters $\alpha > 0$ and $\beta_c > 0$ are linked to the so-called scintillation index $\triangleq \frac{1}{\alpha} + \frac{1}{\beta_c} + \frac{1}{(\alpha\beta_c)}$. α and β_c can be adjusted to achieve good agreement between $f_I(I_{mn})$ and measurement data. Alternatively, assuming spherical wave propagation, α and β_c can be directly linked to physical parameters via

$$\alpha = [\exp(\frac{0.49x^2}{(1+0.18d^2+0.56x^{12/5})^{7/6}}) - 1]^{-1} \tag{4.19}$$

$$\beta_c = [\exp(\frac{0.51x^2(1+0.69x^{12/5})^{-5/6}}{(1+0.9d^2+0.62d^2x^{12/5})^{5/6}}) - 1]^{-1} \tag{4.20}$$

where $x^2 = 0.5C_n^2K_c^{7/6}L_c^{11/6}$, $d = (K_cD_c^2/4L_c)^{1/2}$, and $K_c = 2\pi/\lambda_c$. Here λ_c, D_c, C_n^2, and L_c are the wavelength in the meter, the diameter of the receiver aperture in meters, the index of the refraction structure parameter, and the link distance in meters, respectively.

4.4 Performance Analysis of the Chaotic-LDPC-MIMO

In this section, we have derived measures which can describe the BER performance of the proposed LDPC-MIMO system based on chaotic technique. During transmission, we transmit the LDPC encoded codeword whose energy is more than the original chaotic modulated sequence because of the redundant data symbols added due to encoding. Thus, we have to find the difference between the energies of the codeword and the additional data added.

Let $c_{i,}$ $1 \leq i \leq N$ represent symbols of the codeword, [where $N = 10000$].

Thus,

$$Œ_1 = \sum_{i=1}^{N} \underline{c_i^2} \tag{4.21}$$

where $Œ_1$ is the energy of transmitted codeword.

and

$$Œ_2 = \sum_{i=1}^{B} E_i^2 \tag{4.22}$$

where $Œ_2$ is the energy of sequence at the output of the information source.$(N = 2\beta B)$

Then

$$Œ = Œ_1 - Œ_2 \tag{4.23}$$

Looking at the equation (4.12) and equation (4.13) we can see clearly that the decision variables $\underline{\hat{c}}(2t-1)$ and $\underline{\hat{c}}(2t)$ share the same statistical properties. We compute the statistical properties of the decision variable $\tilde{c}(2t-1)$ for the lth fixed bit.

The mean of $\tilde{c}(2t-1)^{(l)})$ is given as

$$E[\widetilde{c}(2t-1)^{(l)}] = (h_{11}^2 + h_{21}^2 + h_{12}^2 + h_{22}^2)c_1^{(l)}Œ^{(l)} \quad (4.24)$$

For a given fixed bit l, the first and second term in equation (4.25) are equal. The variance $var[.]$ of the decision variable is reduced to variance of the noise term $H * w$

$var[\tilde{c}(2t-1)^{(l)}] = E[(\tilde{c}(2t-1)^{(l)})^2] - E[\tilde{c}(2t-1)^{(l)}]^2 =$

$E[(\sum_{i,j=1}^{2} h_{ij}^2 Œ^{(l)} c_1^{(l)})^2]E(\sum_{i,j=1}^{2} h_{ij}^2 Œ^{(l)} c_1^{(l)})^2$+E$[(h_{11}^* + h_{21} + h_{12}^* + h_{22})w$(4.25)

where

$w = \begin{pmatrix} w_0 \\ w_1 \end{pmatrix}$ from equation (4.12) and equation (4.13)

Since the noise components of the variable w are uncorrelated and independent of the chaotic sequences, and the Gaussian noise samples are independent, the conditional variance of the decision variable for a given bit lth is

$\sigma_{total}^2 = var[w_0] + var[w_1] = var[h_{11}^* n_0 + h_{21} n_1^* + h_{12}^* n_2 + h_{22} n_3^*] +$

$var[h_{21}^* n_0 - h_{11} n_1^* + h_{22}^* n_2 - h_{12} n_3^*]$ (4.26)

then

$$\sigma_{total}^2 = (h_{21}^2 + h_{22}^2)N_0 \quad (4.27)$$

The total error probability of the system is the sum of the error probabilities of symbols in c_1 and c_2, which are independent and equiprobable, and so the total error probability is the error probability of c_1 or c_2.

Thus, the error probability is

$$P_e(Œ^{(l)}) = \frac{1}{2} erfc\left(\frac{E[\widetilde{c}(2t-1)^{(l)}]}{\sqrt{2var[c(2t-1)^{(l)}]}}\right) \quad (4.28)$$

$$P_e(Œ^{(l)}) = \frac{1}{2} erfc\left(\frac{(h_{11}^2+h_{21}^2+h_{12}^2+h_{22}^2)Œ^{(l)}}{\sqrt{2(h_{21}^2+h_{22}^2)N_0}}\right) \quad (4.29)$$

Given the non-periodic nature of chaotic sequence, we cannot consider the bit energy after spreading by chaotic sequence as constant. The overall BER expression of the C-

LDPC-MIMO system is therefore the integral of equation (4.30) over all possible bit energy values.

$$BER = \int_0^{\infty} \frac{1}{2} erfc\left(\frac{(h_{11}^2+h_{21}^2+h_{12}^2+h_{22}^2)Œ^{(l)}}{\sqrt{2(h_{21}^2+h_{22}^2)N_0}}\right) P\,(Œ^{(l)}) dŒ^{(l)} \qquad (4.30)$$

where $P\ Œ^{(l)}$ is the probability density function of the energy $Œ^{(l)}$ which is computed by computing the histogram of the $Œ$ and this followed by numerical integration. The expression in equation (4.28) can be computed numerically, taking into account the bit-energy variation.

For 2×2 Alamouti, the corresponding BER expression is given by,

$$BER = \sum_{l=1}^{m} \frac{1}{2} erfc\left(\frac{(h_{11}^2+h_{21}^2+h_{12}^2+h_{22}^2)Œ^{(l)}}{\sqrt{2(h_{21}^2+h_{22}^2)N_0}}\right) P(Œ^{(l)}) \qquad (4.31)$$

where m is the number of histogram classes and $P(Œ^{(l)})$ is the probability of having the energy in interval centered on $Œ^{(l)}$.

4.5 Simulation Results and Discussions

The LDPC code is characterized by w_r =6 and w_c =3. We set the block length to $N = 10000$ for both regular and irregular LDPC codes and the code rate $\frac{K}{N} = 0.5$.

From Figure 4.2 which (all curves pertain to AWGN channel) it can be observed that using LDPC code gives high BER performance gain in Single-Input-Single-Output (SISO) system.

The use of LDPC code in a SISO system with chaotic modulation gives 6 dB gain at BER of 10^{-4} as compared to similar system without LDPC encoding. In case of 2×2 chaotic-MIMO system, LDPC encoding gives 4.5 dB gain at BER of 10^{-4} as compared to similar system without LDPC encoding. Further, the use of LDPC code in SISO chaotic system gives marginally better BER performance

(0.75 dB) as compared to MIMO chaotic system without LDPC. Finally, with the use of a LDPC code, chaotic MIMO gives 4 dB gain at BER of 10^{-4} as compared to SISO system using the same LDPC code. The circle graph (black) represent BER curve for simulated regular LDPC-MIMO based on CSK which is a large extent align with the blue curve represented theoretical BER computed in equation (4.31)

In Figure 4.3 (all curves pertain to Rayleigh fading channel with $\sigma = 1$), the use of MIMO technique gives 5.5 dB gain at BER of 10^{-4} as compared to SISO technique (without employing LDPC code). After implementing regular LDPC chaotic SISO technique gives 3 dB gain when compared to chaotic MIMO technique without implementing LDPC coding. The BER performance improves further by 3 dB at BER of 10^{-4} if chaotic MIMO technique is combined with LDPC coding.

In Figure 4.4 (all curves pertain to Gamma-Gamma fading channel), where α and β_c were calculated from (4.19) and (4.20) and adopted $\lambda_c = 1550$ nm, $C_n^2 = 10^{-15}$, the diameter of the receiver collecting lens aperture is $D_c = 0.02$ m and the link distance between transmitter and receiver $L_c = 2000$ m, where $\frac{D_c}{L_c} \to 0$. it is seen that implementing chaotic-MIMO scheme without LDPC coding gives 6 dB gain at BER of 10^{-4} as compared to chaotic-SISO technique. The use of regular LDPC code for chaotic SISO technique results in a gain of 1.5 dB at BER of 10^{-4} as compared to chaotic MIMO technique without LDPC coding. Finally, using MIMO technique with regular LDPC coding gives 2 dB gain at BER of 10^{-4} as compared to chaotic-SISO technique with regular LDPC.

Figure 4.5 (all curves pertain to AWGN channel) implementing irregular LDPC coding for chaotic-SISO technique gives 1 dB gain at BER of 10^{-4} as compared to chaotic-MIMO technique without LDPC encoding. So while implementing MIMO technique irregular LDPC coding gives 4.5 dB gain at BER of 10^{-4} as compared to chaotic-SISO irregular LDPC technique. Chaotic-MIMO with irregular LDPC coding enhances the BER performance by 1 dB as compared to chaotic-MIMO with regular LDPC. So MATLAB simulation for Chaotic-MIMO with irregular LDPC coding can use signal with bit energy to noise ratio of 5 dB. The comparison between decoded data and original data gave zero errors.

Under Rayleigh fading channel. Figure 4.6, using irregular LDPC coding for Chaotic-SISO technique gives 1.5 dB gain at BER of 10^{-4} as compared to chaotic MIMO technique without LDPC coding. Implementing MIMO technique with irregular LDPC coding gives further 4.5 dB gain at BER of 10^{-4} as compared to chaotic-SISO technique with irregular LDPC coding. Implementing irregular LDPC coding gives 1.5 dB gain as compared to regular LDPC coding for chaotic-MIMO technique. In our irregular LDPC coding, we generated the signal of bit energy to noise ratio of 8 dB. The decoded data was found to match perfectly with unmodulated original data.

Figure 4.7 under Gamma-Gamma fading channel using irregular LDPC coding gives 3 dB gain at BER of 10^{-4} for chaotic-SISO technique as compared to chaotic-MIMO technique without LDPC coding. Chaotic-MIMO technique with irregular LDPC coding further enhances the BER performance by 2.25 dB. Chaotic-MIMO technique with irregular LDPC gives 1.5 dB gain as compared to chaotic-MIMO technique with regular LDPC coding. In MATLAB simulation, we generated the signal with bit energy to noise ratio of 8 dB. All the original data bits were found to be correctly decoded with zero errors.

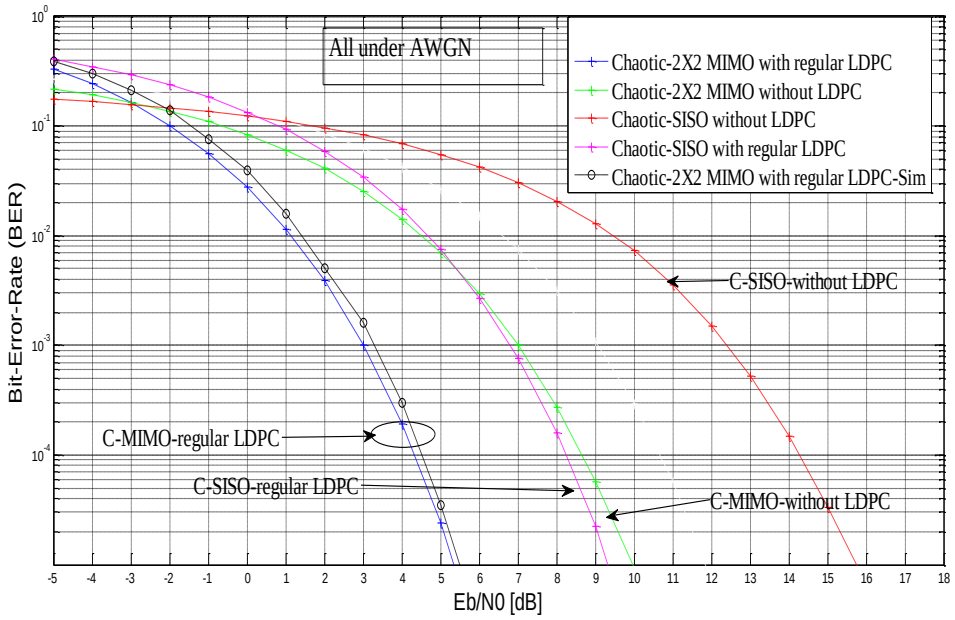

Figure 4.2 BER performance of C-2 × 2 MIMO with regular LDPC under AWGN channel

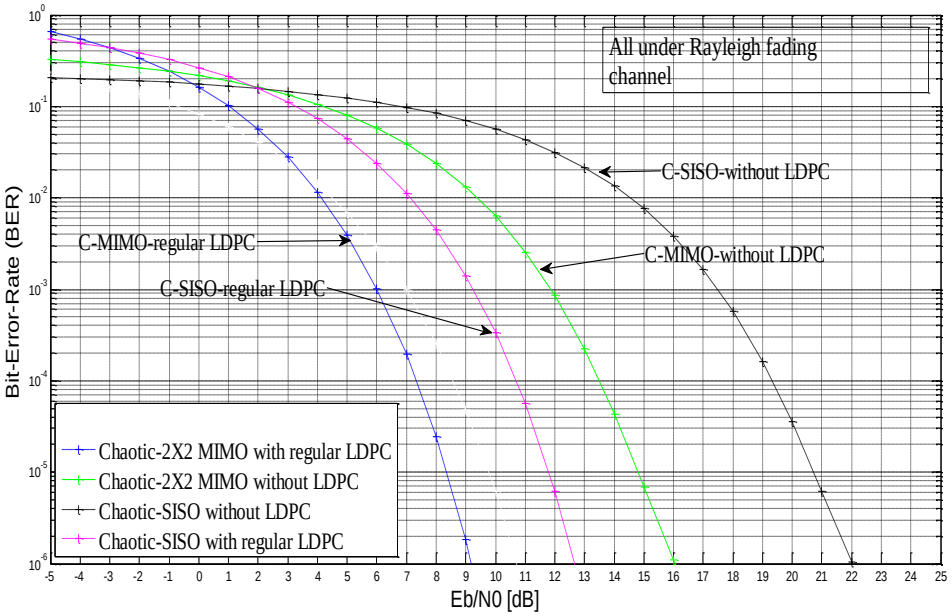

Figure 4.3 BER performance of C-2 × 2 MIMO with regular LDPC under Rayleigh fading channel

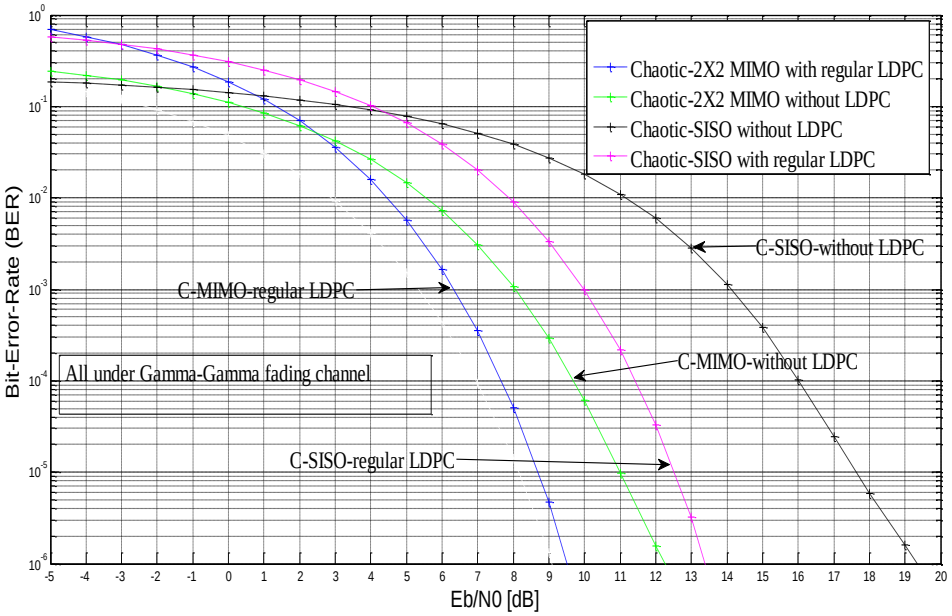

Figure 4.4 BER performance of C-2 × 2 MIMO with regular LDPC under Gamma-Gamma fading channel

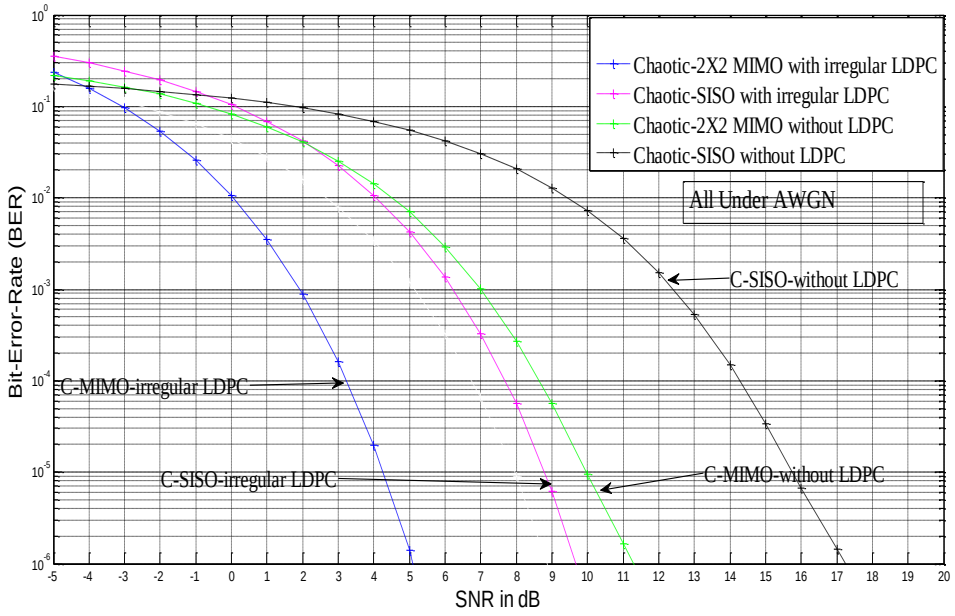

Figure 4.5 BER performance of C-2 × 2 MIMO with irregular LDPC under AWGN channel

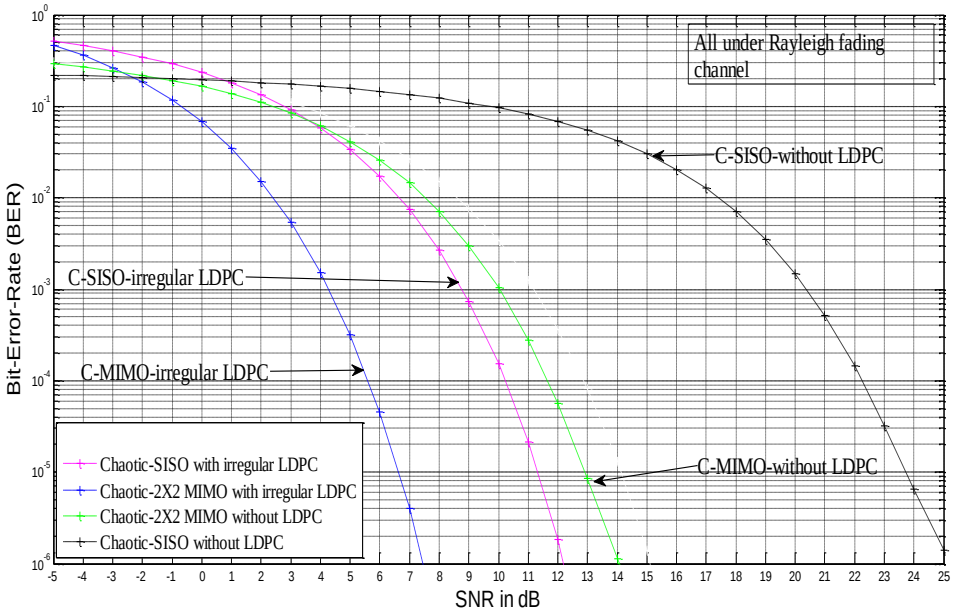

Figure 4.6 BER performance of C-2 × 2 MIMO with irregular LDPC under Rayleigh fading channel

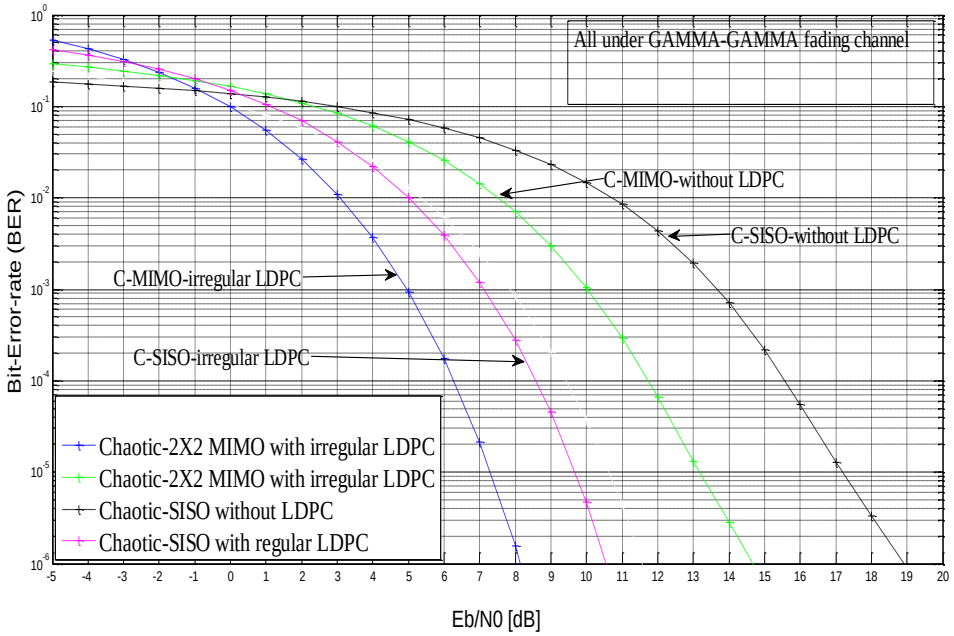

Figure 4.7 BER performance of C-2 × 2 MIMO with irregular LDPC under Gamma-Gamma fading channel

4.6 Conclusions

A communication system employing chaotic modulation, LDPC coding and the Alamouti Space Time Code has been proposed. The main focus of this work is to analyze and study the performance of C-LDPC-MIMO system under different fading channels. We have demonstrated that this system offers benefits of security (because of chaotic modulation) and robust performance over both Rayleigh fading and Gamma-Gamma fading channels because of the use of LDPC codes and the Alamouti STBC. These features make it attractive for deployment in a variety of wireless system including Free Space Optic Systems.

In chapter five we propose a multilevel DCSK system which is coupled with a high rate STBC to improve the system throughput. . We have designed rate-$\frac{5}{4}$ and rate-$\frac{6}{4}$ full diversity orthogonal STBC for QCSK and 2 transmit antennas and 2 receive antennas by enlarging the signaling set used in the Alamouti scheme. The BER performance and effective throughput offered by these schemes has been quantified.

CHAPTER 5

QCSK-MIMO COMMUNICATION SYSTEM USING HIGH-RATE STBC (QCSK-HRSTBC)

5.1 Introduction

It has been shown that the capacity of wireless channels can be significantly increased by the use of multiple antennas [Teletar E., 1999, Basar E. and Aygolu U., 2009]. A number of researchers have worked on the synthesis of STBC and STTC schemes that can significantly improve the performance of wireless systems (capacity, reliability and coverage) operating over fading channels [Siavash M. Alamouti, 1998, Tarokh, V., Vahid T., Jafarkhani and Hamid J., 1999]. Development of chaotic modulation schemes has also attracted the interest of researchers because they can provide high levels of security to information being transacted over wireless channels [Zbigniew G. and Gian M.2001]. Lwaa et.al [2013] has shown that excellent BER performances can be achieved by CSK and its Differential version (DCSK). DCSK system is one of the chaos-based communication schemes that have been shown to be robust against the channel imperfections.

In Chapter 3, we have discussed DCSK modulation in which each symbol is represented by two sets of chaotic signal samples, with the first set representing the reference, and the second carrying data. If $+1$ is transmitted, the data-bearing sequence, is identical to the reference sequence, and if -1 is transmitted, an inverted version of the reference sequence is used as data bearing sequence. QCSK may be considered as the chaotic counterpart of QPSK in conventional digital communications. It is well known that at high SNR values, QPSK exhibits the same BER performance as BPSK with same bandwidth occupation, but provides double the information transfer rate. This is achieved by employing a pair of sinusoidal carriers in phase quadrature to generate an orthogonal signal basis.

Orthogonal basis functions usually sinusoids, are used in digital communications to generate large signal constellations in order to increase the spectral efficiency [Geza K., Michael K. and Leon C., 1997]. The basic idea underlying the QCSK scheme is the generation of chaotic signals which are orthogonal over a specified time interval. This allows the creation of a basis of chaotic functions from which arbitrary constellations of chaotic signals can be constructed [Zbigniew G. and Gian M., 2001].

The QCSK symbol consists of two bits as opposed to one bit in DCSK. QCSK may be considered equivalent to two DCSK systems, with the difference that in QCSK only one reference chip is transmitted for both information-bearing chips.

The advantage of the QCSK scheme is that there is no need to send the orthogonal signal over the channel as its estimate can be reproduced from the received reference signal. The cost is the increased the complexity as QCSK requires the generation of the quadrature signal in both transmitter and receiver. The BER performance of the DCSK and QCSK are similar but QCSK has double data rate [Zbigniew G. and Gian M.,2001]. The availability of a simple ML decoding algorithm and full diversity order are two key features of Alamouti's STBC scheme. However, in order to achieve full diversity, the maximum rates attained with the orthogonal designs have been shown to be 1 symbol per time slot for system with 2 transmits antennas [Duy N., Ha N. and Hoang T, 2008]. In this chapter, we design classes of full diversity high rate (> 1) STBC by exploiting the inherent algebra structure in existing orthogonal designs based on quaternions for 2 transmit antennas.

The Alamouti matrix for symbol s_1 and s_2 is

$$Q(s_1, s_2) \rightarrow \begin{bmatrix} s_1 & -s_2^* \\ s_2 & s_1^* \end{bmatrix} \tag{5.1}$$

This code achieves rate-1 at full diversity and enjoys low-complexity ML decoding. Consider the set $\tilde{Q}$ of s given by 2×2 orthogonal matrices

$$\tilde{Q}(s_1, s_2) \rightarrow \begin{bmatrix} s_1 & -s_2^* \\ -s_2 & -s_1^* \end{bmatrix} = \begin{bmatrix} 1 & 0 \\ 0 & -1 \end{bmatrix} Q(s_1, s_2) \qquad (5.2)$$

In this scheme, the transmitted space time signaling matrix is selected from either Q or $\widetilde{Q}$ according to additional information it 0 or 1, respectively.

Contributions of the thesis in Chapter 5:

- Improve the throughput of transmission for chaos based communication schemes by using High Rate Space-Time Block Codes.

5.2 Quadrature Chaos Shift Keying (QCSK)

The dynamics of the tent map is obtained as shown in equation (2.3).

The first step for introducing QCSK is the generation of a chaotic signal orthogonal to a given chaotic reference signal in a specified time interval. Typically, two independent chaotic signals $f_1(t)$ and $f_2(t)$ exhibits a very low cross-correlation and in that sense they might be considered approximately orthogonal over a sufficiently long interval $[0, \tau]$

$$\int_0^\tau f_1(t)\ f_2(t)dt \approx 0 \qquad (5.3)$$

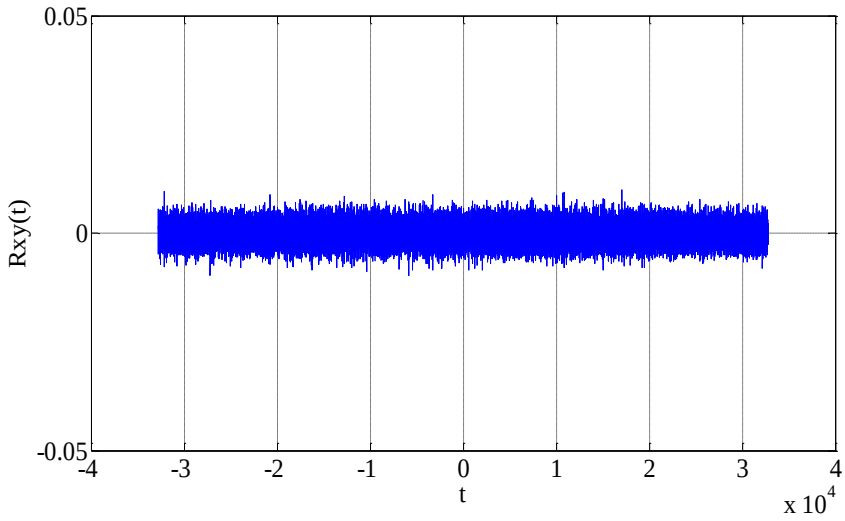

Figure 5.1: Measurement of cross-correlation of a chaotic tent map.

This is demonstrated in Figure 5.1 by computing the cross correlation of two chaotic signals. In order to produce an orthogonal basis function useful for communication purpose, we are interested in the generation of a chaotic signal y exactly orthogonal to a reference chaotic signal x, and which could be generated starting from x. Let $x(t)$ be a chaotic reference signal defined for $t \in [0, \tau]$. We also assume the quadrature signal $y(t)$, with $t \in [0, \tau]$. The requirement is that the signals $x(t)$ and $y(t)$ be orthogonal in the interval $I_\tau = [0, \tau]$ and possess the same power that is,

$$x \perp y \Leftrightarrow \int_0^\tau x(t)y(t)dt = 0 \tag{5.4}$$

$$P_x = P_y \Leftrightarrow \frac{1}{\tau}\int_0^\tau x^2(t)dt = \frac{1}{\tau}\int_0^\tau y^2(t)dt \tag{5.5}$$

An example of chaotic signal x and corresponding orthogonal signal y is shown in Figure 5.2.

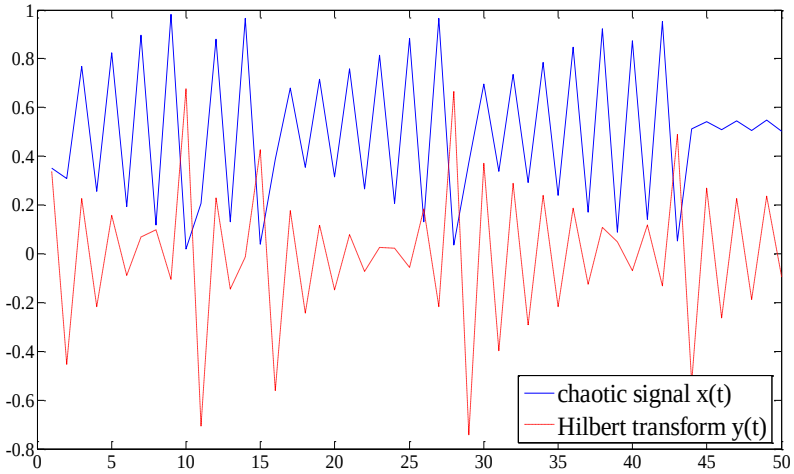

Figure 5.2 Example of chaotic waveform $x(t)$ and corresponding orthogonal signal y(t), computed y(t) taking Hilbert transform of $x(t)$ over the interval [0,50]

In QCSK, similarly to DCSK, to send the symbol s, we transmit the chaotic reference chip $s(t) = \sqrt{E_b}c_x(t)$ for half symbol period. In the second half the information-bearing chip $i(t) = \sqrt{E_b}m_s(t)$, is conveyed. E_b represents the energy per bit.

The transmitted QCSK signal has the analytic form represented by equation (5.6) where $T = 2\tau$, $s = 0,1,2,3$ and $m_s = a_s + ib_s$.

$$S_{QCSK}(t) = \begin{cases} \sqrt{E_b}c_x(t), & 0 \le t < \frac{T}{2} \\ \sqrt{E_b}(a_s c_x\left(t - \frac{T}{2}\right) + b_s c_y(t - \frac{T}{2}), & \frac{T}{2} \le t \le T \end{cases} \quad (5.6)$$

In this chapter, we consider the signal constellation as shown in Figure5.3 [Zbigniew G. and Gian M., 2001].

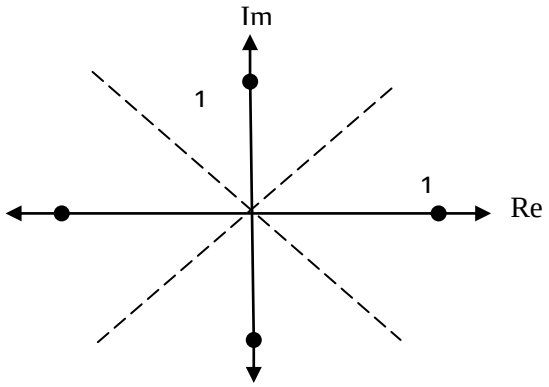

Figure 5.3 Chaotic constellations. Two level signaling (QCSK)

Chaotic Signal Constellation is specified in Table 5.1

QCSK	Chaotic Signal Constellation	
	S	$m_s(t)$
	s=00	$+c_x(t)$
	s=01	$+c_y(t)$
	s=10	$-c_y(t)$
	s=11	$-c_x(t)$

Table 5.1

5.3 High Rate Space-Time Block Code (HRSTBC)

A new class of full-diversity high-rate STBCs were proposed in [Duy N., Ha N. and Hoang T., 2008, Sushanta D., Naufal D. and Robert C., 2006], where the authors exploit inherent algebraic structure in the existing orthogonal designs for 2 transmit antennas. The authors showed that the rate of orthogonal designs could be increased to $\frac{5}{4}$ by accommodating 1 additional bit per space-time codeword and that the rate could be increased to $\frac{6}{4}$ by accommodating 2 additional bits per space-time codeword.

In this case, the expanded set $g = Q \cup \tilde{Q}$ (where Q and $\tilde{Q}$ are defined in equations (5.1) and (5.2) respectively) can be used to construct new high-rate (> 1) full-diversity STBC with low complexity ML decoding and optimized coding gain. This arrangement is described in the above reference. It is briefly reviewed in the following paragraph.

Suppose that G_1 and $G_2 \in g$. The sufficient condition for the STBC g to achieve the full diversity order of 2 is that the matrix $A = (G_1 - G_2)(G_1 - G_2)^H$ (where $(.)^H$ is conjugate transpose operation) is full rank for all $G_1, G_2 \in g$ and $G_1 \neq G_2$. If both G_1 and G_2 belong to either Q or $\tilde{Q}$, then A will be full rank. However, if $G_1 \in Q$ and $G_2 \in \tilde{Q}$, for instance, the matrix A loses its rank. In addition to maximize the coding gain, the determinant of A needs to be maximized. [Tarokh, V., Sheshadri, N. and Calderbank, R., 1998]. A method to maintain the rank of matrix A, proposed in [Duy N., Ha N. and Hoang T., 2008], is to simply scale the constellation in one of the sets, Q or $\tilde{Q}$. Specifically, if the orthogonal design $\tilde{Q}$ is expanded by a factor of $\kappa > 1$ compared to the orthogonal design Q, the matrix A is guaranteed to be full rank. It was stated in [Sushanta D., Naufal D. and Robert C., 2006] that $\kappa = \sqrt{3}$ is the optimal power scaling factor for the case of 2 transmit antennas, in the sense that the coding gain is maximized and the peak to average ratio, a side effect of constellation scaling is minimized. A different way to maintain the rank of matrix A is to apply constellation rotation to one of the STBC design, Q or $\tilde{Q}$. For example, if Q is kept unchanged, $\tilde{Q}$ is defined as

$$\tilde{Q}\left(s_1 e^{j\varphi}, s_2\right) \rightarrow \begin{bmatrix} s_1 e^{j\varphi} & -s_2^* \\ -s_2 & -s_1^* e^{-j\varphi} \end{bmatrix} \tag{5.7}$$

It can be shown that the determinant of $A = (G_1 - G_2)(G_1 - G_2)^H > 0$, for all $G_1, G_2 \in g$ and $G_1 \neq G_2$. In fact, the minimum determinant of A is maximized with $\varphi = \frac{\pi}{4}$.

5.3.1 Rate-$\frac{5}{4}$ STBC Design

Consider QCSK modulation. In the conventional Alamouti scheme, 4 bits select 2 independent QCSK symbols, s_1 and s_2. These symbols are then space-time encoded as described in equation (5.1) or equation (5.2). The space time encoded symbols are sent via 2 transmit antennas and over 2 time slots. One additional bit can be accommodated by simply using it to select one of the encoding schemes in equation (5.1) or equation (5.2). To illustrate this, suppose that b_0 is the third bit after s_1 and s_2 coming to space-time encoder. The QCSK symbols s_1 and s_2 that carry other 4 bits are encoded as follows:

$$b_0 = 0 \Rightarrow \sqrt{\frac{2}{\kappa^2+1}} \begin{bmatrix} s_1 & -s_2^* \\ s_2 & s_1^* \end{bmatrix} \tag{5.8}$$

$$b_1 = 1 \Rightarrow \kappa\sqrt{\frac{2}{\kappa^2+1}} \begin{bmatrix} s_1 & -s_2^* \\ -s_2 & -s_1^* \end{bmatrix} \tag{5.9}$$

Similarly, one can design a rate- $\frac{5}{4}$ STBC by applying constellation rotation as follows.

$$b_0 = 0 \Rightarrow \begin{bmatrix} s_1 & -s_2^* \\ s_2 & s_1^* \end{bmatrix} \tag{5.10}$$

$$b_1 = 1 \Rightarrow \begin{bmatrix} s_1 e^{j\frac{\pi}{4}} & -s_2^* \\ -s_2 & -s_1^* e^{-j\frac{\pi}{4}} \end{bmatrix} \tag{5.11}$$

5.3.2 Rate-$\frac{6}{4}$ STBC Design

In this design, additional two bits are accommodated to increase the transmission rate to $\frac{6}{4}$. This is accomplished by combining the 2 design methods that achieve rate $\frac{5}{4}$ described above. To this end the first bit b_0 is used to choose the constellation scaling factor, the second bit b_1 is used to perform constellation rotation. It is simple to show that this design still guarantees the full diversity of the code. The design is as follows:

$$b_0 b_1 = 00 \Rightarrow \sqrt{\frac{2}{\kappa^2+1}}\begin{bmatrix} s_1 & -s_2^* \\ s_2 & s_1^* \end{bmatrix} \tag{5.12}$$

$$b_0 b_1 = 01 \Rightarrow \sqrt{\frac{2}{\kappa^2+1}}\begin{bmatrix} s_1 e^{j\frac{\pi}{4}} & -s_2^* \\ s_2 & s_1^* e^{-j\frac{\pi}{4}} \end{bmatrix} \tag{5.13}$$

$$b_0 b_1 = 10 \Rightarrow \kappa\sqrt{\frac{2}{\kappa^2+1}}\begin{bmatrix} s_1 & -s_2^* \\ -s_2 & -s_1^* \end{bmatrix} \tag{5.14}$$

$$b_0 b_1 = 11 \Rightarrow \kappa\sqrt{\frac{2}{\kappa^2+1}}\begin{bmatrix} s_1 e^{j\frac{\pi}{4}} & -s_2^* \\ -s_2 & -s_1^* e^{-j\frac{\pi}{4}} \end{bmatrix} \tag{5.15}$$

5.4 QCSK-MIMO System Using High-Rate STBC (QCSK-HRSTB)

The block diagram of proposed QCSK-HRSTBC is shown in Figure 5.4. The QCSK-HRSTBC modulator includes the chaotic generator which generates the chaotic tent map (The dynamic (input-output) relationship of the tent map is specified by equation (2.3)). The corresponding orthogonal signal is generated by the Hilbert Filter. So, the original chaotic signal or the orthogonal version of original chaotic signal modulated by transmitted symbols will be transmitted depending on the two transmitted symbols. Then the signal is transmitted by the antennas T_{x1} and T_{x2}. Tables 5.2 and 5.3 show the structure of the transmitted signals in time, $2T_b = 4\beta T_c$, where the time symbol

$T_b = 2\beta T_c$ for rate $\frac{5}{4}$ and rate $\frac{6}{4}$ respectively. Tables 5.4 and 5.5 show the noisy signal after it has passed through channel and is received on the first antenna R_{x1}, where h_{11}, h_{21}, h_{12} and h_{22} are channel gains. At the receiver, the noisy version of the reference signal and information bearing signal are observed. We assume that the only distortion affecting the received signal is AWGN. As shown in Figure 5.4b, the received signal and delayed version of the received signal are correlated and the output of correlators provides the observation signals. Then the received signal is decoded by STBC decoder. Finally, the Symbol/Bit converter reconstructs the transmitted bits. The block prior to the decision block in Figure 5.4b is the correlator block. The reference chaotic signal is multiplied by the delayed version of the incoming signal (β is the delay element) and correlation is performed.

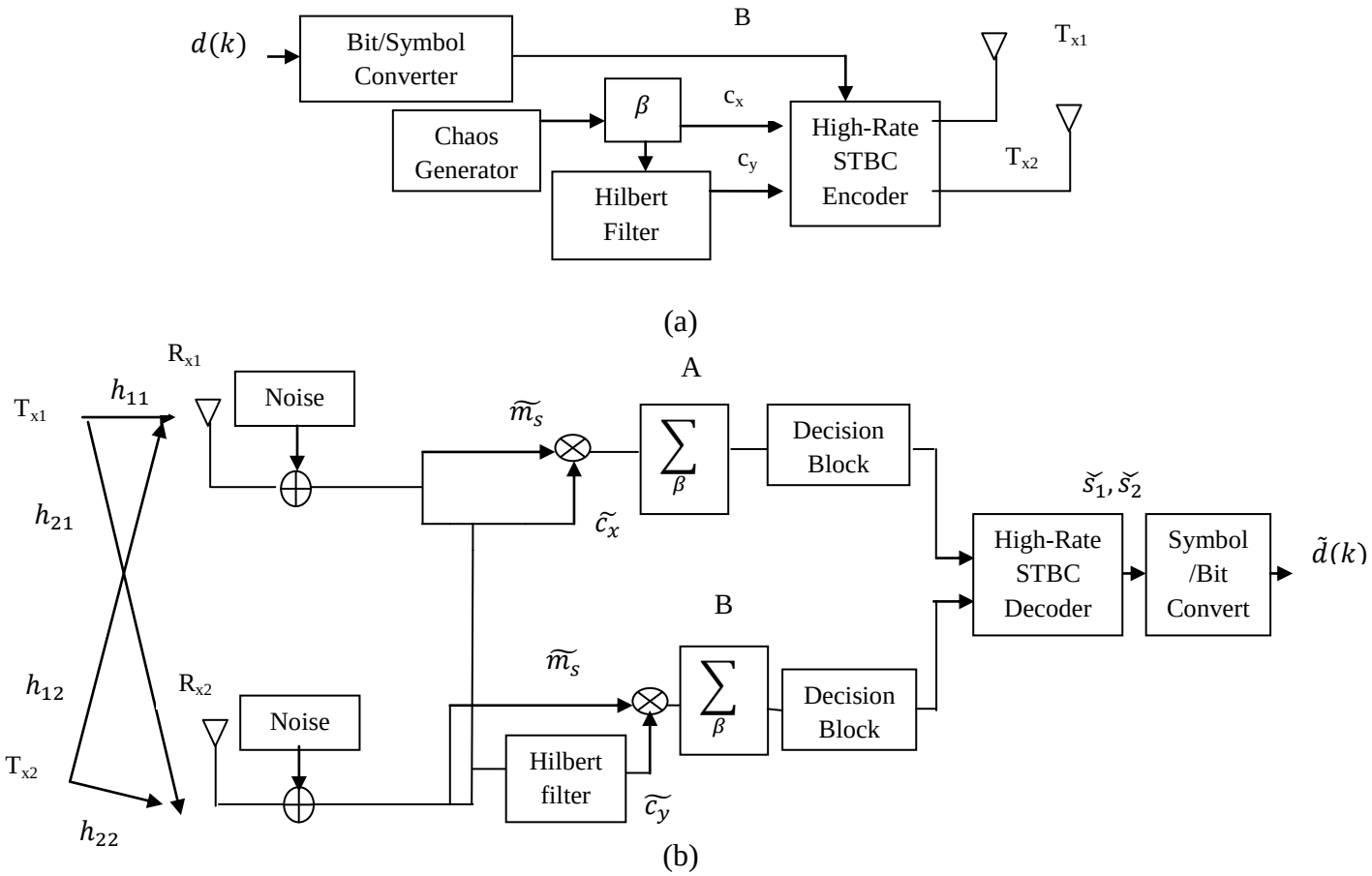

Figure 5.4 Block diagram of proposed QCSK-HRSTBC a) Transmitter b) Receiver

Design of the transmitted signal rate-$\frac{5}{4}$ is specified in Table 5.2

If *b0=0* is accommodated & *s=00*			If *b1=1* is accommodated & *s=00*		
Time	$s_1(t)$ from T_{x1}	$s_2(t)$ from T_{x2}	Time	$s_1(t)$ from T_{x1}	$s_2(t)$ from T_{x2}
$[0, \beta T_c]$	$c_x(t)$	$c_x(t)$	$[0, \beta T_c]$	$c_x(t)$	$c_x(t)$
$[\beta T_c, 2\beta T_c]$	$s_1 c_{x(k-\beta)}(t)$	$s_2 c_{x(k-\beta)}(t)$	$[\beta T_c, 2\beta T_c]$	$s_1 e^{j\pi/4} c_{x(k-\beta)}(t)$	$-s_2 c_{x(k-\beta)}(t)$
$[2\beta T_c, 3\beta T_c]$	$c_{x(k-2\beta)}(t)$	$c_{x(k-2\beta)}(t)$	$[2\beta T_c, 3\beta T_c]$	$c_{x(k-2\beta)}(t)$	$c_{x(k-2\beta)}(t)$
$[3\beta T_c, 4\beta T_c]$	$-s_2^* c_{x(k-3\beta)}(t)$	$s_1^* c_{x(k-3\beta)}(t)$	$[3\beta T_c, 4\beta T_c]$	$-s_2^* c_{x(k-3\beta)}(t)$	$-s_1^* e^{-j\pi/4} c_{x(k-3\beta)}(t)$
If *b0=0* is accommodated & *s=01*			If *b1=1* is accommodated & *s=01*		
Time	$s_1(t)$ from T_{x1}	$s_2(t)$ from T_{x2}	Time	$s_1(t)$ from T_{x1}	$s_2(t)$ from T_{x2}
$[0, \beta T_c]$	$c_y(t)$	$c_y(t)$	$[0, \beta T_c]$	$c_y(t)$	$c_y(t)$
$[\beta T_c, 2\beta T_c]$	$s_1 c_{y(k-\beta)}(t)$	$s_2 c_{y(k-\beta)}(t)$	$[\beta T_c, 2\beta T_c]$	$s_1 e^{j\pi/4} c_{y(k-\beta)}(t)$	$-s_2 c_{y(k-\beta)}(t)$
$[2\beta T_c, 3\beta T_c]$	$c_{y(k-2\beta)}(t)$	$c_{y(k-2\beta)}(t)$	$[2\beta T_c, 3\beta T_c]$	$c_{y(k-2\beta)}(t)$	$c_{y(k-2\beta)}(t)$
$[3\beta T_c, 4\beta T_c]$	$-s_2^* c_{y(k-3\beta)}(t)$	$s_1^* c_{y(k-3\beta)}(t)$	$[3\beta T_c, 4\beta T_c]$	$-s_2^* c_{y(k-3\beta)}(t)$	$-s_1^* e^{-j\pi/4} c_{y(k-3\beta)}(t)$
If *b0=0* is accommodated & *s=11*			If *b1=1* is accommodated & *s=11*		
Time	$s_1(t)$ from T_{x1}	$s_2(t)$ from T_{x2}	Time	$s_1(t)$ from T_{x1}	$s_2(t)$ from T_{x2}
$[0, \beta T_c]$	$-c_x(t)$	$-c_x(t)$	$[0, \beta T_c]$	$-c_x(t)$	$-c_x(t)$
$[\beta T_c, 2\beta T_c]$	$-s_1 c_{x(k-\beta)}(t)$	$-s_2 c_{x(k-\beta)}(t)$	$[\beta T_c, 2\beta T_c]$	$-s_1 e^{j\pi/4} c_{x(k-\beta)}(t)$	$s_2 c_{x(k-\beta)}(t)$
$[2\beta T_c, 3\beta T_c]$	$-c_{x(k-2\beta)}(t)$	$-c_{x(k-2\beta)}(t)$	$[2\beta T_c, 3\beta T_c]$	$c_{x(k-2\beta)}(t)$	$c_{x(k-2\beta)}(t)$
$[3\beta T_c, 4\beta T_c]$	$s_2^* c_{x(k-3\beta)}(t)$	$-s_1^* c_{x(k-3\beta)}(t)$	$[3\beta T_c, 4\beta T_c]$	$s_2^* c_{x(k-3\beta)}(t)$	$s_1^* e^{-j\pi/4} c_{x(k-3\beta)}(t)$
If *b0=0* is accommodated & *s=10*			If *b1=1* is accommodated & *s=10*		
Time	$s_1(t)$ from T_{x1}	$s_2(t)$ from T_{x2}	Time	$s_1(t)$ from T_{x1}	$S_2(t)$ from T_{x2}
$[0, \beta T_c]$	$-c_y(t)$	$-c_y(t)$	$[0, \beta T_c]$	$-c_y(t)$	$-c_y(t)$
$[\beta T_c, 2\beta T_c]$	$-s_1 c_{y(k-\beta)}(t)$	$-s_2 c_{y(k-\beta)}(t)$	$[\beta T_c, 2\beta T_c]$	$-s_1 e^{j\pi/4} c_{y(k-\beta)}(t)$	$s_2 c_{y(k-\beta)}(t)$
$[2\beta T_c, 3\beta T_c]$	$-c_{y(k-2\beta)}(t)$	$-c_{y(k-2\beta)}(t)$	$[2\beta T_c, 3\beta T_c]$	$c_{y(k-2\beta)}(t)$	$c_{y(k-2\beta)}(t)$
$[3\beta T_c, 4\beta T_c]$	$s_2^* c_{y(k-3\beta)}(t)$	$-s_1^* c_{y(k-3\beta)}(t)$	$[3\beta T_c, 4\beta T_c]$	$s_2^* c_{y(k-3\beta)}(t)$	$s_1^* e^{-j\pi/4} c_{y(k-3\beta)}(t)$

Table 5.2

Design of the transmitted signal rate-$\frac{6}{4}$ is specified in Table 5.3

If *b0 b1=00* is accommodated & *s=00*		
Time	$s_1(t)$ from T_{x1}	$s_2(t)$ from T_{x2}
$[0, \beta T_c]$	$c_x(t)$	$c_x(t)$
$[\beta T_c, 2\beta T_c]$	$\sqrt{\frac{2}{\kappa^2+1}} s_1 c_{x(k-\beta)}(t)$	$\sqrt{\frac{2}{\kappa^2+1}} s_2 c_{x(k-\beta)}(t)$
$[2\beta T_c, 3\beta T_c]$	$c_{x(k-2\beta)}(t)$	$c_{x(k-2\beta)}(t)$
$[3\beta T_c, 4\beta T_c]$	$-\sqrt{\frac{2}{\kappa^2+1}} s_2^* c_{x(k-3\beta)}(t)$	$\sqrt{\frac{2}{\kappa^2+1}} s_1^* c_{x(k-3\beta)}(t)$
If *b0 b1=01* is accommodated & *s=00*		
Time	$s_1(t)$ from T_{x1}	$s_2(t)$ from T_{x2}
$[0, \beta T_c]$	$c_x(t)$	$c_x(t)$
$[\beta T_c, 2\beta T_c]$	$\sqrt{\frac{2}{\kappa^2+1}} s_1 e^{j\pi/4} c_{x(k-\beta)}(t)$	$\sqrt{\frac{2}{\kappa^2+1}} s_2 c_{x(k-\beta)}(t)$
$[2\beta T_c, 3\beta T_c]$	$c_{x(k-2\beta)}(t)$	$c_{x(k-2\beta)}(t)$
$[3\beta T_c, 4\beta T_c]$	$-\sqrt{\frac{2}{\kappa^2+1}} s_2^* c_{x(k-3\beta)}(t)$	$\sqrt{\frac{2}{\kappa^2+1}} s_1^* e^{-j\pi/4} c_{x(k-3\beta)}(t)$
If *b0 b1=10* is accommodated & *s=00*		
Time	$s_1(t)$ from T_{x1}	$s_2(t)$ from T_{x2}
$[0, \beta T_c]$	$c_x(t)$	$c_x(t)$
$[\beta T_c, 2\beta T_c]$	$\kappa\sqrt{\frac{2}{\kappa^2+1}} s_1 c_{x(k-\beta)}(t)$	$-\kappa\sqrt{\frac{2}{\kappa^2+1}} s_2 c_{x(k-\beta)}(t)$
$[2\beta T_c, 3\beta T_c]$	$c_{x(k-2\beta)}(t)$	$c_{x(k-2\beta)}(t)$
$[3\beta T_c, 4\beta T_c]$	$-\kappa\sqrt{\frac{2}{\kappa^2+1}} s_2^* c_{x(k-3\beta)}(t)$	$-\kappa\sqrt{\frac{2}{\kappa^2+1}} s_1^* c_{x(k-3\beta)}(t)$
If *b0 b1=11* is accommodated & *s=00*		
Time	$s_1(t)$ from T_{x1}	$s_2(t)$ from T_{x2}
$[0, \beta T_c]$	$c_x(t)$	$c_x(t)$
$[\beta T_c, 2\beta T_c]$	$\kappa\sqrt{\frac{2}{\kappa^2+1}} s_1 e^{j\pi/4} c_{x(k-\beta)}(t)$	$-\kappa\sqrt{\frac{2}{\kappa^2+1}} s_2 c_{x(k-\beta)}(t)$
$[2\beta T_c, 3\beta T_c]$	$c_{x(k-2\beta)}(t)$	$c_{x(k-2\beta)}(t)$
$[3\beta T_c, 4\beta T_c]$	$-\kappa\sqrt{\frac{2}{\kappa^2+1}} s_2^* c_{x(k-3\beta)}(t)$	$-\kappa\sqrt{\frac{2}{\kappa^2+1}} s_1^* e^{-j\pi/4} c_{x(k-3\beta)}(t)$

If *b0 b1=00* is accommodated & *s=01*		
Time	$s_1(t)$ from T_{x1}	$s_2(t)$ from T_{x2}
$[0, \beta T_c]$	$c_y(t)$	$c_y(t)$
$[\beta T_c, 2\beta T_c]$	$\sqrt{\frac{2}{\kappa^2+1}} s_1 c_{y(k-\beta)}(t)$	$\sqrt{\frac{2}{\kappa^2+1}} s_2 c_{y(k-\beta)}(t)$
$[2\beta T_c, 3\beta T_c]$	$c_{y(k-2\beta)}(t)$	$c_{y(k-2\beta)}(t)$
$[3\beta T_c, 4\beta T_c]$	$-\sqrt{\frac{2}{\kappa^2+1}} s_2^* c_{y(k-3\beta)}(t)$	$\sqrt{\frac{2}{\kappa^2+1}} s_1^* c_{y(k-3\beta)}(t)$
If *b0 b1=01* is accommodated & *s=01*		
Time	$s_1(t)$ from T_{x1}	$s_2(t)$ from T_{x2}
$[0, \beta T_c]$	$c_y(t)$	$c_y(t)$
$[\beta T_c, 2\beta T_c]$	$\sqrt{\frac{2}{\kappa^2+1}} s_1 e^{j\pi/4} c_{y(k-\beta)}(t)$	$\sqrt{\frac{2}{\kappa^2+1}} s_2 c_{y(k-\beta)}(t)$
$[2\beta T_c, 3\beta T_c]$	$c_{y(k-2\beta)}(t)$	$c_{y(k-2\beta)}(t)$
$[3\beta T_c, 4\beta T_c]$	$-\sqrt{\frac{2}{\kappa^2+1}} s_2^* c_{y(k-3\beta)}(t)$	$\sqrt{\frac{2}{\kappa^2+1}} s_1^* e^{-j\pi/4} c_{y(k-3\beta)}(t)$
If *b0 b1=10* is accommodated & *s=01*		
Time	$s_1(t)$ from T_{x1}	$s_2(t)$ from T_{x2}
$[0, \beta T_c]$	$c_y(t)$	$c_y(t)$
$[\beta T_c, 2\beta T_c]$	$\kappa\sqrt{\frac{2}{\kappa^2+1}} s_1 c_{y(k-\beta)}(t)$	$-\kappa\sqrt{\frac{2}{\kappa^2+1}} s_2 c_{y(k-\beta)}(t)$
$[2\beta T_c, 3\beta T_c]$	$c_{y(k-2\beta)}(t)$	$c_{y(k-2\beta)}(t)$
$[3\beta T_c, 4\beta T_c]$	$-\kappa\sqrt{\frac{2}{\kappa^2+1}} s_2^* c_{y(k-3\beta)}(t)$	$-\kappa\sqrt{\frac{2}{\kappa^2+1}} s_1^* c_{y(k-3\beta)}(t)$
If *b0 b1=11* is accommodated & *s=01*		
Time	$s_1(t)$ from T_{x1}	$S_2(t)$ from T_{x2}
$[0, \beta T_c]$	$c_y(t)$	$c_y(t)$
$[\beta T_c, 2\beta T_c]$	$\kappa\sqrt{\frac{2}{\kappa^2+1}} s_1 e^{j\pi/4} c_{y(k-\beta)}(t)$	$-\kappa\sqrt{\frac{2}{\kappa^2+1}} s_2 c_{y(k-\beta)}(t)$
$[2\beta T_c, 3\beta T_c]$	$c_{y(k-2\beta)}(t)$	$c_{y(k-2\beta)}(t)$
$[3\beta T_c, 4\beta T_c]$	$-\kappa\sqrt{\frac{2}{\kappa^2+1}} s_2^* c_{y(k-3\beta)}(t)$	$-\kappa\sqrt{\frac{2}{\kappa^2+1}} s_1^* e^{-j\pi/4} c_{y(k-3\beta)}(t)$

If *b0 b1=00* is accommodated & *s=10*		
Time	$s_1(t)$ from T_{x1}	$s_2(t)$ from T_{x2}
$[0, \beta T_c]$	$-c_y(t)$	$-c_y(t)$
$[\beta T_c, 2\beta T_c]$	$-\sqrt{\frac{2}{\kappa^2+1}} s_1 c_{y(k-\beta)}(t)$	$-\sqrt{\frac{2}{\kappa^2+1}} s_2 c_{y(k-\beta)}(t)$
$[2\beta T_c, 3\beta T_c]$	$-c_{y(k-2\beta)}(t)$	$-c_{y(k-2\beta)}(t)$
$[3\beta T_c, 4\beta T_c]$	$\sqrt{\frac{2}{\kappa^2+1}} s_2^* c_{y(k-3\beta)}(t)$	$-\sqrt{\frac{2}{\kappa^2+1}} s_1^* c_{y(k-3\beta)}(t)$
If *b0 b1=01* is accommodated & *s=10*		
Time	$s_1(t)$ from T_{x1}	$s_2(t)$ from T_{x2}
$[0, \beta T_c]$	$-c_y(t)$	$-c_y(t)$
$[\beta T_c, 2\beta T_c]$	$-\sqrt{\frac{2}{\kappa^2+1}} s_1 e^{j\pi/4} c_{y(k-\beta)}(t)$	$-\sqrt{\frac{2}{\kappa^2+1}} s_2 c_{y(k-\beta)}(t)$
$[2\beta T_c, 3\beta T_c]$	$-c_{y(k-2\beta)}(t)$	$-c_{y(k-2\beta)}(t)$
$[3\beta T_c, 4\beta T_c]$	$\sqrt{\frac{2}{\kappa^2+1}} s_2^* c_{y(k-3\beta)}(t)$	$-\sqrt{\frac{2}{\kappa^2+1}} s_1^* e^{-j\pi/4} c_{y(k-3\beta)}(t)$
If *b0 b1=10* is accommodated & *s=10*		
Time	$s_1(t)$ from T_{x1}	$s_2(t)$ from T_{x2}
$[0, \beta T_c]$	$-c_y(t)$	$-c_y(t)$
$[\beta T_c, 2\beta T_c]$	$-\kappa\sqrt{\frac{2}{\kappa^2+1}} s_1 c_{y(k-\beta)}(t)$	$\kappa\sqrt{\frac{2}{\kappa^2+1}} s_2 c_{y(k-\beta)}(t)$
$[2\beta T_c, 3\beta T_c]$	$-c_{y(k-2\beta)}(t)$	$-c_{y(k-2\beta)}(t)$
$[3\beta T_c, 4\beta T_c]$	$\kappa\sqrt{\frac{2}{\kappa^2+1}} s_2^* c_{y(k-3\beta)}(t)$	$\kappa\sqrt{\frac{2}{\kappa^2+1}} s_1^* c_{y(k-3\beta)}(t)$
If *b0 b1=11* is accommodated & *s=10*		
Time	$s_1(t)$ from T_{x1}	$s_2(t)$ from T_{x2}
$[0, \beta T_c]$	$-c_y(t)$	$-c_y(t)$
$[\beta T_c, 2\beta T_c]$	$-\kappa\sqrt{\frac{2}{\kappa^2+1}} s_1 e^{j\pi/4} c_{y(k-\beta)}(t)$	$\kappa\sqrt{\frac{2}{\kappa^2+1}} s_2 c_{y(k-\beta)}(t)$
$[2\beta T_c, 3\beta T_c]$	$-c_{x(k-2\beta)}(t)$	$-c_{x(k-2\beta)}(t)$
$[3\beta T_c, 4\beta T_c]$	$\kappa\sqrt{\frac{2}{\kappa^2+1}} s_2^* c_{y(k-3\beta)}(t)$	$\kappa\sqrt{\frac{2}{\kappa^2+1}} s_1^* e^{-j\pi/4} c_{y(k-3\beta)}(t)$

If *b0 b1=00* is accommodated & *s=11*		
Time	$s_1(t)$ from T_{x1}	$s_2(t)$ from T_{x2}
$[0, \beta T_c]$	$-c_x(t)$	$-c_x(t)$
$[\beta T_c, 2\beta T_c]$	$-\sqrt{\frac{2}{\kappa^2+1}} s_1 c_{x(k-\beta)}(t)$	$-\sqrt{\frac{2}{\kappa^2+1}} s_2 c_{x(k-\beta)}(t)$
$[2\beta T_c, 3\beta T_c]$	$-c_{x(k-2\beta)}(t)$	$-c_{x(k-2\beta)}(t)$
$[3\beta T_c, 4\beta T_c]$	$\sqrt{\frac{2}{\kappa^2+1}} s_2^* c_{x(k-3\beta)}(t)$	$-\sqrt{\frac{2}{\kappa^2+1}} s_1^* c_{x(k-3\beta)}(t)$
If *b0 b1=01* is accommodated & *s=11*		
Time	$s_1(t)$ from T_{x1}	$s_2(t)$ from T_{x2}
$[0, \beta T_c]$	$-c_x(t)$	$-(t)$
$[\beta T_c, 2\beta T_c]$	$-\sqrt{\frac{2}{\kappa^2+1}} s_1 e^{j\pi/4} c_{x(k-\beta)}(t)$	$-\sqrt{\frac{2}{\kappa^2+1}} s_2 c_{x(k-\beta)}(t)$
$[2\beta T_c, 3\beta T_c]$	$-_{x(k-2\beta)}(t)$	$-c_{x(k-2\beta)}(t)$
$[3\beta T_c, 4\beta T_c]$	$\sqrt{\frac{2}{\kappa^2+1}} s_2^* c_{x(k-3\beta)}(t)$	$-\sqrt{\frac{2}{\kappa^2+1}} s_1^* e^{-j\pi/4} c_{x(k-3\beta)}(t)$
If *b0 b1=10* is accommodated & *s=11*		
Time	$s_1(t)$ from T_{x1}	$s_2(t)$ from T_{x2}
$[0, \beta T_c]$	$-c_x(t)$	$-c_x(t)$
$[\beta T_c, 2\beta T_c]$	$-\kappa\sqrt{\frac{2}{\kappa^2+1}} s_1 c_{x(k-\beta)}(t)$	$\kappa\sqrt{\frac{2}{\kappa^2+1}} s_2 c_{x(k-\beta)}(t)$
$[2\beta T_c, 3\beta T_c]$	$-c_{x(k-2\beta)}(t)$	$-c_{x(k-2\beta)}(t)$
$[3\beta T_c, 4\beta T_c]$	$\kappa\sqrt{\frac{2}{\kappa^2+1}} s_2^* c_{x(k-3\beta)}(t)$	$\kappa\sqrt{\frac{2}{\kappa^2+1}} s_1^* c_{x(k-3\beta)}(t)$
If *b0 b1=11* is accommodated & *s=11*		
Time	$s_1(t)$ from T_{x1}	$s_2(t)$ from T_{x2}
$[0, \beta T_c]$	$-c_x(t)$	$-c_x(t)$
$[\beta T_c, 2\beta T_c]$	$-\kappa\sqrt{\frac{2}{\kappa^2+1}} s_1 e^{j\pi/4} c_{x(k-\beta)}(t)$	$\kappa\sqrt{\frac{2}{\kappa^2+1}} s_2 c_{x(k-\beta)}(t)$
$[2\beta T_c, 3\beta T_c]$	$c_{x(k-2\beta)}(t)$	$c_{x(k-2\beta)}(t)$
$[3\beta T_c, 4\beta T_c]$	$\kappa\sqrt{\frac{2}{\kappa^2+1}} s_2^* c_{x(k-3\beta)}(t)$	$\kappa\sqrt{\frac{2}{\kappa^2+1}} s_1^* e^{-j\pi/4} c_{x(k-3\beta)}(t)$

Table 5.3

Table 5.4 Design of the received signals for rate-$\frac{5}{4}$

If b_0 =*0* is received	
Time	Received signal on R_{x1}
$[0, \beta T_c]$	$h_{11}c_x(t) + h_{21}c_y(t) + n_k^1$
$[\beta T_c, 2\beta T_c]$	$h_{11}s_1c_{x(k-\beta)}(t) + h_{21}s_2c_{y(k-\beta)}(t) + n_k^1$
$[2\beta T_c, 3\beta T_c]$	$h_{11}c_{x(k-2\beta)}(t) + h_{21}c_{y(k-2\beta)}(t) + n_k^2$
$[3\beta T_c, 4\beta T_c]$	$-h_{11}s_2^*c_{x(k-3\beta)}(t) + h_{21}s_1^*c_{y(k-3\beta)}(t) + n_k^2$
If b_1 =*1* is received	
Time	Received signal on R_{x1}
$[0, \beta T_c]$	$h_{11}c_x(t) + h_{21}c_y(t) + n_k^1$
$[\beta T_c, 2\beta T_c]$	$h_{11}s_1e^{j\pi/4}c_{x(k-\beta)}(t) + h_{21}s_2c_{y(k-\beta)}(t) + n_k^1$
$[2\beta T_c, 3\beta T_c]$	$h_{11}c_{x(k-2\beta)}(t) + h_{21}c_{y(k-2\beta)}(t) + n_k^2$
$[3\beta T_c, 4\beta T_c]$	$-h_{11}s_2^*c_{x(k-3\beta)}(t) + h_{21}s_1^*e^{-j\pi/4}c_{y(k-3\beta)}(t) + n_k^2$

Table 5.4

Table 5.5 Design of the received signals for rate-$\frac{6}{4}$

If $b_0\ b_1$ =*00* is received	
Time	Received signal on R_{x1}
$[0, \beta T_c]$	$h_{11}c_x(t) + h_{21}c_y(t) + n_k^1$
$[\beta T_c, 2\beta T_c]$	$\sqrt{\frac{2}{\kappa^2+1}}h_{11}s_1c_{x(k-\beta)}(t) + \sqrt{\frac{2}{\kappa^2+1}}h_{21}s_2c_{y(k-\beta)}(t) + n_k^1$
$[2\beta T_c, 3\beta T_c]$	$h_{11}c_{x(k-2\beta)}(t) + h_{21}c_{y(k-2\beta)}(t) + n_k^2$
$[3\beta T_c, 4\beta T_c]$	$-\sqrt{\frac{2}{\kappa^2+1}}h_{11}s_2^*c_{x(k-3\beta)}(t) + \sqrt{\frac{2}{\kappa^2+1}}h_{21}s_1^*c_{y(k-3\beta)}(t) + n_k^2$
If $b_0\ b_1$ =01 is received	
Time	Received signal on R_{x1}

$[0, \beta T_c]$	$h_{11}c_x(t) + h_{21}c_y(t) + n_k^1$
$[\beta T_c, 2\beta T_c]$	$\sqrt{\frac{2}{\kappa^2+1}}h_{11}s_1 e^{j\pi/4}c_{x(k-\beta)}(t) + \sqrt{\frac{2}{\kappa^2+1}}h_{21}s_2 c_{y(k-\beta)}(t) + n_k^1$
$[2\beta T_c, 3\beta T_c]$	$h_{11}c_{x(k-2\beta)}(t) + h_{21}c_{y(k-2\beta)}(t) + n_k^2$
$[3\beta T_c, 4\beta T_c]$	$-\sqrt{\frac{2}{\kappa^2+1}}h_{11}s_2^* c_{x(k-3\beta)}(t) + \sqrt{\frac{2}{\kappa^2+1}}h_{21}s_1^* e^{-j\pi/4}c_{y(k-3\beta)}(t) + n_k^2$
If $b_0\, b_1 = 10$ is received	
Time	Received signal on R_{x1}
$[0, \beta T_c]$	$h_{11}c_x(t) + h_{21}c_y(t) + n_k^1$
$[\beta T_c, 2\beta T_c]$	$\kappa\sqrt{\frac{2}{\kappa^2+1}}h_{11}s_1 c_{x(k-\beta)}(t) - \kappa\sqrt{\frac{2}{\kappa^2+1}}h_{21}s_2 c_{y(k-\beta)}(t) + n_k^1$
$[2\beta T_c, 3\beta T_c]$	$h_{11}c_{x(k-2\beta)}(t) + h_{21}c_{y(k-2\beta)}(t) + n_k^2$
$[3\beta T_c, 4\beta T_c]$	$-\kappa\sqrt{\frac{2}{\kappa^2+1}}h_{11}s_2^* c_{x(k-3\beta)}(t) - \kappa\sqrt{\frac{2}{\kappa^2+1}}h_{21}s_1^* c_{y(k-3\beta)}(t) + n_k^2$
If $b_0\, b_1 = 11$ is received	
Time	Received signal on R_{x1}
$[0, \beta T_c]$	$h_{11}c_x(t) + h_{21}c_y(t) + n_k^1$
$[\beta T_c, 2\beta T_c]$	$\kappa\sqrt{\frac{2}{\kappa^2+1}}h_{11}s_1 e^{j\pi/4}c_{x(k-\beta)}(t) - \kappa\sqrt{\frac{2}{\kappa^2+1}}h_{21}s_2 c_{y(k-\beta)}(t) + n_k^1$
$[2\beta T_c, 3\beta T_c]$	$h_{11}c_{x(k-2\beta)}(t) + h_{21}c_{y(k-2\beta)}(t) + n_k^2$
$[3\beta T_c, 4\beta T_c]$	$\kappa\sqrt{\frac{2}{\kappa^2+1}}h_{11}s_2^* c_{x(k-3\beta)}(t) + \kappa\sqrt{\frac{2}{\kappa^2+1}}h_{21}s_1^* e^{-j\pi/4}c_{y(k-3\beta)}(t) + n_k^2$

Table 5.5

The output of correlator in first line is

$$y_{11} = \sum_{k=1}^{\beta} \left[h_{11}s_1c_x(t) + h_{21}s_2c_y(t) + n_{k+\beta}\right]\left[h_{11}c_x(t) + h_{21}c_y(t) + n_k\right]$$

$$= \sum_{k=1}^{\beta} \left(h_{11}^2 s_1 c_x^2(t) + h_{11}h_{21}s_1c_x(t)c_y(t) + h_{11}c_x(t)s_1n_k\right)$$

$$+ \sum_{k=1}^{\beta} (h_{21}h_{11}s_2c_x(t)c_y(t) + h_{21}^2 s_2 c_y^2(t) + h_{21}s_2c_y(t)n_k)$$

$$+ \sum_{k=1}^{\beta} h_{11}c_x(t)n_{k+\beta} + h_{21}c_y(t)n_{k+\beta} + n_k n_{k+\beta}$$

where $E_b = \sum_{k=1}^{\beta} c_x^2 = \sum_{k=1}^{\beta} c_y^2$ and $c_x \perp c_y = 0$

then

$y_{11} =$

$E_b(h_{11}^2 s_1 + h_{21}^2 s_2) + \sum_{k=1}^{\beta} h_{11}c_x(t)s_1n_k + h_{21}s_2c_y(t)n_k + \sum_{k=1}^{\beta} h_{11}c_x(t)n_{k+\beta} +$

$h_{21}c_y(t)n_{k+\beta} + n_k n_{k+\beta}$

Let

$$\sum_{k=1}^{\beta} h_{11}c_x(t)s_1n_k + h_{21}s_2c_y(t)n_k + \sum_{k=1}^{\beta} h_{11}c_x(t)n_{k+\beta} + h_{21}c_y(t)n_{k+\beta} + n_k n_{k+\beta}$$

$$= N_{11}$$

$$\sum_{k=1}^{\beta} -h_{11}c_x(t)s_2^*n_k + h_{21}s_1^*c_y(t)n_k + \sum_{k=1}^{\beta} h_{11}c_x(t)n_{k+\beta} + h_{21}c_y(t)n_{k+\beta} + n_k n_{k+\beta}$$

$$= N_{21}$$

Let $h_{11}^2 = H_{11}$, $h_{21}^2 = H_{21}$, $h_{12}^2 = H_{12}$ and $h_{22}^2 = H_{22}$

$$Y_{11} = E_b(H_{11}s_1 + H_{21}s_2) + N_{11} \quad (5.16)$$

$$Y_{21} = E_b(-H_{11}s_2^* + H_{21}s_1^*) + N_{21} \quad (5.17)$$

Similarly, for Y_{12} and Y_{22}, where, $N_{11} = N_{12}$ and $N_{21} = N_{22}$.

Then the received signal

$$\begin{pmatrix} Y_{11} \\ Y_{12} \\ Y_{21}^{*} \\ Y_{22}^{*} \end{pmatrix} = E_b \begin{pmatrix} H_{11} & H_{21} \\ H_{12} & H_{22} \\ H_{21}^{*} & -H_{11}^{*} \\ H_{22}^{\wedge} & -H_{12}^{*} \end{pmatrix} \begin{pmatrix} s_1 \\ s_2 \end{pmatrix} + \begin{pmatrix} N_{11} \\ N_{12} \\ N_{21}^{*} \\ N_{22}^{*} \end{pmatrix} \quad (5.18)$$

Finally the channel model is

$$Y = E_b HS + N \quad (5.19)$$

In order to estimate the transmitted bits, the signal Y must be multiplied by conjugate transpose of the channel matrix H

$$\begin{pmatrix} D_{s1} \\ Ds_2 \end{pmatrix} = H^{*}Y \quad (5.20)$$

The decision variables of the bits s_1 and s_2 are then as follows:

$$\begin{aligned} D_{s1} &= E_b s_1(H_{11}^2 + H_{21}^2 + H_{12}^2 + H_{22}^2) + (H_{11} + H_{12} + H_{21}^{*} + H_{22}^{*})N \\ D_{s2} &= E_b s_2(H_{11}^2 + H_{21}^2 + H_{12}^2 + H_{22}^2) + (H_{21} + H_{22} - H_{11}^{*} - H_{12}^{*})N \end{aligned} \quad (5.21)$$

Then the transmitted bits are $\acute{s_1} = sign(D_{s1})$ and $\acute{s_2} = sign(D_{s2})$.

5.5 BER Performance Analysis

Since the decision variables share the same statistical properties, we focus on computing the mean and variance of the decision variable D_{s1}.

E_b and s_1 are computed for lth bit, and the mean of D_{s1} is reduced to the term given in equation (5.22) because the elements of the noise components N are independent and zero mean.

$$E\left[D_{s1}^{(l)}\right] = E_b^{(l)} s_1^{(l)}(H_{11}^2 + H_{21}^2 + H_{12}^2 + H_{22}^2) \quad (5.22)$$

For a given fixed bit l, the first and second term in equation (5.23) are equal. The variance $var[.]$ of the decision variable is reduced to the variance of the noise term $H(1,:) * N$

$$v\left[D_{s1}^{(l)}\right] = E[(D_{s1}^{(l)})^2] - E[D_{s1}^{(l)}]^2 = E[E_b^{(l)} s_1^{(l)} (H_{11}^2 + H_{21}^2 + H_{12}^2 + H_{22}^2)\}^2] - [E_b^{(l)} s_1^{(l)} (H_{11}^2 + H_{21}^2 + H_{12}^2 + H_{22}^2)]^2 + E[\{(H_{11} + H_{12} + H_{21}^* + H_{22}^*)N\}^2] \quad (5.23)$$

Since the noise components of the variable N are uncorrelated and independent of chaotic sequences, and the Gaussian noise samples are independent as well, the conditional variance of the decision variable for a given bit lth is

$$\sigma_{D_{s1}}^2 = var[H_{11}N_{11}] + var[H_{12}N_{12}] + var[H_{21}^* N_{21}^*] + var[H_{22}^* N_{22}^*] \quad (5.24)$$

Then,

$$\sigma_1^2 = var[H_{11}N_{11}]$$

$$= var[H_{11}\{\sum_{k=1}^{\beta} h_{11} c_x(t) s_1 n_k + h_{21} s_2 c_y(t) n_k + \sum_{k=1}^{\beta} h_{11} c_x(t) n_{k+\beta} + h_{21} c_y(t) n_{k+\beta} + \sum_{k=1}^{\beta} n_k n_{k+\beta}\}]$$

$$\sigma_1^2 = H_{11}(h_{11} + h_{21}) \frac{N_0 E_b^{(l)}}{2} + \beta H_{11}(h_{11} + h_{21}) \frac{N_0 E_b^{(l)}}{2} + \frac{H_{11}\beta N_0^2}{2} \quad (5.25)$$

The form of expression (5.25) is obtained because the channel gain $H_{11}$is constant for AWGN assumption and the noise and chaotic signals are independent with zero means.

By analogy, the variances σ_2^2, σ_3^2 and σ_4^2 are given as follows:

$$\sigma_2^2 = var[H_{12}N_{12}] = H_{12}(h_{12} + h_{22}) \frac{N_0 E_b^{(l)}}{2} + \beta H_{12}(h_{12} + h_{22}) \frac{N_0 E_b^{(l)}}{2} + \frac{H_{12}\beta N_0^2}{2} \quad (5.26)$$

$$\sigma_3^2 = var[H_{21}^* N_{21}^*] = H_{21}^*(h_{11}^* + h_{21}^*)\frac{N_0 E_b^{(l)}}{2} + \beta H_{21}^*(h_{11}^* + h_{21}^*)\frac{N_0 E_b^{(l)}}{2} + \frac{H_{21}\beta N_0^2}{2} \quad (5.27)$$

$$\sigma_4^2 = var[H_{22}^* N_{22}^*] = H_{22}^*(h_{12}^* + h_{22}^*)\frac{N_0 E_b^{(l)}}{2} + \beta H_{22}^*(h_{12}^* + h_{22}^*)\frac{N_0 E_b^{(l)}}{2} + \frac{H_{22}\beta N_0^2}{2} \quad (5.28)$$

We can compute the total variance from the above expressions

$$v\left[D_{s1}^{(l)}\right] = 2(1+\beta)(H_{11} + H_{12} + H_{21} + H_{22})(E_b^{(l)}\frac{N_0}{2} + \frac{\beta N_0^2}{2}) \quad (5.29)$$

$$P_e\left(E_b^{(l)}\right) = \frac{1}{2} erfc\left[\frac{E\left[D_{s1}^{(l)}\right]}{\sqrt{2v[D_{s1}^{(l)}]}}\right] \quad (5.30)$$

In order to compute the BER with our approach, the error probability must first be evaluated for a given received energy $E_b^{(l)}$. Considering the bit energy (or chaotic chips) as a deterministic variable, the decision variable at the output of the correlator is necessarily a random Gaussian variable. As a result, this error probability is

$$P_e\left(E_b^{(l)}\right) = \frac{1}{2} erfc\left[\frac{(H_{11}^2+H_{21}^2+H_{12}^2+H_{22}^2)E_b^{(l)}}{\sqrt{2(1+\beta)(H_{11}+H_{12}+H_{21}+H_{22})(E_b^{(l)}\frac{N_0}{2}+\frac{\beta N_0^2}{2})}}\right] \quad (5.31)$$

The overall BER expression of the QCSK-MIMO sytem using high rate STBC is

$$BER = \frac{1}{2} erfc \int_0^\infty \left[\frac{(H_{11}^2+H_{21}^2+H_{12}^2+H_{22}^2)E_b^{(l)}}{\sqrt{2(1+\beta)(H_{11}+H_{12}+H_{21}+H_{22})(E_b^{(l)}\frac{N_0}{2}+\frac{\beta N_0^2}{2})}}\right] P(E_b^{(l)}) dE_b^{(l)} \quad (5.32)$$

where $P(E_b^{(l)})$ is the probability density function of the energy $E_b^{(l)}$.

To compute the integral in equation (5.32), we must first have the energy distrbution. Because the analytical expression of probability density function (PDF) seems intractable, the only way to do this is to compute the histogram of the bit energy as shown in Figure5.5 followed by a numerical integration.

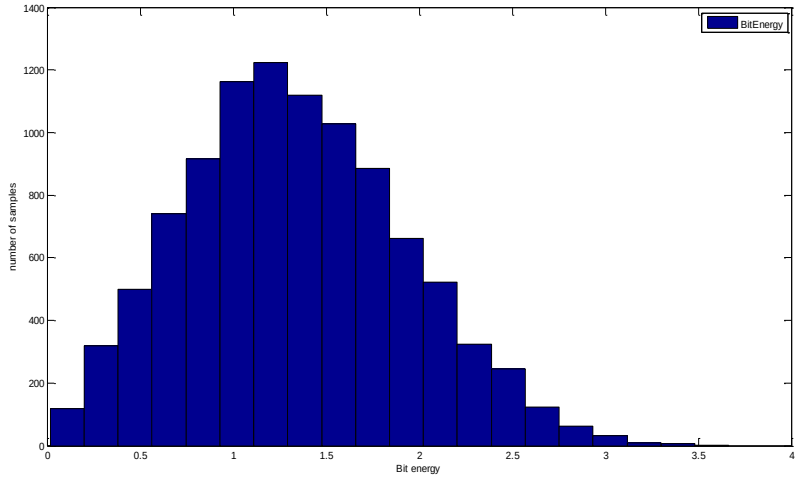

Figure 5.5 Histogram of bit energy for a QCSK-HRSTBC

Since an analytical expression appears to be hard to obtain numerical integration remains a solution for performing the BER computation. The expression in equation (5.30) can be computed numerically, taking into account the bit energy variation.

The numerical integration expression is given by,

$$BER = \sum_{l=1}^{m}\left[\frac{(H_{11}^2+H_{21}^2+H_{12}^2+H_{22}^2)E_b^{(l)}}{\sqrt{2(1+\beta)(H_{11}+H_{12}+H_{21}+H_{22})(E_b^{(l)}\frac{N_0}{2}+\frac{\beta N_0^2}{2})}}\right] P(E_b^{(l)}) \qquad (5.33)$$

where m is the number of histogram classes and $P(E_b^{(l)})$ is the probability of having the energy in interval centered on $E_b^{(l)}$.

5.6 Simulation Results

Figure 5.6 shows the effective throughput in terms of bits/time slot against bit energy to noise ratio implementing 2×2 Alamouti scheme under AWGN channel. The effective throughput $\mathcal{T}$ is defined as $\mathcal{T} = (1 - BER).R.log_2(M)$, where R is the code rate and M is the constellation size (which is 4 for QCSK modulation). The throughput of rate-1 system without chaos approaches 1 bit/time slot at 8 dB bit energy to noise ratio. Rate-1 DCSK, also approaches 1 bit/time slot but compartively slowly at 14 dB bit energy to noise ratio. At 14 dB bit energy to noise ratio rate-1

QCSK can acheve 2 bits/time slot throughput (double as compared to rate-1 DCSK). Rate-$\frac{5}{4}$ QCSK can achieve effective throughput of 2.5 bits/time slot at relatively lower bit energy to noise ratio value of 10 dB (increasing throughput by 25% as compared to rate-1 QCSK).

Figure 5.7 shows that a rate-$\frac{6}{4}$ QCSK can achieve throughput of 3 bits/time slot at bit energy to noise ratio value of 12 dB (increasing throuput by 50% as compared to rate-1 QCSK).

Figure 5.8 shows that rate-$\frac{5}{4}$ QCSK can be implemented to increasae the throughput substationally with the minimum penalty in BER performance. This system gives 3 dB gain as compared to Single-Input-Single-Output (SISO) under AWGN channel.

The circle graph (black) represent BER curve for simulated QCSK rate-5/4 which is overlapped with a maximum deviation of 0.5 dB by the green curve represented theoretical BER computed in equation (5.33).

Figure 5.9 shows that with a further relaxiation in BER performance we can further increase the throughput by implementing rate-$\frac{6}{4}$ QCSK. This system gives 2 dB gain as compared to SISO communication system under AWGN channel.

Thus we can achieve throughput of 2.5 bits/time slot by using rate-$\frac{5}{4}$ QCSK without considerable degredation in BER performance as compared to rate-1 DCSK. We can further increase the throughput to 3 bits/time slot by implementing rate-$\frac{6}{4}$ QCSK with a trade off in BER performance.

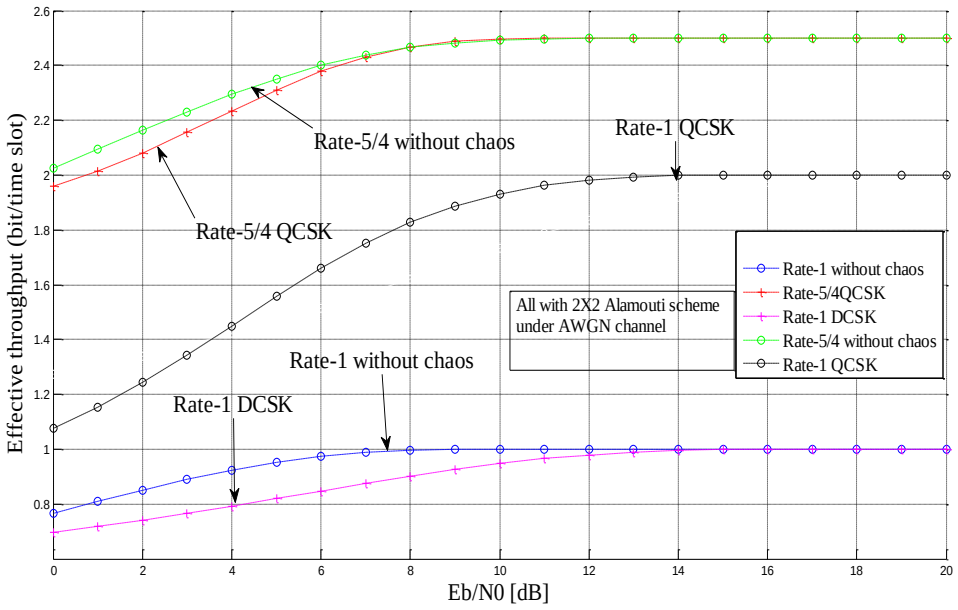

Figure 5.6 Effective throughputs of high rate full-diversity design of rate-$\frac{5}{4}$ for 2 transmit antennas

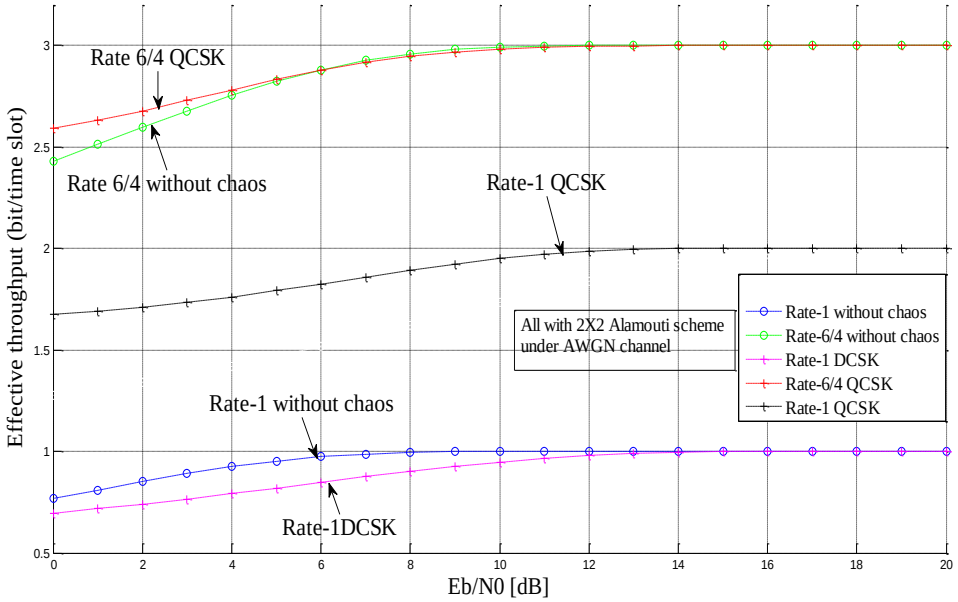

Figure 5.7 Effective throughputs of high rate full-diversity design of rate-$\frac{6}{4}$ for 2 transmit antennas

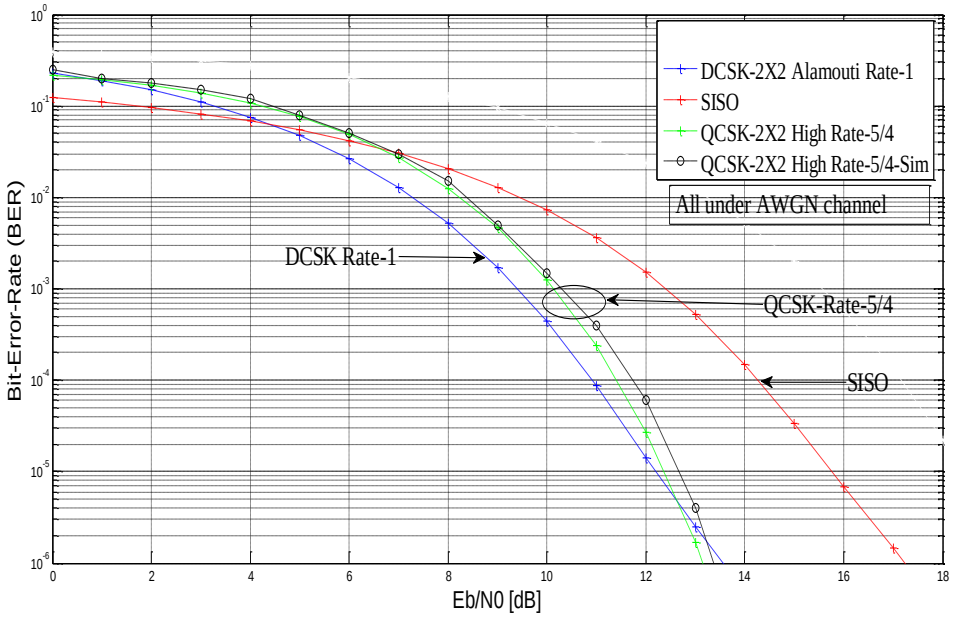

Figure 5.8 BER performances of high rate full-diversity design of rate-$\frac{5}{4}$ for 2 transmit antennas

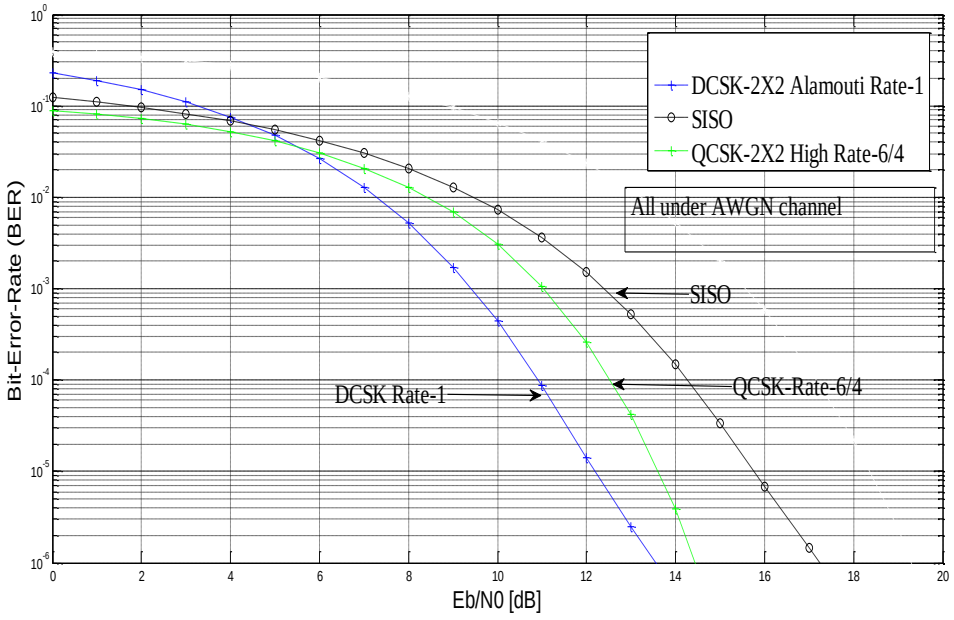

Figure 5.9 BER performances of high rate full-diversity design of rate-$\frac{6}{4}$ for 2 transmit antennas

5.7 Conclusions

In this chapter, we have proposed a multilevel modulation scheme with high rate STBC which has been labelled as (QCSK-HRSTBC). The QCSK scheme is drived from DCSK and exhibits approximately similar BER performance as DCSK for rate-$\frac{5}{4}$ but with 25% information rate increase compared to the traditional Alamouti scheme for QCSK modulation for rate-$\frac{5}{4}$ and 50% information rate increase with rate-$\frac{6}{4}$.

These advantages are realized without paying a penalty (cost) in terms of deterioration in BER. Thus, these schemes can be advantageously employed in communication systems where information security as well as high information fidelity are required.

In the next chapter, we have determined the BER performance of CSK systems under three common types of jamming, namely single-tone jamming, pulsed sinusoidal jamming and multi-tone jamming under different levels of noise power over the AWGN channel. This has been motivated by the desire to evaluate the performance of these schemes in the presence of a jamming signal. We have tried to determine that chaotic modulation scheme which is most resistant to jamming.

CHAPTER 6

ANTI-JAMMING PERFORMANCE OF COMMUNICATION SYSTEMS BASED ON CHAOTIC MODULATION AND MIMO SCHEMES

6.1 Introduction

The chaotic system is a dynamical system which shows complex behavior. The major attribute of a chaotic system is its sensitive dependence on initial conditions. Time series generated from chaotic systems are wideband in nature and noise like in appearance. Because of these special properties, chaotic systems have been widely studied for secure communication applications as well as for encryption and decryption of messages. Encryption of messages is the most common method used for secure communication of sensitive information. [Murthy C., Srilatha G., Anitha K., Ravi Kumar Ch. and Srinivasa Rao M., 2011, Liu. J, Cai. T, Ziao. J, Zhang. Y. and Wu. Y., 1996]. Our purpose in this chapter is to show that chaos based communication systems; specifically the combination of CSK and MIMO communication system has the potential of being employed to design spread-spectrum like systems. The use of CSK modulation scheme provides strong resistance against jamming [Liu. J, Cai. T, Ziao. J, Zhang. Y. and Wu. Y., 1996, Zhi. D, Bing. W. and Peng. L, 2006]. In the previous chapters, we have investigated the feasibility of employing chaotic techniques to enhance information security in MIMO channels by implementing space-time coding schemes combined with CSK modulation. The focus of this chapter is to evaluate some salient performance measures of these systems like determination of their anti-jamming performance. Prior research work on the performance of chaotic communications under the influence of jamming has focused on SISO channels [Lau F., Ye M., Tse C. and Hau S, 2001, Francis C. M., Lau F. and Tse C., 2002]. We have widened the scope of this discussion by analyzing the performance of chaos based communication systems over MIMO channels.

Specifically, CSK combined with 2×2 Alamouti scheme and 2×1 Alamouti scheme have been studied under the influence of jamming. Three common types of jamming signals, namely single-tone jamming, pulsed sinusoidal jamming and multi-tone jamming, have been considered in our study.

Contributions of the thesis in Chapter 6:

Evaluate the BER performance of CSK with 2×1 and 2×2 Alamouti schemes for different jammers. We have analyzed the performance of three common types of jamming, namely single-tone jamming, pulsed sinusoidal jamming and multi-tone jamming by quantifying the BER performance under different levels of noise power over AWGN channel.

6.2 Types of Jammers

Single-tone jamming, pulsed sinusoidal jamming and multi-tone jamming constitute the most common type of jamming signals encountered in practice. The mathematical models and characteristics of these of these jamming arrangements are briefly described below.

6.2.1 Single Tone Jammer

A single-tone jammer is generated by an oscillator whose operating frequency lies within the bandwidth of the signal being jammed (chaotic signal in our case). The single-tone jammer is used to disrupt narrowband communication. The sinusoidal jammer is modeled by a sine wave of frequency f and power P_{jam}. The output of the sinusoidal jammer (using discrete time representation) is depicted by $u_k = \sqrt{2P_{jam}}\sin(2\pi k\frac{F}{\beta})$ where F is the normalized jamming frequency defined as $F = fT_b$, T_b represents the bit duration.[Lau F., Ye M., Tse C. and Hau S., 2001, Francis C. M., Lau F. and Tse C., 2002].

6.2.2 Pulsed Sinusoidal Jammer

A pulsed sinusoidal jammer is a wideband jamming source which turns on and off periodically. This jammer concentrates the jamming power during the "on' time to disrupt a spread-spectrum communication system. The duty factor is the fraction of time during which the jammer turns on [Francis C. M., Lau F. and Tse C., 2010].

We assume that the pulsed sinusoidal jammer transmits pulses of band-limited white Gaussian noise having total average power P_{jam}. Further, it is assumed that the jamming noise occupies the same bandwidth as the chaotic signal. As mentioned before, the pulsed noise jammer concentrates the power during the "on" time to disrupt the spread-spectrum communication system. Since the jammer turns on for a fraction ρ of the time and the average power equals P_{jam}, as defined earlier, the jamming power equals $P_{jam}^{'} = P_{jam}/\rho$ when the jammer is turned on.

There are two types of pulsed sinusoidal jammers, namely slow switching jammer and fast switching jammer. In our case, the jammer is considered as fast switching jammer, meaning that the switching frequency is assumed to be very close to the bit frequency within each bit period. Therefore, the jammer is assumed to be on for a fraction ρ of the symbol period and off for the remaining symbol period [Kaddoum G., Francois G., and Sacha A., 2010].

6.2.3 Multi-tone Jammer

Multi-tone jamming is also called fixed tone jamming. The suitable method for this jamming is to place multiple tones along the transmission band. [Khalid A, 2007].
The power of the jamming signal is $P_{jam} = (M-1).N_j/N_f$.
where M, is the level of digital modulation (in our case BPSK, $M = 2$), $N_j$is the number of jamming frequencies and N_f is the number of frequencies in total bandwidth.

6.3 System Overview

In this chapter, we have investigated the performance of chaos modulation when the channel is subject to a jamming signal in addition to AWGN. Figure 6.1 shows a block diagram of concatenated chaotic and MIMO communication systems with jamming and noise added.

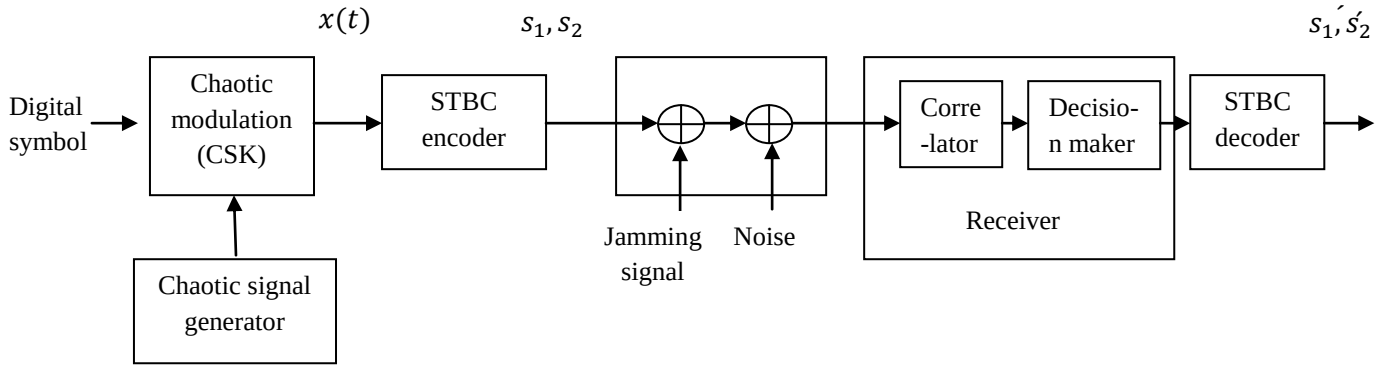

Figure 6.1 Block diagram of chaotic - MIMO communication systems with jamming and noise added [Lwaa F. et al, 2013]

The transmitted signal at the output of the transmitter for CSK communication system is as in equation (3.4). In our analysis, we assume the jamming signal is sine wave of power P_{jam} and frequency f, i.e.,

$$z(t) = \sqrt{2P_{jam}} sin\ (2\pi ft + \theta) \tag{6.1}$$

In this equation, θ is the initial phase angle of the jamming signal and is assumed to be an arbitrary constant angle selected from $[-\pi, \pi]$. Assuming additive jamming and noise, the signal at the input of receiver, $r(t)$, is given by,

$$r(t) = s(t) + n(t) + z(t) \tag{6.2}$$

where $z(t)$is the jamming signal. The transmitted bits can be demodulated by de-spreading the received signal and then integrating over a symbol duration T_s. The transmitted bits are estimated by computing the sign of the decision variable at the output of correlator.

$$Ds_l = sign\ (s_l T_c \sum_{k=0}^{\beta-1} (x_{l\beta+k})^2 + w_l + z_l)) = sign(s_l E_b^{(l)} + w_l + z_l) \tag{6.3}$$

where sign (.) is the sign operator and z_l is the jamming component after dispreading and integration.

The objective of our study is to determine the BER performance when the MIMO chaotic-modulation based digital communication system is affected by a jamming signal in addition to AWGN noise. The design of the transmitted signal is as in Table 3.1.

The received signal at the first time symbol $[0, \beta T_c]$ on R_{x1} is

$$r_{11}(t) = h_{11}s_1x_k + h_{21}s_2x_k + n_k^1 + z_k^1 \tag{6.4}$$

The received signal at the second time symbol $[\beta T_c, 2\beta T_c]$ on R_{x1} is

$$r_{21}(t) = -h_{11}s_2^*x_{k+\beta} + h_{21}s_1^*x_{k+\beta} + n_k^1 + z_k^1 \tag{6.5}$$

The received signal at the first time symbol $[0, \beta T_c]$ on R_{x2} is

$$r_{12}(t) = h_{12}s_1x_k + h_{22}s_2x_k + n_k^2 + z_k^2 \tag{6.6}$$

The received signal at the second time symbol $[\beta T_c, 2\beta T_c]$ on R_{x2} is

$$r_{22}(t) = -h_{12}s_2^*x_{k+\beta} + h_{22}s_1^*x_{k+\beta} + n_k^2 + z_k^2 \tag{6.7}$$

The energy of a given bit l is $E_b^{(l)} = \sum_{k=1}^{\beta} x_k^{(l)2}$.

We will use the first received signal $r_{11}(t)$ in our analysis to get a measure of BER performance. The analysis for other received signals is similar.

Assuming that a correlator-type receiver is employed, the correlator output for the l^{th} bit is given by,

$$Y_{11} = \sum_{K=1}^{\beta l} r_{11}x_k = \underbrace{E_b(h_{11}s_1 + h_{21}s_2)}_{\text{Required signal}} + n_k \underbrace{\sum_{k=1}^{\beta l} x_k}_{\text{Noise}} + \underbrace{z_k \sum_{k=1}^{\beta l} x_k}_{\text{Jamming signal}} \tag{6.8}$$

Suppose the output of the sinusoidal jammer is modeled as, $z_l = \sqrt{2P_{jam}}\sin\left(\frac{k\pi F}{\beta} + \theta\right)$, then equation (6.8) becomes,

$$Y_{11} = \sum_{K=1}^{\beta l} r_{11}x_k = E_b(h_{11}s_1 + h_{21}s_2) + \sum_{k=1}^{\beta l} n_k x_k + \sqrt{2P_{jam}}\sum_{k=1}^{\beta l} x_k \sin\left(\frac{k\pi F}{\beta} + \theta\right) \quad (6.9)$$

Then

$$Y_{11} = E_b(h_{11}s_1 + h_{21}s_2) + \sum_{k=1}^{\beta l} n_k^1 x_k + \sqrt{2P_{jam}}\sum_{k=1}^{\beta l} x_k \sin\left(\frac{k\pi F}{\beta} + \theta\right) \quad (6.10)$$

$$Y_{11} = E_b(h_{11}s_1 + h_{21}s_2) + N_{11} \quad (6\text{-}11)$$

where $N_{11} = \sum_{k=1}^{\beta l} n_k^1 x_k + \sqrt{2P_{jam}}\sum_{k=1}^{\beta l} x_k \sin\left(\frac{k\pi F}{\beta} + \theta\right)$

$$Y_{21} = E_b(-h_{11}s_2^* + h_{21}s_1^*) + N_{21} \quad (6\text{-}12)$$

where $N_{21} = \sum_{k=1}^{\beta l} n_k^2 x_{k+\beta} + \sqrt{2P_{jam}}\sum_{k=1}^{\beta l} x_{k+\beta} \sin\left(\frac{k\pi F}{\beta} + \theta\right)$

The received symbols Y_{12} and Y_{22} on the second antenna R_{x2} are computed in the same way.

Then the received signal is

$$\begin{pmatrix} Y_{11} \\ Y_{12} \\ Y_{21}^* \\ Y_{22}^* \end{pmatrix} = E_b \begin{pmatrix} h_{11} & h_{21} \\ h_{12} & h_{22} \\ h_{21}^* & -h_{11}^* \\ h_{22}^* & -h_{12}^* \end{pmatrix} \begin{pmatrix} s_1 \\ s_2 \end{pmatrix} + \begin{pmatrix} N_{11} \\ N_{12} \\ N_{21}^* \\ N_{22}^* \end{pmatrix} \quad (6.13)$$

In view of these equations, the channel input-output relationship is described by,

$$Y = E_b HS + N \quad (6.14)$$

In order to estimate the transmitted bits, the signal Y must be multiplied by conjugate transpose of the channel matrix H

$$\begin{pmatrix} D_{s1} \\ Ds_2 \end{pmatrix} = H^* Y \tag{6.15}$$

6.4 BER Performance Analysis

We can rewrite Y_{11} in the form

$$Y_{11} = A + B + C \tag{6.16}$$

where A, B and C are the required signal, noise and jamming signal respectively and are defined as,

$A = E_b(h_{11}s_1 + h_{21}s_2)$, $B = \sum_{k=1}^{\beta l} n_k x_k$ and $C = \sqrt{2P_{jam}} \sum_{k=1}^{\beta l} x_k \sin\left(\frac{k\pi F}{\beta} + \theta\right)$.

Where $D_{sA} = \sum_{k=2\beta(l-1)+1}^{2\beta l} x_k^2 \left(\sum_{(i,j)=1}^{2} h_{ij}^2 \; s_1 + [h_{11} + h_{12} + h_{21}^* + h_{22}^*]\right)$

The mean of Y_{11} is $E[Y_{11}] = E[D_{sA}] + E[B] + E[C]$

The mean of D_{sA} is

$$E[D_{sA}] = (h_{11}^2 + h_{21}^2 + h_{12}^2 + h_{22}^2) E_b^{(l)} s_1^{(l)} \tag{6.17}$$

The chaotic sequence, the sinusoidal wave, and the spreading codes are independent with mean equal to zero. So, the mean of the two components B and C are equal to zero, i.e,

$$E[B] = E[C] = 0 \tag{6.18}$$

The variance of Y_{11} is

$$var[Y_{11}] = var[D_{sA}] + var[B] + var[C] \tag{6.19}$$

The required signal variance can be approximated by,

$$var[D_{sA}] = var[x] \tag{6.20}$$

where $var[x]$ is the variance of chaotic signal which is equal to power of the signal (i.e., the mean of chaotic signal is equal to zero). The variance of the variable D_{sA} is equal to

$$var[D_{sA}] = (h_{11}^2 + h_{12}^2 + h_{21}^2 + h_{22}^2)E_b\frac{\Lambda}{2} \tag{6.21}$$

where $p_s = \frac{E_b}{2\beta}$ and Λ is the variance of $\{x_k^2\}$

$$var[D_{sA}] = (h_{11}^2 + h_{12}^2 + h_{21}^2 + h_{22}^2)\beta p_s\Lambda \tag{6.22}$$

where P_s is the average power of the chaotic tent map. The power P_s can computed by numerical simulation, or analytically, if the probability density function of the chaotic sequence is available.

The variance of the variable B is equal to

$$var[B] = \beta p_s N_0 \tag{6.23}$$

And the variance of variable C is equal to

$$var[C] = 2\beta p_s P_{jam} \tag{6.24}$$

Then,

$$var[Y_{11}] = var[D_{sA}] + var[B] + var[C] = 2(h_{11}^2 + h_{12}^2 + h_{21}^2 + h_{22}^2)\beta p_s\Lambda + \beta p_s N_0 + 2\beta p_s P_{jam} \tag{6.25}$$

The overall BER requires the conditional error properties $P(\acute{s} = +1 \mid$ s=-1) or verse versa. These are equal by symmetry and thus the overall BER does not depend on the proportions of the transmitted $\pm$ value and so

BER=$Q\{E(x)/\sqrt{2Var(x)}\}]$ where $Q(x) = \int_x^{+\infty} \frac{1}{\sqrt{2\pi}} \exp(-u^2/2)$

Thus,

$$BER =$$

$$Q[E_{xi}\left(\sum_{n,p=1}^{2} h_{n,p}^2 \sum_{i=0}^{\beta-1} x_i^2\right)(2(\sum_{n,p=1}^{2} h_{n,p}^2)\beta p_s\Lambda + \beta p_s N_0 + 2\beta p_s P_{jam})^{-\frac{1}{2}}] =$$

$$E_{xi}(\sum_{i=0}^{\beta-1} x_i^2)(h_{11}^2 + h_{21}^2 + h_{12}^2 + h_{22}^2).(2(h_{11}^2 + h_{12}^2 + h_{21}^2 + h_{22}^2)\beta p_s\Lambda + \beta p_s N_0 + 2\beta p_s P_{jam})^{-\frac{1}{2}}$$

$\sum_{i=0}^{\beta-1} x_i^2 = \mathrm{E_b^{(l)}}$ is the chaotic symbol energy, and $E_{xi} = \int_0^{\infty} \mathrm{p}\left(\mathrm{E_b^{(l)}}\right)\mathrm{dE_b^{(l)}}$, then

$$\mathrm{BER} = \int_0^{\infty} \frac{1}{2}\mathrm{erfc}\left(\frac{2(h_{11}^2+h_{12}^2+h_{21}^2+h_{22}^2)\beta p_s}{\sqrt{2(h_{11}^2+h_{12}^2+h_{21}^2+h_{22}^2)\beta p_s\Lambda + \beta p_s N_0 + 2\beta p_s P_{jam}}}\right)\mathrm{p}\left(\mathrm{E_b^{(l)}}\right)\mathrm{dE_b^{(l)}} \quad (6.26)$$

The BER expression is the result of the integral given in equations (6.26). To compute the integral in (6.26), we must first have the bit energy distribution.
After numerical integration the BER expression for 2×2 Alamouti is given by,

$$BER = \sum_{l=1}^{m} \frac{1}{2} erfc\left(\frac{2(h_{11}^2+h_{12}^2+h_{21}^2+h_{22}^2)\beta p_s}{\sqrt{2(h_{11}^2+h_{12}^2+h_{21}^2+h_{22}^2)\beta p_s\Lambda + \beta p_s N_0 + 2\beta p_s P_{jam}}}\right) p(E_b^{(l)}) \quad (6.27)$$

For pulsed sinusoidal jamming

$$p_{jam} = P_{jam}^{'}/\rho \quad (6.28)$$

Again, ρ is the fraction of time during which the jammer is on. In our case, jammer is assumed to be a fast switching jammer. Therefore, the jammer is assumed to be on for a fraction ρ of the symbol period and off for the remaining symbol period. Then we have,

$$BER_{on} = \sum_{l=1}^{m} \frac{1}{2} erfc\left(\frac{2(h_{11}^2+h_{12}^2+h_{21}^2+h_{22}^2)\beta p_s}{\sqrt{2(h_{11}^2+h_{12}^2+h_{21}^2+h_{22}^2)\beta p_s\Lambda + \beta p_s N_0 + \frac{2\beta P_s P_{jam}^{'}}{\rho}}}\right) p(E_b^{(l)}) \quad (6.29)$$

$$BER_{off} = \sum_{l=1}^{m} \frac{1}{2} erfc\left(\frac{2(h_{11}^2+h_{12}^2+h_{21}^2+h_{22}^2)\beta p_s}{\sqrt{2(h_{11}^2+h_{12}^2+h_{21}^2+h_{22}^2)\beta p_s \Lambda + \beta p_s N_0}}\right) p(E_b^{(l)}) \quad (6.30)$$

The total BER is then given by,

$$BER_{total} = \rho \mathrm{BER_{on}} + (1-\rho)\mathrm{BER_{off}} \quad (6.31)$$

In case of multi-tone jamming, as illustrated in section 2.3, $P_{jam} = (M-1).N_j/N_f$, then the probability of error is

$$BER = \sum_{l=1}^{m} \frac{1}{2} erfc\left(\frac{2(h_{11}^2+h_{12}^2+h_{21}^2+h_{22}^2)\beta p_s}{\sqrt{2(h_{11}^2+h_{12}^2+h_{21}^2+h_{22}^2)\beta p_s \Lambda + \beta p_s N_0 + \frac{(M-1)N_j}{N_f}}}\right) p(E_b^{(l)}) \quad (6.32)$$

6.5 Simulation Results and Discussion

In this simulation jamming signal introduced as noise signal interfering with the chaos modulated data signal. As shown in Figure 6.2, in absence of jamming signal, the chaotic system implementing 2×2 Alamouti scheme with spreading factor β=4 gives BER performance equivalent to BPSK under AWGN. With the introduction of jamming signal, the BER performance degrades by 2.5 dB for jamming level $\frac{Ps}{Pjam} = -6$ dB and by 3 dB for jamming level $\frac{Ps}{Pjam} = -9$ dB. If an un-spread non chaotic signal is employed in the presence of the jamming signal, a further degradation of the BER performance by 1.25 dB at jamming level $\frac{Ps}{Pjam} = -9$ dB is observed. Thus it can be inferred that spreading signal over wide bandwidth using chaotic techniques improves BER performance in the presence of a jamming signal. The circle graph (black) represent BER curve for simulated jamming level $\frac{P_s}{P_{jam}} = -6\,dB$ which is overlapped by the green curve represented theoretical BER computed in equation (6.27).

As shown in Figure 6.3, in the presence of jamming signal of jamming level $\frac{Ps}{Pjam} = -6$ dB a chaotic system implementing 2×2 Alamouti schemes gives 5 dB improvements in BER performance at BER of 10^{-4} as compared to chaotic SISO system. Similarly, a 2×1 Alamouti chaotic system gives 3 dB gain at BER of 10^{-4} as compared to chaotic SISO system. Hence, the use of chaotic modulation schemes combined with Alamouti schemes helps in enhancement of BER performance under the influence of jamming signals.

In Figure 6.4, we have plotted the BER performance of the CSK-MIMO system under the influence of single-tone, pulsed sinusoidal ($\rho = 0.3$) and multi-tone jamming ($N_j = 3$) for jamming level $\frac{Ps}{Pjam} = -6$ dB. The required bit energy to noise ratio (E_b/N_0) is in the range of 11 dB to 18 dB at BER of 10^{-5}. The single-tone jamming requires a SNR (E_b/N_0) value of 11 dB to achieve a BER of 10^{-5}. While it can be observed that the multi-tone jamming requires a SNR (E_b/N_0) value of 18 dB to achieve a BER of 10^{-5}.

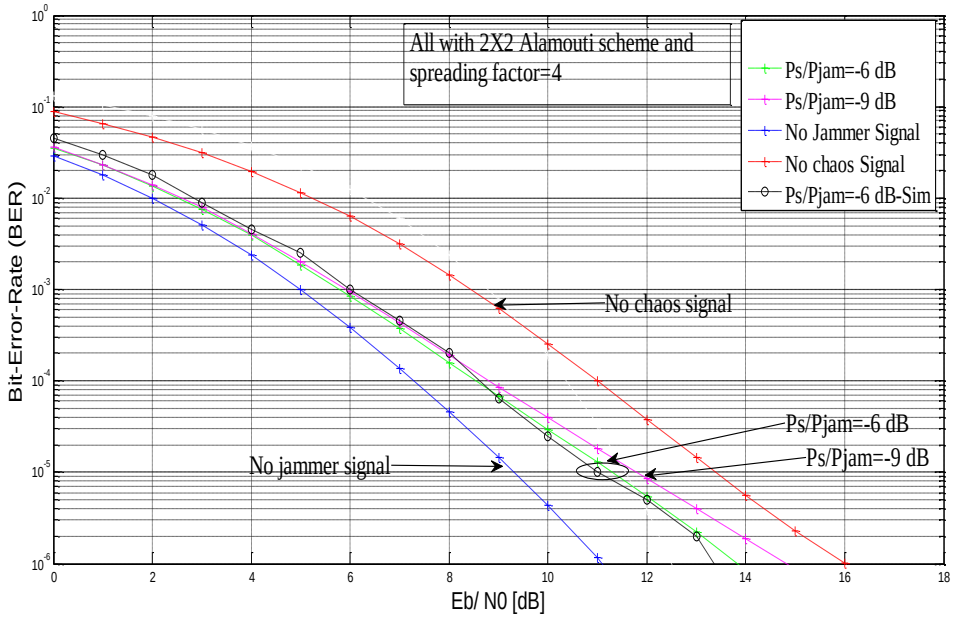

Figure 6.2 BER of CSK system with different values of signal power to the jamming signal ($\frac{Ps}{Pjam}$)

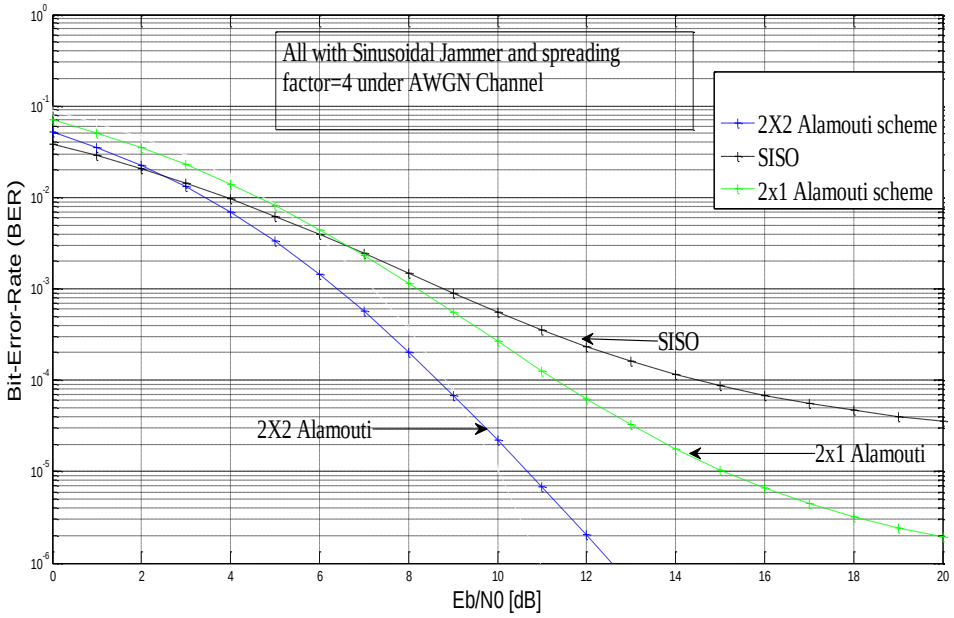

Figure 6.3 BER comparison between 2×2, 2×1 and SISO communication systems for Sinusoidal jamming with jamming level $\frac{Ps}{Pjam} = -6$ dB

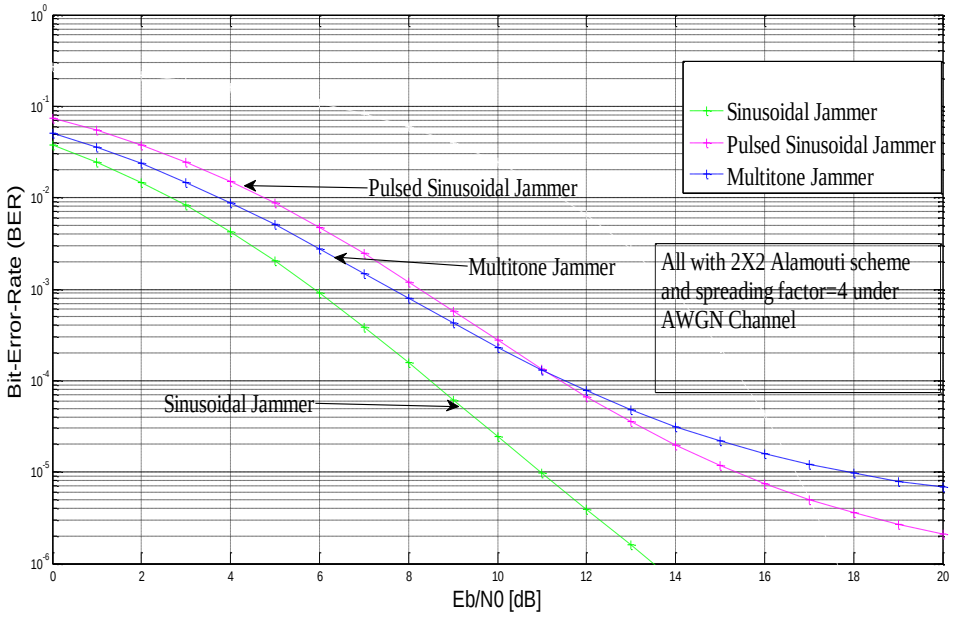

Figure 6.4 BER of common different types of jamming, namely, sinusoidal jamming, pulsed sinusoidal jamming and multi-tone jamming

6.6 Conclusions

In this chapter, the performance of secure CSK-MIMO communication systems in the presence of different types of jamming signals has been analyzed. The analysis has been supported by simulation plots in which the BER associated with the system under different jamming scenarios has been determined and plotted.

The analytical BER expressions obtained for different types of jamming have been derived. Simulation results quantifying the BER levels for different levels of jamming and different types of jamming have been presented.

A comparison of the performance of CSK-MIMO schemes employing $2 \times 2, 2 \times 1$ and SISO systems under sinusoidal jamming has been presented. Based on these results, it can be concluded that CSK-MIMO systems have significant anti-jamming capabilities and have the potential of being employed in designing spread-spectrum systems.

In chapter seven we have design a DS-CDMA-MIMO system based on CSK modulation and have evaluated its performance in a wireless channel with two transmit antennas and one receive antenna as well as with two transmit antennas and two receive antennas.

We have used different chaotic maps under different fading channel models (Rayleigh and Gamma-Gamma) in our study.

CHAPTER 7

CSK BASED MIMO-CDMA SYSTEM: DESIGN AND PERFORMANCE EVALUATION

7.1 Introduction

The primary motivation for the design of a MIMO-DS-CDMA link based on CSK modulation scheme arises from the necessity to have secure communication links with good BER performance. The precise BER specification usually depends on the value dictated by the application. CDMA-MIMO system is based on combination of two technologies, CDMA and MIMO, which have been introduced to optimize the performance in the presence of two sources of degradation: multipath and multiuser interference [Cherni A.,Ben Jemaa Z. and Belghith S. 2011, Inokura H., Kuroyanagi N., Tomita M. and Suehiro N, 2003, Mazzini G., Sitti G. and Rovatti R, 1997].

In DS-CDMA system, all the users of the system employ the same frequency band simultaneously. Individual users are distinguished only by means of spreading waveforms. The dominant impairment and the limiting factor in the detection process of synchronous DS-CDMA system is the loss of orthogonality between the spreading waveforms due to fading multipath propagation. It leads to Multiple Access Interference (MAI) in DS-CDMA system. MAI can be mitigated through the use of MIMO schemes [Thiruvengadam S., Karthikeyan A., Vinothkumar V. and Abhaikumar V., 2003]. A classical set of spreading sequences used in DS-CDMA system are the binary sequences generated by LFSR schemes [Nagarajan V., Dananjayan P. and Nithyanandhan L.,2009]. It has been reported in literature that the chaotic sequences derived from chaotic time series exhibit orthogonality better than the conventional PN sequences. Further, there is a possibility of generating a large number of distinct chaotic sequences, which could be used to support more number of users within allocated bandwidth for DS-CDMA systems [Thiruvengadam S.,

Karthikeyan A., Vinothkumar V. and Abhaikumar V., 2003]. The properties of chaotic signals match the requirements for signals used in communication systems, in particular for spread-spectrum communication and secure communication systems. To correctly demodulate the transmitted CSK signal, the exact initial conditions must be known at the receiver side [Jaedon P. Eunju L., and Giwan Y., 2011]. The possibility of generating an infinite number of uncorrelated chaotic sequences from a given map, which can be uniquely regenerated at the receiver, simplifies the application of these signals in multiuser case. Tent map, Logistic map, Chebyshev map and Tail shift map are typical examples of one-dimensional chaotic maps. One practical approach to realizing a secure communication channel is to have a chaotic generator that is can be used to generate sequences which serve as the symbols of a CSK system. In this case, different sequences can be generated using the same generator but with different initial conditions [Huanfei and Haibin 2009]. A widely used approach known as the Simplified Gaussian Approximation (SGA) considers the sum of dependent variables at the output of correlator as a Gaussian variable [Charge P, Kaddoum G., Lawrance A. and Roviras D., 2011]. This approach does not take into account the non-periodic nature of chaotic sequence, which leads to a low precision of BER approximations, especially when the spreading factor is low.

Since the SGA is very crude in its Gaussian approximation, a better approach is to apply the Gaussian approximation conditionally on the chaotic spreading samples of the active user, and subsequently average over all chaotic spreading samples which the active user might employ.

Contributions of the thesis in Chapter 7:

- Evaluate the BER performance of Code-Division Multiple Access (CDMA)-MIMO system under different fading channels.

7.2 **CSK-DS-CDMA Transmission Systems**

Here, we give a brief description of CSK-DS-CDMA system which is modified in our proposed MIMO-CDMA based on CSK modulation scheme discussed in section 7.4.

The CSK system in Figure 7.1 has L users. A stream of binary data symbols from active user l $(b_{l,i} = \pm 1, i = 1,2,\ldots)$ with bit period T_b is spread by a chaotic signal generated at the transmitter.

The spreading factor (β) is the number of chaotic samples in a bit duration and these constitute a chaotic segment; T_c is the chip duration, so $T_b = \beta T_c$. The chaotic segment $\{x_l\}$ is assumed to have been started with a random initial sample value $x_{l,0}$ from the natural invariant distribution [Lawrance and Yao 2007].
The output of chaotic signal generator

$$U_l(t) = \sum_{i=0}^{\beta-1} x_{l,i} \tag{7.1}$$

The transmitted signal of the lth user is thus

$$S_l(t) = \sum_{i=0}^{\beta-1} (b_l x_{l,i}) \tag{7.2}$$

The energy of a typical bit of lth user is given by

$$E_b^{(l)} = T_c \sum_{i=0}^{\beta-1} x_{l,i}^2 \tag{7.3}$$

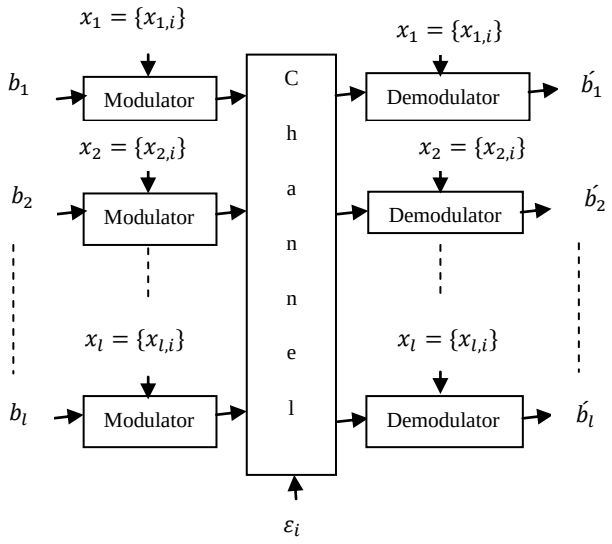

Figure 7.1: Block diagram of a multiuser coherent CSK communication system.

The bit energy depends on the sample values $x_{l,i}$ which are real numbers. Hence, the bit energy is not a constant in contrast to conventional system, such as BPSK.

We assume that the transmitted signal is communicated over a channel perturbed by AWGN channel. Let $n(t)$ be the Gaussian noise effecting reception by the lth user. We assume $n(t)$ has a two sided power spectral density given by

$$S_W(f) = N_0/2 \tag{7.4}$$

Let $\grave{n}(t)$ be the equivalent noise source of $n_t(t)$ specified as

$$\grave{n}(t) = \sum_{i=0}^{\infty} \varepsilon_{l,i} \tag{7.5}$$

where $\{\varepsilon_{l,i}\}$ are independent Gaussian random variables with zero mean and variance

$$\sigma_n^2 = N_0/2T_c \tag{7.6}$$

Furthermore, all users are asynchronous and the received signal $r_l(t)$ of user l at time t includes the sum of $L-1$ interference signals from the other users and AWGN noise. Hence, $r_l(t)$ is given by,

$$r_l(t) = S_l(t) + \sum_{k=1,k\neq l}^{L} S_k(t) + \grave{n}(t) \tag{7.7}$$

By substituting (7.2) in (7.5) and (7.7) we obtain,

$$r_l(t) = h\sum_{i=0}^{\beta-1} b_l x_{l,i} + \sum_{k=1,k\neq l}^{L} b_k x_{k,i} + \varepsilon_i = \sum_{i=0}^{\beta-1} z_{l,i} \tag{7.8}$$

where h is the channel coefficient. In coherent CSK communication systems, perfect synchronization is assumed.

The output of correlator is

$$C_{r,u} = \int_0^{\beta T_c} r_l(t) U_l(t) dt \tag{7.9}$$

By placing (7.1) and (7.8) in (7.9) the correlator output can be expressed as [Ehsan. B., Robert S. and Ranjan. M.,2008],

$$C(z_l, x_l) = T_c \sum_{i=0}^{\beta-1} z_{l,i} x_{l,i} = T_c C_s(z_l, x_l) \tag{7.10}$$

where $C(z_l, x_l)$ is the decision variable and is the discrete covariance sum from (z_l, x_l). and $z_{l,i} = hb_l x_{l,i} + \sum_{k=1,k\neq l}^{L} b_k x_{k,i} + \varepsilon_i, \;\; i = 0,1, \dots, \beta - 1.$

7.3 Fading Channel Models

In addition to Rayleigh fading channel (section 3.3.1) and Gamma-Gamma fading channel (section 4.3), log-normal fading channel are also used also to model wireless optical communication channels.

Lognormal Fading Channel [Mokhtar M and Gupta S., 1992, Laourine A., Stephanne A. and Affes S. 2009]

A random variable X is said to be log-normally distributed, if the random variable $Y = lnx$ is Gaussian distributed. The lognormal distribution is used to model continuous random quantities when the distribution is believed to be skewed, such as certain income and lifetime variables. The PDF of the lognormal distribution is given by

$$f(x) = \begin{cases} \frac{1}{x\sigma\sqrt{2\pi}} e^{-\left[\frac{(\ln(x)-\mu^2)}{2\sigma^2}\right]}, & x > 0 \\ 0, & x \leq 0 \end{cases} \tag{7.11}$$

7.4 MIMO-CDMA System Based on CSK

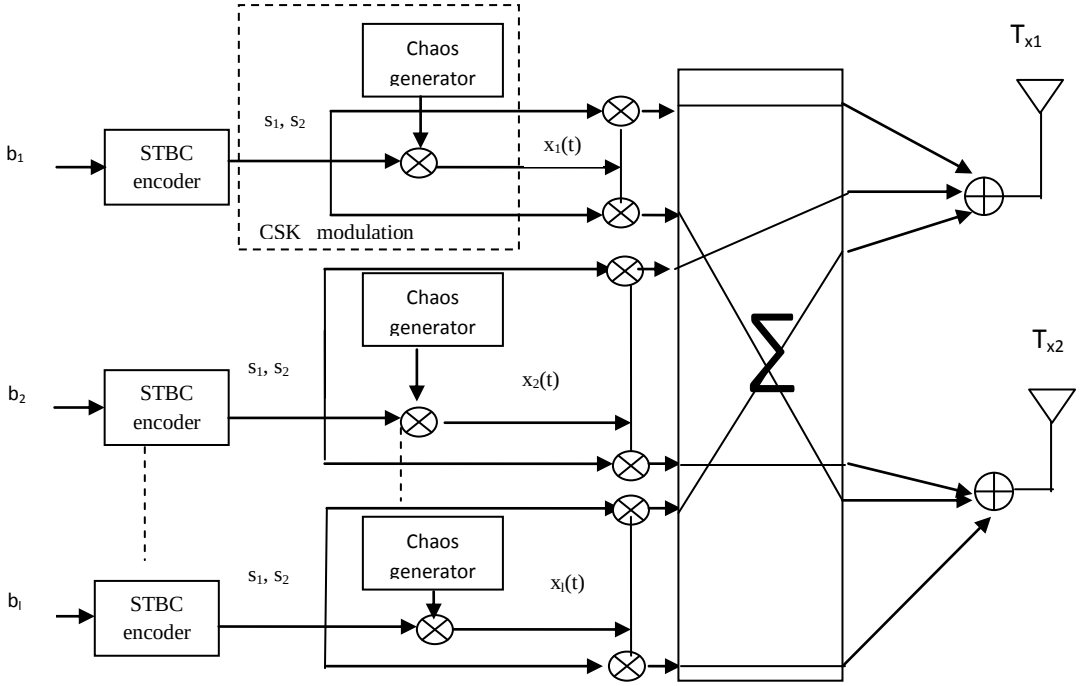

(a)

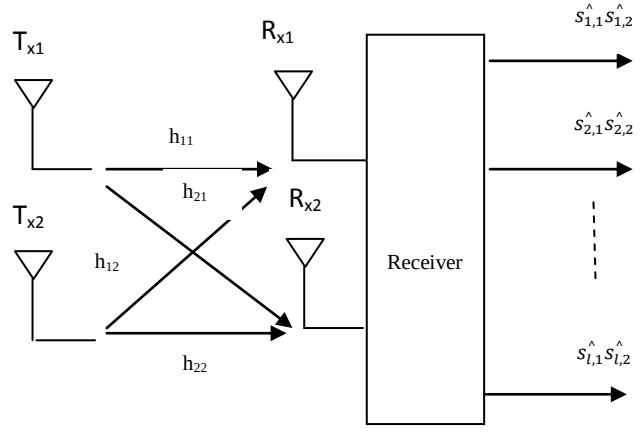

(b)

Figure 7.2 Block diagram of proposed CSK-MIMO-DS-CDMA system a) Transmitter, b) Receiver

In our case, we consider two cases. In the first case, the system is assumed to have two transmitter antennas and one receiver antenna. In the second case, it is assumed to have two transmitter antennas and two receiver antennas. The Almouti matrix for symbols s_1 and s_2 is as in equation (3.10).

The design of the MIMO-DS_CDMA system based on CSK modulation scheme is illustrated in Figure 7.2. The data b_l for each user l are separated by chaotic sequences which generated by chaotic generator.

The design of the transmitted signal is specified in Table 7.1

Time	$s_1(t)$from T_{x1}	$s_2(t)$from T_{x2}
$[0, \beta T_c]$	$s_1 U_{l,i}(t)$	$s_2 U_{l,i}(t)$
$[\beta T_c, 2\beta T_c]$	$-s_2^* U_{l,i+\beta}(t)$	$s_1^* U_{l,i+\beta}(t)$

Table 7.1

In this table, T_c denotes the chip interval.

The block diagram for 2×1 Alamouti for lth user is shown in Figure 3-3.

The received signal of the 2×1 Alamouti for lth user is specified in Table 7.2

Time	Received signal
$[0, \beta T_c]$	$z_l = h_1 s_1 x_k + h_2 s_2 x_k + (\sum_{i=0}^{\beta-1} \sum_{k=1,k\neq l}^{L} N_1 + s_k^1(t))$
$[\beta T_c, 2\beta T_c]$	$z_l = -h_1 s_2^* x_{k+\beta} + h_2 s_1^* x_{k+\beta} + (\sum_{i=0}^{\beta-1} \sum_{k=1,k\neq l}^{L} N_2 + s_k^2(t))$

Table 7.2

As shown in Figure 3.3b, the received signal for lth user is first multiplied by a synchronized replica of chaotic sequence, and then summed over a time symbol βT_c,

and finally decoded by a STBC decoder. In the first time block $[0, \beta T_c]$ of the receiver, the received signal y_1 for lth user after correlation with the local chaotic sequence is

$$y_{l,1} = T_c \sum_{i=0}^{\beta-1}[h_1 s_1 x_{l,i} + h_2 s_2 x_{l,i} + N_1][x_{l,i}] = (h_1 s_1 + h_2 s_2) \sum_{i=0}^{\beta-1} x_{l,i}^2 + (\sum_{i=0}^{\beta-1} \sum_{k=1,k\neq l}^{L} N_1 + s_k^1(t)) x_{l,i} \quad (7.12)$$

Let$((\sum_{i=0}^{\beta-1} \sum_{k=1,k\neq l}^{L} N_1 + s_k^1(t))\, x_{l,i} = \acute{N_1}$ and $\left(\sum_{i=0}^{\beta-1} \sum_{k=1,k\neq l}^{L} N_2 + s_k^2(t)\right) x_{l,i} = \acute{N_2}$.

The energy of a given bit b is as in equation (7.3). The equivalent baseband model on $[0, \beta T_c]$ of the received symbol is

$$Y_{l,1} = E_b(h_1 s_1 + h_2 s_2) + \acute{N_{l,1}} \quad (7.13)$$

In this equation, $\acute{N_1}$ represent noise and interference of other user components. By analogy, the received symbol $Y_{l,2}$ for the second time $[\beta T_c, 2\beta T_c]$ for the lth user is given by,

$$Y_{l,2} = E_b(-h_1 s_2^* + h_2 s_1^*) + \acute{N_{l,2}} \quad (7.14)$$

Again, $\acute{N_2}$ represent noise and interference of other user components.

The received signals of the 2×2 Alamouti for lth user are summarized in Table 7.3.

Time	Received signal on R_{x1}
$[0, \beta T_c]$	$z_l = h_{11} s_1 x_k + h_{21} s_2 x_k + \sum_{i=0}^{\beta-1} \sum_{k=1,k\neq l}^{L} n_k^1 + s_k^1(t)$
$[\beta T_c, 2\beta T_c]$	$z_l = -h_{11} s_2^* x_{k+\beta} + h_{21} s_1^* x_{k+\beta} + \sum_{i=0}^{\beta-1} \sum_{k=1,k\neq l}^{L} n_k^2 + s_k^2(t)$

Table 7.3

Let $\sum_{i=0}^{\beta-1}\sum_{k=1,k\neq l}^{L} n_k^{1,2} + s_k^{1,2}(t) = \acute{n}_k^{1,2}$.

As shown in Figure 3.4 the received signal for lth user is first multiplied by a synchronized replica of chaotic sequence, and then summed over a time symbol βT_c, and finally is decoded by a STBC decoder. In the first time block $[0, \beta T_c]$ of R_{x1}, the received signal y_{11} for the lth user after correlation with the local chaotic sequence is

$$y_{l,11} = \sum_{i=0}^{\beta-1}\left[h_{11}s_1 x_{l,i} + h_{21}s_2 x_{l,i} + \acute{n}_{k,l}^{1}\right]\left[x_{l,i}\right] = (h_{11}s_1 + h_{21}s_2)\sum_{i=0}^{\beta-1} x_{l,i}^2 + \sum_{k=1,k\neq l}^{L}\sum_{i=0}^{\beta-1} \acute{n}_{k,l}^{1} x_{k,i} \quad (7.15)$$

The equivalent baseband model on $[0, \beta T_c]$ of the received symbol on the first antenna is

$$Y_{l,11} = E_b(h_{11}s_1 + h_{21}s_2) + N_{l,11} \quad (7.16)$$

In this equation, $N_{l,11}$ represents a zero mean Gaussian noise component for lth user.

$$N_{l,11} = \sum_{i=0}^{\beta-1} n_l^{1}\acute{x}_{l,i} \quad (7.17)$$

By analogy, the received symbol $Y_{l,21}$ on the first antenna R_{x1} for the second time block $[\beta T_c, 2\beta T_c]$ for the lth user is given by

$$Y_{l,21} = E_b(-h_{11}s_2^* + h_{21}s_1^*) + N_{l,21} \quad (7.18)$$

where the noise component is given by

$$N_{l,21} = \sum_{i=0}^{\beta-1} n_l^{2}\acute{x}_{l,i} \quad (7.19)$$

The received symbols $Y_{l,12}$ and $Y_{l,22}$ on the second antenna R_{x2} are computed in the same way.

The channel model for lth user is given by

$$Y_l = E_b HS + N_l \quad (7.20)$$

The transmitted bits for lth user are estimated by multiplying the symbol Y_l by the conjugate transpose of the channel H, then

$$\binom{D_{s1,l}}{D_{s2,l}} = H^* Y_l \tag{7.21}$$

Finally, the estimated bits are computed from the sign of the decision variable $s_{1,l} = sign(Ds_{1,l})$ and $s_{2,l} = sign(Ds_{2,l})$.

7.5 BER Computation for CSK-MIMO-CDMA System

In this section, we have studied the conditional BER associated with estimating a symbol (bit value) 0 conditional on symbol 1 being transmitted is considered, and vice versa. The aim of this section is to calculate the bit-error probability exactly, rather than approximately from Gaussian approximation. Based on the SGA assumption, the BER can be specified as

$$BER = P\{C_S(z_l, x_l) < 0 | b_l = 1\} \tag{7.22}$$

The Simplified Gaussian Approximation (SGA) technique can be used to accurately determine the BER when the value of the spreading factor β is large (> 50). It does not provide accurate estimates of the BER for small values of β. where $E(C_s)$ and $var(C_s)$ are the mean and variance of $C_S(z_l, x_l)$ [Tam W., Lau F., Tse C. and Lawrance A., 2004].

Because of the SGA presented above is very crude in its Gaussian assumption and a better approach is to apply the Gaussian approximation conditioned on the chaotic spreading samples which the active user might employ.

Thus $E(C_s)$ and $Var(C_s)$ are now considered conditionally on x_l and denoted by $E(C_s|x_l)$ and $Var(C_s|x_l)$.

The overall BER requires the conditional error probabilities $p(\hat{b} = \pm 1 |\ b = \mp 1)$.these are equal by symmetry and thus the overall BER does not depend on the properties of the transmitted $\pm$ symbol values, the conditional Gaussian approximation (CGA) to the BER probability thus becomes [Ji Y. and Lawrance A, 2005, Ohama G., Lawrance A., 2003].

$$E_{xj}[Q\{E(C_s|x_l)/\sqrt{Var(C_s|x_l)}\}], \quad Q(x) = \int_x^{+\infty} \frac{1}{\sqrt{2\pi}} exp\,(-u^2/2) \tag{7.23}$$

Then

$$E(C_s|x_l) = \sum_{n,p=1}^{2} h_{n,p}^2 \sum_{i=0}^{\beta-1} x_{l,i}^2 \tag{7.24}$$

$$Var(C_s|x_l) = (\sum_{n,p=1}^{2} h_{n,p}^2)[(L-1)\sigma_X^2 + \sigma_n^2] \sum_{i=0}^{\beta-1} x_{l,i}^2 + 2\beta(L-1)\sigma_X^2 \sum_{k=1}^{\beta-1}(\beta^{-1} \sum_{i=0}^{\beta-k-1} x_{l,i} x_{l,i+k}) \tag{7.25}$$

Here σ_X^2 denotes the variance of X. Hence using (7.26), CGA result for BER becomes

$$BER = Q[E_{xl} \times \sum_{n,p=1}^{2} h_{n,p}^2 \sum_{i=0}^{\beta-1} x_{l,i}^2 / (\sum_{n,p=1}^{2} h_{n,p}^2 \sum_{i=0}^{\beta-1} \frac{x_{l,i}^2}{\beta\sigma_X^2})^{\frac{1}{2}} (\frac{1}{SNR} + \frac{1}{SOR} + \frac{2}{SOR} \sum_{k=1}^{\beta-1} x_{l,i}\, x_{l,i+k})^{\frac{1}{2}}\}\,] \tag{7.26}$$

The notation $SNR = \beta\sigma_X^2/\sigma_n^2$, eqavinatly E_b/N_0 has been used to define the signal to noise ratio of the system and SOR defines the quantity $\beta/(L-1)$, which will be called the spreading –to-user-interference ratio.

$$BER = Q[E_{xl} \times \sum_{n,p=1}^{2} h_{n,p}^2 \sum_{i=0}^{\beta-1} x_{l,i}^2 / (\sum_{n,p=1}^{2} h_{n,p}^2 \sum_{i=0}^{\beta-1} \frac{x_{l,i}^2}{\beta\sigma_X^2})^{\frac{1}{2}} (\frac{1}{SNR} + \frac{1}{SOR} + \frac{2}{SOR} \sum_{k=0}^{\beta-1} (1 - \frac{k}{\beta}))^{\frac{1}{2}}\}] \tag{7.27}$$

Now, according to CGA result (7.27), the BER result for 2×1 Alamouti scheme can be written as the integral

$$BER = Q[E_{xl} \times (h_1^2 + h_2^2) \sum_{i=0}^{\beta-1} x_{l,i}^2 / ((h_1^2 + h_2^2) \sum_{i=0}^{\beta-1} \frac{x_{l,i}^2}{\beta \sigma_X^2})^{\frac{1}{2}} (\frac{1}{SNR} + \frac{1}{SOR} + \frac{2}{SOR} \sum_{k=0}^{\beta-1} (1 - \frac{k}{\beta}))^{\frac{1}{2}}\}] \quad (7.28)$$

$\sum_{I=0}^{\beta-1} x_{l,i}^2 = e_{bc}$ is the chaotic symbol energy, and $\frac{E_{xl}}{(\beta \sigma_X^2)^{1/2}} = \int_0^{\infty} \mathrm{p}(e_{bc}) \mathrm{d}e_{bc}$ then

$$BER_{CSK} = \int_0^{+\infty} Q\{\sqrt{\frac{(h_1^2 + h_2^2) e_{bc}}{\frac{1}{SNR} + \frac{1}{SOR} + \frac{2}{SOR} \sum_{k=0}^{\beta-1} (1 - \frac{k}{\beta})}}\} * f(e_{bc}) de_{bc} \quad (7.29)$$

And according to CGA result (7.27), the BER result for 2×2 Alamouti scheme can be written as the integral,

$$BER = Q[E_{xl} \times h_{11}^2 + h_{21}^2 + h_{12}^2 + h_{22}^2 \sum_{i=0}^{\beta-1} x_{l,i}^2 / (h_{11}^2 + h_{21}^2 + h_{12}^2 + h_{22}^2 \sum_{i=0}^{\beta-1} \frac{x_{l,i}^2}{\beta \sigma_X^2})^{\frac{1}{2}} (\frac{1}{SNR} + \frac{1}{SOR} + \frac{2}{SOR} \sum_{k=0}^{\beta-1} (1 - \frac{k}{\beta}))^{\frac{1}{2}}\}] \quad (7.30)$$

$$BER_{CSK} = \int_0^{+\infty} Q\{\sqrt{\frac{(h_{11}^2 + h_{21}^2 + h_{12}^2 + h_{22}^2) e_{bc}}{\frac{1}{SNR} + \frac{1}{SOR} + \frac{2}{SOR} \sum_{k=0}^{\beta-1} (1 - \frac{k}{\beta})}}\} * f(e_{bc}) de_{bc} \quad (7.31)$$

Where e_{bc} is the standardized chaotic bit energy variable for the typical jth bit and $f(e_{bc})$ is its probability density function.

However, an analytical expression for $f(e_{bc})$ is difficult because the chaotic samples are not statistically independent, rather they are functionally dependent. Since an analytical expression appears to be hard to obtain, numerical integration remains a

solution for performing the BER computation taking into account the bit-energy variation. The BER expression for 2×1 Alamouti scheme is given by,

$$BER_{CSK} = \sum_{j=1}^{m} Q\{\sqrt{\frac{(h_1^2+h_2^2)e_{bc}}{\frac{1}{SNR}+\frac{1}{SOR}+\frac{2}{SOR}\sum_{k=0}^{\beta-1}\left(1-\frac{k}{\beta}\right)}}\}p(e_{bc}^{(j)}) \quad (7.32)$$

And for 2×2 Alamouti scheme is given by,

$$BER_{CSK} = \sum_{j=1}^{m} Q\{\sqrt{\frac{(h_{11}^2+h_{21}^2+h_{12}^2+h_{22}^2)e_{bc}}{\frac{1}{SNR}+\frac{1}{SOR}+\frac{2}{SOR}\sum_{k=0}^{\beta-1}\left(1-\frac{k}{\beta}\right)}}\}p(e_{bc}^{(j)}) \quad (7.33)$$

Where m is the number of histogram classes created from the simulated spreading segment and $p(e_{bc}^{(j)})$ is the probability of having the energy in integral centered on $e_{bc}^{(j)}$.

7.6 Results and Discussions

The BER performance of DS-CDMA system for SISO and MIMO communication systems using different kinds of chaotic maps is quantified in Table (7.4).

From Table (7.4) it is inferred that chaotic sequences perform well when compared to conventional maximal length sequences.

A second goal of this chapter is to verify the performance of chaos in CDMA systems taking into consideration the dynamic properties of chaotic sequences specially the non-periodicity.

A comparative study is made taking into consideration different fading channels, different chaotic maps, SISO and different MIMO Alamouti modes (2×1 and 2×2).

Figure 7.3 shows the plots of autocorrelation function and cross correlation function of the signal generated by a chaotic tent map.

From the graph we find that the autocorrelation of the chaotic tent map is δ-like, and the cross correlation is very close to zero. The signal isolation is achieved by the using spreading sequences that have low cross correlation properties.

Figure 7.4 shows increase the BER performance by using 2×2 and 2×1 Alamouti scheme as compared to SISO. 2×2 Alamouti scheme gives 1.75 dB gain as compared to 2×1 at a BER of 10^{-5}.

Figure 7.5 shows the BER performance of different chaotic maps implemented in SISO DS-CDMA systems.

It is seen that tent map gives the best BER performance when compared to the performance of Chebyshev map, Logistic map and Tail shift map.

Figure 7.6 shows the BER performance of different chaotic maps implemented in MIMO-DS-CDMA system.

It is observed that the tent map yields the best BER performance when compared to other chaotic maps. As compared to SISO-DS-CDMA system, MIMO-DS-CDMA system gives a gain of 2 dB. The circle graph (black) represent BER curve for simulated CDMA-MIMO based on CSK modulation scheme for chaotic tent map which is overlapped with a maximum deviation of 0.5 dB by the magenta curve represented theoretical BER computed in equation (7.33).

Figure 7.7 shows the BER performance of CSK-MIMO-DS-CDMA system for different fading channels. The required bit energy to noise ratio (E_b/N_0) is in the range of 9 dB to 15dB at BER of 10^{-5}, considering AWGN, Gamma-Gamma, Log-normal and Rayleigh fading channels.

The Gamma-Gamma distribution is widely accepted as the fading channel distribution for wireless optical links. In Gamma-Gamma distribution channel the Chaos-MIMO-DS-CDMA system requires a SNR (E_b/N_0) value of 10.5 dB to achieve a BER of 10^{-5}.

It can be observed from Figure 7.8 that the BER of chaotic SISO system with β=10 increases above 10^{-5}, if the number of user are more than 5.

By using chaotic MIMO system with β=10, the BER gets degraded from 10^{-8} to 10^{-6} as the number of users increases from 1 to 20. If we increase the number of users beyond 20, the BER in chaotic MIMO system remain constant at 10^{-6}. Thus, we can extensively increase the number of users in cell without substantial degradation in BER.

In Table 7.4, column labeled I denotes BER for SISO; column labeled II represents the BER for 2×1 Alamouti scheme and column labeled III denotes the BER encountered with 2×2 Alamouti scheme.

Input SNR in dB	PN Sequences (length 31)			PN Sequences (length 63)		
	I	II	III	I	II	III
0	0.1992	0.1565	0.0528	0.1283	0.0490	0.0660
2	0.1267	0.0784	0.0139	0.103	0.0267	0.0290
4	0.1105	0.0288	0.0016	0.0761	0.0114	0.0085
6	0.1065	0.0062	0.0004	0.0500	0.0035	0.00134
8	0.0985	0.0009	0.0000	0.0278	0.0007	7.92×10^{-5}
10	0.0534	0.0000	0.0000	0.0124	9.87×10^{-5}	1.009×10^{-6}
Input SNR in dB	Tent map			Logistic map		
	I	II	III	I	II	III
0	0.0868	0.0501	0.0353	0.1451	0.1189	0.0747
2	0.0598	0.0267	0.0160	0.1216	0.0924	0.0480
4	0.0342	0.0106	0.0049	0.09521	0.0648	0.0254
6	0.0154	0.0067	0.0008	0.03303	0.0391	0.0101
8	0.0047	0.0003	5.75×10^{-5}	0.01452	0.0188	0.0026
10	0.0008	1.387×10^{-5}	1.23×10^{-7}	0.00427	0.0065	0.0003
Input SNR in dB	Chebyshev map			Tailed shift map		
	I	II	III	I	II	III
0	0.1451	0.111	0,.0747	0.1492	0.1861	0.0747
2	0.1216	0.0953	0.0480	0.1267	0.1704	0.0480
4	0.0952	0.0651	0.0254	0.1002	0.1514	0.0512
6	0.0674	0.0413	0.0113	0.0932	0.1290	0.0282
8	0.0201	0.0316	0.0058	0.0622	0.1035	0.0120
10	0.0069	0.0136	0.0004	0.0331	0.0761	0.0035

Table 7.4

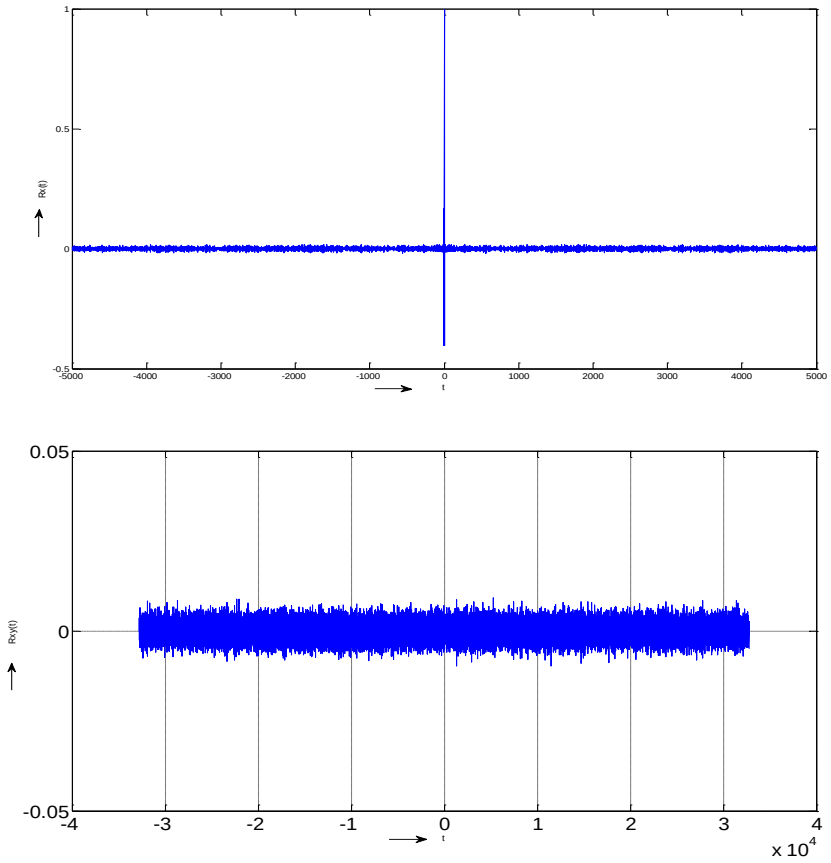

Figure 7.3 Measurement of auto- and cross-correlation of a chaotic tent map

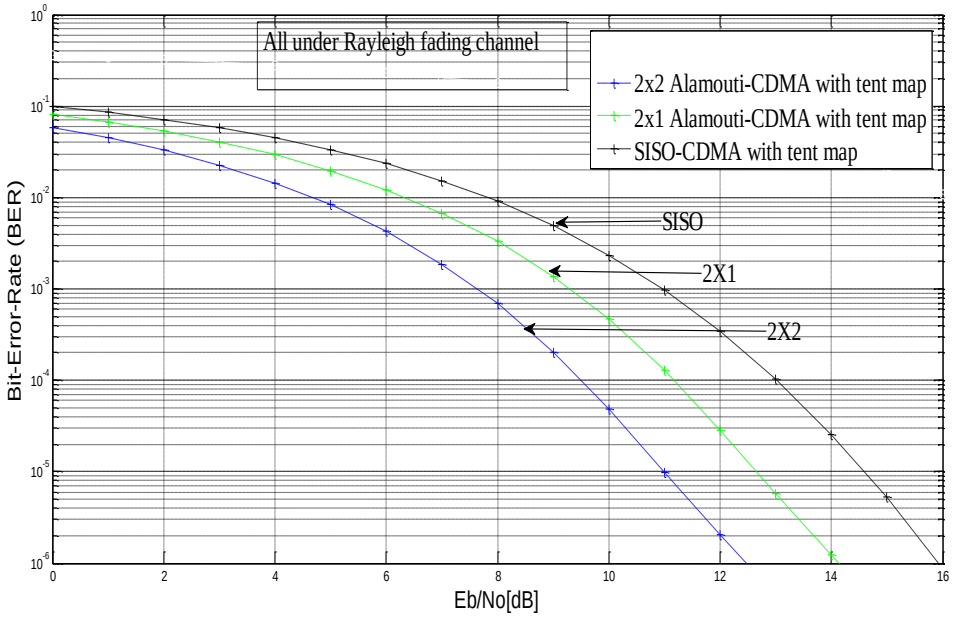

Figure 7.4 BER performance comparison between 2×2 , 2×1 and SISO communication systems for DS-CDMA under Rayleigh fading channels

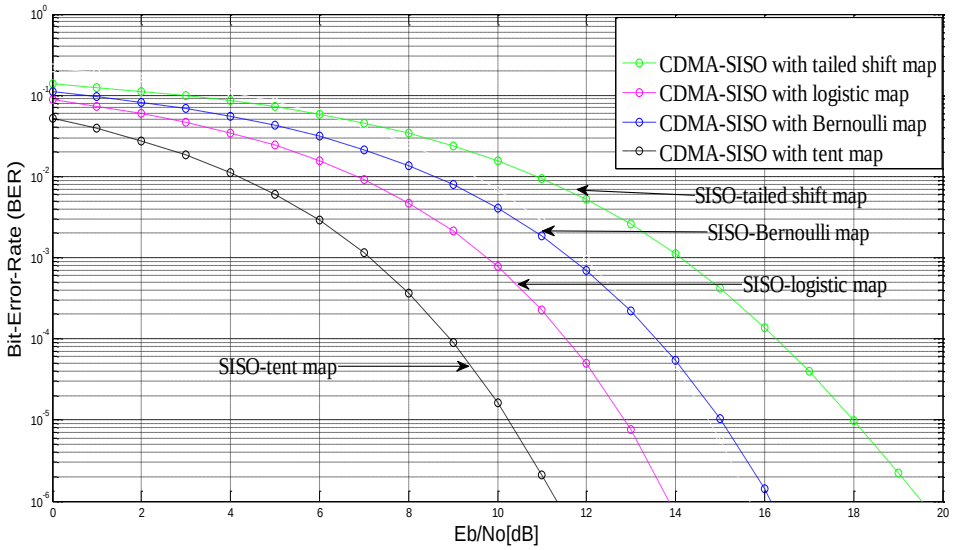

Figure 7.5 SISO-DS-CDMA for different chaotic maps

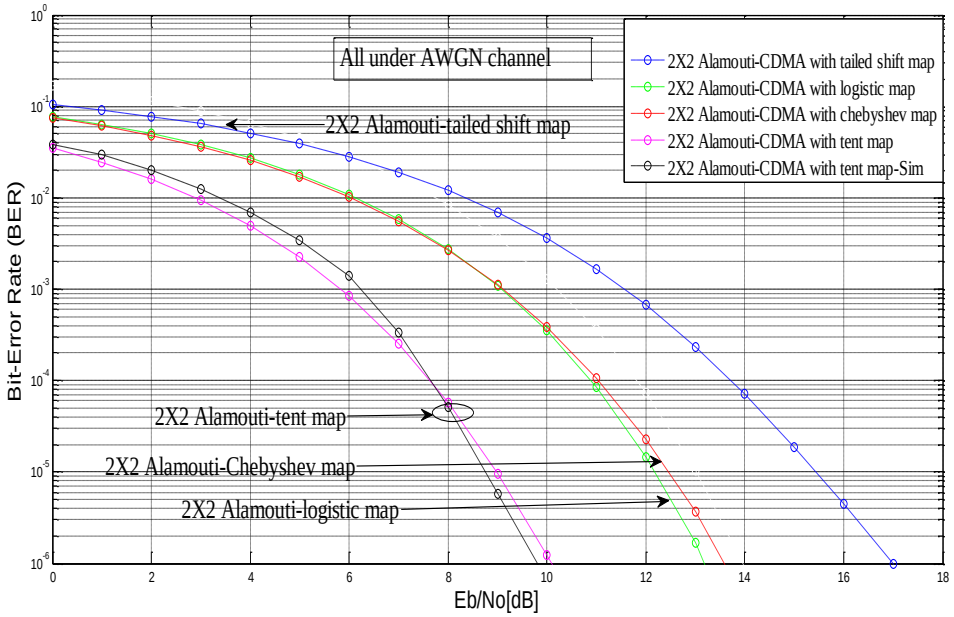

Figure 7.6 2×2 Alamouti-DS-CDMA for different chaotic maps

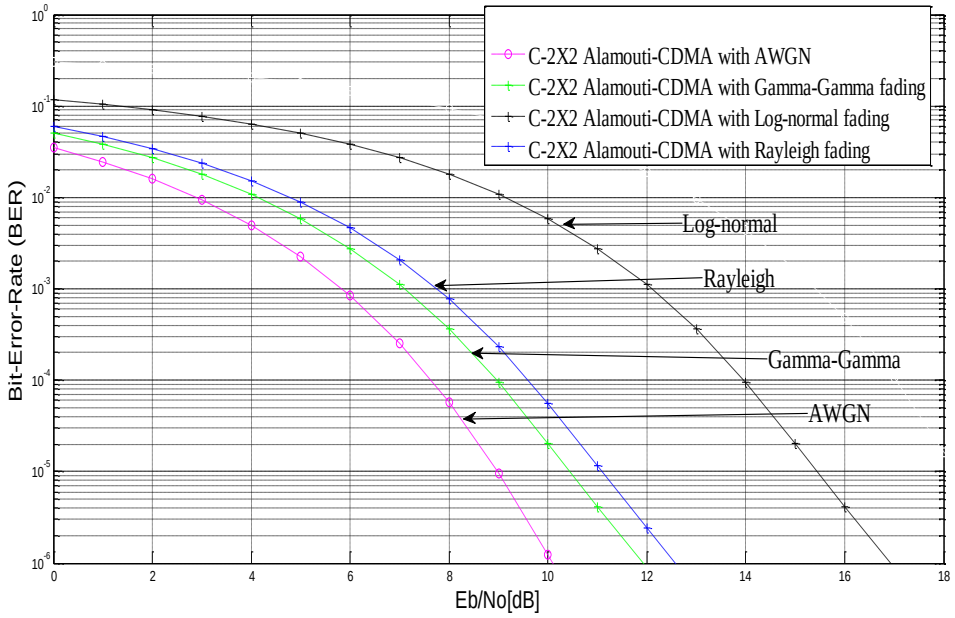

Figure 7.7 Chaotic-2×2 Alamouti-DS-CDMA for different fading channels

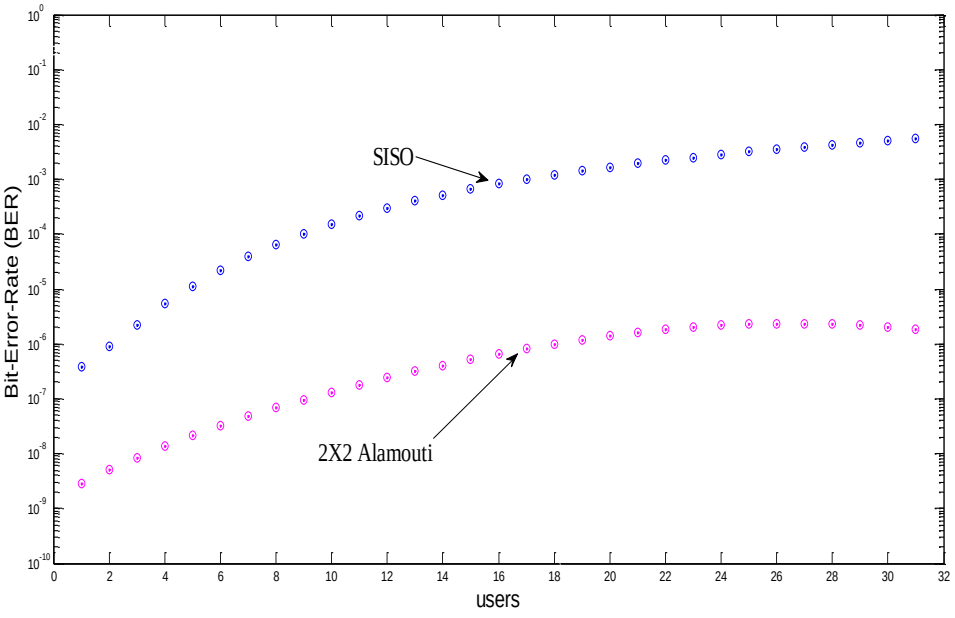

Figure 7.8 BER versus user number

7.7 Conclusions

In this chapter, various performance issues concerning the use of different chaotic maps combined with MIMO communication channel in a CDMA system have been studied.

We have considered a system where the output of a CSK modulation scheme is combined with MIMO-DS-CDMA for two transmit antennas and one receive antenna as well as with two transmit antennas and two receive antennas under different fading channels.

The Alamouti scheme with chaotic technique based CDMA system has many advantages over traditional CDMA systems including BER performance and increase the number of users. Simulation results show that 2×2 Alamouti scheme gives an additional 1.75 dB coding gain as compared to 2×1.

From the results presented in this chapter, we conclude that the use of CDMA-MIMO systems based on chaotic technique have several advantages when compared with CDMA systems based on conventional PN sequences. It is also observed that MIMO systems also present several advantages over SISO systems when the same chaotic sequences are used for spreading.

In the chapter eight, we have considered the application of the chaotic techniques in to enhance information security and improve reliability of communication in FSO systems.

CHAPTER 8

SECURE WIRELESS OPTICAL COMMUNICATION LINK BASED ON CHAOTIC TECHNIQUES

8.1 Introduction

In chapter eight, we have disscused a possible application of chaotic techniques to secure communications over wireless optical communication link. FSO technology can provide highly directional, high bandwidth communication channels. This technology can provide fiber-like data rate over a short distances. A secure communication method based on chaotic techniques is presented to improve security associated with data transmission in FSO networks. In the first part of this chapter, we have turned our attention to a specific class of piece wise linear one-dimensional chaotic maps. We examine the security vulnerabilities of single FSO links and propose a solution to this problem by considering FSO transmission which employs a chaotic signal generator with "reconfigurable tent map". In order to examine and quantify the suitability of these techniques for secure communication, we have determined parameters such as autocorrelation and cross correlation associated with chaotic sequences that determine the ease with which synchronization between transmitter and receiver can be achieved. It is demonstrated that cross correlation is very close to zero and autocorrelation is δ-like. In the second part of this chapter, we have concentrated on investigating the error rate performance of chaotic-wireless optical communication links operating over atmospheric channel, where the turbulence induced fading is described by the Gamma-Gamma and log-normal distributions.

The main aim of this part is to assess the feasibility of employing Space-Time Coded chaotic communications over MIMO communication channels. In this work, we have chosen the spreading factor to be β =4.

In the MIMO set up, a SISO link is simulated by assuming the placement of one laser diode at transmitter and one photo-detector at receiver. A 2×1 link is simulated by assuming the placement of two laser diode transmitters and one photo-detector at receiver while 2×2 link is simulated by assuming the placement of two lasers diodes at transmitter and two photo-detectors at receiver. The Gamma-Gamma fading model is adopted for FSO link because of its excellent fit with measurement data over wide range of turbulence conditions (weak to strong).

In order to understand the relative merits of various chaotic maps in this application, we have computed the BER performance of CSK under different chaotic maps (tent map, logistic map, Chebyshev map and Bernoulli map) in the presence of AWGN and under fading described by the Gamma-Gamma distribution for both 2×1 and 2×2 Alamouti schemes.

Our simulations indicate that the combination of the STBC and tent map provides the best BER performance in addition to security when compared to the choice of other maps.

Hence, this work shows that the use of these schemes can allow the user to enhance security without degrading the BER performance while communicating over these channels. Thus, we have outlined an approach that can be used to mitigate the problem of BER performance degradation as well as enhance security over free space atmospheric channels.

In the third part of chapter eight, we have evaluated the BER performance for STBC in chaotic FSO communication systems with Gamma-Gamma fading channel using OPTSIM Simulator. Thus this chapter is devoted to the design, simulation and BER performance evaluation of different optical chaotic modulation schemes under the MIMO-FSO communication regime.

Contributions of the thesis in Chapter 8:

- Evaluate the BER performance and security of Free Space Optical (FSO) link under turbulent channel conditions modeled by Gamma-Gamma distribution.

8.2 Enhancement of Security for Free Space Optics based on Reconfigurable Chaotic Technique

In Chapter 2 equation (2.3) shows the technique employed to generate chaotic sequences using tent map. By choosing a control parameter p and an initial condition, a sequence of chaotic random numbers between zero and one can be generated. The random numbers are iteratively generated with the x_{n+1} value of previous step becoming the x_n value for present step. Figure 8.1, shows a noise equivalent chaotic signal

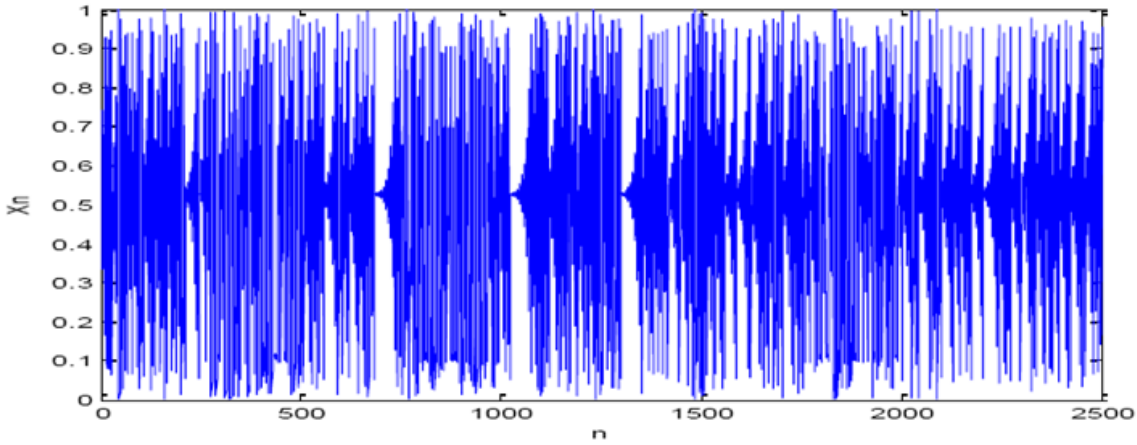

Figure 8.1 Random equivalent chaotic sequence.

8.2.1 FSO Communication System

FSO communications operate in a band of frequencies centered at either 850 nm or 1550 nm. The two wavelengths are chosen because absorption by water or the atmosphere is minimal at these frequencies. A transmitter transmits a light signal through free-space that is received by a receiver.

The emitted signal will undergo broadening that may be characterized by the diffraction angle, and in most cases, the projected beam size will be significantly larger than the dimensions of the receiver [Morgan C., 2003].

Optical wireless communication has received a lot of attention from the research community in the past two decades. This is because FSO offers a highly directional, high bandwidth communication channel [Heba S., Salma D. Abd A. and Mustafa H.,2010, Xiaomin J., Xian W. and Chi Y.,2008].

FSO communication systems are built by transmitting a modulated laser beam through the atmosphere between two LOS points. FSO systems exhibit robustness against channel impairments in the form of rain and snow. However, if the distance between LOS points is greater than a few hundred meters or more, inhomogeneties in the temperature and pressure of the atmosphere can deteriorate the quality of the signal received at the receiver [Premaratne M. and Zheng E.,2007].

Fading induced by atmospheric turbulence is one of the main impairments in FSO communications. However, it has been demonstrated that similar to RF communications, the effect of fading in FSO systems can be considerably reduced by deploying multiple lasers at the transmitter and multiple photo-detectors at receiver [Ehsan B., Robert S. and Ranjan Mallik K., 2009, Ehsan B., Robert S., Ranjan Mallik K., 2010].

Further, the security of the system can be increased by using chaotic-FSO system with optical generators. Although end devices may use cryptographic tools to protect the integrity of data, it is still important to ensure that the FSO links are also secure at the physical layer. Our results show that the use of chaotic techniques and MIMO schemes can provide additional security and reliability to the operation of FSO links.

The need to secure FSO communications is illustrated by Figure 8.2. As can be seen, the FSO beam is thin and is conically divergent. As a result, after traversing a distance of about one kilometer, the circular cross section is few meters in diameter. This is much larger than the aperture of the receiver which is only several centimeters.

Because of the difference in the diameters of the beam and the receiver, there is beam overspill, which can be exploited by an eavesdropper unless the communication is secured by the use of a suitable cryptographic arrangement [Stamatios V., 2010].

In traditional communication systems, information security issues are handled using public key cryptosystems. In these systems, security depends on computational complexity (difficulty) associated with the process of deciphering that has to be undertaken by the eavesdropper. These systems employ a key that is used to encode the message directly. These systems are suitable for exchanging private information on a large network of subscribers, where everyone can send and receive message to and from anyone.

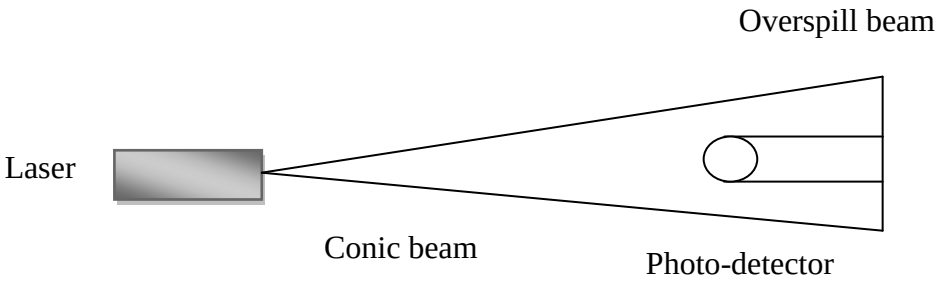

Figure 8.2 The overspill FSO beam which provides an opportunity for snoopers if it is not blocked

The level of security can be enhanced by increasing the key length and making periodic changes in the key sequence. The principle drawback is that it requires suitable means have to be adopted to distribute and validate various key sequences.

An attractive way to improve the security of an encrypted message is to have additional encoding at the physical layer using chaotic carriers generated by components operating in the electrical domain and optical domains [Silvano D. and Claudio R., 2002].

The various approaches that are used to generate chaotic sequences and their application to optical system have resulted in the opening up of new and interesting research areas.

Transmitter

The transmitter is composed of a light source and telescope. Firstly, the light source may be constructed using either LEDs or a laser. Secondly, the telescope construction is usually a simple lens assembly that focuses light onto the receiver. This is because the LED is placed at the focus and images light to infinity, so smaller devices call for smaller focal lengths. The block diagram of chaotic FSO transmitter is sketched in Figure 8.3.

Receiver

The receiver device is the means by which the signal is detected. Receivers implement optical filters, electrical filters, and decision circuits to control and interpret the signal.

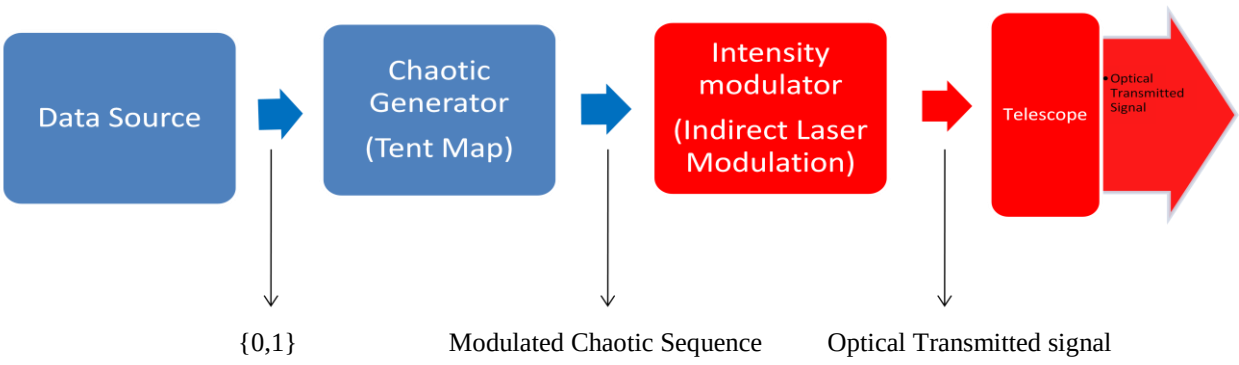

Figure 8.3 Block diagram of Chaotic-FSO transmitter

Once the signal is obtained, appropriate amplification and processing is usually required to decode the transmission. Detectors are characterized by their responsively ζ, and rise time t_r. The responsively ζ, is defined as $\zeta = [\frac{A}{W}]$, where A represents the output current and W represents the input power. The responsively can also be related to the quantum efficiency, η, by $\zeta = e\eta/h_P f$, where e is the charge on an electron, h_P is Planck's constant, and f is the frequency of the detected light. This equation can be

reasoned out as follows. $h_P f$ is the energy of a single photon and e is the charge that is excited by the single photon. By multiplying the factor $e/h_P f$ by η (the quantum efficiency), the total excited charge per unit energy is obtained. In general, semiconductor photodiodes are small, fast, and sensitive, so that they are well-suited for FSO application. Two types of detectors that are commonly used in receivers are p-i-n diodes and APDs [Hemmati H., 2000].

8.3 Reconfigurable chaotic tent map

When the control parameter p is chosen outside the range $(0 < p < 1)$, the chaotic sequence enters into a recursive cycle and the system losses its randomness and become predictable. Thus the security of system is compromised. This problem can be solved by including a linear feedback shift register before the chaotic generator block as shown in Figure 8.4.

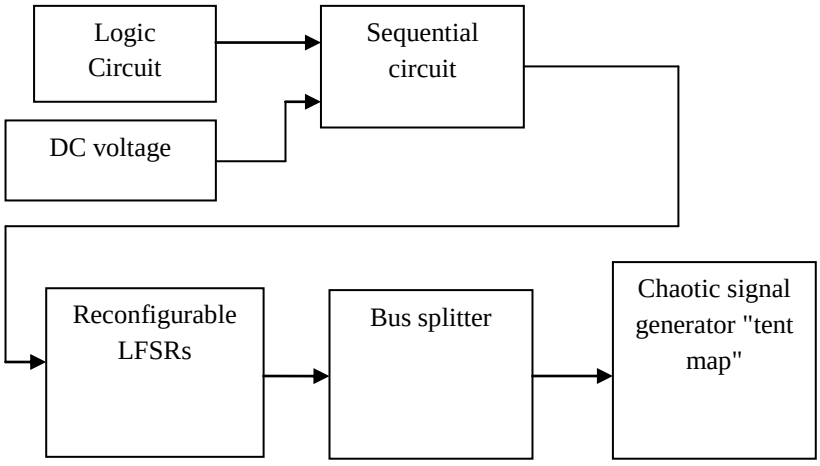

Figure 8.4 Block diagram of the reconfigurable LFSRs/ chaotic tent map signal generator combination design [Lwaa F. et al, 2013]

The reconfigurable tent sequence is given by,

$$x_{i+1=}\begin{cases} f(x_i); when\ 0 \le p \le 1 \\ f(x_i) \oplus Q_1(n) + Q_2(n) + \cdots + Q_l(n); \quad otherwise \end{cases} \tag{8.1}$$

where $Q_i(n)$ is a Linear Feedback Shift Register sequence, N_i is the precision of the system (here it is chosen to be 16 bits), q is a polynomial degree and $f(x_i)$ is chaotic tent map as shown in equation (2-3). The purpose of this test is to check for correlations between the binary sequences generated by the proposed map.
The auto-correlation function of $\{f_i\}$ is

$$AC(m) = \lim_{N_i \to \infty} \frac{1}{N_i} \sum_{i=0}^{N_i - 1} (x_i - \overline{x})(x_{i+m} - \overline{x}) \tag{8.2}$$

For any two different initial parameters f_{01} and f_{02}, the cross-correlation function of the two generated sequences is,[Liu G. J.,, 2009]

$$CC_{12}(m) = \lim_{N_i \to \infty} \frac{1}{N_i} \sum_{i=0}^{N_i - 1} (x_{i1} - x)(x_{(i+m)2} - \overline{x}) \tag{8.3}$$

The design consists of two basic parts: reconfigurable LFSR and chaotic signal generator specially the tent map. The reconfigurable LFSR consists of four LFSR each with different polynomial and with different initial condition. The LFSRs components consist of 70- D-Flip Flops (DF/F), 64-DF/F, 58-DF/F and 52 DF/F. Each group is driven by different initial conditions.

The simulation results of the auto- and cross-functions are shown in Figures. (8.5 and 8.6). The Period Length is calculated as the length of Linear Feedback Shift Register (2^q-1) divided by the Frequency (100MHz) where 'n' is number of Flip Flops.

The period length is (11805916207174, 184467440737, 2882303761and 11258999 respectively at 100 MHz) and the initial values are selected to be (FACDA1543476FFFF00, 64FCFFFFED52DECA, FFFF0120EEEEFFFF and FFF0000EEEEFFFFF, FFF6AAEC654300, 43FF33DDEEFFCC, EEEE5437FFDDA and FFFF5476DE321 in hexadecimal).

The auto-correlation result is $\delta - like$ and the cross-correlation result is very close to 0 which are good accordance with theoretical values.

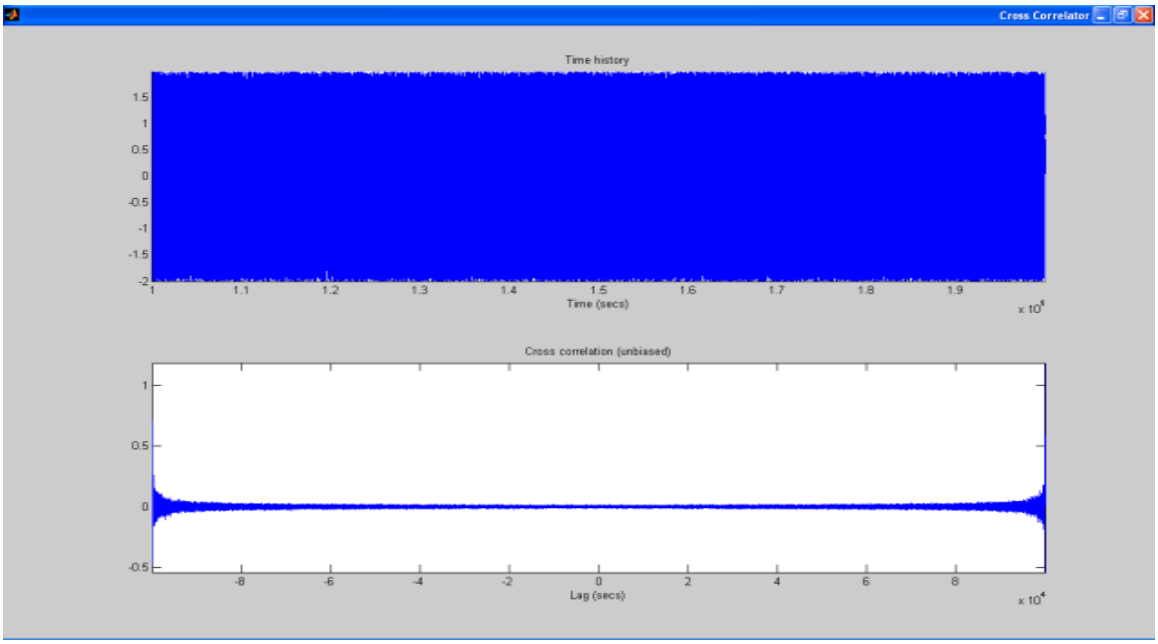

Figure 8.5 Plot of cross correlation

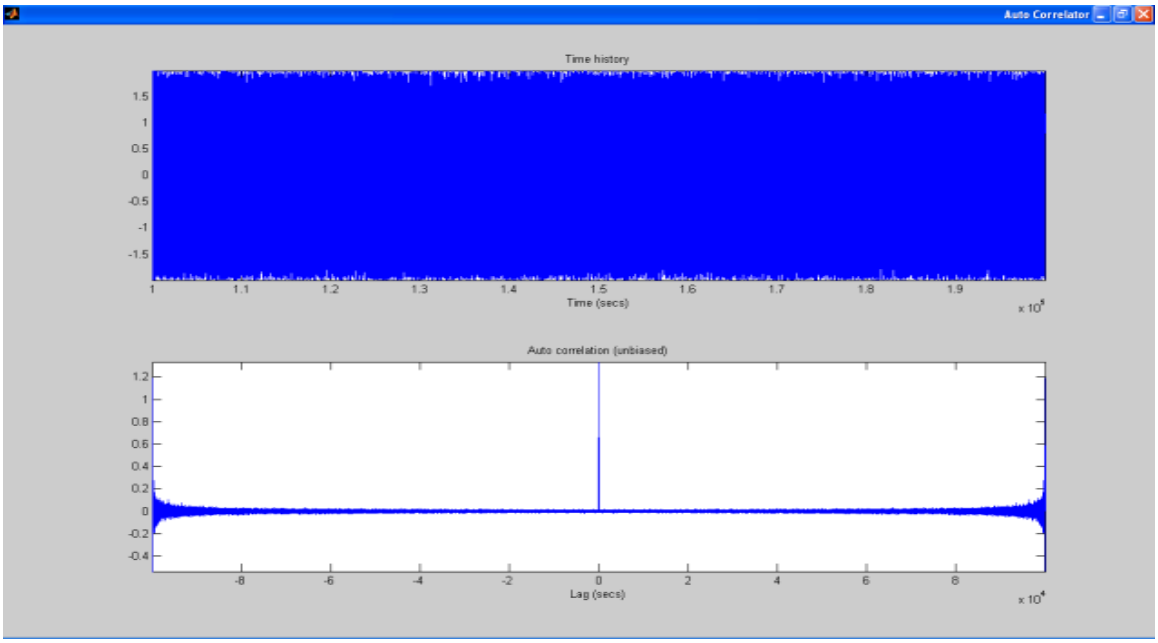

Figure 8.6 Plot of auto correlation

8.4 Secure Wireless Optical Communication System Based on Chaotic communication Systems

In this section we provide a design of MIMO-FSO system based on chaotic technique which improves the security and capacity of the transmission and enhances the BER performance. In the proposed systems STBC is used to overcome the influence of the turbulence induced fading. We show that the proposed systems can achieve the better BER than the BER of FSO system with SISO.

8.4.1 Analysis of Optical STBC

Consider a binary Intensity Modulated (IM) where symbols '0' and '1' are represented by x_0 and x_1.

A description of CSK technique method that can be employed in microchip lasers for effecting secure communications is described in [Shinozuka M., Uchida A., Ogawa T. Yoshmori S. and Kannari F., 2001].

The CSK modulated data symbols are from the set {-1,1}. After IM, the data symbols sent to Optical Alamouti Block are from the set {0,I}.

$$\begin{aligned} s_0(t) &= 0, \qquad 0 \le t \le \beta T_c \\ s_1(t) &= I, \qquad 0 \le t \le \beta T_c \end{aligned} \tag{8.4}$$

Consider the data information symbols ($s_l = \pm 1$) with period T_s spread by a sequence of chaotic sample (or chip).

The time interval of each chip is equal to $T_c(x_k = x(kT_C))$. I is the constant intensity of the laser at the transmitter for symbol 1. The emitted signal at the output of the transmitter is

$$u(t) = \sum_{l=0}^{\infty} \sum_{k=0}^{\beta-1} s_l x_{l\beta+k} \tag{8.5}$$

Recall that the spreading factor β is equal to the number of chaotic samples in symbol duration ($\beta = \frac{T_s}{T_c}$)., the received signal is

$$r(t) = hu(t) + n(t) \tag{8.6}$$

where h is the channel coefficient and $n(t)$ is the AWGN with zero mean and power spectral density equal to $N_0/2$.

In order to demodulate the transmitted bits, the received signal is first de-spread by the local chaotic sequence, and then integrated over symbol durationT_s.

Finally, the transmitted bits are estimated by computing the sign of the decision variable at the output of correlator,

$$Ds_l = sign\left(s_l T_c \sum_{k=0}^{\beta-1}\left(x_{l\beta+k}\right)^2 + w_l\right) = sign(s_l E_b^{(l)}) + w_l \tag{8.6}$$

We recall that the $sign(.)$ is the sign operator,$E_b^{(l)}$is the bit energy of the l^{th} bit and w_l is the noise after despreading and integration.
Let,

$$s_i(t) = -s_j(t) + I, \qquad i \neq j, \;\; i,j \in \{0,1\} \tag{8.7}$$

The complement of signal a_i is $\overline{a_i}$ that represents the opposite binary state of the signal a_i (i.e., if $a_i = s_0$ then $\overline{a_i} = s_1$ and if $a = s_1$ then $\overline{a_i} = s_0$).

Applying this definition to equation (8.7) results in the following relationship,

$$\bar{a}(t) = -a(t) + I, \qquad a(t) \in \{s_0, s_1\} \tag{8.8}$$

We can note that $a(t) = 0, I$ the relationship in equation (8.8) ensure that $a(t)$ is non-negative. The primary property of a space-time code $A(a_1, \ldots\ldots\ldots, a_m) = A(x)$ with $a = (a_1, \ldots\ldots\ldots a_m)^T$ is

$$A^T(a)A(a) = I_M\|a\|^2 \tag{8.9}$$

Where,$(*)^T$ denotes transpose operation, I_M is the $M \times M$ unit matrix, M is the number of transmitter antennas and $\|a\|^2 = (a_1^2 + a_2^2 + \cdots + a_m^2)$.

However, a coding scheme satisfying (8.9) cannot be implemented in IM/DD system because transmitted IM signal must be non-negative at all times.

The above coding scheme shows that certain transmitter outputs must be negated to get the orthogonality. Therefore the above coding scheme cannot be used for free-space IM/DD systems.

To overcome the above problem, we use the following STBC matrix

$$(|A|(a,\bar{a}))_{i,j} = \begin{cases} (A(a))_{i,j} \;\; if \;\; (A(a_1 = 1, \ldots\ldots\ldots a_m = 1))_{i,j} \geq 0 \\ -(A(a))_{i,j} \;\; otherwise \end{cases} \tag{8.10}$$

This definition ensures that the transmitted symbols are always non-negative for an IM/DD system.

Assume the channel gain and the transmitted signal level have a perfect knowledge, the estimated signal at receiver is

$$\tilde{a} = A^T(h)J_K \times (J_K A(h)x + z) \tag{8.11}$$

Using the relation $\mathrm{J_K} \times \mathrm{J_K} = \mathrm{I_K}$, we obtain

$$\tilde{a} = \|\mathrm{h}\|^2\mathrm{x} + \mathrm{A^T(h)J_K n} \tag{8.12}$$

Where K represents the transmission time slots, $\mathrm{J_K}$ is K × K diagonal matrix, with -1 in the diagonal except 1 for $\mathrm{J_{1,1}}$ (i.e., $\mathrm{J} = \mathrm{diag}(1, -1, -1, -1, \ldots, -1)$, $\bar{x} = (\overline{x_1} \ldots\ldots\ldots\ldots \overline{x_m})^T$, $n = (n \ldots\ldots\ldots\ldots n)^T$ are Gaussian noise, which may include

contribution from thermal and/or shot noise and $h = (h_1 \dots\dots\dots h_m)^T$ is the quasi-static channel response for transmitters $i = 1,2, \dots\dots\dots M$ respectively [Premaratne M. and Zheng E.,, 2007, Ehsan B., Robert S. and Ranjan K, 2010, Hiroshi Y. and Tomoaki O.,2003, Wang H. and Ke X.,, 2007].

Then,

The optical Alamouti matrix becomes

$$X(x, \bar{x}) = \begin{pmatrix} a_1 & a_2 \\ \overline{a_2} & a_1 \end{pmatrix} \tag{8.13}$$

For 2×1 optical Alamouti, the estimated signal at receiver

$$\begin{pmatrix} \widetilde{a_1} \\ \widetilde{a_2} \end{pmatrix} = (h_1^2 + h_2^2) \begin{pmatrix} a_1 \\ a_2 \end{pmatrix} + \begin{pmatrix} h_1 z_1 + h_2 z_2 \\ h_2 z_1 - h_1 z_2 \end{pmatrix} \tag{8.14}$$

Where $h = (h_1, h_2)^T$ is the channel response vector for two lasers (antennas).

For 2×2 optical Alamouti and from equation (8.13), the estimated signal at receiver

$$\begin{pmatrix} \widetilde{a_1} \\ \widetilde{a_2} \end{pmatrix} = (h_{11}^2 + h_{21}^2 + h_{12}^2 + h_{22}^2) \begin{pmatrix} a_1 \\ a_2 \end{pmatrix} + \begin{pmatrix} h_{11} z_1 + h_{21} z_2 \\ h_{22} z_1 - h_{12} z_2 \end{pmatrix} \tag{8.15}$$

8.4.2 CSK-MIMO-FSO Communication Systems

The block diagram of CSK-2 × 1-FSO communication system is shown in Figure 8.7

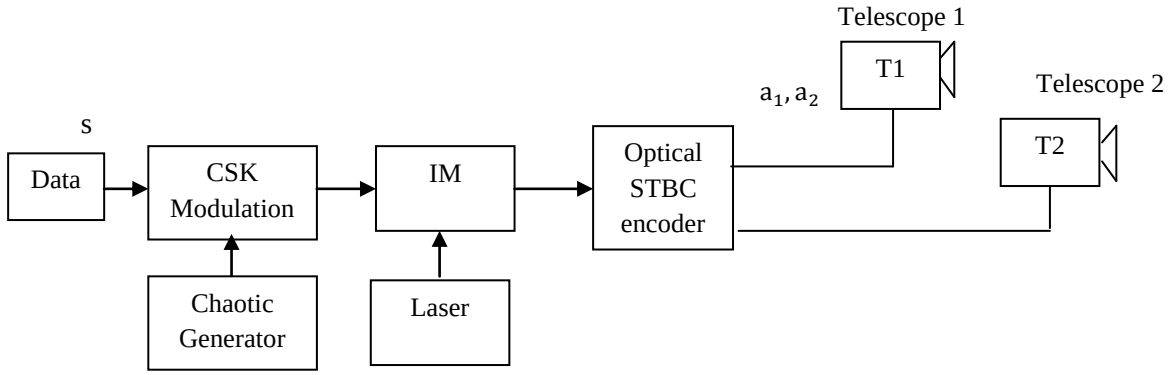

(a)

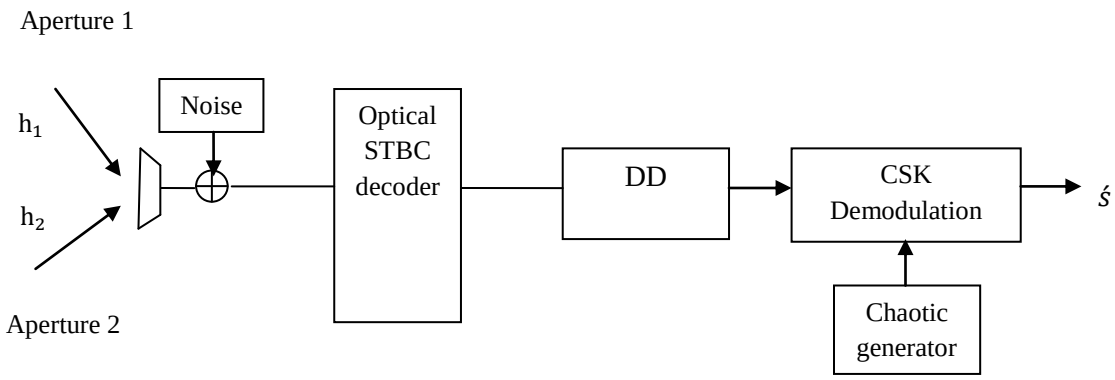

(b)

Figure 8.7 Chaotic-MIMO, a) transmit with two antennas, b) receiver with one antenna [Lwaa F. et al, 2013]

Starting from equation (8.4) and from equations (8.13) and (8.14)

The design of the transmitted signal is

The design of the transmitted signal is specified in Table 8.1

Time	$a_1(t)$from T_{x1}	$a_2(t)$from T_{x2}
$[0, \beta T_c]$	$a_1 x_k$	$a_2 x_k$
$[\beta T_c, 2\beta T_c]$	$\overline{a_2} x_{k+\beta}$	$a_1 x_{k+\beta}$

Table 8.1

The received signal of the 2×1 STBC is specified in Table 8.2

Time	Received signal
$[0, \beta T_c]$	$h_1 a_1 x_k + h_2 a_2 x_k + z_k^1$
$[\beta T_c, 2\beta T_c]$	$h_1 \overline{a_2} x_{k+\beta} + h_2 a_1 x_{k+\beta} + z_k^2$

Table 8.2

The equivalent baseband model of the received symbol is specified in Table 8.3

Time	The equivalent baseband model of the received symbol
$[0, \beta T_c]$	$Y_1 = E_b(h_1 a_1 + h_2 a_2) + Z_1$
$[\beta T_c, 2\beta T_c]$	$Y_2 = E_b(h_1 \overline{a_2} + h_2 a_1) + Z_2$

Table 8.3

where $Z_1$and Z_2 represent noise components while $h_1$and h_2 represent the channel gains.

The channel model can be written as

$$Y = E_b HA + Z \tag{8.16}$$

The transmitted bits are estimated by multiplying the signal Y by the conjugate transpose of the channel H:

$$\begin{pmatrix} D_{s1} \\ D_{s2} \end{pmatrix} = H^* Y \tag{8.17}$$

The estimated bits are computed from the sign of the decision variables,

$$\acute{a_1} = sign\ D_{a1}; \quad \acute{a}_2 = sign\ D_{a2} \tag{8.18}$$

The transmitter of 2×2 STBC is same as in Figure 8.7a. the receiver is shown in Figure 8.8.

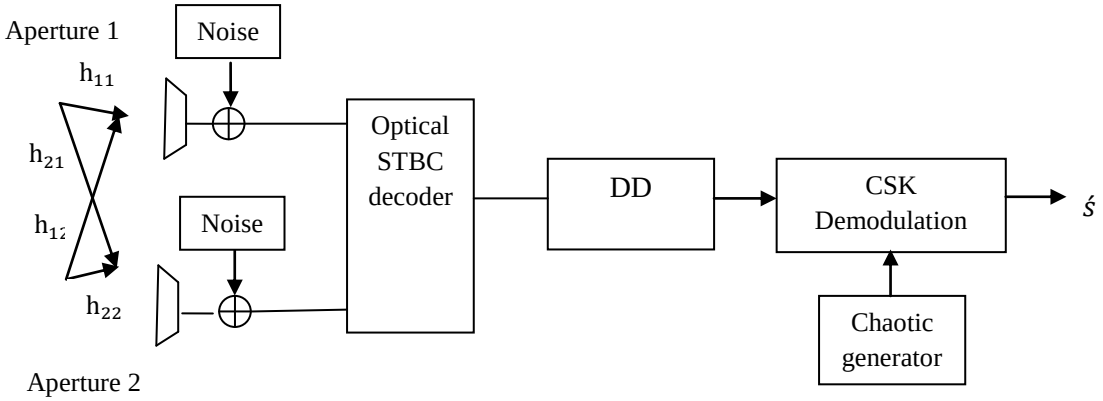

Figure 8.8 Chaotic-MIMO, receiver with two antennas [Lwaa F. et al, 2013]

The design of the transmitted signal of 2×2 Alamouti is as in Table (8.2). From equation (8.15)

The received signal on R_{x1} is specified in Table 8.4

Time	Received signal on R_{x1}
$[0, \beta T_c]$	$h_{11}a_1x_k + h_{21}a_2x_k + z_k^1$
$[\beta T_c, 2\beta T_c]$	$h_{11}\overline{a_2}x_{k+\beta} + h_{21}a_1x_{k+\beta} + z_k^2$

Table 8.4

The received signal on R_{x2}

Time	Received signal on R_{x2}
$[0, \beta T_c]$	$h_{12}a_1x_k + h_{22}a_2x_k + z_k^1$
$[\beta T_c, 2\beta T_c]$	$h_{12}\overline{a_2}x_{k+\beta} + h_{22}a_1x_{k+\beta} + z_k^2$

Table 8.5

The energy of a given bit l is $E_b^{(l)} = \sum_{k=1}^{\beta} x_k^{(l)2}$.

The equivalent baseband model of the received symbol on the first antenna R_{x1} is specified in Table 8.6

Time	The equivalent baseband model of the received symbol on the first antenna R_{x1}
$[0, \beta T_c]$	$Y_{11} = E_b(h_{11}a_1 + h_{21}a_2) + Z_{11}$
$[\beta T_c, 2\beta T_c]$	$Y_{21} = E_b(h_{11}\overline{a_2} + h_{21}a_1) + Z_{21}$

Table 8.6

where $Z_{11} = \sum_{K=1}^{\beta} z_k^1 \, x_k$ and $N_{21} = \sum_{K=1}^{\beta} z_k^2 \, x_{k+\beta}$.

The equivalent baseband model of the received symbol on the second antenna R_{x2} is specified in Table 8.7

Time	The equivalent baseband model of the received symbol on the second antenna R_{x2}
$[0, \beta T_c]$	$Y_{12} = E_b(h_{12}a_1 + h_{22}a_2) + Z_{12}$
$[\beta T_c, 2\beta T_c]$	$Y_{22} = E_b(h_{12}\overline{a_2} + h_{22}a_1) + Z_{22}$

Table 8.7

where $Z_{12} = Z_{11}$ and $Z_{22} = Z_{21}$.

The channel model, estimation and computation of the transmitted bits is similar to 2×2 STBC using equations (8.16), (8.17) and (8.18) respectively.

8.4.2.1 Simulation Results

In Figure 8.9 we have compared the performance of different chaotic maps under Gamma-Gamma fading channel.

The chosen spreading factor is β=4. Our simulations indicate that the tent map gives best performance when compared to other chaotic maps. Hence, the use of tent map is preferred over other maps because it offers superior BER performance in addition to security.

It is observed in Figure 8.10 that under Gamma-Gamma fading conditions, where α and β_c were calculated from (4.19) and (4.20) and adopted $\lambda_c = 1550$ nm, $C_n^2 = 10^{-15}$, the diameter of the receiver collecting lens aperture is $D_c = 0.02$ m and the link distance between transmitter and receiver $L_c = 2000$ m, where $\frac{D_c}{L_c} \to 0$. Tent map gives the best BER performance as compared to other maps. In addition from Figs. 8.9 and 8.10 it is clear that the 2×2 STBC gives 2 dB gain in BER performance as compared to 2×1 STBC under Gamma-Gamma fading conditions.

In Figure 8.11 it is observed that with the use of 2×2 STBC under AWGN, the system is required 9.6 dB SNR at BER=10^{-5}.

Under Gamma-Gamma fading channel, the system is required 10.25 dB E_b/N_0 at BER=10^{-5}, while under Lognormal fading channel the system is required 13.25 dB E_b/N_0 at BER 10^{-5}.

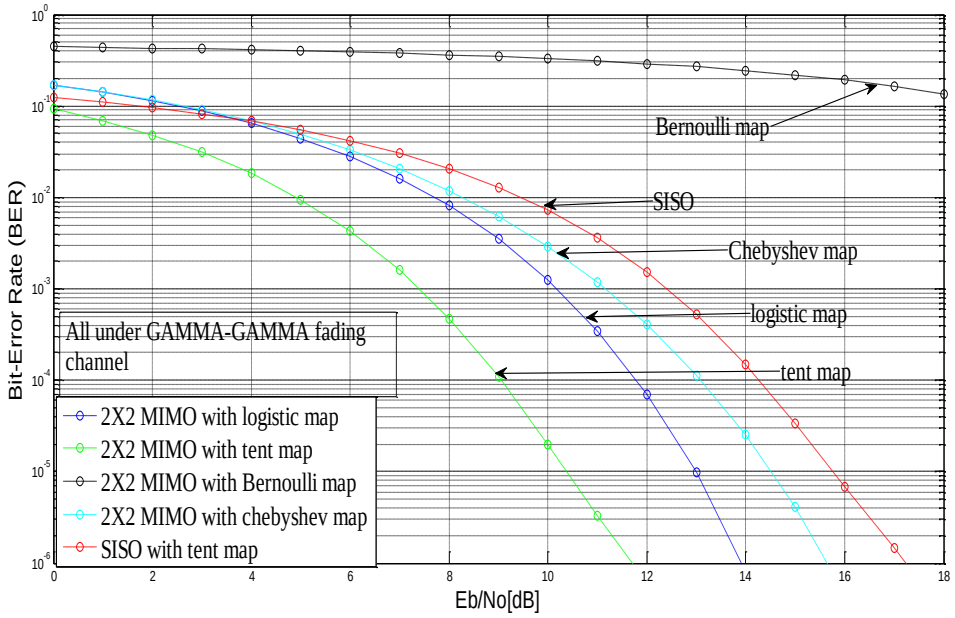

Figure 8.9 BER of 2 × 2 STBC for various types of chaotic maps under Gamma-Gamma fading channel

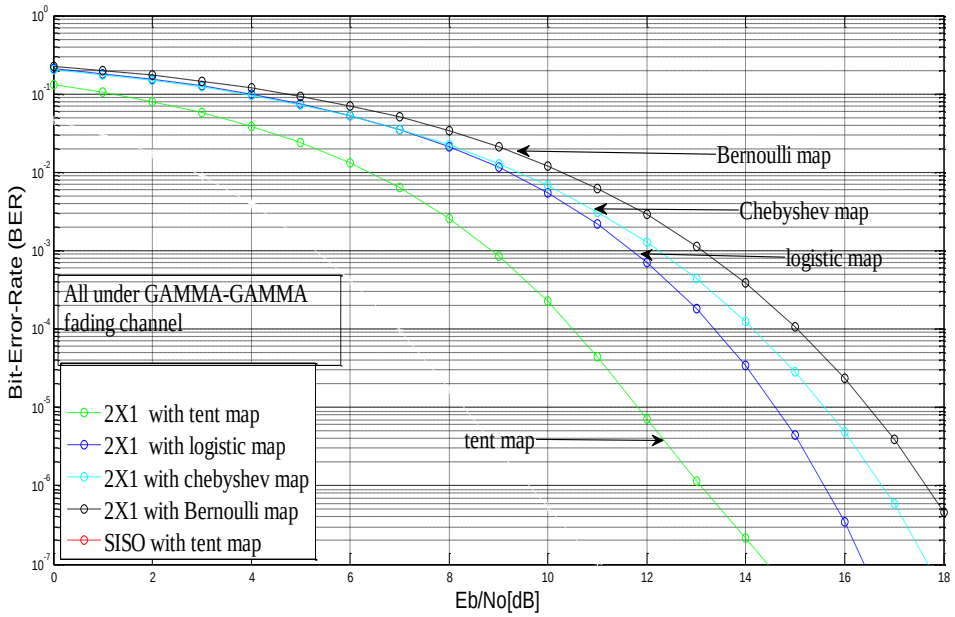

Figure 8.10 BER of 2 × 1 STBC for various types of chaotic maps under Gamma-Gamma fading channel

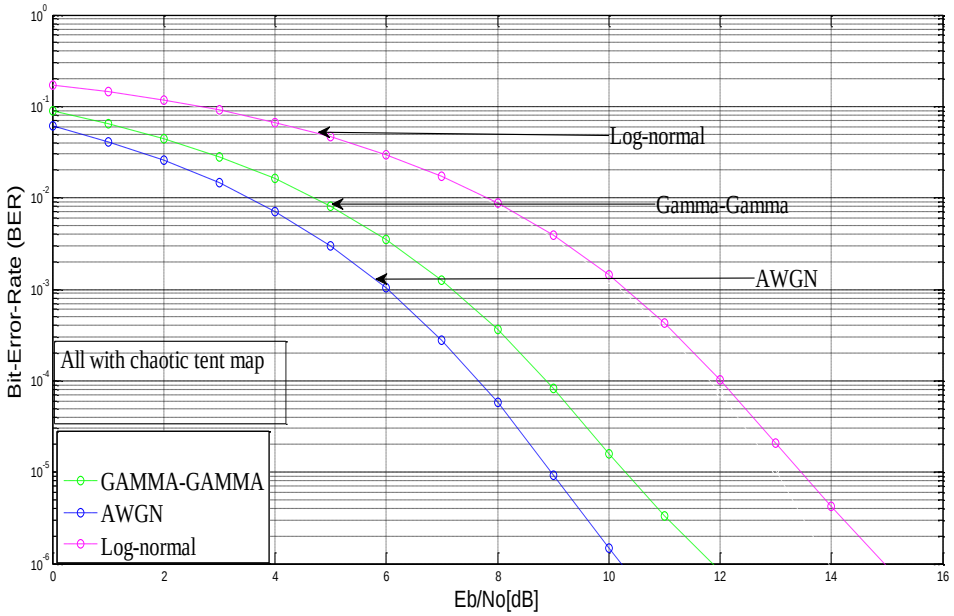

Figure 8.11 BER performance of AWGN, Gamma-Gamma and Log-normal fading channels for 2 × 2 STBC schemes

Hence increasing the diversity along with the use of MIMO communication system reduces the degradation in a fading optical channel employing CSK. Such combined MIMO-CSK schemes can be gainfully employed on optical channels where high levels of data integrity and security are simultaneously required. This improvement is realized with only a marginal increase in computational complexity at the transmitter and receiver.

We have also implemented Chaotic-SISO and Chaotic-MIMO modulation and demodulation in the OPTSIM simulator and the results obtained are in very close agreement with those obtained by MATLAB simulation.

8.4.3 Chaotic-SISO-FSO System Using OPTSIM

Figure 8.12 shows the chaotic sequence generated by chaotic generator

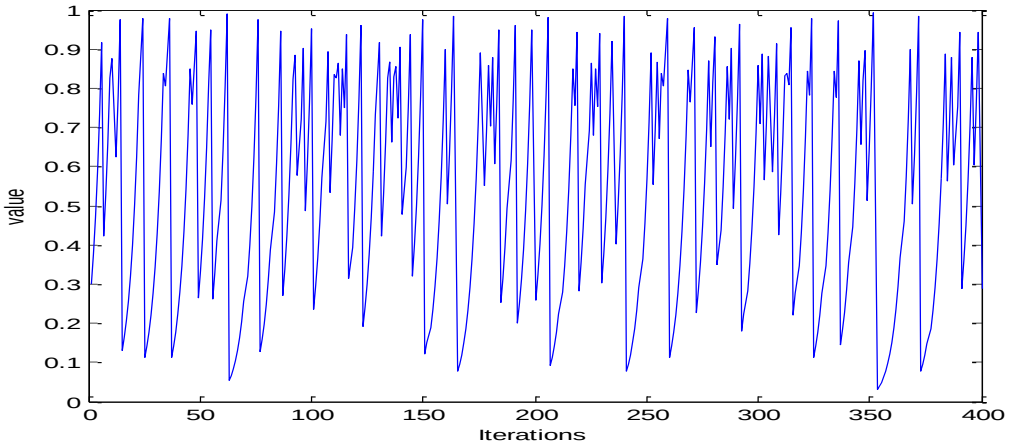

Figure 8.12 Chaos generation by chaotic generator

We consider SISO-FSO link, i.e., $M = N = 1$. Figure 8.13 shows the design and implementation Chaotic-SISO chaotic modulation and demodulation. The modulated optical beam is passed through Gamma-Gamma distributed fading channel.

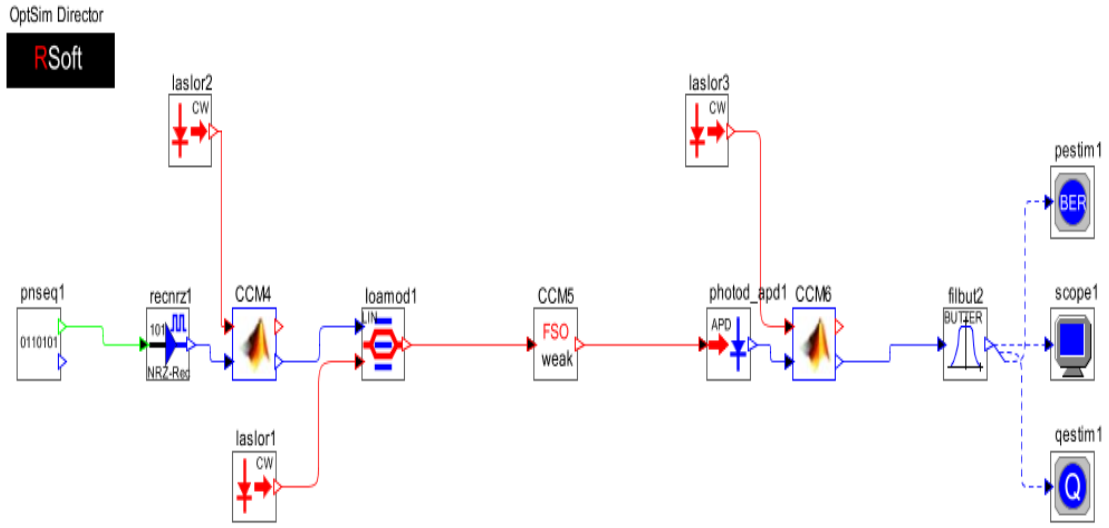

Figure 8.13 Proposed Chaotic-SISO-FSO system architecture and simulation set up using OPTSIM

The MATLAB blocks CCM4 is the chaotic modulator it takes raw data as input and gives chaotic sequence at output using electrical chaotic generator (tent map).

Similarly, CCM6 is the chaotic demodulator it takes received detected signal as input and gives demodulated data as output.

8.4.4 2×1- Chaotic -FSO system Using OPTSIM

Figure 8.14 shows the design of 2×1-Chaotic modulation and demodulation systems linked through Gamma-Gamma distributed FSO channel i.e., $M = 2, N = 1$. Here,

Figure 8.14 contains two lasers on the transmitter side and one photo-detector at receiver side. The digital message is introduced into transmitter chaos through chaotic modulation.

The encoded sequence is then transmitted to the receiver through FSO channel with transmission distance 2 Km.

The MATLAB blocks CCM7 is the chaotic modulator it takes raw data as input and gives chaotic sequence at output using electrical chaotic generator (tent map)..

CCM1 and CCM2 are the Alamouti modulators which frame the signal according to Alamouti in the above equations.

Similarly, CCM10 is the chaotic and Alamouti demodulator it takes received detected signal as input and gives demodulated data as output.

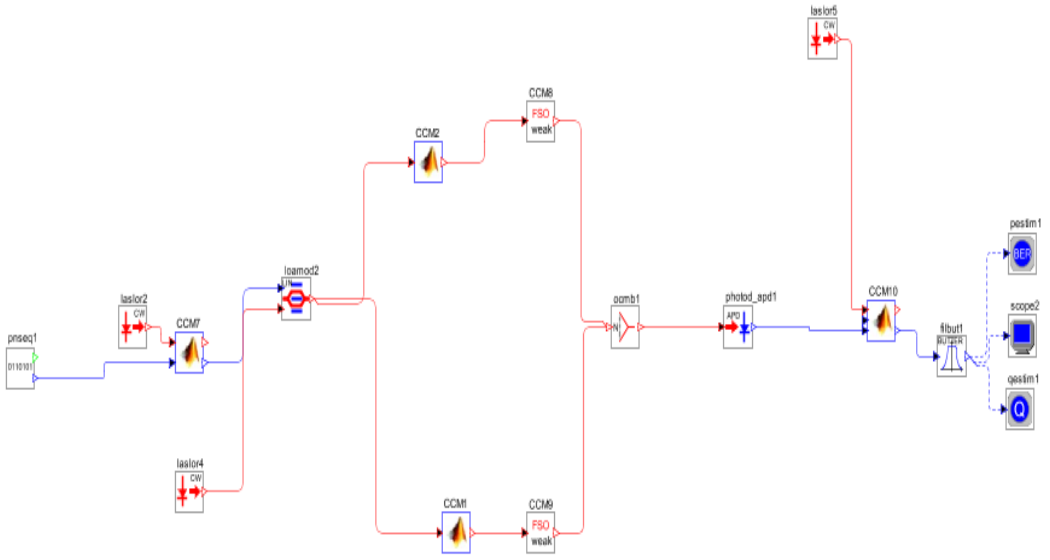

Figure 8.14 Proposed 2×1-Chaotic- FSO system architecture and simulation set up using OPTSIM

8.4.5 2×2- Chaotic -FSO system Using OPTSIM

Figure 8.15 shows the design of 2×2-Chaotic modulation and demodulation systems linked through Gamma-Gamma distributed FSO channel. Here, Figure 8.16 contains two lasers on the transmitter side and two photo-detectors at receiver side i.e. $M = 2, N = 2$. The digital message is introduced into transmitter chaos through chaotic modulation. The encoded sequence is then transmitted to the receiver through FSO channel with transmission distance 2 Km.

The MATLAB blocks CCM is the chaotic modulator it takes raw data as input and gives chaotic sequence at output using electrical chaotic generator (tent map)..CCM11 and CCM12 are the Alamouti modulators which frame the signal according to Alamouti in the above equations. Similarly, CCM10 is the chaotic and Alamouti demodulator it takes received detected signal as input and gives demodulated data as output.

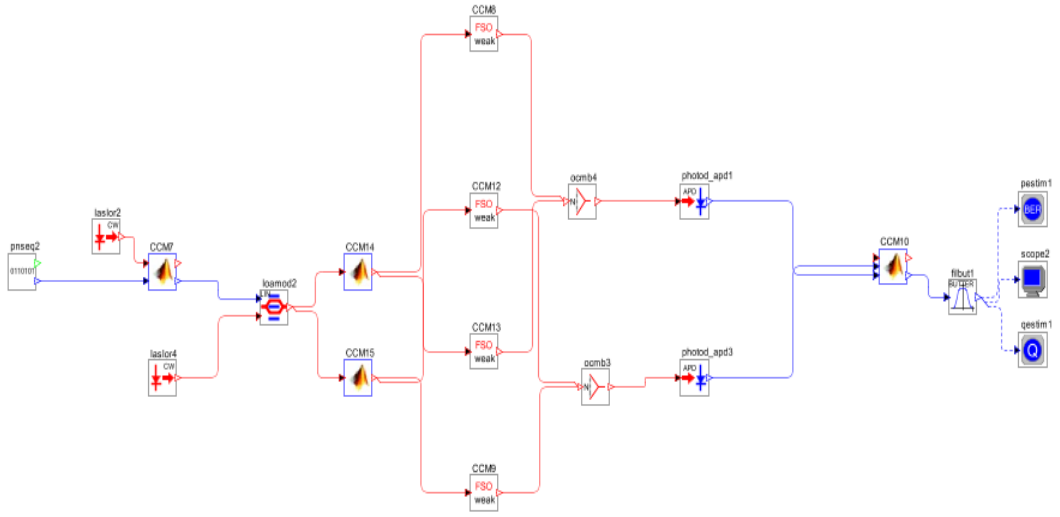

Figure 8.15 Proposed 2×2-Chaotic- FSO system architecture and simulation set up using OPTSIM

8.4.6 Simulation Results Using OPTSIM

We have simulated results for CSK combined with (SISO and MIMO). We have used OPTSIM software package version (5.2) to simulate the results.

Our design uses MATLAB co-simulation for chaotic sequence generation, for Alamouti design and for message decoding linked with optical components in OPTSIM.

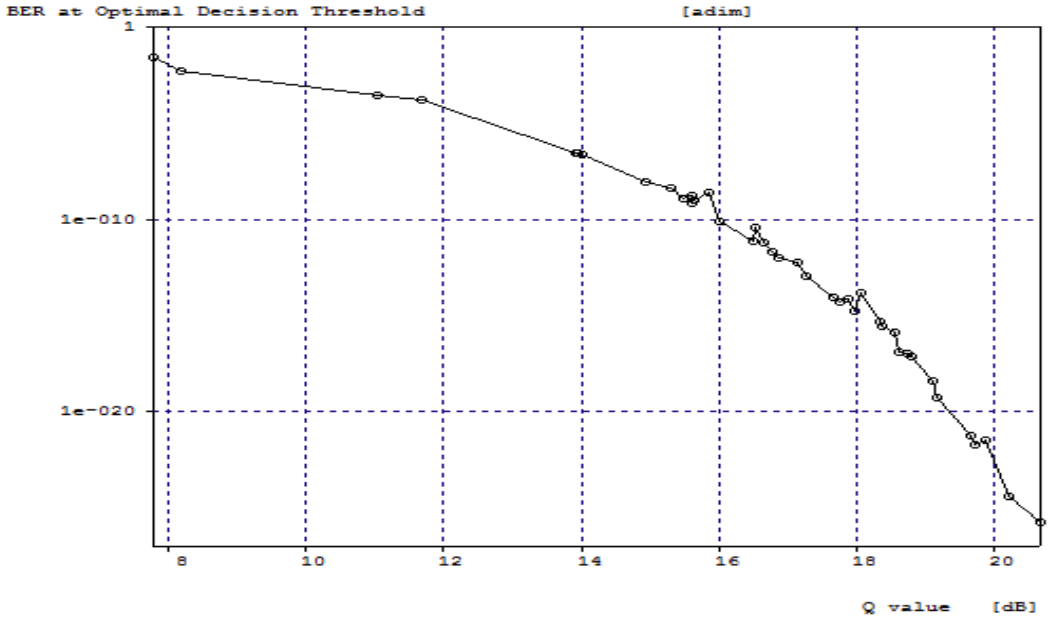

Figure 8.16 BER performance of Chaotic-SISO-FSO

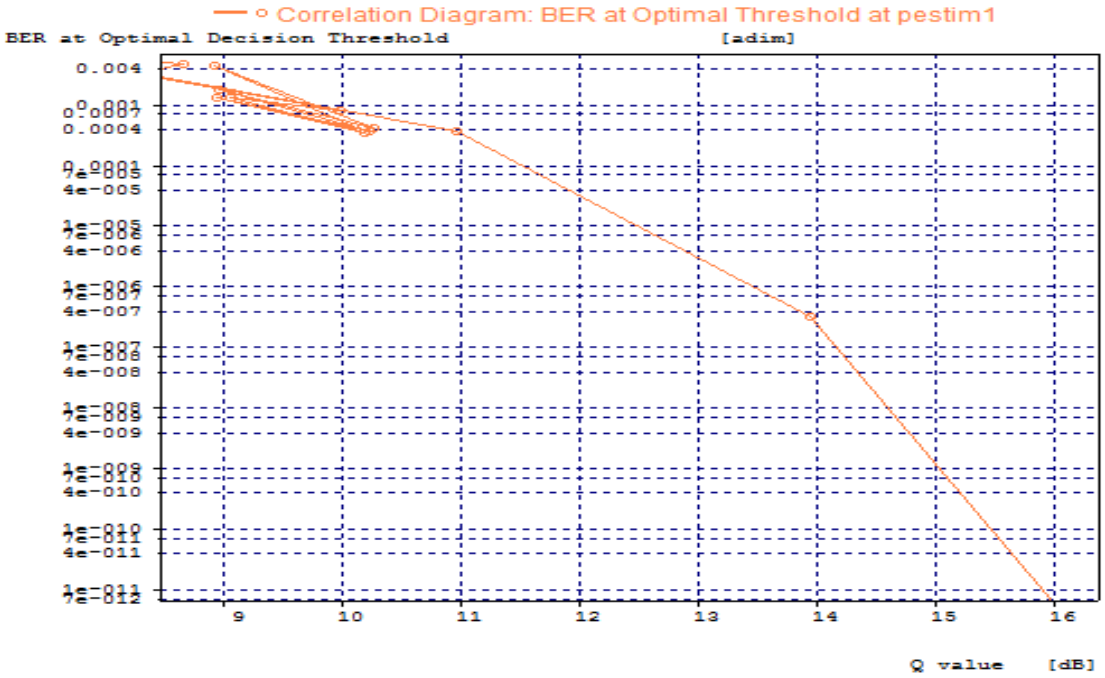

Figure 8.17 BER performance of Chaotic-2×1-FSO

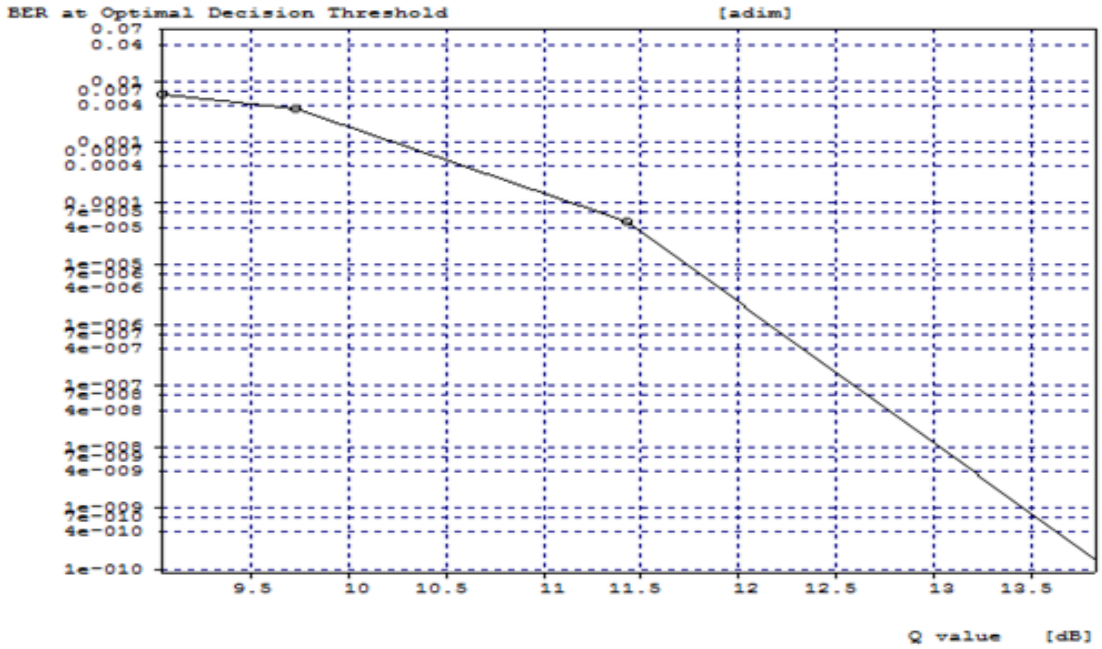

Figure 8.18 BER performance of Chaotic-2×2-FSO

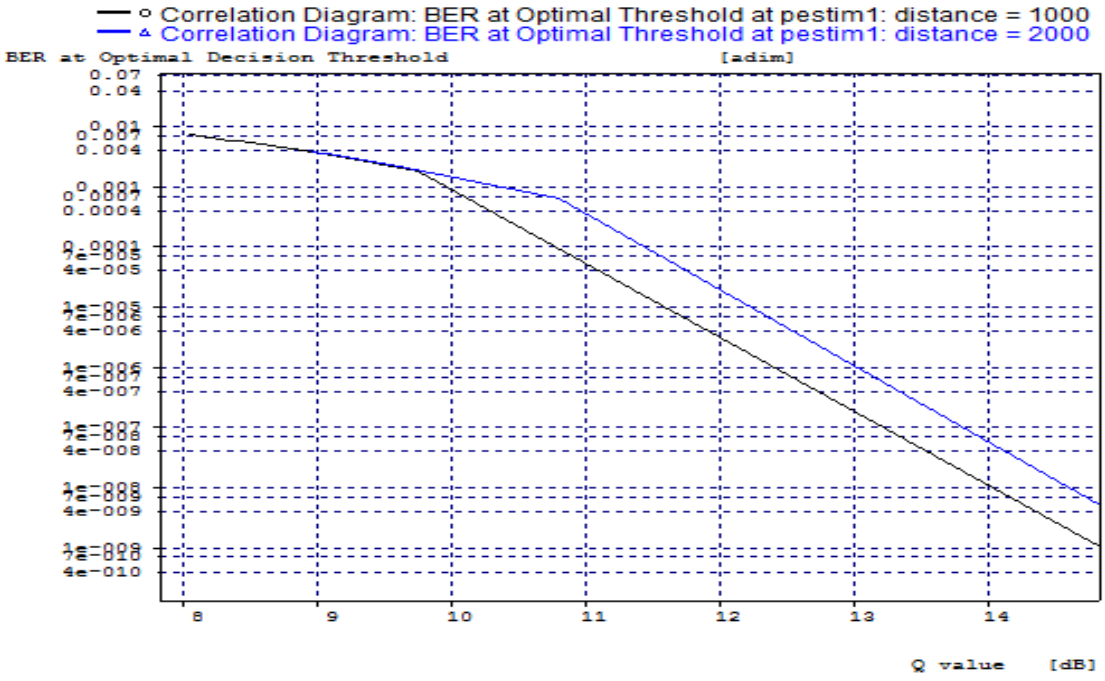

Figure 8.19 BER performance of Chaotic-2×2-FSO for different distances

Figures above shows the BER performance of three different modulation techniques compared at 10^{-5}. It can be observed that chaotic 2×1 (Figure 8.17) gives 1 dB gain to

chaotic SISO (Figure 8.16). Chaotic 2×2 (Figure 8.18) gives 1.75 dB gain as compared to chaotic SISO (Figure 8.16).

Figure 8.19 shows 0.5 dB degradation of BER performance with increase in FSO link distance by 1000 meters.

8.5 Conclusions

In the first part of this chapter, we have described the design of a secure FSO communication scheme using chaotic signal. The simulation results indicate that the algorithm has excellent correlation property. We examined the security vulnerabilities of single FSO links by implementing the chaotic signal generator "reconfigurable tent map" and test auto-correlation and cross-correlation. The synchronization between them is good since the cross correlation is very close to zero and auto-correlation is δ-like as shown in Figures (8.5 and 8.6).

In the second part of this chapter, the BER performance of 2×2 STBCand 2×1 STBC schemes combined with CSK for different chaotic maps under different fading channel conditions have been computed and plotted. These schemes give the benefit of providing additional security while maintaining BER performance at levels similar to that obtained by the use of simple BPSK alone.

In the third part of chapter eight, the design and implementation, simulation and BER performance evaluation of CSK modulation scheme with FSO communication system are presented using OPTSIM simulator. We have evaluated the BER performance for STBC in chaotic FSO communication systems with Gamma-Gamma fading channel. Use of STBCs with multiple transmitters and receivers can improve signal quality.

In the next (and last) chapter, we shall recall all the work done in this thesis and suggest a few directions for further research.

CHAPTER 9

CONCLUSIONS AND FUTUTRE DIRECTIONS

9.1 Summary of the Results

The primary motivation of this thesis has been to design and evaluate techniques based on chaotic modulation combined with MIMO and Space Time Codes that can provide the important requirements of very low BER, high bandwidth efficiency along with information security over both static and fading channels. Specifically, the thesis has dealt with the study and analysis of techniques that can provide security and reliability to wireless RF and Optical communication links. While conventional techniques based on the use of PN sequences, DES, triple DES or various key generations have been employed, they are unable to simultaneously provide information security and good BER performance. The work presented in this thesis has been designed to simultaneously meet these twin requirements without sacrificing bandwidth efficiency.

A brief introduction to chaotic techniques and their applications in various fields is presented in the first Chapter. The motivation for carrying out this work is also explained. This is followed by the derivation of the nonlinear control factor for chaotic tent map to enforce the synchronization between transmitter and receiver. It has been demonstrated that the use of an LDPC channel code can result in a reduction in the number of errors even with a low value of spreading factor ($\beta = 4$) under AWGN channel conditions. The use of low spreading factors helps to reduce the complexity of the system, compensating for the increase in the complexity due to use of LDPC codes.

The use of dual chaotic maps to enhance information security is also suggested in this chapter. Our results indicate that while use of dual map increases security, the single tent map provides the best BER performance with acceptable security.

In chapter three, we have evaluated the BER performance for different chaotic coherent and non-coherent schemes (CSK, DCSK and CDSK). These schemes have been combined with MIMO communication systems and their performance has been evaluated under AWGN and Rayleigh fading channel conditions. We have employed an exact method to analyze the BER performance.

This method takes into consideration the non-periodic nature of chaotic sequences. We have compared the performance of coherent and non-coherent chaotic schemes in terms of BER performance. Our simulation results indicate that the BER performance of modulation scheme employing tent map is superior to the performance offered by other modulation schemes employing other chaotic maps.

A careful inspection of the combination of CSK with 2×2 Alamouti scheme reveals that the performance of 2×2 Alamouti scheme without chaos and the performance of CSK modulated 2×2 Alamouti scheme are nearly identical. This implies that the BER degradation seen in the use of chaotic schemes has been successfully overcome by the 2×2 Alamouti STBC. Thus the system offers security as well as good BER performance.

It is a common observation that exact synchronization can be difficult to establish and maintain over long intervals of time. Our results in chapter three suggest that DCSK modulation scheme can be employed in wireless communication systems if the synchronization is difficult to achieve. The use of Alamouti scheme can reduce the degradation in fading channel which employ DCSK. Such a scheme combining MIMO with DCSK can be efficiently employed on channels where high level of data integrity and security are simultaneously required.

This improvement is realized with only a marginal increase in computational complexity at the transmitter and receiver.

The use of DCSK and CDSK is preferred in practice because they can operate in the absence of synchronization between the transmitter and receiver. This reduces the

complexity of the receiver as compared to coherent schemes. However, our results indicate that under AWGN the BER performance of CSK is better than that of non-coherent schemes. Thus, coherent schemes inherently yield better reliability over AWGN channels. Further, it has been demonstrated that the bandwidth efficiency of CDSK is superior to that of DCSK. However, the BER performance of DCSK is better than that of CDSK.

In chapter four, we evaluated the BER performance for a concatenated scheme comprising of LDPC-MIMO and chaotic modulation under different fading channels. Synchronization between transmitter and receiver is achieved as described in chapter two.

From simulation results we observed that for proposed system the system employing irregular LDPC code outperforms the system employing regular LDPC code in term of BER performance.

Improvement in throughput is always an important requirement in any communication system. With this objective in mind (that is improving the throughput of the chaotic communication system), we have proposed the use of QCSK combined with high rate STBC (rate-$\frac{5}{4}$ and rate-$\frac{6}{4}$) in Chapter Five. In addition, we have derived the exact formula for the BER of this system. We computed the effective throughput and BER for both rate-$\frac{5}{4}$ and rate-$\frac{6}{4}$ with QCSK and DCSK implementing 2×2 Alamouti scheme. We have achieved throughput of 2.5 bit/time slot by using rate-$\frac{5}{4}$ QCSK as compared to rate-1 DCSK (increasing throughput 25% as compared to rate-1 QCSK). This is achieved with a certain tradeoff in BER performance. In addition, we have further increased the effective throughput to 3 bit/time slot by implementing rate-$\frac{6}{4}$ QCSK with a certain tradeoff in BER performance (increasing throughput 50 % as compared to rate-1 QCSK).

In chapter six, we have derived the BER performance of CSK-MIMO scheme under sinusoidal jamming. We have compared the BER performance this combination of

chaotic modulation and MIMO with three common types of jamming, namely sinusoidal jamming, pulsed sinusoidal jamming and multi-tone jamming under different levels of noise power over AWGN channel.

Our simulation results indicate that in absence of jamming signal, the chaotic system implementing 2×2 Alamouti scheme with $\beta = 4$ provides BER performance equivalent to BPSK under AWGN. We have studied the BER performance with jamming signal levels corresponding to jamming level $\frac{P_s}{P_{jam}} = -6$ dB outperforms to that of the jamming level $\frac{P_s}{P_{jam}} = -9$dB. We have concluded that from a study of the BER performance that the chaotic modulation system is more immune (resistant) to sinusoidal jamming as compared to other jamming methods.

In chapter seven, we have designed a communication system that combines a MIMO scheme with chaotic sequence based on DS-CDMA. This is designated as a MIMO-CDMA scheme based on chaotic technique. We have computed the BER performance for different chaotic maps with 2×2 Alamouti scheme, 2×1 Alamouti scheme (MIMO) and SISO communication system and compared them with BER of a DS-CDMA system based on PN sequences. We have determined that the autocorrelation of chaotic tent map is δ-like and the cross-correlation value is close to zero.

From simulation results, we observed that the tent map provides superior BER performance when compared to Chebyshev map, logistic map and tailed shift map.

For different fading channels, the required E_b/N_0 range is 9 dB to 15 dB at BER of 10^{-5}. We have also computed the number of users who can use the cell without degradation in BER.

In chapter eight we discussed the applications of chaotic technique in wireless optical communication link. In the first part of this chapter, we examined the security vulnerabilities of single FSO link and proposed a solution to this problem by implementing the chaotic signal generator (reconfigurable tent map). The

autocorrelation result of this configuration is δ-like and the crosscorrelation is close to zero which are in accordance with requirements.

In the second part of chapter eight, we concentrated on investigating the error rate performance of chaotic wireless optical communication links operating over atmospheric channels. Our simulation results indicate that the combination of the STC and tent map provides the best BER performance in addition to security when compared with other chaotic maps.

Thus, combination of CSK-MIMO scheme can be gainfully employed on channels where high levels of data integrity and security are simultaneously required. This improvement is realized with only a marginal increase in computational complexity at the transmitter and receiver.

In the third part of chapter eight, we have proposed a chaotic-MIMO-FSO communication system which can improve the security and capacity of the transmission and enhance the BER performance. We used a 2×2 Alamouti scheme, 2×1 Alamouti scheme to overcome the influence of the turbulence induced fading. Simulations studies were carried out using available simulator from RSOFT OPTSIM version 5.2. Performance has been evaluated in term of BER and Q factor to verify the results of the second part.

9.2 Scope for Future Work

The use of chaotic techniques to secure communications against channel induced perturbations and eavesdroppers have attracted the attention of many researchers and could be a promising approach in the near future. In order to make this technique attractive to designers of communication systems, a few more problems need to be addressed. Some of the problems that have to be addressed and solved are listed below. They are listed for the use of other potential researchers entering this dynamic research area.

- In chapter 3, we looked at Alamouti STBC with different chaotic modulation schemes to improve the signal quality. Other techniques of MIMO communications have not been explored. These can be studied. In addition, possible improvement of BER performance (with reduced power consumption) with implementation of beamforming techniques instead of MIMO systems can also be explored.
- In this thesis, we have employed a LDPC code to improve the BER performance. A similar study involving other powerful channel codes such as Turbo codes can be carried out.
- We have presented different applications of chaos in secure communications. Our focus has been on simultaneous improvement of BER performance and security. Our claim that the system provides security is based on the unpredictability of the chaotic waveform. However, we have not quantified the strength of these systems in terms of the computational complexity associated with breaking the cipher. These issues require study. Encryption and cryptanalysis using chaotic dynamics requires further research.
- Another important research problem which can be addressed is the scaling of the system from QCSK to MCSK (M-ary CSK) to increase bandwidth efficiency.
- The possibility of implementing these schemes as constituents of WCDMA, CDMA 2000 and 4G telecommunication standards for spreading and authentication can be examined.
- The use of chaotic sequences in RADAR and LIDAR systems for spreading and security can be examined. They have the potential to be gainfully used in such systems as well.

The potential of chaotic systems in securing communication systems against channel impairments is immense. We have tried to take a small step in this direction by means of the work done in this thesis. It is hoped that many researchers in the field will address unresolved problems in this discipline and that these techniques will find popularity and acceptance in the community of Communication Engineers.

REFERENCES

Abir A., Safwan. A, Wang Q. Calin V. and Bassem. B., (2008). "Comparative study of 1-D chaotic generator for digital data encryption". IAENG International Journal of Computer Science, 35:4, IJCS_35_4_05.

Akinori O. and Tomoaki O., (2004). "Performance Analysis and Code Design of Low Density Parity-Check (LDPC) Coded Space-Time Transmit Diversity (STTD) System". IEEE Communication Society GlobeCom, pp. 3118-3122.

Anjam R. and Maaruf A., (2008). "Chaotic Communications, their Applications and Advantages over Traditional Methods of Communication". IEEE International Symposium on Communication System, Networks and Digital Signal Processing, pp. 21-24.

Bart S. and Vincent N. (2010). "Pseudo-Random Binary Sequence Selection for Delay and Add Direct Sequence Spread Spectrum Modulation Scheme". IEEE Communication Letters, Vol. 14, No. 11.

Basar E. and Aygolu U., (2009). "High-rate full-diversity space-time block codes for three and four transmit antennas. IET Communications", Vol.3 Issue, pp. 1371-1378.

Charge P, Kaddoum G., Lawrance A. and Roviras D, (2011). "Chaos Communication Performance: Theory and Computation". Springer, Circuit and System Signal Processing, 185-207.

Cherni A.,Ben Jemaa Z. and Belghith S., (2011). "Performance of Conventional Receiver in a CDMA MIMO System Using Non classical Spread Spectrum Sequences". IEEE, International conference of communications, computing and control applications, PP. 1-5.

Chi C. and Chao C., (2012). “Robust Synchronization of Chaotic Systems Subject to Noise and Its Application to Secure Communication”. Fourth International Conference on Computational Intelligence. Communication Systems and Networks. pp. 206-210.

Chris W., (2001). “Chaotic Communication over Radio Channels”. IEEE Transactions of Circuits and Systems: Fundamental Theory and Applications, Vol. 48, No. 12, pp. 1394-140.

Chunyan H. and Fenguan M., (2010). “Noise Performance Analysis of Chaotic Coherent CSK Communication System”**,** IEEE International Conference on Computational Intelligence and Software Engineering, pp. 1-4.

Daniela K. and Marcio E., (2007). “On the Power Spectral Density of Chaotic Signals Generated by Skew Tent Maps”., IEEE International Symposium on Signals, Circuits and Systems, Vol. 1, pp. 1-4.

David C., Simon W. and Matthew D., (1999). “Comparison of Constructions of Irregular Gallager Codes”. IEEE Transaction on Communications, Vol. 47, No. 10, pp. 1449-1454.

Douglas F., (1993). “Chaotic Digital Encoding: An Approach to Secure Communication”, IEEE Transaction of Circuits and Systems: Analog and Digital Signal Processing, Vol. 40, No. 10. pp. 660-666.

Duy N., Ha N. and Hoang T., (2008). “High-Rate Space-Time Block Coding Schemes”, IEICE Transactions on Fundamentals of Electronics, Communications and Computer Sciences, Vol. E91, Issue 11, 3393-3397.

Ehsan. B., Robert S. and Ranjan. M., (2008). “Performance Analysis of Free–Space Optical Systems in Gamma Gamma Fading”, IEEE, Global Telecommunication Conference, 1-6.

Ehsan B., Robert S.Ranjan Mallik K., (2010). “On Space–Time Coding for Free–Space Optical Systems”, IEEE Transactions on Communications, Vol. 58, No. 1, pp. 58-62.

Eiji O., (2011). “A chaos MIMO transmission scheme for secure communications on physical layer”. IEEE Vehicular Technology Conference, pp. 1-5.

Francis C. M., Lau F. and Tse C., (2002). “Study of Anti-Jamming Capabilities of Chaotic Digital Communication Systems”. International Symposium on Information Theory and Its Applications, P.P. 65-68.

Francis L., Chi T., Ming Y. and Sau H., (2004). “Coexistence of Chaos Based and Conventional Digital Communication Systems of Equal Bit Rate”. IEEE Transactions on Circuits and Systems-I, Vol. 51, No. 2.

Francis L., (2012). “Chaotic Communications: the Past, the Present and the Future”. IEEE International Conference on Advanced Technologies for Communications, pp. 1.

Gallager, R.G., (1962). “Low density Parity Check Codes”. Transactions of the IRE Professional Group on Information Theory, Vol. IT-8, pp. 21-28.

Gerard F., (1996). “Layered Space-Time Architecture for Wireless Communication in a Fading Environment when Using Multi-Element Antennas”. Bell Labs Technical Journal, pp. 41-59.

Geza K., Michael K. and Leon C., (1997). “The Role of Synchronization in Digital Communications Using Chaos—Part I: Fundamentals of Digital Communications”. IEEE Transaction on Circuits and Systems-I: Fundamental Theory and Applications, Vol. 44, No. 10, pp.927-936.

Geza K., Michael K. and Leon C., (1998). “The Role of Synchronization in Digital Communications Using Chaos—Part II: Chaotic Modulation and Chaotic Synchronization”. IEEE Transaction on Circuits and Systems-I: Fundamental Theory and Applications, Vol. 45, No. 11, pp.1129-1139.

Geza K., Michael K., Gabor K. and Zoltan J, (1998).” FM-DCSK A Novel Method for Chaotic Communications”. IEEE International Symposium on Circuits and Systems, p.p. 477-480.

Guopeng T., Xiaofeng L. Di. X. and Chuandong l., (2004). “A Secure Communication Scheme Based on Symbolic Dynamics”. IEEE International Conference on Communications, Circuits and Systems, p.p. 13-17.

Guangyi W., Xun Z., Lingling S., Caifen L. and Yan Z., (2006). “Performance Analysis of Antipodal CSK Communication System in a Noisy Multiuser Environment”. IEEE, International Conference on Wireless, Mobile and Multimedia Networks, pp. 1-3.

Hang K., and The L., (2009). “A new structure of chaotic secure communication in wireless AWGN channel”. IEEE, International Workshop on Chaos-Fractals Theories and Applications, pp. 182-185.

Heba S., Salma D. Abd A. and Mustafa H., (2010). Probability of Error Performance of Free Space Optical Systems in Severe Atomspheric Turbulence Channels. IEEE Microwave Symposium, pp. 355-359.

Hemmati H., (2000). “Status of Free-Space Optical Communications Program at JPL”. IEEE Aerospace Conference, Vol. 3, pp. 101-105.

Henry L. and Jennifer L., (1997). “Design of Demodulator for the Chaotic Modulation Communication System”. IEEE Transactions of Circuits and Systems: Fundamental Theory and Applications Vol. 44, No. 3.

Hiroshi Y. and Tomoaki O., (2003). “Atmospheric Optical Subcarrier Modulation Systems using Space-Time Block Code”. IEEE Global Telecommunication Conference, Vol. 6, p.p.3326-3330.

Huanfei M. and Haibin K , (2009). “Space-Time Coding and Processing With Differential Chaos Shift Keying Scheme”. IEEE International Conference on Communications, pp. 1-5.

Ibarra E., Vazquez R., Cruz M. and Del R., (2008). “Numerical Calculation of the Lyapunov Exponent for the Logistic Map”. International Conference on Mathematical Methods in Electromagnetic Theory, pp. 409-411.

Inokura H., Kuroyanagi N., Tomita M. and Suehiro N., (2003). “A CDMA MIMO System with Multiple-Dimension-Decorrelating-Detectors”. IEEE Vehicular Technology Conference, Vol 2, 1364-1368.

Jaedon P. Eunju L., and Giwan Y., (2011). “Average Bit-Error Rate of the Alamouti Scheme in Gamma-Gamma Fading Channels”. IEEE Photonic Technology Letters, Vol.23, No.4, 269-271.

Jaejin L. and Douglas W., (1995). “Secure Communication Using Chaos”. IEEE Global Telecommunication Conference, p.p. 1183-1187.

Ji Y., (2004). “Optimal Chaotic Shift Keying Communications with Correlation Decoding, IEEE International Symposium on Circuits and Systems”. pp. 593-596.

Ji Y. and Lawrance A., (2005). “Optimal Spreading in Multi-User Non-coherent Binary Chaos-Shift-Keying Communication Systems”. IEEE, International Conference on Circuits and Systems, Vol. 2 876-879.

Jiamin P. and He Z., (2009). “Design of FM-QACSK Chaotic Communication System”. IEEE International Conference on Wireless Communications and Signal Processing, pp. 1-4.

Jianmeng Z. and Shuqing W., (2000). “A Chaos Scheme for Secure Communication Based on Neural Network”. IEEE Asia-Pacific Conference on Circuits and Systems, P.P. 371-374.

Jiang P, Yanbin Z, Lei N and Qun D,, (2012). “A New Viewpoint on Chaotic Signal in Communication: Viewing from random variables and random process”. IEEE Fifth International Workshop on Chaos-fractals Theories and Applications, pp. 176-180.

Jin Y., Hanyu L., Yu Y. and Neil V., (1999). “Chaotic generation of PN sequences: A VLSI implementation”. IEEE International Symposium on Circuits and Systems, pp. 454-457.

Jiu F and Chi T, (2008). “Reconstruction of Chaotic Signals with Applications to Chaos-Based Communications”. © Word Scientific.

Jose L. and Sebastien R., (2010). “Spectrally Efficient Maximum-Likelihood Detection for Chaotic Underdetermined MIMO Systems”. IEEE Workshop on Signal Processing Systems, p.p. 186-191.

Jovic B. and Unsowrth C. P., (2010). “Fast synchronization of chaotic maps for secure chaotic communications”. IEEE Electronic Letters, Vol. 46, Issue 1, pp. 49-50.

Jovic B., (2011). “Synchronization Techniques for Chaotic Communication Systems”. © Springer.

Kaddoum G., Roviras D., (2007). “Charge P. and Prunaret F.: Analytical calculation of BER in communication systems using a piecewise linear chaotic map”. IEEE 18th International Conference on Circuit theory and Design, pp. 691-694.

Kaddoum G., Roviras D., Charg´e., (2009). “Robust synchronization for asynchronous multi-user chaos-based DS-CDMA”. Elsevier Signal Process, vol. 89, pp. 807–818.

Kaddoum G., Francois G., and Sacha A., (2010). “Performance Analysis of A Chaotic Symbolic Communication System Under Sinusoidal Jammer”. Military Communications Conference-Waveform and Signal Processing Track, pp. 1678-1683.

Kaddoum G., Francois G., Pascal C and Daniel R., (2010). “A Generalized BER Prediction Method for Differential Chaos Shift Keying System through Different Communication Channels”. Springer, Wireless Personal Communications, Vol. 64, No. 2, pp.425-437.

Kaddoum G., Mai V. and Francois G., (2011). “On the performance of chaos shift keying in MIMO communications systems”. IEEE Wireless Communication and Networking Conference, pp. 1432-1437.

Kaddoum G., Mai V. and Francois G., (2011). “Performance Analysis of Differential Chaotic Shift Keying Communications in MIMO Systems”. IEEE International Symposium on Circuits and Systems, pp. 1580-1583.

Kai X., Peiyu T., Ng and Jing L., (2009). “Analog Turbo Codes: A Chaotic Construction”. ISIT Seoul, Korea, pp. 894-898.

Kathleen A., Tim S. and James Y., (1996). “Chaos, An Introduction to Dynamical Systems”. © Springer.

Khalid A., (2007). “Design and Simulation of Band pass Digital Filter for Frequency Hopping Spectrum Transceiver System”. Ph.D. Thesis, University of Technology.

Kwok W., Qiuzhen L. and Jianyong C., (2010). “Simultaneous Arithmetic Coding and Encryption Using Chaotic Maps”. IEEE Transactions on Circuits and Systems, Vol. 57, No. 2, pp. 146-150.

Laourine A., Stephanne A. and Affes S., (2009). “On the Capacity of Log-Normal Fading Channels. IEEE Transactions on Communications”. Vol. 57, No. 6, pp. 16.3-16.7.

Lau F., Ye M., Tse C. and Hau S., (2001). “Anti-Jamming Performance of Chaotic Digital Communication Systems”. IEEE Transaction on Circuits and Systems-I: Fundamental Theory and Apllications, Vol 49, No. 10, pp.1486-1494.

Lawrence L, Jia L and Lev T, (2006). “Digital Communications Using Chaos and Nonlinear Dynamics”., © Springer.

Lawrance A. and Yao J., (2007). “Likelihood-Based Demodulation in Multi-User Chaos Shift Keying Communication”. Circuits, Systems and Signal Processing, Springer, pp. 847-864.

Li H. Gang Z. and Zeng T., (2010). “A Chaotic Secure Communication Scheme based on Logistic Map”. IEEE International Conference on Computer Application and System Modeling, Vol. 8, pp. 589-591.

Ling C. and Sun S., (1996). Coherent Demodulation of Chaos Shift Keying. IEEE, International Conference on Communication Technology, p.p. 926-929.

Liu J., Cai. T. Xiao J. Zhang Y and Wu Y., (1996). “Chaos-Shift-Keying Secure Digital Communications using Feedback to Synchronize Chua's Circuit :Simulation and Realization”. IEEE International Conference on Communication Technology, p.p. 552-554.

Liu J., Chen H. and T. Tang S., (2001). “Optical-Communication Systems Based on Chaos in Semiconductor Lasers”. IEEE Transactions of Circuits and Systems: Fundamental Theory and Applications Vol. 48, No. 12, pp. 1475-1483.

Liu J., (2009). “A High Quality PN Sequence Generator Based on Chaotic Maps. Fifth International Conference on Natural Computation”. IEEE International Conference on Natural Computation, pp. 432-436.

Ljupco K., Janusz S., Jose A. and Igor T., (2006). “Discrete Chaos-I: Theory”. IEEE Transaction of Circuits and Systems-I, Vol 53, No. 6, pp. 1300-1309.

Lwaa F., Jokhakar J, Sripati U. and Muralidhar K., (2013). “BER Performance Enhancement for Secure Wireless Communication Systems based on Chaotic- MIMO Techniques”. SPIE International Conference on Communication and Electronics System Design, Vol. 8760 87600V, pp.1-11.

Lwaa F., Jokhakar D., U. Sripati and Muralidhar K., (2013). **“**On the Security of Free Space Optics based on Reconfigurable Chaotic Technique”. SPIE International Conference on Communication and Electronics System Design, Vol. 8760 87600O, pp.1-7.

Lwaa F., Jokhakar D., U. Sripati and Muralidhar K., (2013). “BER Performance Enhancement for Secure Wireless Optical Communication Systems Based on Chaotic MIMO Techniques”. Nonlinear Dynamics, An international Journal of Nonlinear

Dynamics and Chaos in Engineering Systems, (SPRINGER), DOI: 10.1007/s11071-013-1044-z.

Lwaa F., Jokhakar D., U. Sripati and Muralidhar K., (2013). "Anti-Jamming Performance of Communication Systems based on Chaotic Modulation and MIMO Schemes over AWGN Channels". European Journal of Scientific Research, Vol. 102, Issue, pp. 462-473.

Mackay, D.J.C., (1999). "Good error correcting codes based on very sparse matrices". IEEE Transactions on Information Theory, Vol. 45, No. 3, pp. 399-431.

Martin H and Yuri M., (1997). "An Introduction to the Synchronization of Chaotic Systems: Coupled Skew Tent Maps"., IEEE Transactions on Circuits and Systems-I: Fundamental Theory and Applications, Vol. 44, No. 10, pp. 856-866.

Martin H. and Thomas S., (2002). "Potential of Chaos Communication Over Noisy Channels-Channel Coding Using Chaotic Piecewise Linear Maps". IEEE International Symposium on Circuits and Systems, p.p. 568-571.

Mazzini G., Sitti G. and Rovatti R., (1997). "Chaotic Complex Spreading Sequences for Asynchronous DS-CDMA—Part I: System Modeling and Results". IEEE Transactions on Circuits and Systems-I; Fundamental Theory and Applications, Vol. 44, No. 10, 937-947.

Mekhail S, Lev T. and Alexander V., (2000). "Performance Analysis of Correlation-Based Communication Schemes Utilizing Chaos". IEEE Transactions on Circuits and Systems, Vol. 47, No. 12, pp. 1684-1691.

Michael L., Michael M., Amin S. and Daniel S., (1998). "Improved Low-Density Parity-Check Codes Using Irregular Graphs and Belief Propagation". IEEE, PP. 117.

Mihir M., Laxmi M. and Saumendra M., (2011). “Design of MIMO Space-Time Code for High Data Rate Wireless Communication”. International Journal on Computer Science and Engineering, pp. 693-696.

Mokhtar M and Gupta S., (1992). “Capacity for Cellular CDMA PCS’s IN Nakagami Fading Log-normal Shadowing Channels”. IEEE International Conference on Universal Personal Communications, pp. 1-5.

Morgan C., (2003). “Review of Free-Space Optical Communications Links”. Cite seer California at Berkeley, CA9 4720 USA.

Mozsary A., Azzinari L., Krol K. and Porra V., (2001). “Theoretical connection between PN-sequences and chaos makes simple FPGA pseudo-chaos sources possible”. IEEE International Conference on Electronics, Circuits and Systems, Vol. 1, pp. 457-460.

Murthy C., Srilatha G., Anitha K., Ravi Kumar Ch. and Srinivasa Rao M., (2011). “Counter Jamming Method based on Chaos for Secure Communication in Multiuser Environment”. IJECT Vol. 2, Issue 3, pp. 199-203.

Nagarajan V., Dananjayan P. and Nithyanandhan L., (2009). “On The Performance of Chaotic Spreading Sequence MIMO MC-DS/CDMA Systems Using NPGP”. International Conference on Control, Autonomous, Communication and Energy Conservation, 1-5.

Nuwan B., Pradeepa Y., Telex N. and Attahiru A., (2009). “Low-Complexity Iterative Detection and Decoding in Finite Geometry LDPC-Coded MIMO Systems”. International Symposium on Personal, Indoor and Mobile Radio Communication, pp. 1752-1756.

Ohama G., Lawrance A., (2003). “Exact Calculation of Bit Error Rates in Communication Systems with Chaotic Modulation”. IEEE Transaction of Circuits and Systems, Vol 50, No. 11.

Parlitz U., (1993). “Lyapunov Exponents from Chau’s Circuit”. Journal of Circuits, Systems and Computers, Vol. 3, No. 2, pp. 507-523.

Pecora M. and Carroll L., (1990). “Synchronization in Chaotic Systems”., Physical Review Letters Vol. 64, No. 8. pp. 821-825.

Pingping C., Lin W. and Francis L., (2013). “One Analog STBC-DCSK Transmission Scheme not Requiring Channel State Information”. IEEE Transactions on Circuits and Systems-I, Vol. 60, No. 4, pp. 587-597.

Peng L., Xueying W., Wakamori K., Pham T., Alam M. and Matsumoto M., (2011). “Bit Error Rate Performance Analysis of Optical CDMA Time-Diversity Links Over Gamma-Gamma Atmospheric Turbulence Channel”. IEEE WCNC Conference, 1932-1936.

Premaratne M. and Zheng E., (2007). “Orthogonal space–time block codes for free-space IM-DD optical links”. IEEE Electronic Letter, Vol. 43,Issu: 15, p.p. 822-823.

Ranjan B and Amitbha B., (1996). “Implementing Symmetric Cryptography Using Chaos Function”. Citeseer, pp. 1-4.

Sae C., Daived G., Thomas R. and Rudiger U., (2001). “On the Design of Low-Density Parity-Check Codes within 0.0045 dB of the Shannon Limit”. IEEE Communication LetterVol. 5, No. 2, pp. 58-60.

Safwan and Chadi T., (2005). “Design and Implementation of Chaotic Codec”. IEEE, The European Conference on Wireless Technology, pp. 351-354.

Shilian W. and Xiaodong W., (2010). “M-DCSK-Based Chaotic Communications in MIMO Multipath Channels With No Channel State Information”. IEEE Transactions on Circuits and Systems, Vol. 57, No. 12.

Shilian W., Jiang Z. and Jie Z., (2012). “OFDM-based Chaotic Spread Spectrum Communications with High Bandwidth Efficiency”. IEEE International Conference on Control Engineering and Communication Technology, pp. 940-943.

Siavash M. Alamouti, (1998). “A Simple Transmit Diversity Technique for Wireless Communications”. IEEE Journal on Select Areas in Communications, Vol. 16, No. 8, p.p. 1451-1458.

Silvano D. and Claudio R., (2002). “Introduction to the Feature Section on Optical Chaos and Applications to Cryptography”. IEEE Quantum of Electronics Vol. 38, No. 9, pp. 1138-1140.

Songsheng Z., Yinlin X. and Kiuxi., (2009). “Design of a Quadrature Differential Chaotic Phase Shift Keying Communication System”. IEEE International Conference on Networks Security, Wireless Communications and Trusted Computing, pp. 518-521.

Soobul Y. Chady K. and Rughooputh H., (2002). “Digital Chaotic Coding and Modulation in CDMA”. IEEE African Conference , Vol. 2, PP. 841-846.

Stamatios V., (2010). “Chaos in WDM Mesh FSO for Enhanced Link Security”. IEEE Communication Society, pp 1-5.

Stavroulakis P., (2006). “Chaos Applications in Telecommunications”. © Taylor & Francis Group.

Surbhi S. and Rajesh K., (2011). “LDPC concatenated space-time block coded system in multipath fading environment”. Analysis and evaluation. Maejo International Journal of Science and Technology, pp. 204-214.

Sushanta D., Nawfal D. and Robert C., (2006). “Novel Full-Diversity High Rate STBC for 2 and 4 Transmit Antennas”. IEEE Communication Letters, Vol. 10 No. 3, pp. 171-173.

Sushanta D. and Monisha G., (2008). “High-Rate Full-Diversity STBC Design with Option to Provide Unequal Error Protection”. IEEE, Vehicular Technology Conference, PP. 1448-1452.

Tam W., Lau F., Tse C., Lawrance A., (2004). “Exact analytical bit error rates for multiple access chaos-based communication systems”. IEEE Transactions on Circuits and Systems, Vol. 51, No. 9. PP. 473-481.

Tarokh, V., Sheshadri, N. and Calderbank, R., (1998). “Space-Time codes for high data rate wireless communication: Performance criterion and code construction”. IEEE Transactions on Information Theory, Vol. 44, No. 2, pp. 744-765.

Tarokh, V., Vahid T., Jafarkhani and Hamid J., (1999). “Space-Time Block Coding for Wireless Communications: Performance Results”. IEEE Journal on Selected Areas in Communications, Vol. 17, Issue 3, pp. 451-460.

Teletar E., (1999). “Capacity of Multi-antenna Gaussian Channel”. European Transactions on Telecommunications, Vol. No. 6, pp. 585-595.

Thiruvengadam S., Karthikeyan A., Vinothkumar V. and Abhaikumar V., (2003). “Performance Analysis of DS-CDMA System with Space-Time Multiuser Detection Using a Class of Chaotic Spreading Sequences”, IEEE TENCON, Vol. 2, 801-805.

Thomas R.,Amin S., Rudiger U., (2001). “Design of Capacity Approaching Irregular Low-Density Parity Check Codes”. IEEE Transaction on Information Theory, Vol 47, No. 2, pp. 619-637.

Thomas S. and Martin H., (2003). “Coded Modulation Based on Controlled 1-D and 2-D Piecewise Linear Chaotic Maps”. IEEE International Symposium on Circuits and Systems, p.p. 762-765.

Vahid T. Hamid J. and Robert C., (1999). “Space–Time Block Coding for Wireless Communications: Performance Results”. IEEE Journal on Selected Area in Communications. Vol 17, No. , p.p. 451-460.

Wai T, Francis L., and Chi T., (2006). “Generalized Correlation-Delay-Shift-Keying Scheme for Non-coherent Chaos-Based Communication Systems”. IEEE Transactions on Circuits and Systems-I, Vol. 53, No. 3.

Wai T, Francis L and Chi T., (2007). “Digital Communication with Chaos, Multiple Access Techniques and Performance”. © Elsevier.

Wang H. and Ke X., (2007). “Application of STBC in MIMO Atmosphere Laser Communication”. The Eighth International Conference on Electronic Measurement and Instruments, pp. 630-633.

Wang J. and Xu Z., (2002). “A New Version of DCSK Data Transmission scheme”. IEEE International Symposium om Electromagnetic Compatibility, p.p.685-687.

Wang L. and Li W., (2007). “Code Design of Space-Time Block Codes Coded Low-Density Parity-Check Code and System Performance Analysis”. IEEE International Conference on Electronic Measurement and Instruments, pp. 305-308.

Wang Y. Wang J and Si F., (2013). Study on Chaotic Behavior of the Stock Price's Volatility. IEEE Third International Conference on Intelligent System Design and Engineering Applications, PP. 1323-1325.

Xiaomin J., Xian W. and Chi Y., (2008). "Design and Implementation of Mobile Free Space Optical Communication System". IEEE Conference of Avionics, Fiber Optic and Photonics Technology, pp. 37-38.

Yi C, Li Z. and Yifang W., (2010). "A Data Encryption Algorithm based on Dual Chaotic System". International Conference on Computer Application and System Modeling, pp. V4-431V4-435.

Yi F., Jing X. Lin W. and Guanrong C., (2013). "Performance of MIMO Relay DCSK-CD Systems Over Nakagami Fading Channels". IEEE Transactions on Circuits and Systems-I, Vol. 60, No. 3, pp. 757-767.

Yuu L., Kevin L. and Zahir H., (2005). "Space-Time Encoded Secure Chaos Communications with Transmit Beamforming". IEEE Region 10 TENCON, pp.1 -5.

Yuu S. and Zahir H., (2005). "A New Approach in Chaos Shift Keying for Secure Communication". IEEE Proceedings of the Third International Conference on Information Technology and Applications, pp. 630-633.

Zakria N. S., Elkouny and Sobhy M., (2002). "Digital Chaotic DS-CDMA Communication". IEEE 45th Midwest Symposium on Circuits and Systems, Vol. 3, pp. III- 629-31.

Zbigniew G. and Gian M., (2001). "Quadrature Chaos-Shift Keying: Theory and Performance Analysis". IEEE Transaction on Circuits and Systems-I: Fundamental Theory and Applications, Vol. 48, No. 12, pp. 1510-1519.

Zheng G., Boutat D., Floquet T. and Barbot J., (2008). “Secure Communication Based on Multi-input Multi-output Chaotic System with Large Message Amplitude”. Elsevier, Chaos, Solitons and Fractals, Vol. 41, Issue 3, pp. 1-14.

Zhi D. Bing W. and Peng L., (2006). “Wireless Secure Communication Systems Design Based on Chaotic Synchronization”. IEEE, International Conference on Communication Technology, pp 1-4.

Zhibo Z., Tong Z. and Jinxiang W., (2008). “Exact BER Analysis of Differential Chaos Shift Keying Communication System in Fading Channels”. IEEE International Conference on Wireless Communication, Networking and Mobile Computing, pp. 1-4.

Zhinggou L., Kun L., Changyun W. and Yeng S., (2003). “A new chaotic communication system”. IEEE Transaction on Communication, Vol. 51, No.8, pp. 1306-1312.

Zhong J., (2002). A note on Chaotic Communication Systems. IEEE Transaction on Circuits and Systems: Fundamental Theory and Applications, Vol.49, No.1, pp. 92-96.

Zongjie T Shiyong Z., (2007). “Overview of LDPC Codes”. IEEE International Conference on Computer and Information Technology, pp. 469-474.

PUPLICATIONS BASED ON THE RESEARCH WORK DESCRIBED IN THIS THESIS

International Journal Papers:

[1] Lwaa Faisal Abdulameer, Jokhakar Jignesh D., U. Sripati and Muralidhar Kulkarni, "BER Performance Enhancement for Secure Wireless Optical Communication Systems Based on Chaotic MIMO Techniques", Nonlinear Dynamics, An international Journal of Nonlinear Dynamics and Chaos in Engineering Systems, (SPRINGER), DOI: 10.1007/s11071-013-1044-z., September 2013.

[2] Lwaa Faisal Abdulameer, Jokhakar Jignesh D., U. Sripati and Muralidhar Kulkarni, "BER Performance Enhancement for Secure Wireless Communication Systems based on DCSK- MIMO Techniques under Rayleigh Fading Channel", Radioelectronics and Communications Systems", (SPRINGER) Vol. 56, No. 10, pp. 481-492, September 2013.

[3] Lwaa Faisal Abdulameer, Jokhakar Jignesh D., U. Sripati and Muralidhar Kulkarni "Anti-Jamming Performance of Communication Systems based on Chaotic Modulation and MIMO Schemes over AWGN Channels, European Journal of Scientific Research, Vol. 102, Issue, pp. 462-473, May 2013

International Conference Papers:

[1] Lwaa Faisal Abdulameer, Jokhakar Jignesh D., U. Sripati and Muralidhar Kulkarni, "BER Performance Improvement for Secure Wireless Communication Systems Based on CSK-STBC Techniques", Presented in International Conference on RADAR, Communication and Computing (IEEE), December 2012, thiruvannamalai pp. 1-5.

[2] Lwaa Faisal Abdulameer, Jokhakar Jignesh D., U. Sripati and Muralidhar Kulkarni, **"**BER Performance Enhancement for Secure Wireless Communication Systems based on Chaotic- MIMO Techniques", SPIE, International conference on Communication and Electronics System Design, 2013.

[3] Lwaa Faisal Abdulameer, Jokhakar Jignesh D., U. Sripati and Muralidhar Kulkarni," On the Security of Free Space Optics based on Reconfigurable Chaotic Technique", SPIE International Conference on Communication and Electronics System Design, 2013.

Communicated Papers:

[1] Lwaa Faisal Abdulameer, Jokhakar Jignesh D., U. Sripati and Muralidhar Kulkarni, "Chaotic Shift Keying (CSK) based MIMO-CDMA System: Design and Performance Evaluation". Springer, "Telecommunication Systems".

[2] Lwaa Faisal Abdulameer, Jokhakar Jignesh D., U. Sripati and Muralidhar Kulkarni, "BER Performance Analysis of Chaotic-LDPC Coded Space Time Block Code (STBC) System". International Journal of Electronics and Communications, ELSEVIER.

BIO DATA OF LWAA FAISAL ABDULAMEER

LWAA FAISAL ABDULAMEER
Research Scholar,
Department of Electronics and Communication Engineering,
National Institute of Technology Karnataka (NITK), Surathkal.
E-mail: lwaa@kecbu.uobaghdad.edu.iq
E-mail: lwaakhamass@gmail.com

Qualifications:

- Bs.C (1999) (Electrical Engineering), Al Rasheed College of Engineering and Science, Baghdad, Iraq.
- Ms.C. (2004) (Communication Engineering), Al Rasheed College of Engineering and Science, University of Technology, Baghdad, Iraq.

Total Teaching Experience: 6 years (Information and Communication Engineering Department, Al-Khwarizmi College of Engineering, University of Baghdad, Baghdad, Iraq).

No. of International Journal Publications: 5

No. of International Conference Proceedings/Publications: 3

No. of National Conference Proceedings/Publications: 1

No. of awards obtained during the research period: 1 (SPIE, USA)

No. of Workshops Attended: 2